Does oil emplacement stop diagenesis and quartz cementation in deeply buried sandstone reservoirs

UNIVERSITY OF LIVERPOOL

Thesis submitted in accordance with the requirements of the University of Liverpool for the Degree of Doctor of Philosophy by

Mohammed Bukar

January 2013

Abstract

Reservoir quality relates to the presence of porosity and the connectivity of the pores of the reservoir rock which controls permeability. Deeply buried sandstones in sedimentary basins lose their reservoir quality due to compaction and cementation. Quartz cement is the most volumetrically important porosity occluding cement in sandstones buried to depths greater than about 3000m. Precipitation of quartz cement requires a source of silica, transportation of the silica in solution from source to the point of precipitation and clean grain surfaces to grow on. For these processes to take place water is required to dissolve the mineral grains that provide the source of silica, to provide aqueous fluid pathway from the site of mineral dissolution to the site of precipitation and water is required at the site of mineral precipitation to enable mineral growth. In oil or gas fields, displacing the aqueous pore fluid by petroleum disrupts the pathway between the reactants and points of precipitation. If the oil saturation becomes high; (i) the residual (irreducible) water becomes isolated within a continuous hydrocarbon phase or (ii) the aqueous pathway becomes tortuous and diffusion becomes slow or (iii) grain surfaces become coated by oil if the sandstone is oil wet. However, over the years a controversy has developed as to whether oil emplacement into reservoir stops quartz cementation and preserves porosity at depth.

The research presented in this thesis used core samples, wireline logs and well reports collected from the oil and water legs and the transition zone of Upper Jurassic marine sandstones of the Ula and Tambar fields from the Norwegian North Sea. They were studied using a range of techniques: core analysis, core logging, downhole wireline analysis, optical microscopy, scanning electron microscope (SEM), cathodoluminescence (CL), X-ray diffraction (XRD), fluid inclusion UV-petrology and thermometry. The distributions of all potential controls on porosity and permeability have been quantified so that it has been possible to assess the influence of all possible controls on quartz cement as well as fluid type. Thus the roles of depositional facies, grain size, sorting, chlorite coats and microcrystalline quartz coats have all been assessed.

The main diagenetic cements in both Ula and Tambar fields are quartz overgrowths, grain coating microcrystalline quartz, K-feldspar cement, illite, dolomite and minor

amounts of calcite and chlorite. Fluid inclusion evidence shows that quartz cementation was probably a continuous process and is still taking place in both fields. Quartz cementation occurred in the presence of some oil, as shown by the presence of oil inclusions within quartz cement in both Ula and Tambar. However, there are far fewer oil inclusions in quartz cement in Tambar than Ula suggesting that oil emplacement occurred later in Tambar than Ula. There is less quartz cement in the coarser grained sandstones in the oil legs than the water legs of Ula and Tambar suggesting that quartz cementation has been inhibited, in these facies, by the addition of oil. Finer-grained facies in both fields have more grain-coating microcrystalline quartz that has effectively inhibited quartz cementation in both oil and water legs. Stable isotope data show that the carbonate cements in the oil leg grew at relatively lower temperatures than those in the water legs. Precipitation temperature for carbonate cement in the oil leg stopped at the time of oil emplacement but carbonate cements in the water leg carried on growing or recrystallising at higher temperatures and show progressive input of source-rock derived CO_2 (as the carbon isotopes get progressively lighter) in both Ula and Tambar fields.

Reservoir quality in the Ula field is primarily controlled by a combination of depositional facies, mechanical compaction and early oil emplacement and locally by facies-controlled microcrystalline quartz. In the Tambar field early-formed grain-coating microcrystalline quartz mainly controls the reservoir quality and effects of oil emplacement are not as significant as in Ula due to the later oil charge.

The results of this work have academic and economic significance. Understanding the controls on reservoir quality and the effect of oil emplacement on quartz cementation may be used (1) as analogues in other basins of known petroleum charge history, (2) to improve appropriate reserve calculation and well planning during the appraisal stage and (3) to assist in reliable prediction of aquifer performance during production, and lead to proper decision on number and positions of injection wells during the later life of the field.

TABLE OF CONTENTS

List of Figures

List of Tables

Dedication

To my parents who are the foundation on which I stand

Acknowledgments

First of all I would like to thank my supervisor Professor Richard H. Worden who came with the idea for this research, provided many hours of guidance, critical discussions and advice. Under his tutelage I learned not only the most exciting part of geology, but also the attributes of great researcher, wonderful supervisor and an exceptional teacher. I will forever remain grateful.

Second, I would like to express my appreciation to my co-supervisor Elizabetha Mariani for her invaluable help and encouragement throughout this research work.

This project greatly benefited from collaboration with experienced and talented industry geologists Philip Shell of British Petroleum, who willingly provided data, technical and financial support. I thank you Phil for the keen interest you have shown in this research.

Funding for this research was provided by Petroleum Technology Development Fund of Nigeria (PTDF). This funding is gratefully appreciated. I extend my appreciation to British Petroleum for providing cores and other assistance for this research work. I am also grateful to Reslab Laboratories Stavanger for the access to sample the cores.

This work could not have been completed without the contribution of the following committed staff of the department. I deeply appreciate the contributions of Carmel Pinnington for teaching me how to use SEM, CL and EBSD, Dan Tatham for help in the EBSD scan and processing, Stephen Crowley for assisting in the stable isotope analysis and the elegant James Utley for teaching me how to prepare samples for XRD analysis and assisting in running the samples. I thank Ian Bamber, Paula Houghton, Karen Li, Maureen Dodd, Moira, John Kavanagh, Alan, Dave and Chris Hunt for being there whenever I need their assistance.

A big thank you to Nigel Clarke of British Petroleum for the invaluable guidance in petrographic studies, Simon Thomas for the hospitality accorded to us in Reslab laboratories in Stavanger, Norway during core sampling.

I have benefitted immensely from the company and support of the following colleagues: Salah Elgarmadi, Shanvas Sathar, Oshaine Blake, Mohammed

Benshatwan, Gemma Byrne, Wasiu Raji, Elizabeth Rushworth, John McDonalds, Peter Armitage and Patrick Dowey. It has been interesting sharing an office with Ehsan Daneshver and Lei Jiang for the years I spent here in Liverpool. Thank you to Fauziya for her encouragements and Binta for her troubles.

I owe my deepest gratitude to my parents and my siblings for their unconditional love, encouragement and support throughout this research period. Thank you very much Mum and Dad for all that you have done which made me what I am today.

CHAPTER 1

1. Diagenesis and reservoir quality

1.2 Introduction

Accurate prediction of reservoir quality is needed throughout the entire "life cycle" of a reservoir (Sneider, 1990). The accurate prediction of reservoir quality is, and will continue to be a key challenge for petroleum exploration and development. Prediction is a logical and critically important extension of the description and interpretation of geological processes (Kupecz et al., 1997). Assessing reservoir quality risk is important in plays and prospects where objective sandstones have been exposed to elevated temperatures (>100^{o}C) and /or high effective stress for significant period of time (Taylor et al., 2010).

The importance of accurate pre-drill assessment, including reservoir quality, is growing as oil and gas exploration is increasingly focused on deeper targets. Since we have direct access to a only limited part of the reservoir in form of cores, better understanding has to be model-driven. Presently most models that predict quartz cement distribution are empirical, developed using assumptions and data superimposed on predicted values. Careful integration of basin modeling with reservoir quality modeling can be used to quantify, prior to drilling, the potential impact of hydrocarbon emplacement on porosity and permeability.

All diagenetic reactions take place through an aqueous phase, by dissolution and re-precipitation. There is no possibility of significant solid state reactions at diagenetic temperatures, as diffusion is too slow even on geological time scales (Wilkinson et al., 2006). Hence, for diagenetic reaction to occur there must be a fluid pathway from the site of mineral dissolution to the site of precipitation. Displacing the aqueous pore fluid by oil disrupts the pathway between the reactants and points of precipitation. If the oil saturation becomes high, the residual water (irreducible) becomes isolated within a continuous hydrocarbon phase or the aqueous pathway becomes tortuous and diffusion becomes slow and grain surface becomes coated by oil if the sandstone is oil wet (Worden and Barclay, 2003). Hence, in theory,

cementation could be effectively halted and porosity preserved after oil emplacement. However, recently, contrary ideas have been reported (Aase and Walderhaug, 2005; Molenaar et al., 2008).

This research is intended to assess the effect of oil emplacement on diagenesis with special reference to quartz cementation and porosity-loss in deeply buried reservoir sandstones. In this research work, data from Ula and Tambar oil fields, offshore Norway, have been used to understand diagenesis and reservoir quality with special attention to the effect of the addition of oil. To get a clear idea of the effects of early oil emplacement on quartz cementation, attempt will be made to eliminate all other controls on porosity and permeability (grain size and sorting, chlorite coats, microcrystalline quartz coats). The distribution of quartz cement and porosity will be assessed as a function of pore fluid type for sandstone of the same initial characteristics (in terms of grain size, mineralogy and earlier diagenetic processes).

1.2 Nature of the problem

Quartz is the most important porosity destroying cement in medium and deeply buried sandstone reservoirs. Understanding the controls on quartz cement and being able to predict its occurrence, volume and distribution are becoming more important as oil and gas exploration progresses to ever deeper levels in mature basins. Two opposing schools of thought have evolved over recent years: (1) that quartz cementation ceases or slows dramatically in oil (or gas) fields once petroleum has replaced water in the pores leading to the preservation of porosity and permeability (Boles and Hickey; Cox et al., 2010; Dixon et al., 1989; Emery et al., 1993; Gluyas et al., 1993; Hawkins, 1978; Marchand et al., 2000; Marchand et al., 2002; Saigal et al., 1992; Wilkinson and Haszeldine, 2011) because water is essential for the dissolution-transport-precipitation process that creates cement; a view based on reduced volume of quartz cement above oil water contact; (2) that quartz cement can continue to grow unhindered in oil fields (Aase and Walderhaug, 2005; Bjørkum and Nadeau, 1998; Bjørkum et al., 1998; Bjørlykke, 1994; Ehrenberg, 1990, 1993; Giles et al., 1992; Molenaar et al., 2008; Ramm, 1992; Ramm and Bjorlykke, 1994), utilizing the residual water clinging to grain surfaces for transport and precipitation since petroleum never flushes all water out of the reservoir; a view based on the

occurrence of oil-bearing fluid inclusions trapped in quartz cement and examples of reservoirs that do not show a significant difference in volumes of cement between oil and water zones.

The two schools of thought both of which cannot both be correct - lead to entirely different predictions of the distribution of porosity in oil fields. The "oil stops diagenesis" school of thought would predict that, where oil emplacement predates quartz cementation or is contemporaneous with quartz cementation, early filled reservoirs or structural crest (if the oil charge is gradual), will have less quartz cement and so have better reservoir quality (Emery et al., 1993). This could result in serious overestimation of oil-leg porosities and preservation of deep reservoir quality by early petroleum emplacement. The “oil does not stop diagenesis” school of thought will predict no porosity - permeability variation in relation to filling history. Poor understanding of the effect of oil emplacement on quartz cementation could lead to errors in field volume calculations during the appraisal stage and erratic assessment of reservoir performance (e.g., aquifer influx) during the production stage and improper decisions on number and positions of injection wells at the later life of the field.

- The "oil emplacement inhibits quartz" cementation school of thought based their arguments on:
- Reduced volume of quartz cement above oil-water contacts in some fields,
- Inverse relationship between abundance of petroleum inclusions and quartz cement volume,
- Some sandstones may be oil wet,
- Timing of oil generation is episodic,
- Quartz cementation often coincidental with oil filling.

Diagenesis in sandstone reservoirs is "not affected by oil emplacement" school of thought based their evidence on the following reasons:

- Equal volumes of quartz cement above and below oil-water contacts *in some fields*,
- Presence of primary petroleum inclusions in quartz cement,
- Quartz is apparently water-wet in most oil fields,
- Quartz cementation reported to be a continuous process in some oil fields.

1.3 Aims of the thesis

The aim of this project is to understand the effect of oil emplacement on diagenesis in sandstone reservoir rocks with emphasis on quartz cementation and preservation of porosity at depth. To achieve these, efforts have been made to eliminate all other possible factors that can stop or influence quartz cementation such as early chlorite coats, microcrystalline quartz coats, depth of burial, facies variation and overpressure so that only similar samples at similar depths can be compared. In order to do this, core data covering oil leg, transition zone and water leg have been collected from producing oil fields. The wells selected for the project are those that were drilled at the early stages in the field so that the oil-water contacts are the true ones and not the artifact of oil production.

The specific objectives are:

To characterize the distribution of diagenetic cements in the Upper Jurassic Ula and Tambar fields sandstone reservoirs.

To determine the timing of quartz cement precipitation relative to oil emplacement in Ula and Tambar fields.

To determine whether oil emplacement has stopped/retarded diagenetic quartz cements precipitation and preserved porosity in the Ula and Tambar fields.

To determine what other diagenetic factors (chlorite or even illite coats, microquartz coats, carbonate cement, facies, and compaction) affect the reservoir quality distribution of the Ula and Tambar fields.

To compare and contrast diagenesis and reservoir quality distribution between the Ula and Tambar oil fields.

1.4 Techniques used in this project

Core sampling: to systematically select samples covering oil leg, transition zone and the water leg for statistical representation of the fields.

Thin section petrography, modal analysis: to determine qualitative and quantitative composition of the detrital and authigenic minerals within each sample and to determine relative timing of the diagenetic events.

Whole rock semi-quantitative X-ray diffraction (XRD) analysis: to quantify the mineralogical composition of the samples with emphasis on clay mineralogy.

Scanning Electron Microscopy: to further investigate composition, microstructure and precise relationship of the components of the samples that are beyond the resolution of the optical microscope and identification of some minerals based on morphology and energy dispersion.

Cathoduluminescence (CL): to highlight the amount of authigenic quartz, check for zoning in the authigenic cements and microfractures in both detrital and authigenic minerals.

Fluid inclusion thermometry and petrography: to determine temperature of precipitation of quartz cement in the samples, relative timing of oil emplacement and formation water chemistry at the time of quartz cement precipitation.

Wireline log analysis: to determine porosity and water saturation.

Carbonate stable isotope analysis: to determine possible sources of the carbonate cements and determine formation water temperature at the time of carbonate cement precipitation.

1.5 Research database

The database for this research work comprises core data sampled at different depths on which the various analytical techniques were carried out (Table 1.1), set of wireline logs, maps and supporting documents.

Table 1. 1 Database used in the project and the analytical techniques carried out.

Well	Depth (mDD)	Analytical techniques used						
		Modal analysis	Textural analysis	SEM	CL	XRD	Fluid Inclusion	Stable Isotope
7/12-A13	5020.80	•	•	•	•	•		
7/12-A13	5020.80	•	•					
7/12-A13	5021.00	•	•			•		
7/12-A13	5022.70	•	•	•	•	•		
7/12-A13	5025.80	•	•	•	•			•
7/12-A13	5027.80	•	•					
7/12-A13	5028.65	•	•	•		•		
7/12-A13	5030.00	•	•			•		
7/12-A13	5034.70	•	•					
7/12-A13	5035.00	•	•			•	•	
7/12-A13	5047.60	•	•					
7/12-A13	5051.60	•	•	•	•			
7/12-A13	5057.00	•	•			•		
7/12-A13	5060.00	•	•	•				
7/12-A13	5060.70	•	•			•	•	•
7/12-A13	5065.20	•	•			•		•
7/12-A13	5101.40	•	•					
7/12-A13	5109.30	•	•				•	
7/12-A13	5110.50	•	•			•		
7/12-A13	5111.50	•	•					
7/12-A13	5104.00	•	•	•	•	•	•	•

Well	Depth (mDD)	Analytical techniques used						
		Modal analysis	Textural analysis	SEM	CL	XRD	Fluid Inclusion	Stable Isotope
7/12-A3	3642.10	•	•	•	•	•		•
7/12-A3	3645.66	•	•					
7/12-A3	3648.70	•	•			•		
7/12-A3	3654.00	•	•					
7/12-A3	3661.00	•	•	•	•	•		
7/12-A3	3665.50	•	•					
7/12-A3	3669.00	•	•	•				
7/12-A3	3675.50	•	•			•	•	
7/12-A3	3679.20	•	•					
7/12-A3	3680.10	•	•	•			•	
7/12-A3	3686.60	•	•					
7/12-A3	3690.90	•	•	•	•	•	•	
7/12-A3	3694.80	•	•					
7/12-A3	3698.00	•	•					
7/12-A3	3703.00	•	•			•		
7/12-A3	3708.10	•	•					
7/12-A3	3711.00	•	•	•	•	•	•	
7/12-A3	3715.00	•	•					
7/12-A3	3718.02	•	•					
7/12-A3	3720.55	•	•					
7/12-A3	3722.30	•	•	•	•	•		•
7/12-A3	3725.10	•	•					

7/12-A3	3727.90	•	•	•		•	•	
7/12-A3	3729.20	•	•					
7/12-A3	3730.10	•	•	•	•	•		

Well	Depth (mDD)	Analytical techniques used						
		Modal analysis	Textural analysis	SEM	CL	XRD	Fluid Inclusion	Stable Isotope
7/12-2	3395.70	•	•		•	•		
7/12-2	3402.85	•	•					•
7/12-2	3409.00	•	•	•	•	•		
7/12-2	3414.93	•	•					•
7/12-2	3419.90	•	•					
7/12-2	3424.50	•	•			•		
7/12-2	3429.50	•	•					
7/12-2	3435.00	•	•	•	•		•	
7/12-2	3440.00	•	•					
7/12-2	3444.20	•	•	•	•	•		
7/12-2	3448.10	•	•					
7/12-2	3451.20	•	•					
7/12-2	3455.20	•	•	•		•		
7/12-2	3460.00	•	•	•			•	
7/12-2	3467.00	•	•					
7/12-2	3470.00	•	•					
7/12-2	3475.05	•	•	•		•		
7/12-2	3479.00	•	•	•	•		•	
7/12-2	3484.00	•	•					
7/12-2	3643.00	•	•	•				
7/12-2	3648.00	•	•	•	•	•	•	

Well	Depth (mDD)	Analytical techniques used						
		Modal analysis	Textural analysis	SEM	CL	XRD	Fluid Inclusion	Stable Isotope
7/12-A08	4347.50	•	•	•	•	•		
7/12-A08	4349.35	•	•				•	
7/12-A08	4351.37	•	•					
7/12-A08	4354.90	•	•	•	•	•	•	
7/12-A08	4358.35	•	•					
7/12-A08	4361.00	•	•					
7/12-A08	4364.40	•	•	•		•	•	
7/12-A08	4365.50	•	•					
7/12-A08	4366.00	•	•	•	•			
7/12-A08	4367.00	•	•					
7/12-A08	4367.70	•	•					
7/12-A08	4373.10	•	•	•	•	•	•	•
7/12-A08	4375.50	•	•	•			•	
7/12-A08	4378.42	•	•					
7/12-A08	4381.50	•	•					
7/12-A08	4383.00	•	•			•		
7/12-A08	4385.30	•	•					
7/12-A08	4386.00	•	•					
7/12-A08	4388.21	•	•	•		•		
7/12-A08	4389.30	•	•					
7/12-A08	4390.51	•	•					
7/12-A08	4393.00	•	•	•	•	•		

Well	Depth (mDD)	Analytical techniques used						
		Modal analysis	Textural analysis	SEM	CL	XRD	Fluid Inclusion	Stable Isotope
7/12-5	3844.45	•	•	•	•	•		
7/12-5	3847.20	•	•				•	
7/12-5	3850.00	•	•		•			
7/12-5	3853.50	•	•			•		
7/12-5	3857.10	•	•	•			•	
7/12-5	3861.40	•	•					
7/12-5	3865.30	•	•					
7/12-5	3863.00	•	•					
7/12-5	3872.65	•	•	•	•	•	•	
7/12-5	3876.00	•	•					
7/12-5	3877.00	•	•	•		•	•	•
7/12-5	3881.00	•	•			•		
7/12-5	3886.00	•	•					
7/12-5	3889.87	•	•					
7/12-5	3893.43	•	•					
7/12-5	3895.65	•	•	•	•	•	•	
7/12-5	3899.20	•	•					
7/12-5	3901.40	•	•	•			•	
7/12-5	3904.30	•	•	•	•	•		
7/12-5	3907.00	•	•					
7/12-5	3908.20	•	•					
7/12-5	3910.50	•	•					

7/12-5	3911.45	•	•			•		
7/12-5	3912.35	•	•					•

Well	Depth (mDD)	Analytical techniques used						
		Modal analysis	Textural analysis	SEM	CL	XRD	Fluid Inclusion	Stable Isotope
1/3-3	4131.50	•	•			•		•
1/3-3	4133.20	•	•					
1/3-3	4138.80	•	•					
1/3-3	4144.10	•	•					•
1/3-3	4147.36	•	•			•		
1/3-3	4181.67	•	•					
1/3-3	4195.42	•	•					
1/3-3	4198.30	•	•	•	•	•		
1/3-3	4202.90	•	•					
1/3-3	4210.50	•	•	•	•		•	
1/3-3	4215.00	•	•					
1/3-3	4220.77	•	•					
1/3-3	4224.10	•	•			•	•	•
1/3-3	4225.50	•	•	•				
1/3-3	4229.70	•	•	•	•	•	•	•
1/3-3	4231.50	•	•					
1/3-3	4241.70	•	•					
1/3-3	4243.81	•	•					
1/3-3	4246.5	•	•					•
1/3-3	4247.35	•	•	•	•	•		

Well	Depth (mDD)	Analytical techniques used						
		Modal analysis	Textural analysis	SEM	CL	XRD	Fluid Inclusion	Stable Isotope
2/1-10	4193.25	•	•			•		
2/1-10	4196.00	•	•					
2/1-10	4199.00	•	•					
2/1-10	4201.50	•	•					•
2/1-10	4204.80	•	•			•		
2/1-10	4210.80	•	•					
2/1-10	4216.20	•	•					
2/1-10	4220.00	•	•	•	•	•	•	
2/1-10	4222.00	•	•	•				
2/1-10	4224.40	•	•					
2/1-10	4229.15	•	•	•		•		
2/1-10	4235.00	•	•					
2/1-10	4238.15	•	•					
2/1-10	4241.20	•	•			•		
2/1-10	4245.00	•	•					
2/1-10	4247.20	•	•					
2/1-10	4250.25	•	•					
2/1-10	4256.90	•	•	•	•	•		
2/1-10	4259.80	•	•					
2/1-10	4263.00	•	•	•	•	•	•	
2/1-10	4267.00	•	•					
2/1-10	4268.00	•	•				•	

2/1-10	4270.10	•	•	•		•		
2/1-10	4272.77	•	•				•	
2/1-10	4278.00	•	•					
2/1-10	4283.00	•	•					
2/1-10	4287.00	•	•	•	•		•	

Well	Depth (mDD)	Analytical techniques used						
		Modal analysis	Textural analysis	SEM	CL	XRD	Fluid Inclusion	Stable Isotope
1/3-9ST2	4273.20	•	•			•		
1/3-9ST2	4278.00	•	•					
1/3-9ST2	4278.45	•	•	•	•	•	•	
1/3-9ST2	4281.78	•	•					
1/3-9ST2	4284.49	•	•					
1/3-9ST2	4286.60	•	•	•	•	•	•	
1/3-9ST2	4291.49	•	•					
1/3-9ST2	4294.80	•	•					
1/3-9ST2	4297.49	•	•	•		•	•	
1/3-9ST2	4301.52	•	•					
1/3-9ST2	4304.80	•	•			•		
1/3-9ST2	4308.00	•	•	•	•	•	•	
1/3-9ST2	4311.30	•	•			•		
1/3-9ST2	4313.50	•	•					
1/3-9ST2	4317.30	•	•	•			•	
1/3-9ST2	4318.78	•	•					
1/3-9ST2	4321.78	•	•					
1/3-9ST2	4323.20	•	•					
1/3-9ST2	4331.78	•	•	•	•	•	•	
1/3-9ST2	4334.78	•	•					
1/3-9ST2	4337.78	•	•					

1/3-9ST2	4340.65	•	•			•		
1/3-9ST2	4343.78	•	•			•		
1/3-9ST2	4347.78	•	•					
1/3-9ST2	4354.78	•	•			•		
1/3-9ST2	4357.78	•	•					
1/3-9ST2	4361.50	•	•	•	•	•		
1/3-9ST2	4364.50	•	•					
1/3-9ST2	4367.80	•	•					
1/3-9ST2	4370.78	•	•					
1/3-9ST2	4373.65	•	•		•	•		
1/3-9ST2	4376.78	•	•					
1/3-9ST2	4378.20	•	•	•		•		

• Techniques performed on the samples

SEM Scanning electron microscopy

CL Cathodulominces

XRD X-ray diffraction

1.6 Thesis structure

Chapter 1 gives a brief introduction of the topic and the rationale behind the project. It also gives a brief overview of the aims and objectives of the thesis and how they will be addressed.

Chapter 2 elaborates on the key concepts of the topic. It reviews the controversies over oil emplacement and quartz cementations and porosity preservation in literatures. Sources of the quartz cement in sandstones and the process through which the oil emplacement can bring about quartz cement retardation are also reviewed. Other factors reported to have stopped quartz cementation in deeply buried sandstones in some oil fields are also reviewed.

Chapter 3 presents and discusses the general diagenetic changes as it affects the reservoir rock from Ula in a paper format titled "Diagenesis and reservoir quality of the shallow marine sandstones of Ula field, offshore Norway".

Chapter 4 presents the relationship between diagenesis and oil emplacement as it relates to quartz cementation in a paper format titled "Does oil emplacement stop quartz cementation and porosity lost in deeply buried reservoirs: Evidences from Ula fields Norwegian North Sea".

Chapter 5 presents diagenesis and controls on reservoir quality in the Tambar field in a paper format titled "Is it grain coating microcrystalline quartz or the early oil charge that preserved porosity in the Tambar Field Central Graben, North Sea".

Chapter 6 is a synthesis and the general summary and conclusion for the whole work carried out and suggestions for further work.

For the chapters written in paper formats, it may involve some degree of repetition of material from one chapter to another, especially the methods sections. Key concepts related to the geological background of the study area may also contain some repetition.

1.6 References

Aase, N. E., and Walderhaug, A., 2005, The effect of hydrocarbons on quartz cementation: diagenesis in the Upper Jurassic sandstones of the Miller Field, North Sea, revisited: Petroleum Geoscience, v. 11, no. 3, p. 215-223.

Bjørkum, P. A., and Nadeau, P. H., 1998, Temperature controlled porosity/permeability reduction, fluid migration, and petroleum exploration in sedimentary basins: Australian Petroleum Production and Exploration Association Journal, v. 38, p. 453-464.

Bjørkum, P. A., Oelkers, E. H., Nadeau, P. H., Walderhaug, O., and Murphy, W. M., 1998, Porosity prediction in quartzose sandstones as a function of time, temperature, depth, stylolite frequency, and hydrocarbon saturation: American Association of Petroleum Geologists Bulletin, v. 82, no. 4, p. 637-648.

Bjørlykke, K., 1994, Pore-water flow and mass transfer of solids in solution in sedimentary basins: Natural Resources Research, v. 453, p. 189-189.

Boles, J. R., and Hickey, J. J., Inhibition of quartz cementation by the presence of hydrocarbons, Point McIntyre Field, North Slope, Alaska, *in* Proceedings Second international conference on fluid evolution, migration and interaction in sedimentary basins and orogenic belts, Belfast, Ireland, 10-14 March 1997, p. 272-274.

Cox, P. A., Wood, R. A., Dickson, J. A. D., Al Rougha, H. B., Shebl, H., and Corbett, P. W. M., 2010, Dynamics of cementation in response to oil charge: Evidence from a Cretaceous carbonate field, UAE: Sedimentary Geology, v. 228, no. 3-4, p. 246-254.

Dixon, S. A., Summers, D. M., and Surdam, R. C., 1989, Diagenesis and preservation of porosity in Norphlet Formation (Upper Jurassic), southern Alabama: Americam Association of Petroleum Geologists Bulletin, v. 73, no. 6, p. 707-728.

Ehrenberg, S. N., 1990, Relationship between diagenesis and reservoir quality in sandstones of the Garn Formation, Haltenbanken, mid-Norwegian continental shelf: American Association of Petroleum Geologists Bulletin, v. 74, no. 10, p. 1538-1558.

-, 1993, Preservation of anomalously high porosity in deeply buried sandstones by grain-coating chlorite: examples from the Norwegian continental shelf: American Association of Petroleum Geologists Bulletin, v. 77, p. 1260-1260.

Emery, D., Smalley, P. C., Oxtoby, N. H., Ragnarsdottir, K. V., Aagaard, P., Halliday, A., Coleman, M. L., and Petrovich, R., 1993, Synchronous oil migration and cementation in sandstone reservoirs demonstrated by quantitative description of diagenesis [and discussion]: Philosophical Transactions of the Royal Society of London. Series A: Physical and Engineering Sciences, v. 344, no. 1670, p. 115-125.

Giles, M. R., Stevenson, S., Martin, S. V., Cannon, S. J. C., Hamilton, P. J., Marshall, J. D., and Samways, G. M., 1992, The reservoir properties and diagenesis of the Brent Group: a regional perspective, *in* Morton, A. C., Haszeldine, R. S., Giles, M. R., and Brown, S., eds., Geology of the Brent Group, Geological Society, London, Special Publications, v. 61, p. 329-350.

Gluyas, J. G., Robinson, A. G., Emery, D., Grant, S. M., and Oxtoby, N. H., 1993, The link between petroleum emplacement and sandstone cementation, *in* Parker, J., ed., Petroleum Geology of the North west Europe, Geological Society of London, v. 4, p. 1395-1402.

Hawkins, P. J., 1978, Relationship between diagenesis, porosity reduction, and oil emplacement in late Carboniferous sandstone reservoirs, Bothamsall Oilfield, E Midlands: Journal of the Geological Society, v. 135, no. 1, p. 7-24.

Kupecz, J. A., Gluyas, J., and Bloch, S., 1997, Reservoir quality prediction in sandstones and carbonates: An overview, *in* Kupecz, J. A., Gluyas, J., and Bloch, S., eds., Reservoir quality prediction in sandstones and carbonates, American Association of Petroleum Geologist Memoir 69.

Marchand, A. M. E., Haszeldine, R. S., Macaulay, C. I., Swennen, R., and Fallick, A. E., 2000, Quartz cementation inhibited by crestal oil charge: Miller deep water sandstone, UK North Sea: Clay Minerals, v. 35, no. 1, p. 201-210.

Marchand, A. M. E., Smalley, P. C., Haszeldine, R. S., and Fallick, A. E., 2002, Note on the importance of hydrocarbon fill for reservoir quality prediction in sandstones: American Association of Petroleum Geologists Bulletin, v. 86, no. 9, p. 1561-1571.

Molenaar, N., Cyziene, J., Sliaupa, S., and Craven, J., 2008, Lack of inhibiting effect of oil emplacement on quartz cementation: Evidence from Cambrian reservoir sandstones, Paleozoic Baltic Basin: Geological Society of America Bulletin, v. 120, no. 9-10, p. 1280-1295.

Ramm, M., 1992, Porosity depth trends in reservoir sandstones - theoretical models related to Jurassic sandstones offshore Norway: Marine and Petroleum Geology, v. 9, no. 5, p. 553-567.

Ramm, M., and Bjorlykke, K., 1994, Porosity depth trends in reservoir sandstones - assessing the quantitative effects of varying pore-pressure, temperature history and mineralogy, Norwegian shelf data: Clay Minerals, v. 29, no. 4, p. 475-490.

Saigal, G. C., Bjorlykke, K., and Larter, S., 1992, The effects of oil emplacement on diagenetic processes - examples from the Fulmar Reservoir sandstones, central North Sea: American Association of Petroleum Geologists Bulletin, v. 76, no. 7, p. 1024-1033.

Sneider, R. M., 1990, Introduction: Reservoir description of sandstones, *in* Barwis, J. H., McPherson, J. G., and Studlick, J. R. J., eds., Sandstone petroleum reservoirs: New York, Springer-Verlag, p. 1-3.

Taylor, T. R., Giles, M. R., Hathon, L. A., Diggs, T. N., Braunsdorf, N. R., Birbiglia, G. V., Kittridge, M. G., Macaulay, C. I., and Espejo, I. S., 2010, Sandstone diagenesis and reservoir quality prediction: Models, myths, and reality: American Association of Petroleum Geologists Bulletin, v. 94, no. 8, p. 1093-1132.

Wilkinson, M., and Haszeldine, R. S., 2011, Oil charge preserves exceptional porosity in deeply buried, overpressured, sandstones: Central North Sea, UK: Journal of the Geological Society, v. 168, no. 6, p. 1285-1295.

Wilkinson, M., Haszeldine, R. S., and Fallick, A. E., 2006, Hydrocarbon filling and leakage history of a deep geopressured sandstone, Fulmar Formation, United Kingdom: American Association of Petroleum Geologists Bulletin, v. 90, no. 12, p. 1945-1961.

Worden, R. H., and Barclay, S. A., 2003, The effect of oil emplacement on diagenetic clay mineralogy: the Upper Jurassic Magnus Sandstone Member, North Sea, *in* Worden, R. H., and Morad, S., eds., Clay mineral cements in sandstones, Volume 34, International Association of Sedimentologists Special Publication, p. 453-469.

CHAPTER 2

2. Sandstone diagenesis and the effect of oil emplacement on quartz cementation

2.1 Introduction

Diagenesis comprises a broad spectrum of physical, chemical and biological post-depositional processes by which original sedimentary assemblages and their interstitial pore waters react in an attempt to reach textural and geochemical equilibrium with their environment (Curtis et al., 1977). Diagenesis commences from the deposition of the sediment and continues to the onset of metamorphism (Figure 2.1). It involves the lithification, compaction and cementation of deposited sediments facilitated by alterations in pore water chemistry, temperature, pressure during burial and exhumation cycle of the basin history. Compaction causes a decrease in volume, largely by squeezing out water and reducing the volume of ductile grains; cementation introduces chemical precipitates of new authigenic minerals (quartz, calcite, hematite, clays etc.), and lithification converts sediments from loose into a cohesive rock.

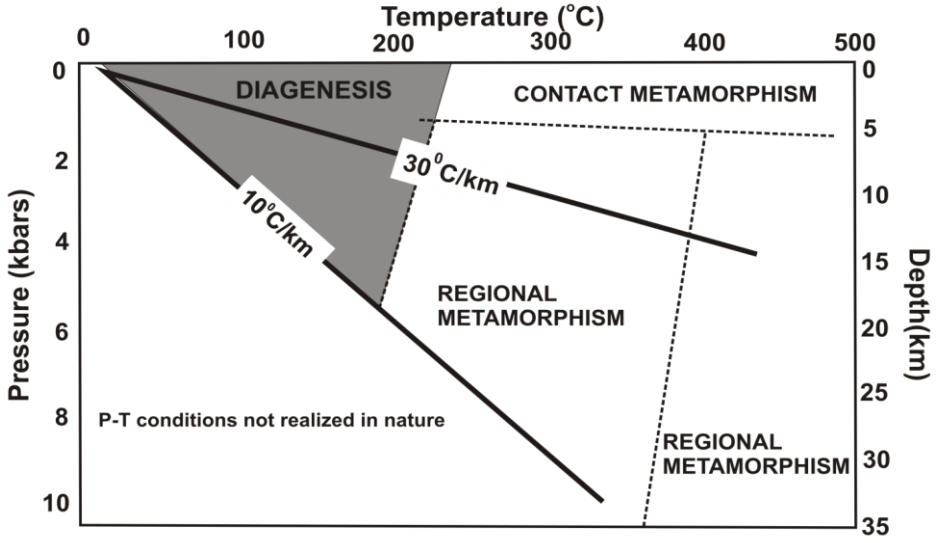

Figure 2. 1 Pressure – temperature diagram showing relationship between diagenesis and metamorphism. 10 ^{o}C km^{-1} and 30 ^{o}C km^{-1} crustal geotherms are for typical stable cratons and rifted sedimentary basins respectably, after Worden and Burley (2003).

2.2 Process of quartz cementation

The nature and rate of silica cement formation is dictated by dissolution of silica from a source, the mechanism by which the silica is transported from source to the point of precipitation and the precipitation mechanism. The slowest of any of these three processes can be rate-limiting to quartz cement precipitation (Worden and Morad, 2000). Several variables, including pH, temperature, pressure, and site locations, play integral roles in determining which of the three processes (dissolution, transportation, and precipitation) is rate-limiting for a particular setting. Each of these processes will be discussed in detail.

2.3 Sources of quartz cement in sandstones

Numerous studies have been performed to analyse silica cementation in sandstones. Despite these efforts the sources of silica cement remains unresolved. Some investigations have suggested that huge volumes of water, released through compaction could provide the silica precipitated as quartz cement in sandstones (Baccar and Fritz, 1993; Land and Dutton, 1979; McBride, 1989; Robinson and Gluyas, 1992b; Siever, 1959). Chemical mass balance calculations and fluid flow modelling, however, indicate that significant transport of silica by advection from thick sandstones would require orders of magnitude higher pore water fluxes than are likely in compactional regimes of sedimentary basins (Bjørlykke, 1983; Bjørlykke and Egeberg, 1993; de Caritat, 1989). As a result it is likely that bulk of the silica originates within the sandstone body. However, many models attempting to explain quartz cementation still conclude that external sources of silica are needed to explain the observed quantity of quartz cement e.g. (Gluyas and Coleman, 1992). A detailed account of likely sources of silica for quartz cement in sandstones (Figure 2.2) was given by Worden and Morad (2000) as:

1. Illitization and chloritization of smectite,
2. Detrital feldspar-related sources,
3. Pressure dissolution and stylolites within sandstones,
4. Dissolution of amorphous silica,
5. Biogenic source, and
6. External source.

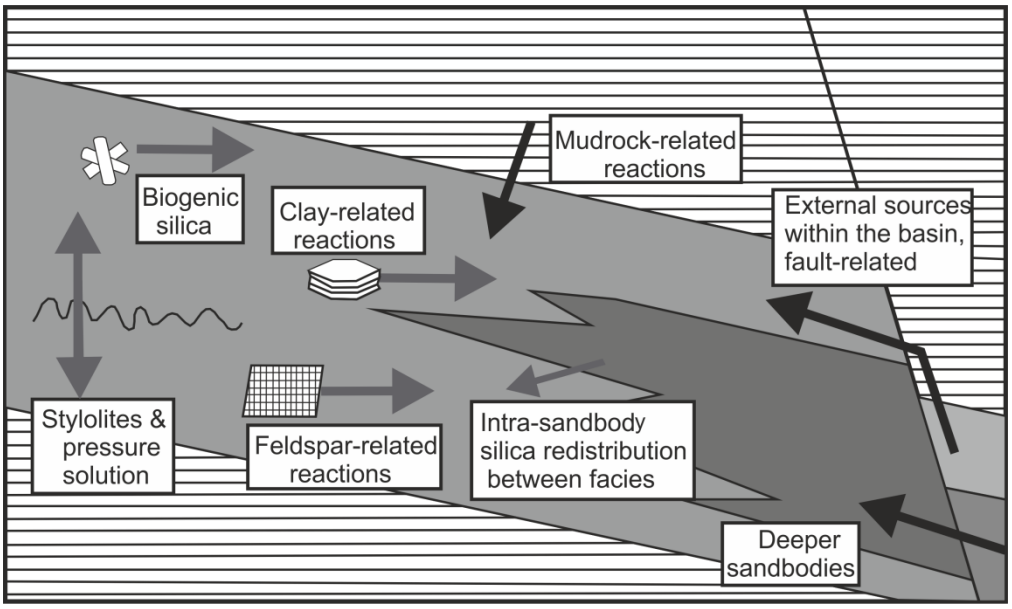

Figure 2. 2 Schematic diagram showing sources of quartz cement (Worden and Morad, 2000). Grey arrows are internally derived sources while black arrows are externally derived sources.

2.3.1 Illitization and chloritization of smectite

The smectite to illite transformation as a source of silica for quartz cement has been studied by many geologist (Boles and Franks, 1979; Curtis et al., 1985; Drief and Nieto, 2000; Huang et al., 1993; Leder and Park, 1986; Towe, 1962; van de Kamp, 2008). Smectite varies greatly in chemical composition but has relatively high Si/Al ratio and thus it is a potential source of silica for quartz cementation (Boles and Franks, 1979). It is commonly found at shallow depth as mud intraclast, infiltrated clays, and as neighbouring mudstones (Worden and Morad, 2003). A model reaction for the illitization of smectite into illite was described by Abercrombie et al., (1994).

$$KAlSi_3O_8 + 2K_{0.3}Al_{1.9}Si_4O_{10}(OH)_2 = 2K_{0.8}Al_{2.4}Si_{3.5}O_{10}(OH)_2 + 4SiO_2 \quad \text{eq1}$$

K-feldspar K-smectite illite quartz

The decrease in smectite and increase in illite and chlorite with depth (Figure 3) are documented in many sedimentary basins (Hoffman and Hower, 1979; Lynch et al.,

1997; Perry and Hower, 1970; Weaver, 1956, 1958). It is suggested that iron-magnesium-rich smectite layers react more slowly and that conversion of these layers to illite at higher temperatures releases iron and magnesium. The implications of this diagenetic model are that silica is released over temperatures of 60-210°C potentially forming quartz overgrowths in sandstones (Boles and Franks, 1979).

Experimental investigation of laboratory-induced smectite-illite transformation have shown it is, in fact, accompanied by the precipitation of quartz (Small et al., 1992) and results from previous studies on mudstones have also indicated that some of the Si released from smectite-illite reaction is precipitated as authigenic quartz (Eberl and Hower, 1977; Hower et al., 1976; Thyberg and Jahren, 2011; Yeh and Savin, 1977). The transformation of smectite to ~95% illite occurs within the temperature range of 20^{o} – 200^{o}C (Merriman and Frey, 1999).

Chloritization of smectite which occurs in sediment rich in detrital iron silicate, iron oxides and iron-titanium oxides may cause the release of silica to pore water in similar way as illitization of smectite described above. The original composition of smectite may have an influence on whether it transforms into illite or chlorite. Mg-Fe-rich smectite tend to be chloritized (Chang et al., 1986), whereas K-, Ca- and Na-rich smectite tend to be illitized.

The post-depositional transformation of montmorillonite and/or mixed-layer illite-montmorillonite to illite has been suggested as a source of silica cement in some sedimentary rocks (Uuoa, 1991). Using petrographic and computational investigation he stated that much of the silica cement found in the Jurassic quartzose sandstones of the North Sea is as a result of the dissolution of quartz at mica/illitic clay interface due to chemically catalysed processes and that a major factor controlling the distribution of cement is the time/temperature history of a given sandstone unit.

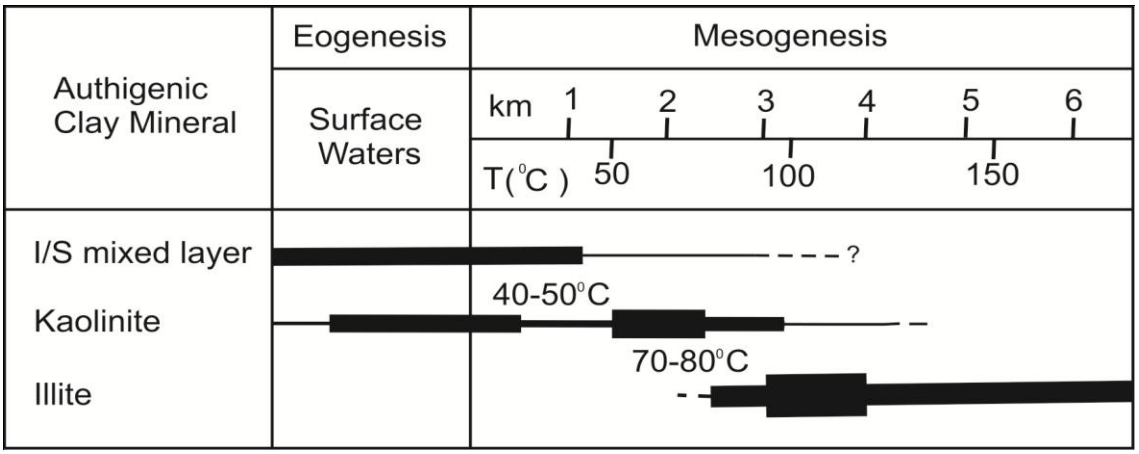

Figure 2. 3 Diagram showing diagenetic sequence of clay minerals. The thickness of each line approximates the abundance of each mineral over a particular burial/temperature range after (Burley and Macquaker, 1992).

2.3.2 Detrital feldspar related source

Feldspars are the second most common group of minerals in most sandstones and they are mainly derived from igneous and metamorphic rocks formed under relatively high temperature and pressure compared to depositional and diagenetic environments. The main reason why feldspars are a source of silica is that they have higher Si/Al ratios than the clays they produce. Alkali feldspars (K-Na series) have an Si/Al ratio of three compared to illite and kaolinite which have Si/Al ratios of ~1(Worden and Morad, 2000).

A decrease in detrital feldspar volume with increase in depth of burial, after a threshold depth (temperature), has been documented in many sedimentary basins e.g. (Berger et al., 1999; Giles et al., 1992; Glasmann, 1992; Hower et al., 1976; Wilkinson and Haszledine, 1996; Wilkinson et al., 2001). The type of clay mineral that is produced as a result of feldspar alteration is controlled by the chemistry of the formation water and temperature.

Although silica is released from feldspar leaching during meteoric water flushing, very little quartz is likely to precipitate during the flushing due to low temperatures and continued removal of the released silica. Therefore, dissolution of feldspars by

meteoric water at a shallow burial depth close to the surface is not likely to be the source of silica that precipitates quartz cements in sandstones during burial diagenesis. This type of early diagenesis may be referred to as subsurface weathering and results in the precipitation of kaolinite (Bjørlykke, 1998):

$$\underset{\text{Feldspar}}{2K(Na)AlSi_3O_8} + 2H^+ + 9H_2O = \underset{\text{kaolinite}}{Al_2SiO_5(OH)_4} + 2H_4SiO_4 + 2K(Na^+) \quad \text{eq2}$$

Worden and Morad (2000) stated that this type of reaction also occurs during burial diagenesis but can results in growth of illite or kaolinite at higher temperature depending on the compostion (K/H ratio) of the formation water:

$$\underset{\text{K-feldspar}}{3KAlSi_3O_8} + 2H^+ = \underset{\text{illite}}{KA_{l3}Si_3O_{10}(OH)_2} + \underset{\text{quartz}}{6SiO_2} + 2K^+ \quad \text{eq3}$$

$$\underset{\text{K-feldspar}}{2KAlSi_3O_8} + 2H^+ + H_2O = \underset{\text{kaolinite}}{Al_2Si_2O_5(OH)_4} + \underset{\text{quartz}}{4SiO_2} + 2K+ \quad \text{eq4}$$

As the temperature increases to about 125^{o}C the remaining K-feldspars and diagenetic kaolinite can react to produce illite and quartz as shown below:

$$\underset{\text{K-feldspar}}{KASi_3O_8} + \underset{\text{kaolinite}}{Al_2SiO_5(OH)_4} = \underset{\text{illite}}{KAl_3Si_3O_{10}(OH)_2} + \underset{\text{quartz}}{2SiO_2} + H_2O \quad \text{eq5}$$

The source of quartz for the first phase of cementation in the Jurassic sandstones of offshore Norway is feldspar dissolution by fresh meteoric water which produced kaolinite and silica. A second phase of feldspar alteration duing burial diagenesis can result in either kaolinite or illite as a function of water composition, while a final phase can result from the reaction of feldspar with early diagenetic kaolinite.

2.3.3 Pressure solution and stylolites within sandstones

Pressure solution refers to dissolution of quartz at a point of grain contacts as a result of stress, generally caused by effective load. Pressure solution can act as a source of

cement (Renton et al., 1969; Tada and Siever, 1989) and it is an important mechanism of intergranular compaction. Stylolites are localised dissolution surfaces locally found in sandstones and carbonate rocks which can account for dissolution of more than 50% of the original rock volume (Alvarez et al., 1978; Stockdale, 1922).

Stylolites have never been produced experimentally in the laboratory (except on the sub-grain scale (Gratier et al., 2005), and the mechanism of their formation is not well understood. The formation of stylolites is not limited to quartz grains but can occur between quartz grain and calcite, or between feldspar grain and mica (Heald, 1955). It has long been recognized that pressure solution of quartz is enhanced at grain contact surfaces in contact with potassium-rich phyllosilicates (Heald, 1955). The driving mechanism for pressure solution in a chemically closed system is the enhanced solubility at the grain contacts due to differences in concentration of the effective stress along the grain-grain interface (Lehner, 1995; Rutter, 1983). This leads to the development of gradients in chemical potential along grain contacts with the maximum chemical potential localized at centre of the grain contacts to minimal chemical potential values at the pore walls (Sheldon et al., 2003). Among the various silica sources, quartz pressure solution and stylolitezation have received particular attention (Oelkers et al., 1996).

Experimental investigations of quartz pressure solution indicate that, under certain conditions, substantial quartz dissolution can occur at quartz/quartz interfaces (De Boer, 1977; Maxwell, 1960; Sathar et al., 2012). The relevance of these experiments to natural systems have been questioned (Tada and Siever, 1989), because they have been carried out at substantially greater stresses and temperatures than typically found in sedimentary basins. Variations in factors such as stress, temperature, grain size, sorting, chemistry of the pore fluid, and the nature of the grain contacts have a strong effect on the rate of pressure solution (Oelkers et al., 1996; Sheldon et al., 2003, 2004). It has been noticed (Oelkers et al., 1996) that the distribution of silica cement in some sedimentary basins is a function of distance from the nearest stylolite which indicates that much of the cement originates from stylolites. Stylolites can be a significant cement source (Wong and Oldershaw, 1981). Thus if stylolitisation is inhibited by petroleum emplacement then so might be cementation.

2.3.4 Biogenic and amorphous silica sources

Biogenic silica is derived from siliceous tests and skeletal elements of organisms. Siliceous opaline fossils have existed since the Cambrian. Dissolution and reprecipitation of this silica into quartz takes place at low temperatures and shallow depths and produces mainly microcrystalline grain coating quartz. In the Jurassic sandstones of the Moray Firth, quartz overgrowths are only common in sandstone which contains a few sponge spicules and quartz cement distribution is largely a result of sedimentary processes which concentrated sponge spicules in the finest-grained intervals of the sand body (Vagle et al., 1994).

Amorphous silica and opal CT may be important internal sources of quartz cement at burial depths of 1.5-2.0 km (70-80°C) (Bjørlykke and Egeberg, 1993). Giles et al. (2000) mentioned all the sources above as likely sources for large scale quartz cementation.

2.3.5 Ttransport of silica from an external source

Pore-water flow by convection has been put forward by several authors as a mechanism to move solutes in the subsurface (Davis et al., 1985; Haszeldine et al., 1984; Wood and Hewett, 1982). There have been many publications in which an external sources of silica flux has been proposed (Curtis, 1978; Dutton and Diggs, 1990; Gluyas and Coleman, 1992; Haszeldine et al., 1984; Lahann, 1980; Nedkvitne et al., 1993; Wood and Boles, 1991; Worden et al., 1998). Haszeldine (1984) used quartz cementation within highly permeable sandstone as evidence to support the importance of fluid flow in quartz cementation. The correlation of quartz cement with other late diagenetic phases that appear to require advective transport potentially supports this (Gluyas and Leonard, 1995). It has been suggested by Gluyas and Coleman (1992) that silica seem to have been added to porous sandstones relative to the now non-porous and impermeable early carbonate-cemented nodules suggesting the import of silica. Possible external sources of quartz cement were proposed to include clay transformation reactions in adjacent mudstones (Burley and Flisch, 1989; Gluyas and Leonard, 1995; Haszeldine et al., 1984; Land and Dutton, 1979; Towe, 1962), mixing of meteoric and basinal fluids within the reservoir (Graham et al., 1996), burial metamorphism of shales (Land et al., 1987), and illite to muscovite

transformation (Totten and Blatt, 1996). A combination of internal and external sources of diagenetic silica cement has also been proposed (Dutton and Diggs, 1990; Stone and Siever, 1996; Wood and Boles, 1991). Whether sandstone becomes an exporter or importer of silica probably depends on the local degree of silica saturation (Worden and Morad, 2000). For example volcanic lithic fragments in sandstones are chemically unstable and tend to alter into smectite and chloritic clay minerals, zeolites, calcite, and releasing silica (opal-cristobalite-tridymite, microcrystalline quartz, or chalcedony) during diagenesis (De Ros et al., 1997; Pirrie et al., 1994) and could lead to export of silica from a sandstone.

2.4 Transport mechanism for quartz cementation

Worden et al., (1998) proposed two end member mechanisms for the transport of silica cement into a reservoir: (1) covection/advection of fluids, and (2) diffusion of fluids. The majority of those who favoured internal sources (Aplin and Warren, 1994; Bjørlykke and Egeberg, 1993; Nedkvitne et al., 1993; Walderhaug, 1990) favour transport by diffusion and workers who favour external sources for silica cement (Burley et al., 1989; Glasmann et al., 1989; Glasmann, 1992; Gluyas and Coleman, 1992; Haszeldine et al., 1984; Land and Dutton, 1979; Leder and Park, 1986) seem to favour transport by convection/advection.

The maximum range of diffusional transport is restricted to a sand-body scale of tens of meters which may only be enough if the source of diagenetic cement is derived internally (Berner, 1980). Convectional/advectional transport can be active for distance over hundreds of kilometres in favourable intra-cratonic basins. This can transport cement materials from an external source to a petroleum reservoir (Bethke and Marshak, 1990). If petroleum is emplaced in a reservoir transport of dissolved silica from source to point of precipitation will be hampered. If silica supply is sourced internally and the mode of transport is diffusive, oil emplacement increase tortuosity of the residual water in the reservoir. Worden et al. (2008) stated that rate of diffusion in reservoir filled with oil will be two or more orders of magnitude slower than underlying aquifer. If the silica is sourced externally and the mode of transport is advective, the presence of oil in the reservoir decreases the effective permeability reducing supply of silica saturated fluid into the reservoir. Worden et

al. (1998) demonstrated that the ratio of the rates of diffusion is a function of water saturation and saturation exponent (n):

$$J_t/J_o=S^n_w$$

where J_t is the diffusive flux within the irreducible water in the oil leg and J_o is the diffusive flux in the water leg and n is the saturation exponent. Sodena et al. (1989) showed that a saturation exponent tends to increase as oil saturation increases. This means that the rate of diffusion will be slowed with increase in oil saturation (Figure 2.5)

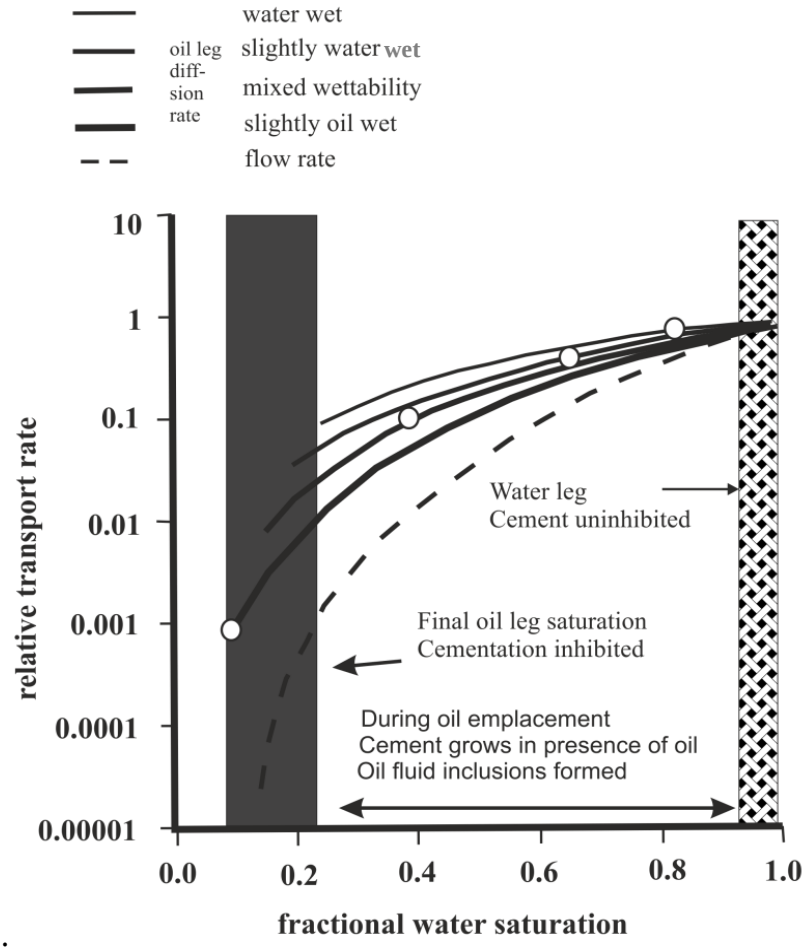

Figure 2. 4 showing how oil emplacement retards diffusion and flow in sandstones (Worden et al., 1998).

2.5 Quartz cement precipitation

Quartz cement precipitation takes place when the following conditions are fulfilled. The aqueous fluid is supersaturated with silica, the silica solutions have access to clean grain surfaces, and threshold temperature (about 70^{o}C) for quartz cementation is attained. When oil is emplaced in a reservoir, dissolved silica solution may not reach the surface of the grains for precipitation to take place depending on grain wettability and degree of oil saturation, even if all other factors are favourable. If the sandstone is water wet, the potential rate of quartz cement precipitation will not be significantly affected as the irreducible water saturation around the grain will make a favourable surface for precipitation of cement. If the reservoir is oil wet, the silica solution may not reach the grain surface and therefore, the presence of oil will affect the rate of quartz cement precipitation.

2.6 Factors affecting quartz cement precipitation

2.6.1 Temperature

Temperature affects both the equilibrium thermodynamics and kinetics of geochemical process that cause cementation in sandstones. Thermodynamics is the measure of change in energy of a system during chemical reactions relative to the equilibrium position.

Temperature is commonly accepted as one of the main controls on quartz cementations in sandstone reservoirs. Based on fluid inclusion thermometry and burial history curve, quartz cementations mostly begins at temperatures of about 90-130°C (Giles, 1997; Gluyas et al., 1993a). The rate at which quartz cement precipitates increases exponentially with temperature, rising by a factor of approximately 5% between 70 and 100°C and another factor of 5 between 100 - 135°C. Detailed petrographic analysis of core material from wells from the Tahiti field (Gulf of Mexico) indicates that the presence of minor amount of quartz cement (1-2%) in clean sands with porosities that range between 21 and 24% at sub-salt depths of more than 7000m, in contrast to sandstones of equivalent age and comparable composition from Poseidon field where temperatures are more than 40°C

hotter at roughly the same depth, having substantially more quartz cement (2-7%) and porosities of only 12-17% (Taylor et al., 2010).

Increases in temperature and pressure during diagenesis also accelerate reaction kinetics by increasing solubility of quartz and amorphous silica providing a greater amount of soluble silica available for quartz cementation (Dove and Rimstidt, 1994).

Fluid inclusion homogenization temperatures that are close to present day in-situ temperature have been used as a proof of on-going quartz cementation. Worden and Morad (2000) concluded that the temperature at which quartz cementation begins coincides with the onset of several important temperature-dependant silica releasing diagenetic processes (intergranular pressure dissolution of detrital quartz, stylolite formation in siltstones and sandstones, dissolution, albitization and alteration into clay minerals of detrital feldspars, and illitization of kaolinite and smectite) which are considered to be the main sources of silica for quartz cementation (Worden and Morad, 2000). It should be noted that illite growth has been proposed for almost the entire range of diagenetic temperatures (e.g. 15 -20°C, Brent Group; 35 – 40°C, Oxfordian Sand, Inner Moray Firth; 50 – 90°C, Brae Formation; 100 – 110°C, Brent Group; 130 - 140°C, Haltenbanken (Wilkinson et al., 2006). In the southern Viking Graben, low-porosity sandstones are found where the exposure to high temperatures over time was above the regional average (Maast et al., 2011). Walderhaug (1990) using fluid inclusion homogenization temperature to characterize the minimum temperature for quartz cementation stated that quartz cementation commences at 70 - 80^{o}C. The temperature range of quartz cementation deduced from fluid-inclusion thermometry depends on the subsidence history of the basin, and hence the residence time of the sequence within a certain temperature interval. In slowly subsiding, cratonic basins, considerable quartz cementation may occur during long residence times (tens of millions of years) at relatively low temperatures (< 100°C) (Morad et al., 1994). However, quartz cement precipitations at lower temperature of 40 - 60°C have been reported (Grant and Oxtoby, 1992; Haszeldine et al., 1984; Nedkvitne et al., 1993).

2.6.2 Reservoir heterogeneity

Significant reservoir heterogeneity arises from heterogeneity in the primary detrital properties of the sediment, change in sediment supply during deposition, change in water chemistry, sediment residence time under particular physico-chemical condition, or fluctuation in depositional current energy level. The presences of barriers to solute transport in a reservoir have effect on quartz cementations.

Convectional transport which brings silica solution into a reservoir could occur on an intrabasinal scale (Barclay and Worden, 1998). But, due to presence of barriers (carbonate-cemented intervals and shales/mudstones), the conditions for Rayleigh convection are rarely met in sandstones (Bjørlykke et al., 1988). The type of convective flow occurring in a system is defined by Raleigh numbers. The Raleigh number is a numerical description of the stability of a convection-driven fluid flow system (Wood and Hewett, 1982).

The effect of barriers on diffusive transport of solutes can be shown using Fick's first law (Murphy et al., 1989):

$$J = -Ø\phi D\rho.(\delta m/\delta x)$$

Where J = rate of diffusional transport, Ø = porosity, D = diffusion coefficient, ρ = density, δm/δx = change in molality (m) of diffusion species over distance (x), i.e. concentration gradient. From the above equation diffusional flux is proportional to porosity.

Internal sources of diagenetic silica will also vary in distribution. It has been shown that distribution of quartz cement precipitation is inversely proportional to the distance between stylolites (Oelkers et al., 1996), and that there is more quartz cement closer to stylolite than away from stylolite (Walderhaug and Bjorkum, 2003).

2.6.3 Water saturation and wettability

The diagenetic process of dissolution, transportation and precipitation in a reservoir take place in the presence of aqueous fluid solution (Worden et al., 1998). Before any oil enters the reservoir, the pore space is filled with formation water. As oil is

introduced into the reservoir, the formation water is replaced gradually and a gradational boundary known as transition zone or oil-water contact is formed between the oil dominated interval and the water dominated interval (Archer and Wall, 1986). The measure of the amount of water and oil in the reservoir is given by water saturation (S_w).

The water in the reservoir is never completely replaced. Even as the reservoir is charged with oil, some of the initial formation water is left behind referred to as irreducible water saturation (S_{wi}). An S_w value equals to 1 means that the reservoir contains no oil and S_w value of 0 means the reservoir contains no water. If the S_w = 1, it means there is water readily available for all diagenetic activities in the reservoir and no control from oil charge. If S_w <1, then oil has entered the reservoir and diagenetic activity will depend on a number of factors which include amount of water saturation and wettability of the grains. Under this circumstance there are number of possible scenarios: (1) There is high water saturation and the grains are water wet thereby allowing all dissolution, transportation and precipitation to continue unhindered. (2) Low water saturation but the grains are water wet allowing water to remain on the grain surface giving room for dissolution and clean grain surface for precipitation, though transport of dissolve material will be hindered severely (3) Grains are oil wet and water cannot reach the grain surface for dissolution and precipitation regardless of level of water saturation even though transportation may go on unhindered. In sandstones, if the source of the silica is external, low S*w* affects the source and transportation (relative permeability of two phase solutes) even if the grains are water wet thereby reducing chance of cement precipitation.

Oil emplacement has been reported to have stopped the precipitation of quartz cements in some sandstone reservoirs (Emery et al., 1993; Kantorowicz, 1985) and carbonate (Feazel and Schatzinger, 1985; Heasley et al., 2000; Murphy et al., 1989; Neilson et al., 1998). At a water saturation of 0.3, for a reservoir within an irreducible water saturation of 0.2, the relative permeability of water is more than four orders of magnitude lower in the oil zone than in the water leg (Worden and Barclay, 2003).

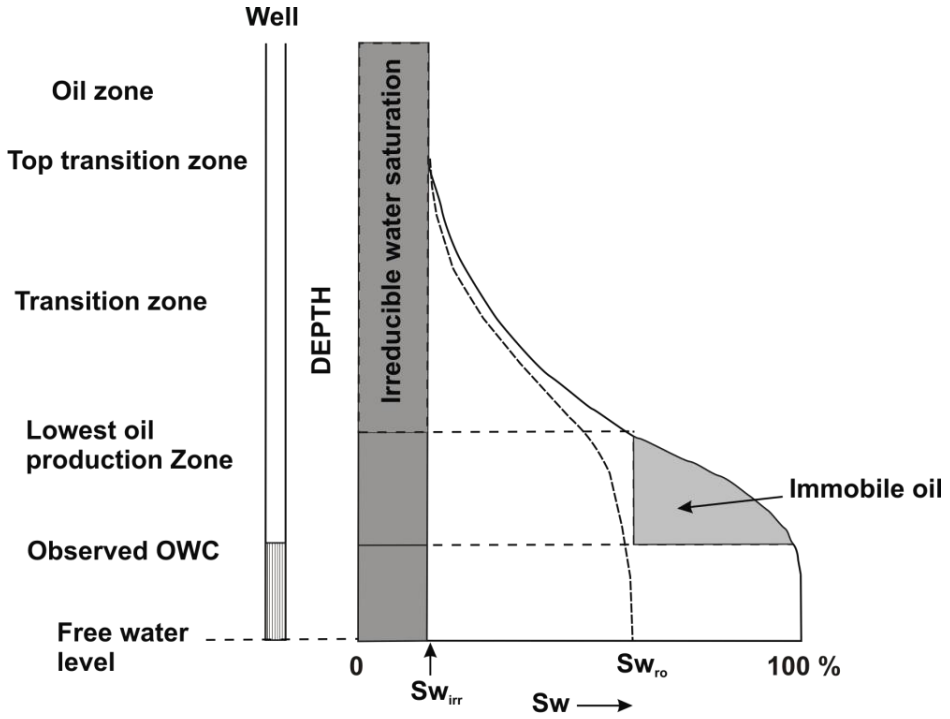

Figure 2. 5 Schematic illustrations of different zones within an oil-water transition zone and variation in static water saturation in homogeneous reservoir (after Archer and Wall, 1986).

Wettability of the mineral grains in a rock is influenced by mineralogy, water chemistry and oil chemistry. Barclay and Worden (2000) provided an explicit account of these factors. Quartz, single crystals of unweathered feldspar, illite and single crystals of kaolinite are all water wet. Carbonates, Fe-clays and oxides and kaolinite booklets are all oil wet. Oil containing significant amount of resin compounds or asphaltine will tend to make reservoirs to become oil wet. A low pH, high salinity, oxidising and transition metals rich pore water are more likely to produce oil wet reservoir compared to a high pH, low salinity, and reducing and transition metal-poor pore water. The most oil wet scenario is the reservoirs containing low maturity and biodegraded oils, clay, haematite and carbonate rich sandstones.

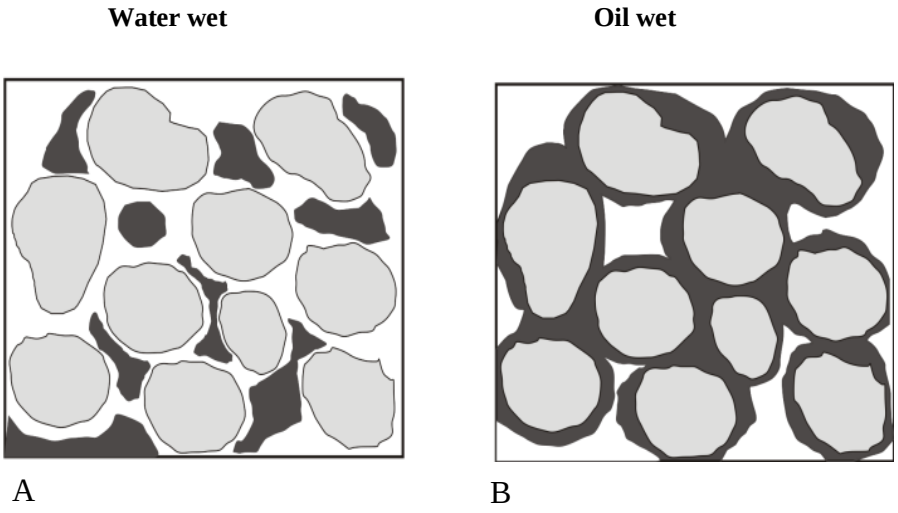

Figure 2. 6 Schematic diagram showing sandstone grains with varying wettability (A) water wet (B) oil wet.

Residual oil saturation depends on the rock/fluid wetting characteristic, whereas it markedly increase by alternating the reservoir wettability from oil wet to water wet (Al-Garni and Al-Anazi, 2008).

2.6.4 Sandstone composition

The mineralogical composition of sandstone has great impact on quartz cementation because it can affect the diagenetic reactions that take place. The surface area available for quartz nucleation, abundance of precursor minerals altered to release silica solution and detrital framework stability of sandstone depends on mineralogical composition. In experimental studies of quartz cementation (Heald and Renton, 1966) showed that quartz cementation takes place more rapidly in pure quartz sandstone than arkoses. The difference in porosity between the quartz arenite and the feldspathic sandstone never exceeds 4%. Sandstones rich in rock fragments contain less quartz cement than detrital quartz rich sandstones (Rezaee and Lemon, 1996). Sandstones rich in ductile materials have a high potential of minimising quartz cementation by the material filling in pore space during diagenesis and making pseudo-matrix that will cover detrital grains (Worden et al 1997). Sandstones rich in monocrystalline quartz grain will be more rapidly cemented than sandstones rich in polycrystalline grains, and cherts (James et al., 1986; Lander et al.,

2008; McBride, 1989; Worden and Morad, 2000). The view of (Heald and Renton, 1966) is that the slower cementation rate in polycrystalline quartz is because the overgrowths that form on the smaller domain reach euhedral termination more rapidly, while Worden and Morad (2000) stated that the slow rate of cementation is due to mutual interference of overgrowth crystals that have nucleated on neighbouring domains with different crystallographic orientations.

A published quartz cementation model (Lander et al., 2008) (Figure 2.7) comes to similar conclusions to that of Heald and Renton (1966), that the dominant cause of reduced cementation on polycrystalline quartz and chert compared to monocrystalline quartz grains is the more rapid development of euhedral terminations on smaller nucleation substrate. The growth-competition also acts to decrease net growth rates; however it is much smaller than the domain size effect. Sandstones that have a high percentage of carbonate precursor minerals will result in early carbonate cement precipitation leaving no space for quartz cementation. Microcrystalline quartz and clay coating around detrital grains can prevent quartz cement growth by preventing silica nucleating on the grain surface. Details are given in sub-sections 2.7.1 and 2.7.2.

2.6.5 Sandstone texture

Primary rock texture has an important control on diagenesis. As diagenetic minerals require space to grow during diagenesis, this space is provided by the pore spaces in between detrital grains. Quartz precipitation occurs in greater volume in coarse-grained sandstones compared to fine-grained sandstones as a result of the greater porosity and permeability in the coarse-grained sandstone (Leder and Park, 1986). Increasing the tortuosity of a system reduces the transport rate of a solute around the pore network of a reservoir (Worden et al., 1998), therefore the rate of transport of cementing species around a reservoir could be retarded in fine-grained sandstone compared to coarse-grained sandstones, resulting in smaller volume of diagenetic cement in finer-grained sandstone when compared with coarse-grained sandstone.

Clastic petrologists have recognized that quartz cementation rates are significantly slower for overgrowths that nucleate on chert and polycrystalline quartz grains

compared to monocrystalline quartz grains within the same sample e.g., (James et al., 1986; McBride, 1989). Chert grains, in particular, have little associated quartz cement even in reservoirs that have had high thermal exposures over considerable geologic time. Consequently, chert-rich sandstones may have significantly better reservoir quality than otherwise similar intervals with greater proportions of monocrystalline quartz grains (Larese and Hall, 2003).

In natural sandstones, textural and compositional characteristics that influence quartz cementation rates such as grain shape and composition, clay-size matrix, non-quartz cements, and grain coatings may vary with grain size even within a given sandstone unit. Many researchers are of the opinion that finer grained detrital materials will become cemented at faster rate than coarser materials because the surface area available on finer-grained particles is larger. This may be even more prominent if the source of the quartz cement is pressure solution (Houseknecht, 1984; Sprunt and Nur, 1977). However, most larger data sets for quartz cement volumes do not indicate a strong correlation between the amount of quartz cement and grain size (Dutton and Diggs, 1990) and many data sets indicate a tendency toward greater quartz cement in coarser sandstones (McBride, 1989). It is reported that thickness of quartz overgrowths increase systematically with grain size in the Cambrian Galesville Sandstones (Makowitz and Sibley, 2001).

Nevertheless, to facilitate the analysis of the significance of the grain size effect alone on growth kinetics Lander et al., (2008) conducted an experiment to evaluate the origin of the phenomena in quartz by precipitating synthetic overgrowths on nucleation surface of various sizes using constant fluid chemistry, temperature, pressure, and seed-crystal characteristics. The result showed that sandstone rich in monocrystalline quartz grains predict a substantial decrease in net quartz cementation rates. Simulation on fine-grained also has the fastest overall rate of quartz cementation (Figure 2.7).

A)

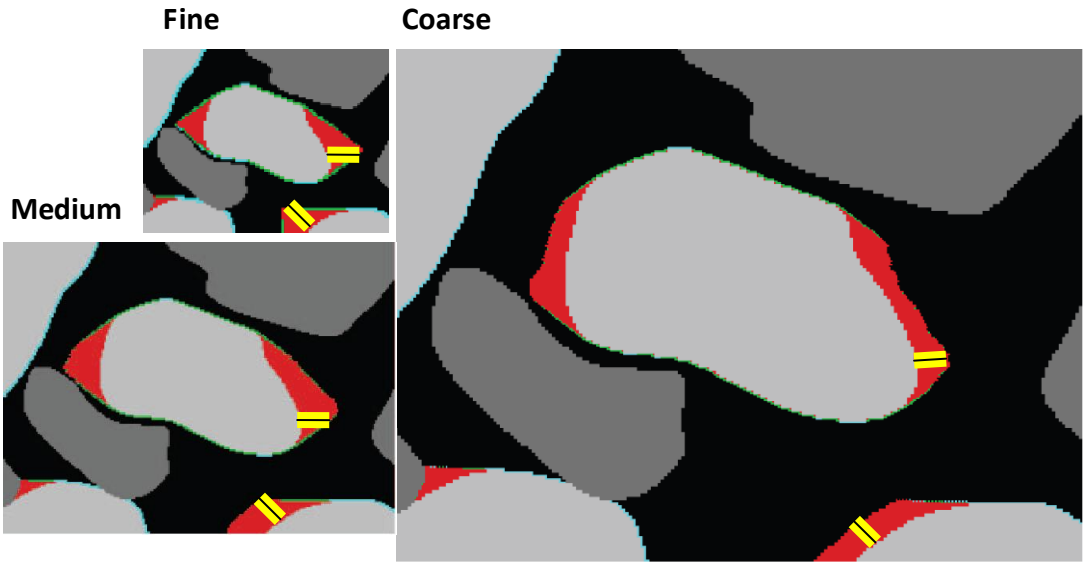

B)

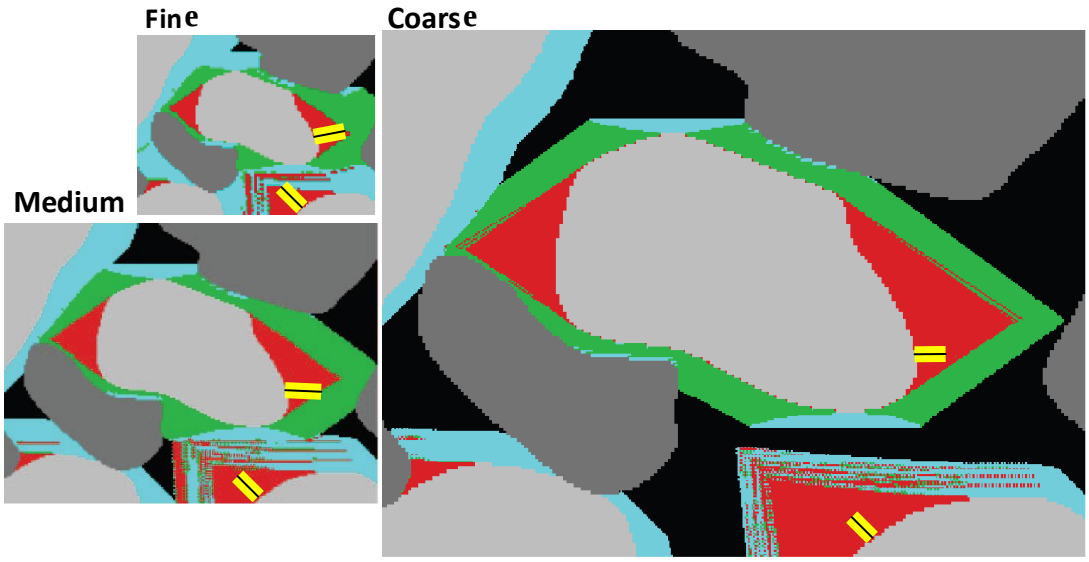

Figure 2. 7 Sketches showing the effect of grain size on quartz cement precipitation rate on equivalent regions of fine, medium and coarse simulation samples. The results show that the fine simulation achieves euhedral geometries and lose porosity and nucleation surface area at faster rate than medium and coarse after Lander et al. (2008). The lengths of the yellow doted are based on the maximum c-axis overgrowth thicknesses (a) before significant cementation (b) after significant cementation.

2.7 Other factors that retard quartz cementation

Other factors reported as capable of inhibiting quartz cementation and leading to preservation of high porosity and permeability at deeply buried clastic reservoir sandstones are; (1) grain coats and grain rims, and (2) shallow development of fluid overpressure (Pittman et al., 1992; Walderhaug, 1996). The most commonly reported types of grain coat observed in sandstones are clay minerals and microcrystalline quartz. Other less effective and less commonly discussed types of grain coats are detrital clay rims, fine crystalline carbonates (e.g. siderites), phosphate, and bitumen.

2.7.1 Microcrystalline quartz coats

Microcrystalline quartz crystals typically have sizes that range from 0.5-5 micron diameter (Aase and Walderhaug, 2005), 5-10 micron diameter, quartz overgrowths typically has crystal size from 10 -100 microns and greater in diameter (Worden et al., 2012). Microquartz is very difficult to observe with a standard light microscope or even by viewing polished thin section in SEM. It is commonly studied by viewing a freshly broken surface of a rock in an SEM with secondary electron imaging.

Microcrystalline quartz in sandstones has been found in rocks that fall within the age range of Devonian to Miocene sandstones (Haimson and Lee, 2004; Lima and De Ros, 2002), from regions as diverse as Brazil (Lima and De Ros, 2002), Colombia (Warren and Pulham, 2001), the United States (Haimson and Lee, 2004), the North Sea basins (Aase et al., 1996; Aase and Walderhaug, 2005; Hendry and Trewin, 1995; Ramm, 1992; Vagle et al., 1994; Weibel et al., 2010), North Africa (Goldstein and Rossi, 2002), and Germany (Worden et al., 2012).

Aase and Walderhaug (2005) stated that the source of microquartz crystals in Jurassic sandstones of the Miller field is probably biogenic silica such as opaline sponge spicules, which occur in trace amounts. Volcanic rock fragments can also alter to various forms of silica including microcrystalline quartz together with some clay minerals (De Ros et al., 1994; Mathisen and McPhearson, 1991; Pirrie, 1991). Microquartz in sandstones is typically derived from biologically-derived silica (Hendry and Trewin, 1995; Lima and De Ros, 2002), and occurs as fine coatings of

crystallites on quartz grains, allegedly preventing the growth of ordinary quartz cement (Aase et al., 1996; Bloch et al., 2002; Jahren and Ramm, 2000; Lima and De Ros, 2002; McBride, 1989; Vagle et al., 1994).

The inhibiting effect of microcrystalline quartz coating on the growth of normal quartz overgrowths is probably due to the microcrystalline quartz crystals being slightly more soluble than larger quartz crystals. They lead to increased silica concentration in the pore water, which is apparently large enough to inhibit quartz dissolution in stylolites, but not enough to permit further growth of the microquartz (Aase et al., 1996; Ramm et al., 1997). Recent work (French, 2012) showed that microcrystalline quartz inhibits the growth of quartz cement because of the crystallographic misorientation relative to the substrate. In the Late Cretaceous Heidelberg Formation, Germany, Worden et al., (2012) described thin film of (amorphous) silica found between the detrital quartz and the microquartz as the precursor to the microcrystalline quartz. Microcrystalline quartz crystals are misoriented relative to the host grain (Haddad et al., 2006), and the c-axis is oriented parallel to the host surface inhibiting the growth of large single crystal of quartz (Ramm et al., 1997; Worden et al., 2012). This microquartz blockes nucleation sites for quartz cement precipitation and the c-axis parallel to the surface of the host grain prevents significant growth into the pore space.

Vagle et al. (1994) described chalcedonic quartz overgrown by microquartz in the presence of *Rhaxella* spicules in Jurassic sandstones of the Inner Moray Firth (UK). When biogenic silica is abundant (e.g. sponge spicules), it will dissolve and create a highly supersaturated silica system were microcrystalline quartz will precipitate. The microcrystalline quartz will grow as long as there is a source of biogenic silica is present, but halt when the biogenic silica is exhausted and silica saturation drops.

Amorphous silica and opal CT may be important sources of silica for quartz cementation at 70-80°C, and the existence of such metastable silica phases at lower temperatures is evidence that quartz does not then precipitate for kinetic reasons. If microcrystalline quartz distribution can be modelled and environments of occurrence can be predicted, the distribution of reservoir rocks with high porosity can be predicted with greater confidence.

2.7.2 Clay coats

The importance of clay mineral coats in preserving porosity in sandstone reservoirs has been well documented (Cecil and Heald, 1971; Ehrenberg, 1993; Ehrenberg and Boassen, 1993; Heald and Larese, 1974; Moraes and De Ros, 1990; Pittman et al., 1992; Storvoll et al., 2002; Taylor et al., 2010; Thomson, 1979; Wilson, 1992). Authigenic chlorite and corrensite are the most commonly reported effective coats occurring in hydrocarbon reservoirs (Pittman et al., 1992). Authigenic chlorite coats are commonly iron-rich (Ehrenberg, 1993; Pittman et al., 1992), but magnesium-rich chlorite have been reported also (Kugler and McHugh, 1990; Pittman et al., 1992).

Illite and illite/chlorite coatings have apparently prevented quartz cementation and thereby helped preserve the primary porosity in the Garn Formation (particularly Garn A); in the Kristin and Lavrans fields, offshore Mid-Norway (Storvoll et al., 2002). In the Cretaceous sandstones of the Sawan gas field, Pakistan, well-developed chlorite rims inhibited quartz cementation, preserved porosities of up to 20%, and led to good permeabilities. Porosity-preserving chlorite cementation in Sawan is restricted to sediments of a shallow-marine environment (Berger et al., 2009). However, the fibrous habit of illite causes severe permeability decrease in sandstone reservoirs (Ehrenberg and Nadeau, 1989; Wilson and Pittman, 1977).

Chlorite crystals are smaller and cause less severe occlusion of pores, particularly in medium to coarse-grained sandstones (Morad et al., 2010). Many important examples of chlorite coatings stopping quartz cementation and preserving porosity are from deltaic and near-shore marine sandstone facies (Grigsby, 2001; Hillier, 1994). These are typically iron-rich varieties of chlorite and are associated with areas of river discharge into marine environments (Taylor and Machent, 2010). It has been reported (Taylor et al., 2004) and (Ajdukiewicz et al., 2010) that Jurassic aeolian Norphlet sandstone in offshore Alabama is an excellent gas reservoir with porosities commonly in the range of 15–20% at depths of 6600–7000 m below surface because detrital grain surfaces are coated with chlorite, and only minor amounts of quartz cement are found. Where small discontinuities in the chlorite rims occur in the uppermost part of the section, authigenic quartz has nucleated on the uncoated surface and filled the adjacent intergranular pore space. In the same way,

quantitative data confirmed that inverse relationship exists between the volume of quartz cement and the percentage of detrital quartz grain surface coated with clay in Jurassic and Triassic sandstones with maximum temperature of 130–160°C in the North Sea. Appreciable primary porosity was preserved in Cunningham (Springer Formation) and Primrose (Morrowan) sandstones (as much as 20% in one sample of Primrose sandstone) by the formation of chlorite grain coats on detrital quartz during the early stages of burial and diagenesis. The chlorite grain coats inhibited the occlusion of pore space by preventing pervasive cementation of the rocks by quartz overgrowths. Cross-plots of porosity versus the abundance of authigenic quartz and grain-coating chlorite document the relationship in two of the cores (McBride, 1987).

Clay coatings on detrital quartz grains that inhibit precipitation of burial diagenetic quartz overgrowths and help preserve porosity and permeability in Unayzah sandstones, Saudi Arabia (Shammari et al., 2011). The grain coating is grain size dependent, the finer the grains, the more clay coatings (~ 90%); and the coarser the grains, the fewer grain coatings (~ 50%) in the samples. Other porosity preservation by grain coating chlorite resulting in stopping quartz cementation include Prairie Chein sandstone, Michican basin (Peck et al., 1988), Santos basin, offshore eastern Brazil (Anjos et al., 2003), Tuscaloosa sandstone in Louisiana (Ryan and Reynolds, 1996), Norphlet sandstone in Mississippi and Alabama.

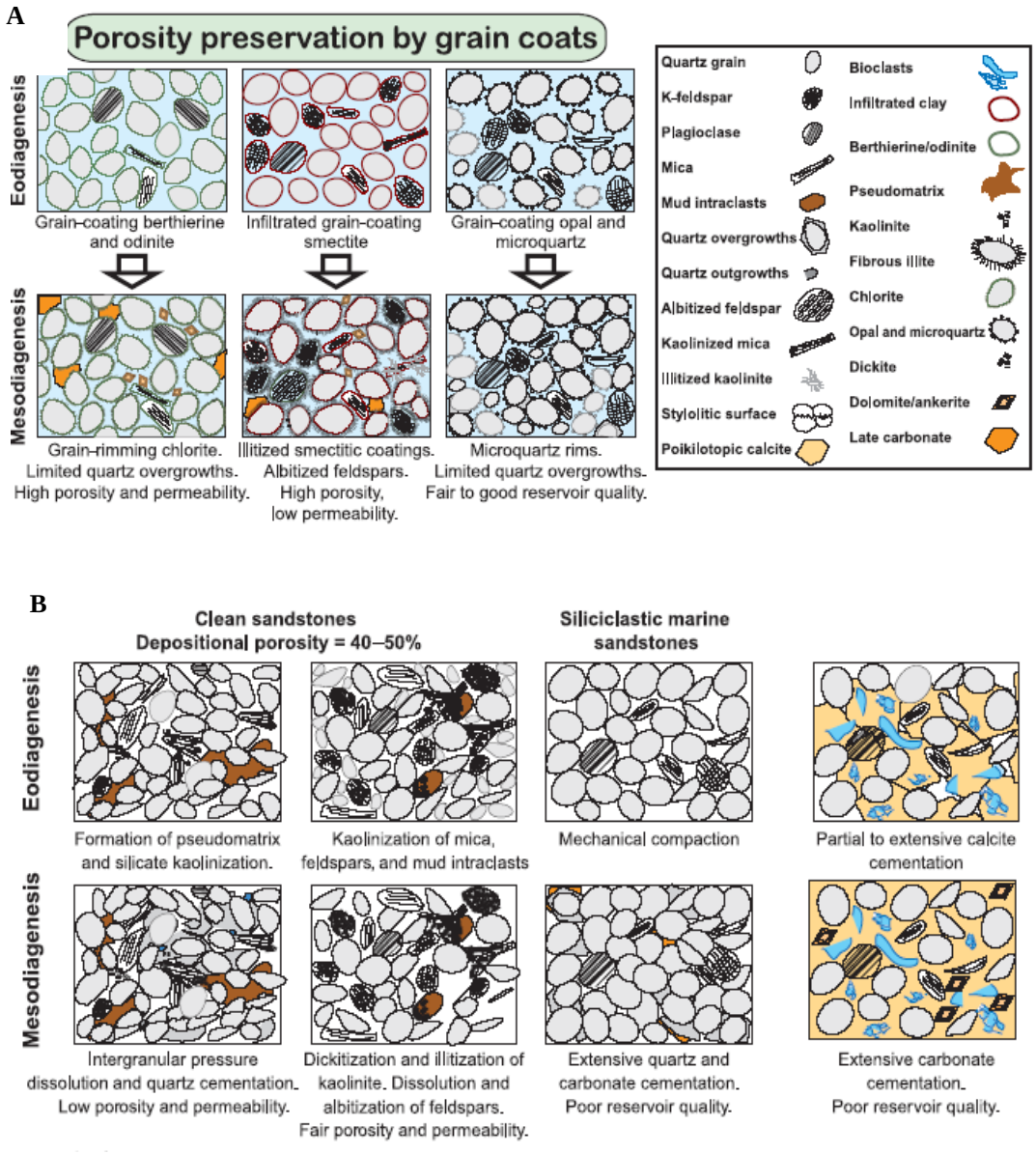

Figure 2. 8 Idealised diagram showing importance of grain coating and reservoir quality. A) Show how grain coating chlorite, illite and microcrystalline quartz preserve porosity by inhibiting quartz cementation. B) Clean sandstone without grain coating leading to precipitation of quartz cement occluding porosity (Morad et al., 2010).

2.8 Phosphate and bitumen coating

Phosphate poisoning has been interpreted as the cause of anomalously high porosity in deeply buried sandstone interval in the late Cretaceous Guadalupe Group in the Cusiana field of Columbia (Warren and Pulham, 2001). Their interpretation was

based on the observation that lithic sandstone composed of quartz and a variety of phosphate grains has porosity of 20% compared to inter bedded clean quartz arenite that were heavily cemented. Adukiewicz et al (1991) proposed the isolation of high porosity and negligible quartz cement in deeply buried Norphlet sandstone were caused by the unit's isolation from the source of silica bearing fluids by the presence of underlying evaporites. This hypothesis however required that silica was not sourced internally and did not explain the occurrence of quartz cement in other isolated sandstones of Gulf of Mexico. From petrographic studies, Maast (2011) revealed that the bitumen coated sandstone zones of the South Viking Graben contain little quartz cement; the bitumen has efficiently shut down quartz cementation.

2.8 Controversy over oil emplacement on quartz cementation and porosity

The idea that oil emplacement could halt quartz cementation and influence preservation of porosity in sandstone reservoirs became known to many geologists in the 1920's (Johnson, 1920). Over the years there has been series of publications which accepted early oil emplacement as a mechanism for porosity preservation in sandstone reservoirs.

2.8.1 Cement volume trends in oil and water leg

Quartz cement volume distribution in water leg and oil leg in different oil fields have been used as evidence for and against "the concept that oil emplacement halts diagenesis" and thereby preserves porosity in deeply buried reservoirs (Aase and Walderhaug, 2005; Barclay et al., 2000; Bonnell et al., 2006; Dixon et al., 1989; Emery et al., 1993; Gluyas et al., 1993b; Lowry, 1956; Marchand et al., 2000; Marchand et al., 2001; Marchand et al., 2002; Molenaar et al., 2008; Ramm, 1992; Ramm and Bjorlykke, 1994).

Barclay and Worden (2000), using petrographic and petrophysical analysis, did not find significant difference in quartz cement volume across oil-water contact in the Magnus field, N. Sea. Higher quartz cement volumes in the oil leg compared to the

water leg in the Fulmar reservoir sandstones of the North Sea have been reported (Saigal et al., 1992). From petrographic data and porosity measurements Wilkinson and Hazeldine (2011) concluded that early oil charge has preserved exceptional porosity in deeply buried, invariably homogeneous, overpressured, sandstones of the Fulmar Formation, North Sea. In similar ways Marchand et al. (2002) studied the distribution of quartz cement in Brae Formation sandstones of the Miller and Kingfisher fields (United Kingdom North Sea). They reported significant difference in quartz cement volume between the oil leg and the water leg. Quartz cementation rates were reduced by at least two orders of magnitude in the oil legs relative to water legs. Marchand et al. (2002) presented data indicating that average volume of quartz cement increases from 6% in the oil bearing zones at the structural crest to 13.3% in the water bearing sands along the structural flank.

Aase and Walderhaug (2005) used additional petrographic data that was not included in the earlier work and disputed the previous work of Marchand and co-workers. When all the data were taken into account, no discernible relationship between quartz cement volume and pore-fluid type was apparent in the Miller field. They regarded porosity-preservation as being the result of microcrystalline quartz coats and concluded that the misinterpretation was a consequence of the previous study failing to recognise microquartz coating (Bonnell et al., 2006).

Similarly, Maast et al., (2011) claimed that on regional scale, in the Upper Jurassic sandstones of the south Viking Graben, North Sea, no correlation exists between hydrocarbon saturated sandstones and the high porosity sandstones previously described. On the contrary, hydrocarbon saturated sandstones were found in the high-, the normal-, and the low-porosity sandstone. The water leg and the oil leg display similar amounts of quartz cement.

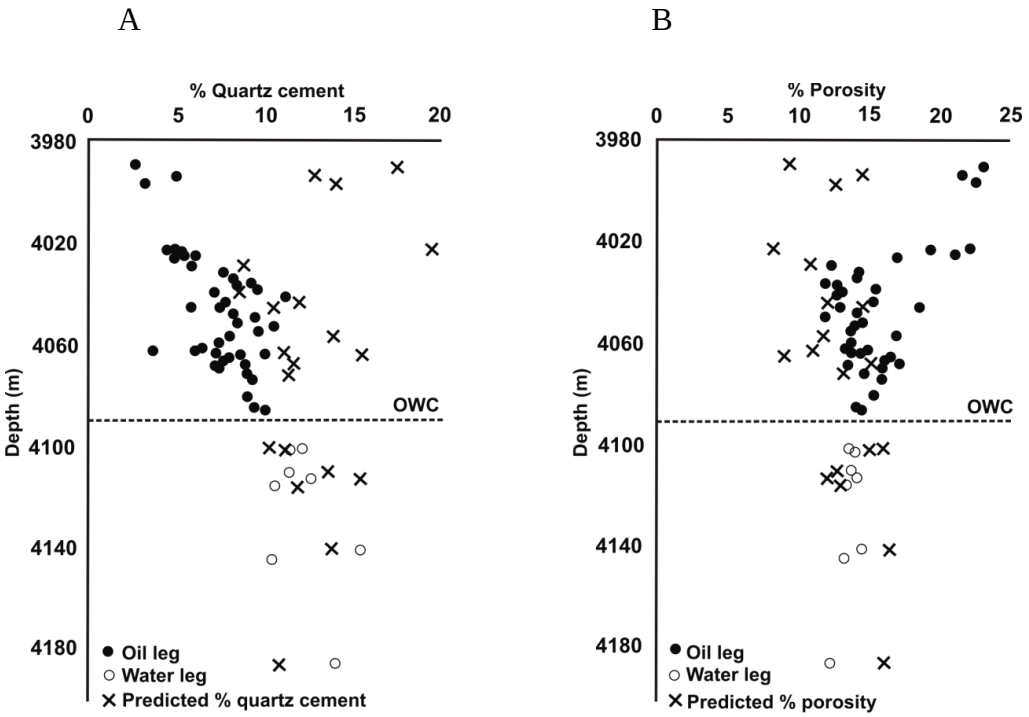

Figure 2. 9 (A) Depth versus quartz cement distribution determined by (SEM-CL) in the Miller oil field (B) Core helium porosity distribution relative to oil-water-contact (OWC) (after Marchand et al., 2002). The oil charge is gradual in this field as a result quartz cement volume is lower at the crest than the calculated volume and increased systematically from the crest to the OWC and porosity decrease from the crest toward the OWC.

On the other hand, Molenaar et al., (2008) showed that there is no noticeable difference in porosity distribution between oil leg and the water leg of the Cambrian reservoir sandstones, Palaeozoic Baltic Basin. According to them, the lack of any difference in properties of oil filled sandstones, dry structures as well as water filled sandstones below the oil-water contact, indicates that oil had no noticeable effect on diagenesis and did not lead to preservation of porosity. It is possible that water saturation was either too high, or variable to inhibit quartz cementation, or thermal modelling was incorrect, or that oil was emplaced after the main phase of quartz cementation.

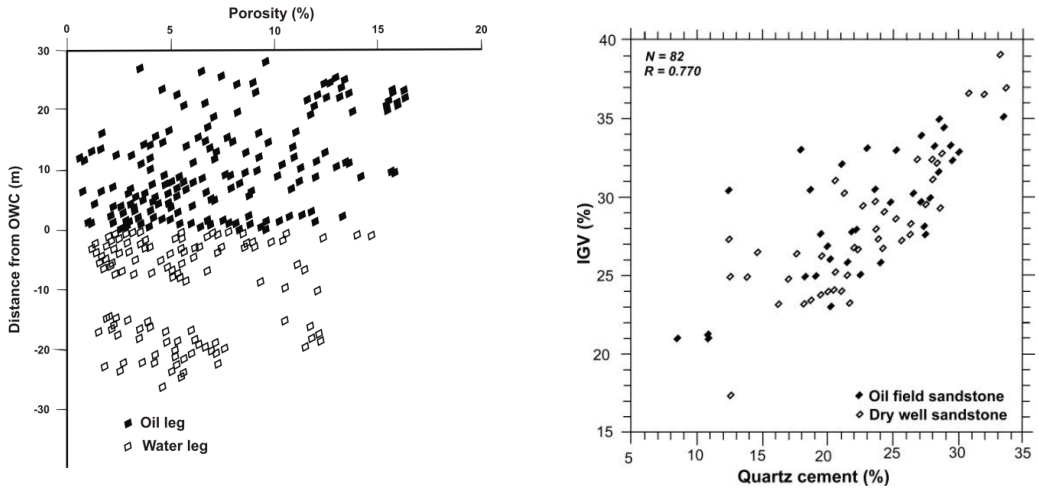

A **B**

Figure 2. 10 (A) Distribution of porosity with respect to distance to the oil-water contact (OWC) in the Cambrian reservoir sandstones of the Kretinga oil field, Baltic Basin. Filled symbols are from the oil leg, while open symbols are from the water leg below the oil-water contact. (B) Correlation between quartz cement volume and intergranular volume (IGV) of oil field sandstone and dry well sandstone (after Molenaar et al., 2008). Filled symbols are from the oil leg, while open symbols are from the water leg. No significant difference in porosity or quartz cement volume is observed.

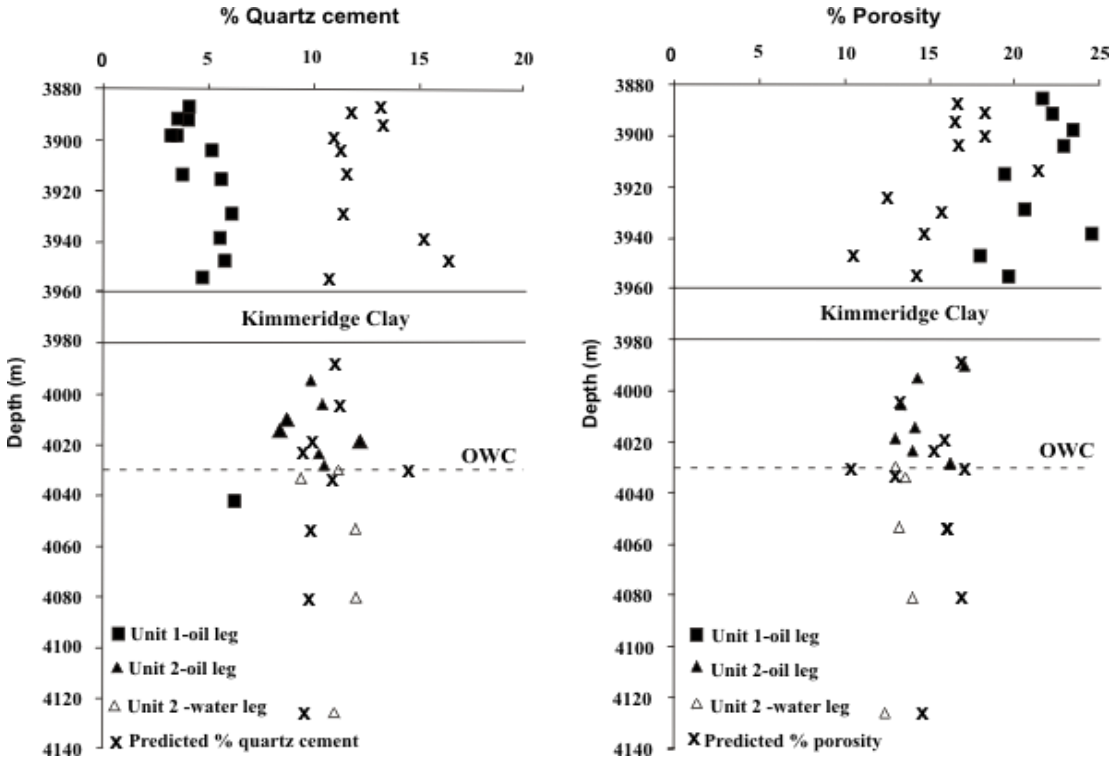

A B

Figure 2. 11 (A) Plot of quartz cement abundance determined by scanning electron microscopy-based CL (%) and image analysis versus depth (B) core helium porosity (%) versus depth in the King Fisher field (after Marchand et al., 2002). The upper unit above the Kimmeridge clay received early oil charge and porosity is preserved and quartz cement is low throughout. The lower unit received late oil charge, quartz cement is high and porosity is low throughout the reservoir.

2.8.2 Presence of oil inclusions in quartz cement

Fluid inclusions are fluids trapped during crystal growths (or during grain fracturing and rehealing). The trapped fluids may be liquid, vapour, or subcritical fluid, and the composition of the trapped fluid may include essentially pure water, brines of various salinity, gas or gas bearing liquids, and silicate, sulphide or carbonate melts, amongst others (Bodnar, 2003). Since fluid inclusions occur mainly at the boundary between the detrital grain and the overgrowth, therefore homogenization temperatures could be the same as the temperature at the onset of quartz cementation (Walderhaug, 1994; Wilson and Stanton, 1994). Hydrocarbon inclusions can also provide evidence for the timing of hydrocarbon migration and filling of reservoir (Pagel et al., 1986).

Homogenization temperatures of fluid inclusions in quartz cement from different basins are variable within 75°–150°C range (Walderhaug, 1994). Petroleum inclusions are often colourless, but may in some cases show brown coloration. The colour is a function of composition and size of the inclusion (Burruss, 1981). The most common and most effective way of differentiating between aqueous inclusion and petroleum inclusion is by ultraviolet light (UV); petroleum emits light in the visible range while aqueous fluids are non-fluorescent.

Fluid inclusion of authigenic minerals have been used in an attempt to understand the diagenetic history of sedimentary rocks (Burruss, 1981; Haszeldine et al., 1984; Nedkvitne et al., 1993; Parnell et al., 2001; Roedder and Bodnar, 1997). The compositions of hydrocarbon in oil-filled inclusions can provide valuable information about the filling history of reservoirs (George et al., 1997; Isaksen et al., 1998; Karlsen et al., 1993), in addition to information about in *situ* PVT conditions at the time of inclusion formation that can be gained from homogenization temperatures (Munz et al., 1999). Aqueous fluids are dominant in sedimentary systems and actively participate in diagenetic processes (Goldstein, 2001). Due to the general inhibiting effect of petroleum on cementation, it is, however, likely that trapping mechanisms are most active during filling of the reservoir than at arbitrary later time, when most of the water has been displaced (Munz et al., 1999). A key factor is that diagenetic processes often slow down subsequently as the sandstone becomes lithified and as petroleum saturation increases above a certain threshold (Worden et al., 1998), although quartz cementation may continue for considerable period under favourable conditions (Barclay and Worden, 2000; Karlsen and Skeie, 2006; Nedkvitne et al., 1993).

The existence of oil-bearing fluid inclusions in quartz cement in some reservoir sandstones is cited as evidence to prove that quartz cementation has continued to take place after oil emplacement (Ramm, 1992; Saigal et al., 1992; Walderhaug, 1996). However, oil inclusions in quartz cements are often considered to form during early phase of oil charging a reservoir and often contain less mature oil than is present in the reservoir (Weedman et al., 1996). This suggests that such inclusions were trapped when water saturation is very high in the reservoir.

Thermal re-equilibration of homogenization temperature of fluid inclusions in authigenic quartz can occur when the host mineral is subjected to high temperatures and pressure higher than those at which it initially formed has been reported, perhaps due to stretching of the inclusions (Osborne and Haszeldine, 1993). However, fluid inclusions in quartz are considered to be resistant to non-elastic deformation, making re-equilibration unlikely under diagenetic condition (Worden et al., 1995). The absence of cleavage and the resistance to re-crystallization make quartz a highly suitable medium to preserve fluid inclusions (Van den Kerkhof and Hein, 2001).

Resetting (re-equilibration) of fluid inclusion homogenization temperature (T*h*) when the host mineral is subjected to higher temperatures and pressure higher than those at which it initially formed have been reported (Osborne and Haszeldine, 1993).

2.9 Duration and timing of quartz cementation

Episodic or short precipitation time is defined as a cement precipitation period of 1 to 10 million years and a long precipitation time as a cement precipitation period of similar duration to the burial history of rock (Gluyas and Oxtoby, 1995). Long period of > 10 million years have been stated for completion of quartz cementation in some basins (Robinson and Gluyas, 1992a; Wood and Boles, 1991). Quartz cementation has been viewed as both a prolonged process that occur overs long period of time once a threshold temperature of about 80°C is reached (Williams et al., 1997) and as an episodic process in which short bursts of activity are punctuated by long period of quiescence (Canals and Meunier, 1995; Gluyas and Oxtoby, 1995; Haszeldine et al., 1984; Robinson and Gluyas, 1992b; Wood and Boles, 1991).

William et al. (1997) used stable isotope and fluid inclusion data from an off shore Jurassic hydrocarbon reservoir in Norway to show that quartz cementation was a continuous process from Middle Cretaceous (around 100 m years) to the present day. Robinson and Gluyas (1992) stated that quartz cement precipitation occurred within a period of 10 million years, a time substantially shorter than the age of the sandstone. Quartz cementation in Beatrice field, North Sea took place in 1.6 m years (Haszeldine et al., 1984). Worden and Morad (2000) concluded that the exact

duration of quartz cementation is dependent on the burial history and age of the basin.

Fluid inclusion data are most commonly used to determine rate of quartz cementation. Ironically this method has supported both episodic (Gluyas et al., 1993a) and prolonged period of time for quartz cementation (Walderhaug, 1990).

Another important aspect of oil emplacement and quartz cementation is the relative timing of the two events. If quartz cementation occurred before the oil charge of a reservoir (Fig. 2.9), there will be no effect on the reservoir quality. If quartz cementation is synchronous with oil charge, there will be gradual increase in quartz cement volume from crest to the flanks toward the oil-water contact (Marchand et al., 2000) case of Miller field (Figure 2.9). If quartz cementation commences after oil charge, then reservoir quality may be enhanced provided the presence of oil has effect on quartz cementation. Barclay and Worden (2000) have shown how quartz cementation relative to oil emplacement can determine the reservoir quality of an oil field (Figure 2.12).

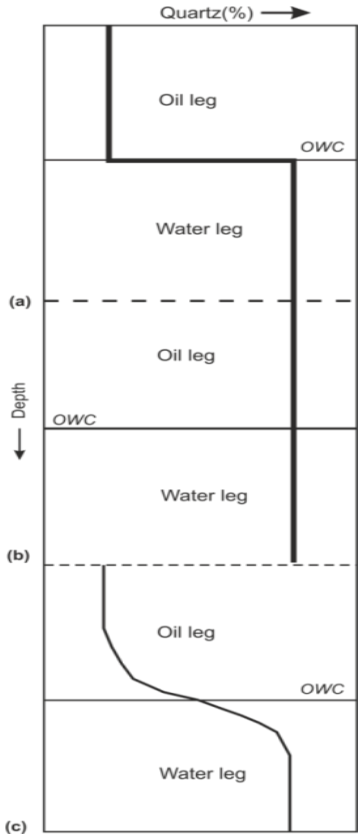

Figure 2. 12 effect of timing on oil emplacement and quartz cementation (a) oil charge before quartz cementation (b) oil charge after quartz cementation (c) oil charge during quartz cementation after (Barclay and Worden, 1998).

2.9 Conclusions

Quartz cementation takes place only when there is source of silica, transport of silica from source to point of precipitation and clean grain surface to precipitate on. Sources of silica can be internal through stylolitization, pressure solution at grain contacts, alteration of feldspar, illitization of smectite or dissolution of biogenic silica. Silica solution can also be introduce to sand bodies from external sources through faults and fractures, or by advection from deep beneath the reservoir or adjacent source. Transport of silica solution from the source to the point of precipitation is mainly by diffusion or advection.

Temperature at which quartz cement precipitation begin determined from fluid inclusion homogenization temperature varies from basin to basin but threshold

temperature >70^{o}C is commonly accepted, while whether quartz cementation is episodic or a continuous is still controversial. Various factors that may inhibit quartz cementation include grain coatings by chlorite, microcrystalline quartz, phosphate and bitumen, early oil emplacement and over pressure. Whether early oil emplacement inhibits quartz cementation and preserves porosity in deeply buried sandstones is still debated. In case of oil emplacement, timing oil charge relative to quartz cementation is very important. Oil emplacement before commencement of quartz cementation or synchronous to quartz cementation will inhibit quartz cementation while oil charge after quartz cementation will have no effect (Fig. 2.12). Rapid versus slow rate of oil charge will also have different effect on quartz cementation (Fig. 2.11)

2.10 References

Aase, N. E., Bjorkum, P. A., and Nadeau, P. H., 1996, The effect of grain-coating microquartz on preservation of reservoir porosity: American Association of Petroleum Geologists Bulletin, v. 80, no. 10, p. 1654-1673.

Aase, N. E., and Walderhaug, A., 2005, The effect of hydrocarbons on quartz cementation: diagenesis in the Upper Jurassic sandstones of the Miller Field, North Sea, revisited: Petroleum Geoscience, v. 11, no. 3, p. 215-223.

Abercrombie, H. J., Hutcheon, I. E., Bloch, J. D., and Decaritat, P., 1994, Silica activity and the smectite-illite reaction: Geology, v. 22, no. 6, p. 539-542.

Ajdukiewicz, J. M., Nicholson, P. H., and Esch, W. L., 2010, Prediction of deep reservoir quality using early diagenetic process models in the Jurassic Norphlet Formation, Gulf of Mexico: American Association of Petroleum Geologists Bulletin, v. 94, no. 8, p. 1189-1227.

Al-Garni, M. T., and Al-Anazi, B. D., 2008, Investigation of wettability effects on capillary pressure, and irreducible saturation for Saudi crude oils, using rock centrifuge: Oil and Gas Bussiness, v. http://www.ogbus.ru/eng.

Alvarez, W., Engelder, T., and Geiser, P. A., 1978, Classification of solution cleavage in pelagic limestones: Geology, v. 6, no. 5, p. 263-266.

Anjos, S. M. C., De Ros, L. F., and Silva, C. M. A., 2003, Chlorite authigenesis and porosity-preservation in the Upper Cretaceous marine sandstones of the Santos Basin, offshore eastern Brazil, *in* Worden, R. H., and Morad, S., eds., In: Clay mineral cements in sandstones International Association of Sedimentologists Special Publications, Volume 34: Oxford, Blackwell Science, p. 319-342.

Aplin, A. C., and Warren, E. A., 1994, Oxygen isotopic indications of the mechanisms of silica transport and quartz cementation in deeply buried sandstones: Geology, v. 22, no. 9, p. 847-850.

Archer, J. S., and Wall, C. G., 1986, Petroleum engineering: principles and practice, Society of Petroleum Engineers, TX, p. 374.

Baccar, M. B., and Fritz, B., 1993, Geochemical modelling of sandstone diagenesis and its consequences on the evolution of porosity: Applied Geochemistry, v. 8, no. 3, p. 285-295.

Barclay, S. A., and Worden, R. H., 1998, Quartz cement volumes across oil-water contacts in oil fields from petrography and wireline logs: preliminary results from the Magnus Field, Northern North Sea, *in* Harvey, P. K., and Lovell, M. A., eds., Core-Log Integration. Geological Society Special Publication, Volume 136: Bath, p. 327-339.

-, 2000, Geochemical modelling of diagenetic reactions in a sub-arkosic sandstone: Clay Minerals, v. 35, no. 1, p. 57-67.

Barclay, S. A., Worden, R. H., Parnell, J., Hall, D. L., and Sterner, S. M., 2000, Assessment of fluid contacts and compartmentalization in sandstone reservoirs using fluid inclusions: an example from the Magnus oil field, North Sea: Americam Association of Petroleum Geologists Bulletin, v. 84, no. 4, p. 489-504.

Berger, A., Gier, S., and Krois, P., 2009, Porosity-preserving chlorite cements in shallow-marine volcaniclastic sandstones: Evidence from Cretaceous

sandstones of the Sawan gas field, Pakistan: American Association of Petroleum Geologists Bulletin, v. 93, no. 5, p. 595-615.

Berger, G., Velde, B., and Aigouy, T., 1999, Potassium sources and illitization in Texas Gulf Coast shale diagenesis: Journal of Sedimentary Research, v. 69, no. 1, p. 151-157.

Berner, R. A., 1980, Early diagenesis: A theoretical approach, Princeton Univ Press, v. 1.

Bethke, C. M., and Marshak, S., 1990, Brine migrations across North America-the plate tectonics of groundwater: Annual Review of Earth and Planetary Sciences, v. 18, p. 287.

Bjørlykke, K., 1983, Diagenetic reactions in sandstones: Sediment Diagenesis: Reading, UK, Reidel Publishing, p. 169-213.

-, 1998, Clay mineral diagenesis in sedimentary basins-a key to the prediction of rock properties. Examples from the North Sea Basin: Clay Minerals, v. 33, no. 1, p. 15-34.

Bjørlykke, K., and Egeberg, P. K., 1993, Quartz cementation in sedimentary basins: American Association of Petroleum Geologists Bulletin, v. 77, p. 1538-1538.

Bjørlykke, K., Mo, A., and Palm, E., 1988, Modeling of thermal convection in sedimentary basins and its relevance to diagenetic reactions: Marine and Petroleum Geology, v. 5, p. 338-351.

Bloch, S., Lander, R. H., and Bonnell, L., 2002, Anomalously high porosity and permeability in deeply buried sandstone reservoirs: Origin and predictability: Americam Association of Petroleum Geologists Bulletin, v. 86, no. 2, p. 301-328.

Bodnar, R. J., 2003, Introduction to aqueous-electrolyte fluid inclusions: Fluid Inclusions Analysis and Interpretation: Vancouver, Mineralogical Association of Canada, Short Course, v. 32, p. 81-100.

Boles, J. R., and Franks, S. G., 1979, Clay diagenesis in Wilcox Sandstones of southwest Texas - implications of smectite diagenesis on sandstone cementation: Journal of Sedimentary Petrology, v. 49, no. 1, p. 55-70.

Bonnell, L., Larese, R. E., and Lander, R. H., 2006, Hydrocarbon versus microquartz inhibition of quartz cementation in North Sea sandstones: Empirical and experimental evidence American Association of Mineralogist Journal Convention Abstract, Volume 15.

Burley, S. D., and Flisch, M., 1989, K-Ar geochronology and timing of detrital I/S clay illitization and authigenic illite precipitation in the Piper and Tartan fields, outer Moray Firth, UK North Sea: Clay Minerals, v. 24, no. 2, p. 285-315.

Burley, S. D., and Macquaker, J. H. S., 1992, Authigenic clays, diagenetic sequences and conceptual diagenetic models in contrasting basin-margin and basin-center North Sea Jurassic sandstones and mudstones In: Origin, diagenesis and petrophysics of clay minerals in sandstones (eds. Houseknecht, D. W. and Pittman, E. D.) Society of Economic Geologists, Sedimentary Petrology Special Publication, v. 47, p. 81-110.

Burley, S. D., Mullis, J., and Matter, A., 1989, Timing and diagenesis in the Tartan reservoir (UK North Sea) - constraints from combined cathodoluminescence microscopy and fluid inclusion studies: Marine and Petroleum Geology, v. 6, no. 2, p. 98-&.

Burruss, R. C., 1981, Analysis of fluid inclusions; phase equilibria at constant volume: American Journal of Science, v. 281, no. 8, p. 1104-1126.

Canals, M., and Meunier, J. D., 1995, A model for porosity reduction in quartzite reservoirs by quartz cementation: Geochimica et Cosmochimica Acta, v. 59, no. 4, p. 699-709.

Cecil, C. B., and Heald, M. T., 1971, Experimental investigation of the effects of grain coatings on quartz growth: Journal of Sedimentary Research, v. 41, no. 2, p. 582-584.

Chang, H. K., Mackenzie, F. T., and Schoonmaker, J., 1986, Comparisons between the diagenesis of dioctahedral and trioctahedral smectite, Brazilian offshore basins: Clays and Clay Minerals, v. 34, p. 407-423.

Curtis, C. D., 1978, Possible links between sandstone diagenesis and depth-related geochemical reactions occurring in enclosing mudstones: Journal of the Geological Society, v. 135, no. 1, p. 107-117.

Curtis, C. D., Burns, R. G., and Smith, J. V., 1977, Sedimentary geochemistry: environments and processes dominated by involvement of an aqueous phase [and discussion]: Philosophical Transactions of the Royal Society of London. Series A, Mathematical and Physical Sciences, v. 286, no. 1336, p. 353-372.

Curtis, C. D., Murchison, D. G., Berner, R. A., Shaw, H., Sarnthein, M., Durand, B., Eglinton, G., Mackenzie, A. S., and Surdam, R. C., 1985, Clay mineral precipitation and transformation during turial diagenesis [and discussion]: Philosophical Transactions of the Royal Society of London. Series A, Mathematical and Physical Sciences, v. 315, no. 1531, p. 91-105.

Davis, S. H., Rosenblat, S., Wood, J. R., and Hewett, T. A., 1985, Convective fluid flow and diagenetic patterns in domed sheets: Amercian Journal of Science, v. 285, no. 3.

De Boer, R. B., 1977, On the thermodynamics of pressure solution—interaction between chemical and mechanical forces: Geochimica et Cosmochimica Acta, v. 41, no. 2, p. 249-256.

de Caritat, P., 1989, Note on the maximum upward migration of pore water in response to sediment compaction: Sedimentary Geology, v. 65, no. 3, p. 371-377.

De Ros, L., Morad, S., and Al-Aasm, I., 1997, Diagenesis of siliciclastic and volcaniclastic sediments in the Cretaceous and Miocene sequences of the NW African margin (DSDP Leg 47A, Site 397): Sedimentary Geology, v. 112, no. 1, p. 137-156.

De Ros, L. F., Sgarbi, G. N. C., and Morad, S., 1994, Multiple authigenesis of K-feldspar in sandstones; evidence from the Cretaceous Areado Formation, Sao Francisco Basin, central Brazil: Journal of Sedimentary Research, v. 64, no. 4a, p. 778-787.

Dixon, S. A., Summers, D. M., and Surdam, R. C., 1989, Diagenesis and preservation of porosity in Norphlet Formation (Upper Jurassic), southern Alabama: Americam Association of Petroleum Geologists Bulletin, v. 73, no. 6, p. 707-728.

Dove, P. M., and Rimstidt, J. D., 1994, Silica-water interactions: Reviews in Mineralogy and Geochemistry, v. 29, no. 1, p. 259-308.

Drief, A., and Nieto, F., 2000, Chemical composition of smectites formed in clastic sediments. Implications for the smectite—illite transformation: Clay Minerals, v. 35, no. 4, p. 665-678.

Dutton, S. P., and Diggs, T. N., 1990, History of quartz cementation in the Lower Cretaceous Travis Peak Formation, East Texas: Journal of Sedimentary Research, v. 60, no. 2, p. 191-202.

Eberl, D., and Hower, J., 1977, The hydrothermal transformation of sodium and potassium smectite into mixed-layer clay: Clays and Clay Minerals, v. 25, no. 3, p. 215-227.

Ehrenberg, S. N., 1993, Preservation of anomalously high porosity in deeply buried sandstones by grain-coating chlorite: examples from the Norwegian continental shelf: American Association of Petroleum Geologists Bulletin, v. 77, p. 1260-1260.

Ehrenberg, S. N., and Boassen, T., 1993, Factors controlling permeability variation in sandstones of the Garn Formation in Trestakk Field, Norwegian continental shelf: Journal of Sedimentary Research, v. 63, no. 5, p. 929-944.

Ehrenberg, S. N., and Nadeau, P. H., 1989, Formation of diagenetic illite in sandstones of the Garn Formation, Haltenbanken area, mid-Norwegian continental shelf: Clay Minerals, v. 24, no. 2, p. 233-253.

Emery, D., Smalley, P. C., Oxtoby, N. H., Ragnarsdottir, K. V., Aagaard, P., Halliday, A., Coleman, M. L., and Petrovich, R., 1993, Synchronous oil migration and cementation in sandstone reservoirs demonstrated by quantitative description of diagenesis [and discussion]: Philosophical Transactions of the Royal Society of London. Series A: Physical and Engineering Sciences, v. 344, no. 1670, p. 115-125.

Feazel, C. T., and Schatzinger, R. A., 1985, Prevention of carbonate cementation in petroleum reservoirs, , *in* Schnedermann, N., and Harris, P. M., eds., Carbonate cements: Society for Sedimentary Geology Special Publication, Volume 36, p. 97-106.

George, S. C., Krieger, F. W., Eadington, P. J., Quezada, R. A., Greenwood, P. F., Eisenberg, L. I., Hamilton, P. J., and Wilson, M. A., 1997, Geochemical comparison of oil-bearing fluid inclusions and produced oil from the Toro sandstone, Papua New Guinea: Organic Geochemistry, v. 26, no. 3-4, p. 155-173.

Giles, M. R., 1997, Diagenesis: a quantitative perspective, Kluwer Academic Publishers.

Giles, M. R., Stevenson, S., Martin, S. V., Cannon, S. J. C., Hamilton, P. J., Marshall, J. D., and Samways, G. M., 1992, The reservoir properties and diagenesis of the Brent Group: a regional perspective, *in* Morton, A. C., Haszeldine, R. S., Giles, M. R., and Brown, S., eds., Geology of the Brent Group, Geological Society, London, Special Publications, v. 61, p. 329-350.

Glasmann, J., Clark, R., Larter, S., Briedis, N. A., and Lundegard, P. D., 1989, Diagenesis and hydrocarbon accumulation, Brent sandstone (Jurassic), Bergen high area, North Sea: American Association of Petroleum Geologists Bulletin, v. 73, no. 11, p. 1341-1360.

Glasmann, J. R., 1992, The fate of feldspar in Brent Group reservoirs, North Sea: a regional synthesis of diagenesis in shallow, intermediate, and deep burial environments, *in* A. C. Morton, S.Haszeldine, R., Giles, M. R., and Brown,

S., eds., Geological Society, London, Special Publications, Volume 61, p. 329-350.
Gluyas, J., and Coleman, M., 1992, Material flux and porosity changes during sediment diagenesis: Nature, v. 356, no. 6364, p. 52-54.
Gluyas, J., and Leonard, A., 1995, Diagenesis of the Rotliegend Sandstone: the answer ain't blowin'in the wind: Marine and Petroleum Geology, v. 12, no. 5, p. 491-497.
Gluyas, J., and Oxtoby, N., 1995, Diagenesis - A short (2-Million year) story - Miocene sandstones of Central Sumatra, Indonesia: Journal of Sedimentary Research Section a-Sedimentary Petrology and Processes, v. 65, no. 3, p. 513-521.
Gluyas, J. G., Grant, S. M., and Robinson, A. G., 1993a, Geochemical evidence for a temporal control on sandstone cementation: In: Diagenesis and basin development (eds. Horbury, A. D. and RobinsonA. G.) American Association of Petroleum Geologists Studies in Geology, v. 36, p. 23-33.
Gluyas, J. G., Robinson, A. G., Emery, D., Grant, S. M., and Oxtoby, N. H., 1993b, The link between petroleum emplacement and sandstone cementation, *in* Parker, J., ed., Petroleum Geology of the North west Europe, Geological Society of London, v. 4, p. 1395-1402.
Goldstein, R. H., 2001, Fluid inclusions in sedimentary and diagenetic systems: Lithos, v. 55, no. 1-4, p. 159-193.
Goldstein, R. H., and Rossi, C., 2002, Recrystallization in quartz overgrowths: Journal of Sedimentary Research, v. 72, no. 3, p. 432-440.
Graham, C. M., Valley, J. W., and Winter, B. L., 1996, Ion microprobe analysis of 18O/16O in authigenic and detrital quartz in the St. Peter Sandstone, Michigan Basin and Wisconsin Arch, USA: contrasting diagenetic histories: Geochimica et Cosmochimica Acta, v. 60, no. 24, p. 5101-5116.
Grant, S. M., and Oxtoby, N. H., 1992, The timing of quartz cementation in Mesozoic sandstones from Haltenbanken, offshore mid-Norway: fluid inclusion evidence: Journal of the Geological Society, v. 149, no. 4, p. 479-482.
Gratier, J. P., Muquet, L., Hassani, R., and Renard, F., 2005, Experimental microstylolites in quartz and modeled application to natural stylolitic structures: Journal of Structural Geology, v. 27, no. 1, p. 89-100.
Grigsby, J. D., 2001, Origin and growth mechanism of authigenic chlorite in sandstones of the lower Vicksburg Formation, south Texas: Journal of Sedimentary Research, v. 71, no. 1, p. 27-36.
Haddad, S. C., Worden, R. H., Prior, D. J., and Smalley, P. C., 2006, Quartz cement in the Fontainebleau sandstone, Paris basin, France: Crystallography and implications for mechanisms of cement growth: Journal of Sedimentary Research, v. 76, no. 2, p. 244-256.
Haimson, B., and Lee, H., 2004, Borehole breakouts and compaction bands in two high-porosity sandstones: International Journal of Rock Mechanics and Mining Sciences, v. 41, no. 2, p. 287-301.
Haszeldine, R. S., Samson, I. M., and Cornford, C., 1984, Quartz diagenesis and convective fluid movement; Beatrice Oilfield, UK North Sea: Clay Minerals, v. 19, no. 3, p. 391-402.
Heald, M. T., 1955, Stylolites in sandstones: The Journal of Geology, p. 101-114.

Heald, M. T., and Larese, R. E., 1974, Influence of coatings on quartz cementation: Journal of Sedimentary Research, v. 44, no. 4, p. 1269-1274.

Heald, M. T., and Renton, J. J., 1966, Experimental study of sandstone cementation: Journal of Sedimentary Research, v. 36, no. 4, p. 977-991.

Heasley, E. C., Worden, R. H., and Hendry, J. P., 2000, Cement distribution in a carbonate reservoir: recognition of a palaeo oil–water contact and its relationship to reservoir quality in the Humbly Grove field, onshore, UK: Marine and Petroleum Geology, v. 17, no. 5, p. 639-654.

Hendry, J. P., and Trewin, N. H., 1995, Authigenic quartz microfabrics in Cretaceous turbidites; evidence for silica transformation processes in sandstones: Journal of Sedimentary Research, v. 65, no. 2a, p. 380-392.

Hillier, S., 1994, Pore-lining chlorite in siliciclastic reservoir sandstones - electron microprobe, SEM and XRD data, implications for their origin: Clay Minerals, v. 29, no. 4, p. 665-679.

Hoffman, J., and Hower, J., 1979, Clay mineral assemblages as low grade metamorphic geothermometers: application to the thrust faulted disturbed belt of Montana, USA, *in* Scholle, P. A., and Schluger, P. S., eds., Aspects of diagenesis: , Volume 26, Society of Sedimentary Petrology Special Publication, p. 55-79.

Houseknecht, D. W., 1984, Influence of grain size and temperature on intergranular pressure solution, quartz cementation, and porosity in a quartzose sandstone: Journal of Sedimentary Research, v. 54, no. 2, p. 348-361.

Hower, J., Eslinger, E. V., Hower, M. E., and Perry, E. A., 1976, Mechanism of burial metamorphism of argillaceous sediment: Mineralogical and chemical evidence: Geological Society of America Bulletin, v. 87, no. 5, p. 725-737.

Huang, W. L., Longo, J. M., and Pevear, D. R., 1993, An experimentally derived kinetic model for smectite-to-illite conversion and its use as a geothermometer: Clays and Clay Minerals, v. 41, p. 162-177.

Isaksen, G. H., Pottori, R. J., and Jenssen, A. I., 1998, Correlation of fluid inclusions and reservoired oils to infer trap fill history in the South Viking Graben, North Sea: Petroleum Geoscience, v. 4, no. 1, p. 41-55.

Jahren, J., and Ramm, M., 2000, The porosity-preserving effects of microcrystalline quartz coatings in arenitic sandstones: examples from the Norwegian continental shelf: In: Quartz cementation in sandstones (eds. Worden, R.H. and Morad, S.) International Association of Sedimentologists Special Publications, v. 29, p. 271-280.

James, W. C., Wilmar, G. C., and Davidson, B. G., 1986, Role of quartz type and grain size in silica diagenesis, Nugget Sandstone, south-central Wyoming: Journal of Sedimentary Research, v. 56, no. 5, p. 657-662.

Johnson, R. H., 1920, The cementation process in sandstone: American Association of Petroleum Geologists Bulletin, v. 4, p. 33-35.

Kantorowicz, J. D., 1985, The origin of authigenic ankerite from the Ninian Field, UK North Sea: Letters to Nature, v. 315, p. 212-216.

Karlsen, D. A., Nedkvitne, T., Larter, S. R., and Bjørlykke, K., 1993, Hydrocarbon composition of authigenic inclusions: application to elucidation of petroleum reservoir filling history: Geochimica et Cosmochimica Acta, v. 57, no. 15, p. 3641-3659.

Karlsen, D. A., and Skeie, J. E., 2006, Petroleum migration, faults and overpressure, part I: calibrating basin modelling using petroleum in traps—a review: Journal of Petroleum Geology, v. 29, no. 3, p. 227-256.

Kugler, R. L., and McHugh, A., 1990, Regional diagenetic variation in Norphlet Sandstone: Implications for reservoir quality and the origin of porosity: Transactions of Gulf Coast Association of Geological Societies, v. 40, p. 411-423.

Lahann, R. W., 1980, Smectite diagenesis and sandstone cement; the effect of reaction temperature: Journal of Sedimentary Research, v. 50, no. 3, p. 755-760.

Land, L. S., and Dutton, S. P., 1979, Cementation of sandstones, reply: Journal of Sedimentary Petrology, v. 49, p. 1359-1361.

Land, L. S., Milliken, K. L., and McBride, E. F., 1987, Diagenetic evolution of Cenozoic sandstones, Gulf of Mexico sedimentary basin: Sedimentary Geology, v. 50, no. 1-3, p. 195-225.

Lander, R. H., Larese, R. E., and Bonnell, L. M., 2008, Toward more accurate quartz cement models: The importance of euhedral versus noneuhedral growth rates: Americam Association of Petroleum Geologists Bulletin, v. 92, no. 11, p. 1537-1563.

Larese, R. E., and Hall, D. L., 2003, Impact of interactive textural, compositional, and diagenetic controls on potential reservoir quality of low permeability sandstones (abst). : Americam Association of Petroleum Geologists Bulletin Annual Convention Program, v. 12.

Leder, F., and Park, W. C., 1986, Porosity reduction in sandstone by quartz overgrowth: American Association of Petroleum Geologists Bulletin, v. 70, no. 11, p. 1713.

Lehner, F. K., 1995, A model for intergranular pressure solution in open systems: Tectonophysics, v. 245, no. 3-4, p. 153-170.

Lima, R. D., and De Ros, L. F., 2002, The role of depositional setting and diagenesis on the reservoir quality of Devonian sandstones from the Solimões Basin, Brazilian Amazonia: Marine and Petroleum Geology, v. 19, no. 9, p. 1047-1071.

Lowry, W. D., 1956, Factors in loss of porosity by quartzose sandstones of Virginia: American Association of Petroleum Geologists Bulletin, v. 40, no. 3, p. 489-500.

Lynch, F. L., Mack, L. E., and Land, L. S., 1997, Burial diagenesis of illite/smectite in shales and the origins of authigenic quartz and secondary porosity in sandstones: Geochimica et Cosmochimica Acta, v. 61, no. 10, p. 1995-2006.

Maast, T. E., Jahren, J., and Bjorlykke, K., 2011, Diagenetic controls on reservoir quality in Middle to Upper Jurassic sandstones in the South Viking Graben, North Sea: American Association of Petroleum Geologists Bulletin, v. 95, no. 11, p. 1937-1958.

Makowitz, A., and Sibley, D., 2001, Crystal growth mechanisms of quartz overgrowths in a Cambrian quartz arenite: Journal of Sedimentary Research, v. 71, no. 5, p. 809-816.

Marchand, A. M. E., Haszeldine, R. S., Macaulay, C. I., Swennen, R., and Fallick, A. E., 2000, Quartz cementation inhibited by crestal oil charge: Miller deep water sandstone, UK North Sea: Clay Minerals, v. 35, no. 1, p. 201-210.

Marchand, A. M. E., Haszeldine, R. S., Smalley, P. C., Macaulay, C. I., and Fallick, A. E., 2001, Evidence for reduced quartz-cementation rates in oil-filled sandstones: Geology, v. 29, no. 10, p. 915-918.

Marchand, A. M. E., Macaulay, C. I., Haszeldine, R. S., and Fallick, A. E., 2002, Pore water evolution in oilfield sandstones: constraints from oxygen isotope microanalyses of quartz cement: Chemical Geology, v. 191, no. 4, p. 285-304.

Mathisen, M. E., and McPhearson, J. G., 1991, Volcaniclastic deposits: implications for hydrocarbon exploration, *in* Richard , V. F., and Gray, A. S., eds., Sedimentation in volcanic settings: , Volume 45, Society for Sedimentary Geology Special Publication, p. 27-36.

Maxwell, J. C., 1960, Experiments on compaction and cementation of sand: Rock Deformation: Geological Society of America, Memoir, v. 79, p. 105-132.

McBride, E. F., 1987, Diagenesis of the Maxon Sandstone (Early Cretaceous), Marathon region, Texas; a diagenetic quartzarenite: Journal of Sedimentary Research, v. 57, no. 1, p. 98-107.

-, 1989, Quartz cement in sandstones: a review: Earth-Science Reviews, v. 26, no. 1, p. 69-112.

Merriman, R. J., and Frey, M., 1999, Patterns of very low grade metamorphism in metapelitic rocks, *in* Frey, M., and Robinson, D., eds., Low Grade Metamorphism: Oxford, Blackwell Sciences, p. 61-107.

Molenaar, N., Cyziene, J., Sliaupa, S., and Craven, J., 2008, Lack of inhibiting effect of oil emplacement on quartz cementation: Evidence from Cambrian reservoir sandstones, Paleozoic Baltic Basin: Geological Society of America Bulletin, v. 120, no. 9-10, p. 1280-1295.

Morad, S., Al-Ramadan, K., Ketzer, J. M., and De Ros, L. F., 2010, The impact of diagenesis on the heterogeneity of sandstone reservoirs: A review of the role of depositional facies and sequence stratigraphy: American Association of Petroleum Geologists Bulletin, v. 94, no. 8, p. 1267-1309.

Moraes, M. A. S., and De Ros, L. F., 1990, Infiltrated clays in fluvial Jurassic sandstones of Recôncavo Basin, northeastern Brazil: Journal of Sedimentary Research, v. 60, no. 6, p. 809-819.

Munz, I. A., Johansen, H., Holm, K., and Lacharpagne, J. C., 1999, The petroleum characteristics and filling history of the Frøy field and the Rind discovery, Norwegian North Sea: Marine and Petroleum Geology, v. 16, no. 7, p. 633-651.

Murphy, W. M., Oelkers, E. H., and Lichtner, P. C., 1989, Surface reaction versus diffusion control of mineral dissolution and growth rates in geochemical processes: Chemical Geology, v. 78, no. 3, p. 357-380.

Nedkvitne, T., Karlsen, D. A., Bjorlykke, K., and Larter, S. R., 1993, Relationship between reservoir diagenetic evolution and petroleum emplacement in the Ula Field, North Sea: Marine and Petroleum Geology, v. 10, no. 3, p. 255-270.

Neilson, J. E., Oxtoby, N. H., Simmons, M. D., Simpson, I. R., and Fortunatova, N. K., 1998, The relationship between petroleum emplacement and carbonate reservoir quality: examples from Abu Dhabi and the Amu Darya Basin: Marine and Petroleum Geology, v. 15, no. 1, p. 57-72.

Oelkers, E. H., Bjorkum, P. A., and Murphy, W. M., 1996, A petrographic and computational investigation of quartz cementation and porosity reduction in North Sea sandstones: American Journal of Science, v. 296, no. 4, p. 420-452.

Osborne, M., and Haszeldine, S., 1993, Evidence for resetting of fluid inclusion temperatures from quartz cements in oilfields: Marine and Petroleum Geology, v. 10, no. 3, p. 271-278.

Pagel, M., Walgenwitz, F., and Dubessy, J., 1986, Fluid inclusions in oil and gas-bearing sedimentary formations: Collection colloques et séminaires-Institut français du pétrole, no. 44, p. 565-583.

Parnell, J., Middleton, D., Honghan, C., and Hall, D., 2001, The use of integrated fluid inclusion studies in constraining oil charge history and reservoir compartmentation: examples from the Jeanne d'Arc Basin, offshore Newfoundland: Marine and Petroleum Geology, v. 18, no. 5, p. 535-549.

Peck, C. J., Elmore, R. D., Gale, P. N., and Carpenter, B., 1988, Porosity preservation and development in Prairie du Chien sandstone, Michigan basin: American Association of Petroleum Geologists Bulletin, v. 72, no. CONF-880301--.

Perry, E. A., and Hower, J., 1970, Burial diagenesis in Gulf Coast pelitic sediments: Clay and Clay Mineral, v. 18, p. 167-177.

Pirrie, D., 1991, Controls on the petrographic evolution of an active margin sedimentary sequence: the Larsen Basin, Antarctica, *in* Morton, A. C., Todd, S. P., and Haughton, P. D. W., eds., Geological Society, London, Special Publications, Volume 57, p. 231-249.

Pirrie, D., Ditchfield, P. W., and Marshall, J. D., 1994, Burial diagenesis and pore-fluid evolution in a Mesozoic back-arc basin: the Marambio Group, Vega Island, Antarctica: Journal of Sedimentary Research Section A: Sedimentary Petrology and Processes, no. 3, p. 541-552.

Pittman, E. D., Larese, R. E., and Heald, M. T., 1992, Clay coats: occurrence and relevance to preservation of porosity in sandstones: eds. Pittman, E. D., Origin, diagenesis, and petrophysics of clay minerals in sandstones: SEPM Special Publication, v. 47, p. 241-255.

Ramm, M., 1992, Porosity-depth trends in reservoir sandstones: theoretical models related to Jurassic sandstones offshore Norway: Marine and Petroleum Geology, v. 9, no. 5, p. 553-567.

Ramm, M., and Bjorlykke, K., 1994, Porosity depth trends in reservoir sandstones - assessing the quantitative effects of varying pore-pressure, temperature history and mineralogy, Norwegian shelf data: Clay Minerals, v. 29, no. 4, p. 475-490.

Ramm, M., Forsberg, A. W., and Jahren, J., 1997, Porosity-depth trends in deeply buried Upper Jurassic Reservoirs in the Norwegian Central Graben: an example of porosity preservation beneath the normal economic basement by grain coating microquartz: In: Reservoir quality prediction in sandstones and carbonates (eds. Kupecz, J.A., Gluyas, J. and Bloch, S.) American Association of Petroleum Geologists Memoir, v. 69, p. 177-200.

Renton, J. J., Heald, M. T., and Cecil, C. B., 1969, Experimental investigation of pressure solution of quartz: Journal of Sedimentary Petrology, v. 39, p. 1107-1117.

Rezaee, M. R., and Lemon, N. M., 1996, Influence of depositional environment on diagenesis and reservoir quality: Tirrawarra sandstone reservoir, southern Cooper Basin, Australia: Journal of Petroleum Geology, v. 19, no. 4, p. 369-391.

Robinson, A., and Gluyas, J., 1992a, Duration of quartz cementation in sandstones, North Sea and Haltenbanken Basins: Marine and Petroleum Geology, v. 9, no. 3, p. 324-327.

-, 1992b, Model calculations of loss of porosity in sandstones as a result of compaction and quartz cementation: Marine and Petroleum Geology, v. 9, no. 3, p. 319-323.

Roedder, E., and Bodnar, R. J., 1997, Fluid inclusion studies of hydrothermal ore deposits: Geochemistry of hydrothermal ore deposits, v. 3, p. 657-697.

Rutter, E. H., 1983, Pressure Solution in Nature, Theory and Experiment: Journal of the Geological Society, v. 140, no. Sep, p. 725-740.

Ryan, P. C., and Reynolds, R. C., 1996, The origin and diagenesis of grain-coating serpentine-chlorite in Tuscaloosa Formation sandstone, US Gulf Coast: American Mineralogist Journal, v. 81, no. 1-2, p. 213-225.

Saigal, G. C., Bjorlykke, K., and Larter, S., 1992, The effects of oil emplacement on diagenetic processes - examples from the Fulmar Reservoir sandstones, central North Sea: American Association of Petroleum Geologists Bulletin, v. 76, no. 7, p. 1024-1033.

Sathar, S., Worden, R. H., Faulkner, D. R., and Smalley, P. C., 2012, The Effect of Oil Saturation On the Mechanism of Compaction In Granular Materials: Higher Oil Saturations Lead To More Grain Fracturing and Less Pressure Solution: Journal of Sedimentary Research, v. 82, no. 8, p. 571-584.

Shammari, S., Franks, S., and Soliman, O., 2011, Depositional and facies controls on infiltrated/Inherited clay coatings: Unayzah sandstones; Saudi Arabia, American Association of Petroleum Geologist Annual conference and exhibition: Houston, Texas, USA.

Sheldon, H. A., Wheeler, J., Worden, R. H., and Cheadle, M. J., 2003, An analysis of the roles of stress, temperature, and pH in chemical compaction of sandstones: Journal of Sedimentary Research, v. 73, no. 1, p. 64-71.

-, 2004, An Analysis of the Roles of Stress, Temperature, and pH in Chemical Compaction of Sandstones: Reply: Journal of Sedimentary Research, v. 74, no. 3, p. 449-450.

Siever, R., 1959, Petrology and geochemistry of silica cementation in some Pennsylvanian sandstones, *in* Ireland, H. A., ed., Silica in sediments: Society for Sedimentary Geolgist Spececial Publication, Volume 7, p. 55-79.

Small, J. S., Hamilton, D. L., and Habesch, S., 1992, Experimental simulation of clay precipitation within reservoir sandstones: techniques and examples: Journal of Sedimentary Petrology, v. 62, no. 3, p. 508-519.

Sprunt, E. S., and Nur, A., 1977, Experimental study of the effects of stress on solution rate: Journal of Geophysical Research, v. 82, no. 20, p. 3013-3022.

Stockdale, P. B., 1922, Stylolites: Their nature and origin, Indiana University press, v. 55, 97 p.:

Stone, W. N., and Siever, R., 1996, Quantifying compaction, pressure solution and quartz cementation in moderately-and deeply-buried quartzose sandstones from the Greater Green River Basin, Wyoming, *in* Crossey, J. L., Loucks, R.,

and Totten, M. W., eds., Siliciclastic diagenesis and fluid flow: Concepts and applications, Volume 55: Tulsa, Oklahoma, Society for Sedimentary Geology Special Publication p. 125-150.

Storvoll, V., Bjørlykke, K., Karlsen, D., and Saigal, G., 2002, Porosity preservation in reservoir sandstones due to grain-coating illite: a study of the Jurassic Garn Formation from the Kristin and Lavrans fields, offshore Mid-Norway: Marine and Petroleum Geology, v. 19, no. 6, p. 767-781.

Tada, R., and Siever, R., 1989, Pressure solution during diagenesis: Annual Review of Earth and Planetary Sciences, v. 17, p. 89.

Taylor, K. G., Gawthorpe, R. L., and Fannon-Howell, S., 2004, Basin-scale diagenetic alteration of shoreface sandstones in the Upper Cretaceous Spring Canyon and Aberdeen Members, Blackhawk Formation, Book Cliffs, Utah: Sedimentary Geology, v. 172, no. 1-2, p. 99-115.

Taylor, K. G., and Machent, P. G., 2010, Systematic sequence-scale controls on carbonate cementation in a siliciclastic sedimentary basin: Examples from Upper Cretaceous shallow marine deposits of Utah and Coloradao, USA: Marine and Petroleum Geology, v. 27, no. 7, p. 1297-1310.

Taylor, T. R., Giles, M. R., Hathon, L. A., Diggs, T. N., Braunsdorf, N. R., Birbiglia, G. V., Kittridge, M. G., Macaulay, C. I., and Espejo, I. S., 2010, Sandstone diagenesis and reservoir quality prediction: Models, myths, and reality: American Association of Petroleum Geologists Bulletin, v. 94, no. 8, p. 1093-1132.

Thomson, A., 1979, Preservation of porosity in the deep Woodbine/Tuscaloosa trend, Louisiana: Gulf Coast Association of Geological Societies Transactions, v. 30, p. 396-403.

Thyberg, B., and Jahren, J., 2011, Quartz cementation in mudstones: sheet-like quartz cement from clay mineral reactions during burial: Petroleum Geoscience, v. 17, no. 1, p. 53-63.

Totten, M. W., and Blatt, H., 1996, Sources of silica from the illite to muscovite transformation during late-stage diagenesis of shales, *in* Crosser, L., Loucks, R., and Totten, M. W., eds., Society for Sedimentary Geologist Special Publication, Volume 55, p. 85-102.

Towe, K. M., 1962, Clay mineral diagenesis as a possible source of silica cement in sedimentary rocks: Journal of Sedimentary Research, v. 32, no. 1, p. 26-28.

Uuoa, M. N., 1991, Smectite-to-chlorite transformation in thermally metamorphosed volcanoclastic rocks in the Kamikita area, northern Honshu, Japan Arsuyuxr lNour: American Minerologist Journal, v. 76, p. 682-640.

Vagle, G. B., Hurst, A., and Dypvik, H., 1994, Origin of quartz cements in some sandstones from the Jurassic of the Inner Moray Firth (UK): Sedimentology, v. 41, no. 2, p. 363-377.

van de Kamp, P. C., 2008, Smectite-illite-muscovite transformations, quartz dissolution, and silica release in shales: Clays and Clay Minerals, v. 56, no. 1, p. 66-81.

Van den Kerkhof, A. M., and Hein, U. F., 2001, Fluid inclusion petrography: Lithos, v. 55, no. 1-4, p. 27-47.

Walderhaug, O., 1990, A fluid inclusion study of quartz cemented sandstones from offshore mid-Norway - possible evidence for continued quartz cementation

during oil emplacement: Journal of Sedimentary Petrology, v. 60, no. 2, p. 203-210.
-, 1994, Temperatures of quartz cementation in Jurassic sandstones from the Norwegian continental shelf; evidence from fluid inclusions: Journal of Sedimentary Research, v. 64, no. 2a, p. 311-323.
-, 1996, Kinetic modeling of quartz cementation and porosity loss in deeply buried sandstone reservoirs: American Association of Petroleum Geologists Bulletin, v. 80, no. 5, p. 731-745.
Walderhaug, O., and Bjorkum, P. A., 2003, The effect of stylolite spacing on quartz cementation in the Lower Jurassic Sto Formation, southern Barents Sea: Journal of Sedimentary Research, v. 73, no. 2, p. 146-156.
Warren, E. A., and Pulham, A. J., 2001, Anomalous porosity and permeability preservation in deeply buried Tertiary and Mesozoic sandstones in the Cusiana field, Ilanos foothills, Colombia: Journal of Sedimentary Research, v. 71, no. 1, p. 2-14.
Weaver, C. E., 1956, The distribution and identification of mixed-layer clay in sedimentary rocks: American Association of Mineralogist Journal, v. 141, p. 202-221.
-, 1958, Geologic interpretation of argillaceous sediments. Part I. Origin and significance of clay minerals in sedimentary rocks: American Association of Petroleum Geologists Bulletin, v. 42, no. 2, p. 254-271.
Weedman, S. D., Brantley, S. L., Shiraki, R., and Poulson, S. R., 1996, Diagenesis, compaction, and fluid chemistry modeling of a sandstone near a pressure seal: Lower Tuscaloosa Formation, Gulf Coast: Americam Association of Petroleum Geologists Bulletin, v. 80, no. 7, p. 1045-1064.
Weibel, R., Friis, H., Kazerouni, A. M., Svendsen, J. B., Stokkendal, J., and Poulsen, M. L. K., 2010, Development of early diagenetic silica and quartz morphologies—Examples from the Siri Canyon, Danish North Sea: Sedimentary Geology, v. 228, no. 3, p. 151-170.
Wilkinson, M., Haszeldine, R. S., and Fallick, A. E., 2006, Hydrocarbon filling and leakage history of a deep geopressured sandstone, Fulmar Formation, United Kingdom North Sea: American Association of Petroleum Geologists Bulletin, v. 90, no. 12, p. 1945-1961.
Wilkinson, M., and Haszledine, R. S., 1996, Aluminium loss during sandstone diagenesis: Journal of the Geological Society, v. 153, no. 5, p. 657-660.
Wilkinson, M., Milliken, K. L., and Haszeldine, R. S., 2001, Systematic destruction of K-feldspar in deeply buried rift and passive margin sandstones: Journal of the Geological Society, v. 158, no. 4, p. 675-683.
Williams, L. B., Hervig, R. L., and Bjorlykke, K., 1997, New evidence for the origin of quartz cements in hydrocarbon reservoirs revealed by oxygen isotope microanalyses: Geochimica et Cosmochimica Acta, v. 61, no. 12, p. 2529-2538.
Wilson, M. D., 1992, Inherited grain-rimming clays in sandstones from eolian and shelf environments: their origin and control on reservoir properties: in D. W. Houseknecht, & E. D. Pittman, eds., Origin, diagenesis, and petrophysics of clay minerals in sandstones: Society for Sedimentary Geology Special Publication, v. 47, p. 209-225.

Wilson, M. D., and Pittman, E. D., 1977, Authigenic clays in sandstones; recognition and influence on reservoir properties and paleoenvironmental analysis: Journal of Sedimentary Research, v. 47, no. 1, p. 3-31.

Wilson, M. D., and Stanton, P. T., 1994, Diagenetic mechanisms of porosity and permeability reduction and enhancement, *in* Wilson, M. D., ed., Reservoir quality assesment and prediction in clastic rocks, Volume 21, Society of Sedimentary Petrologist, p. 59-118.

Wong, P. K., and Oldershaw, A., 1981, Burial cementation in the Devonian, Kaybob reef complex, Alberta, Canada: Journal of Sedimentary Research, v. 51, no. 2, p. 507-520.

Wood, J. R., and Boles, J. R., 1991, Evidence for episodic cementation and diagenetic recording of seismic pumping events, North Coles Levee, California, USA: Applied Geochemistry, v. 6, no. 5, p. 509-521.

Wood, J. R., and Hewett, T. A., 1982, Fluid convection and mass transfer in porous sandstones—a theoretical model: Geochimica et Cosmochimica Acta, v. 46, no. 10, p. 1707-1713.

Worden, R. H., and Barclay, S. A., 2003, The effect of oil emplacement on diagenetic clay mineralogy: The Upper Jurassic Magnus Sandstone Member, North Sea: In: Clay mineral cements in sandstones (eds. Worden, R.H. and Morad, S.) International Association of Sedimentologists Special Publications, v. 34, p. 453-469.

Worden, R. H., French, M. W., and Mariani, E., 2012, Amorphous silica nanofilms result in growth of misoriented microcrystalline quartz cement maintaining porosity in deeply buried sandstones: Geology, v. 40, no. 2, p. 179-182.

Worden, R. H., and Morad, S., 2000, Quartz cementation in sandstones: a review of the key controversies *in* Worden, R. H., and Morad., S., eds., Quartz cementation in sandstones International Association of Sedimentologists Special Publication v. 29, p. 1-20.

Worden, R. H., and Morad, S., 2003, Clay minerals in sandstones: controls on formation, distribution and evolution, *in* Worden, R. H., and Morad, S., eds., Clay Cements in Sandstones, International Association of Sedimentologist Special Publication, 34 Wiley Online Library, p. 3-9.

Worden, R. H., Oxtoby, N. H., and Smalley, P. C., 1998, Can oil emplacement prevent quartz cementation in sandstones?: Petroleum Geoscience, v. 4, no. 2, p. 129-137.

Worden, R. H., Warren, E. A., Smalley, P. C., Primmer, T. J., and Oxtoby, N. H., 1995, Discussion of evidence for resetting of fluid inclusion temperatures from quartz cements in oilfields' by Osborne and Haszeldine (1993): Marine and Petroleum Geology, v. 12, no. 5, p. 566-570.

Yeh, H. W., and Savin, S. M., 1977, Mechanism of burial metamorphism of argillaceous sediments: O-isotope evidence: Geological Society of America Bulletin, v. 88, no. 9, p. 1321-1330.

CHAPTER 3

3. Diagenesis and reservoir quality of the shallow marine sandstones of Ula field, offshore Norway

3.1 Abstract

The Upper Jurassic Ula Formation sandstone is the principal reservoir rock in the Ula oil field, located in the southern part of the Norwegian sector of the North Sea. Detailed petrographic study of the Ula Formation sandstone was carried out on core samples recovered from oil wells using light optics, scanning electron microscope, X-ray diffraction (XRD), carbonate stable isotope analysis and fluid inclusion studies. The Ula Formation sandstones are dominantly very fine to very coarse-grained; moderately to well sorted arkosic sandstones. The main diagenetic cements are quartz overgrowths, grain coating microcrystalline quartz, K-feldspar cement, illite, dolomite and minor amounts of calcite, chlorite and pyrite. Kaolinite is conspicuously absent which might be the result of reactions with K-feldspar producing illite and quartz cement. Fluid inclusion evidence shows that quartz cementation is a continuous process and is still taking place in the field. Stable isotope data show that the carbonate cements in the oil leg grew at about 100 ± 8^{o}C, before oil emplacement, and were largely sourced from dissolved and precipitated bioclastic debris. Precipitation of carbonate cement in the oil leg stopped at 104 ± 8^{o}C but carbonate cements in the water carried on growing to higher temperature (150 ± 8^{o}C) and show progressive input of source-rock derived CO_2 (as the carbon isotopes get progressively lighter). The formation water has changed from high to low salinity during diagenesis probably as a result of meteoric water flushing meteoric water.

Reservoir quality is primarily controlled by a combination of depositional facies, mechanical compaction and quartz cementation. Quartz cement was sourced internally from stylolites, grain-grain pressure solution, alteration of detrital feldspar and transformation of smectite to illite and chlorite. Distribution and abundance of quartz cement is mainly controlled by pore fluid type and the occurrence of early

formed grain coating microcrystalline quartz. Chlorite occurs as pore filling clay and played no more than a limited role in porosity preservation.

3.2 Introduction

Diagenesis comprises a broad spectrum of physical, chemical and biological post depositional process by which original sedimentary mineral assemblages and their interstitial pore waters interact in an attempt to reach textural and thermodynamic equilibrium with the environment (Worden and Barclay, 2003). The complex and variable interplay of factors such as sand composition, texture, and fluid chemistry under conditions of variably increasing temperature and effective stress through time yields a wide range of potential outcomes with respect to reservoir porosity and permeability (Taylor et al., 2010). During burial the deposited sand never retains its original porosity, fabric or mineralogy as it becomes sandstone (Worden and Barclay, 2003). Three main processes occur during diagenesis; compaction, mineral dissolution and mineral precipitation. In addition, alteration of detrital grains and minerals also take place but this is a special case of dissolution and precipitation at the same site (Worden and Barclay, 2003). Compaction includes mechanical rearrangement of grains and chemical compaction (also known as pressure solution). Cementation in sandstones is dominated by growth of quartz, clay mineral, carbonate and other cements (e.g. anhydrite, barite) and even feldspars can be volumetrically-important.

Reservoir quality depends on the presence of porosity and the connectivity of the pores (controlling permeability) of the reservoir rock. There are many aspects of diagenesis which are still controversial even though it is an important control on the prospectivity during petroleum exploration. Reservoir quality also influences well locations during appraisal and reservoir management. Assessing reservoir quality is important especially in plays and prospects where the reservoir sandstone has been exposed to elevated temperatures (>100 ^{o}C) and high effective stress for significant period of geologic times as in the Upper Jurassic sandstones of Ula field. It is important to understand the controls on reservoir quality and diagenetic changes in sandstones so that it is possible to predict reservoir quality distribution in the subsurface. It is very important to understand the geological process controlling the

evolution of pore systems in the Ula reservoirs. Depositional system which controls the initial distribution of lithofacies (especially grain size and clay content) should be understood as they influence the post depositional diagenetic activities of the sandstones.

In this paper we report a study of the shallow marine, Upper Jurassic sandstone in the Ula field, Norwegian North Sea to assess key factors that control the reservoir quality. Key questions to be addressed are:

1. What are the most volumetrically important cements?
2. What is the paragenetic sequence of events?
3. What are the sources of the diagenetic minerals?
4. What controls the reservoir quality of the Ula Formation sandstone?
5. What diagenetic process occurred in the shallow marine sandstone?

3.3 Geological background

The Ula field (in Norwegian: *Ula feltet*) is an offshore oil field situated in the Central Graben of the North Sea in block 7/12, 280 km south-west of Stavanger (Fig. 3.1) in a water depth of about 70m. The field consists of Upper Triassic to Upper Jurassic sandstones in an anticlinal structure. The structure is a result of Upper Jurassic rifting followed by inversion in the Cretaceous and Tertiary (Brown et al., 1992). Oil was generated from the Upper Jurassic Mandal Formation (equivalent to the Kimmeridge Clay Formation) beginning in the Late Cretaceous from the deeper parts of the Central Graben and currently being generated within the Ula trend (Taylor et al., 1999). The reservoir rock is the Upper Jurassic Ula Formation (Fig. 3.2); (Bergan et al., 1989; Karlsen et al., 1993; Partington et al., 1993; Underhill, 1998). This unit is a shallow marine sandstone up to 200m thick that prograded across outer-shelf mudstones, following a sea level fall in the Kimmeridgian (Harris, 2006). The Ula Formation sandstones are typically fine-grained, well sorted and highly biotubated with beds rich in lithic shale fragments. The Ula Formation unconformably overlies the partly-eroded Middle Jurassic to Triassic fluvial Skagerrak Formation (Fig. 3.2). This unit is in turn overlain by Late

Jurassic Mandal mudstones, which include the Upper Jurassic source rock (Wilhelms and Larter, 1994).

The Ula Formation sandstone has been intensively burrowed. Even where burrows are not apparent, physical sedimentary structures are nonetheless absent. This suggests that the unit may have been completely biotubated. Trace fossils are dominated by *Ophiomorpha*, suggesting a shallow marine origin for the sandstone (Brown et al., 1992). The Ula Formation sandstone was interpreted as shallow marine on the basis of their bioclastic content (mostly bivalves and belemnites), microflora, ichnofacies (*Opiomorpha, Teichichnus, Rhizocorallium, Chondrites*) and the presence of glauconite (Bjornseth and Gluyas 2006).

The Ula Formation sandstone has undergone more than 2000m of subsidence since the early Oligocene (Harris, 2006). The Ula Formation sandstone is overpressured; multiple pressure measurement by repeat formation tester (RFT) gave an average gradient of 0.703 psi/foot (15.9 Mpa/km), in Jurassic sandstones of the Central Graben equivalent to a significantly higher fluid pressure than hydrostatic pressure within the formation.

The Ula Formation sandstones have-lower-than expected overpressures compared with overpressures in the overlying Chalk and on the opposite margin of the Central Graben at the same burial depth (O'Connor et al., 2001). This high pressure is considered to be the result of a combination of rapid late Tertiary subsidence (Harris, 2006) and petroleum generation in the overlying Upper Jurassic organic rich Mandal Formation (Nedkvitne et al., 1993). Porosity values in the Ula Formation range mostly between 14% and 28%, with permeabilities within therange 650 - 850 mD in the better reservoir units (extremes 0.2-2800 mD) (Karlsen et al., 1993). The reservoir temperature at 3450 m is between 143 and 145^{o}C (Home, 1987).

The Ula Formation sandstone in the Ula field has been described as arkosic (Gluyas, 1997) and has been interpreted as being derived from nearby Triassic sandstones. Gluyas (1997) also stated that Ula sandstones are significantly affected by quartz cementation, with quartz cement volume as determined from point

counting ranged from as little as 3% to as much as 19%. The variation in quartz cement volume, which occurs over a very narrow range of burial depths, was considered to have been controlled principally by the timing of cementation relative to oil emplacement. Where oil was emplaced relatively early, formation of quartz cement was inhibited, and cement volumes are low; in rocks where oil was emplaced late or not at all and in water legs, quartz cement volumes are high. However, the high porosity in the Ula Formation sandstones in Ula and Gyda fields has been attributed to the presence of grain coating microcrystalline quartz, seen under SEM examination (Aase et al., 1996). The microcrystalline quartz was interpreted to have been sourced from primary depositional sponge spicules.

This work was largely intended to establish the general suite of controls on reservoir quality in the Ula Formation sandstones in the Ula field.

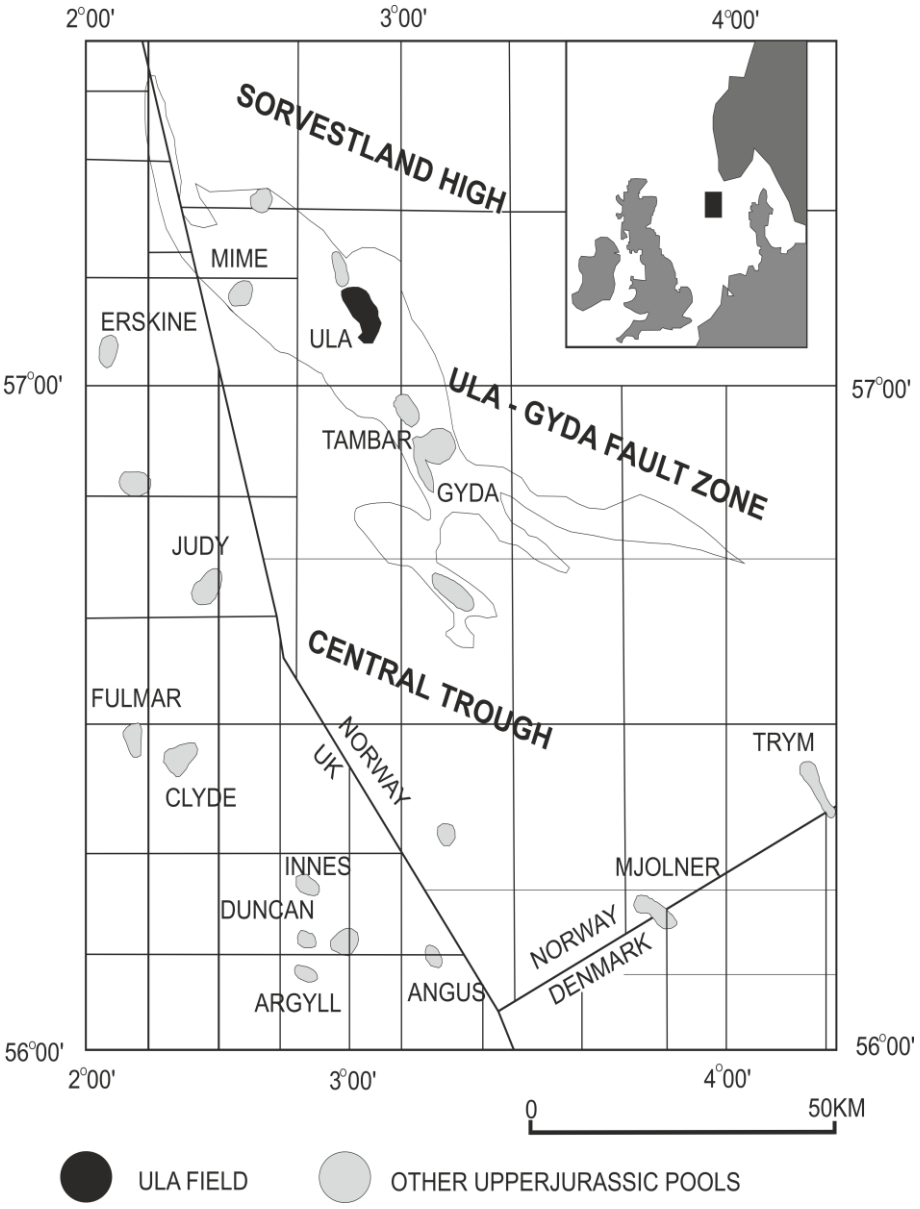

Figure 3. 1 Regional map of the Central Graben showing the Ula field (modified from Bjornseth and Gluyas., 1993).

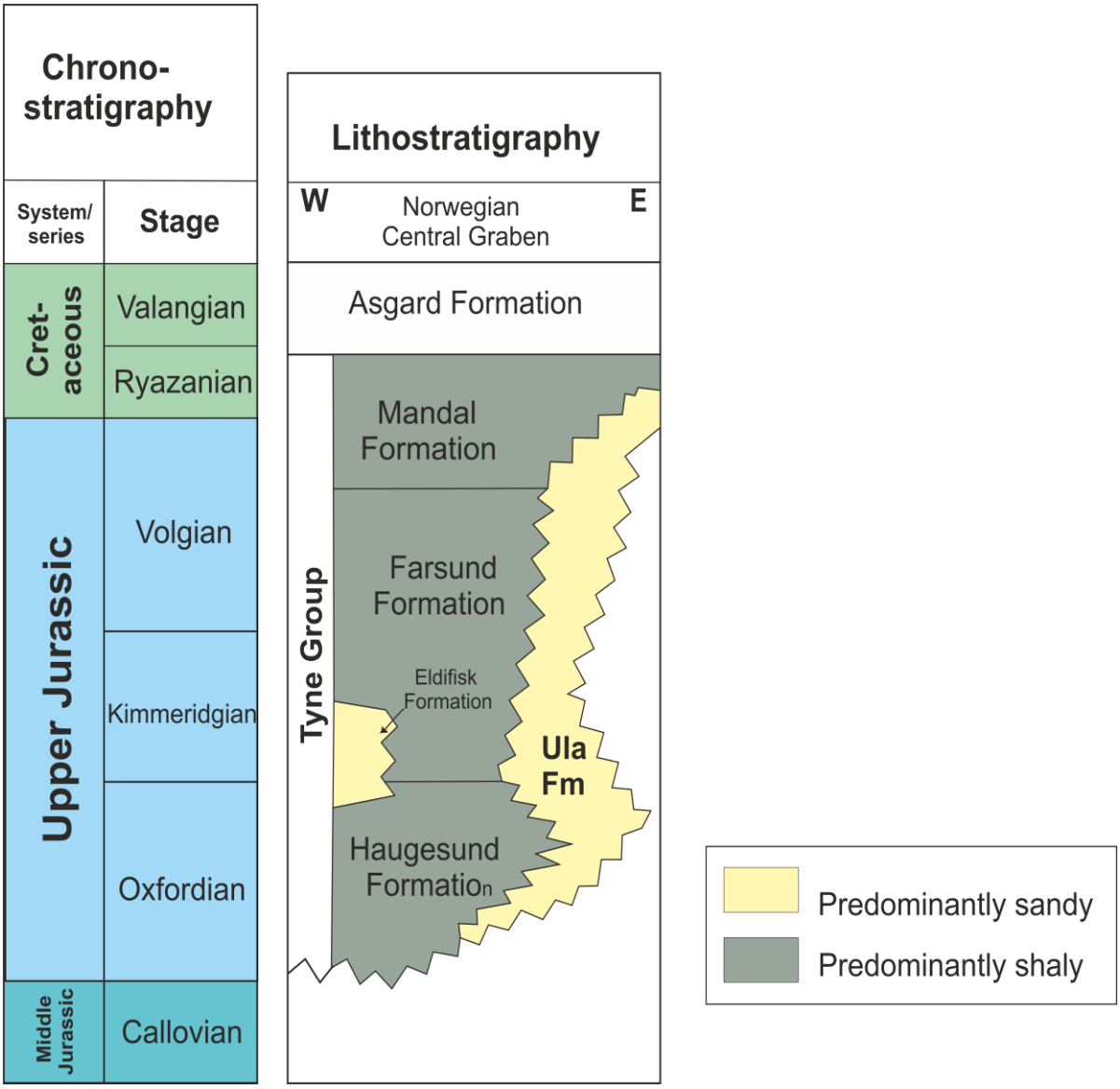

Figure 3. 2 Generalised stratigraphy of the Norwegian Central Graben

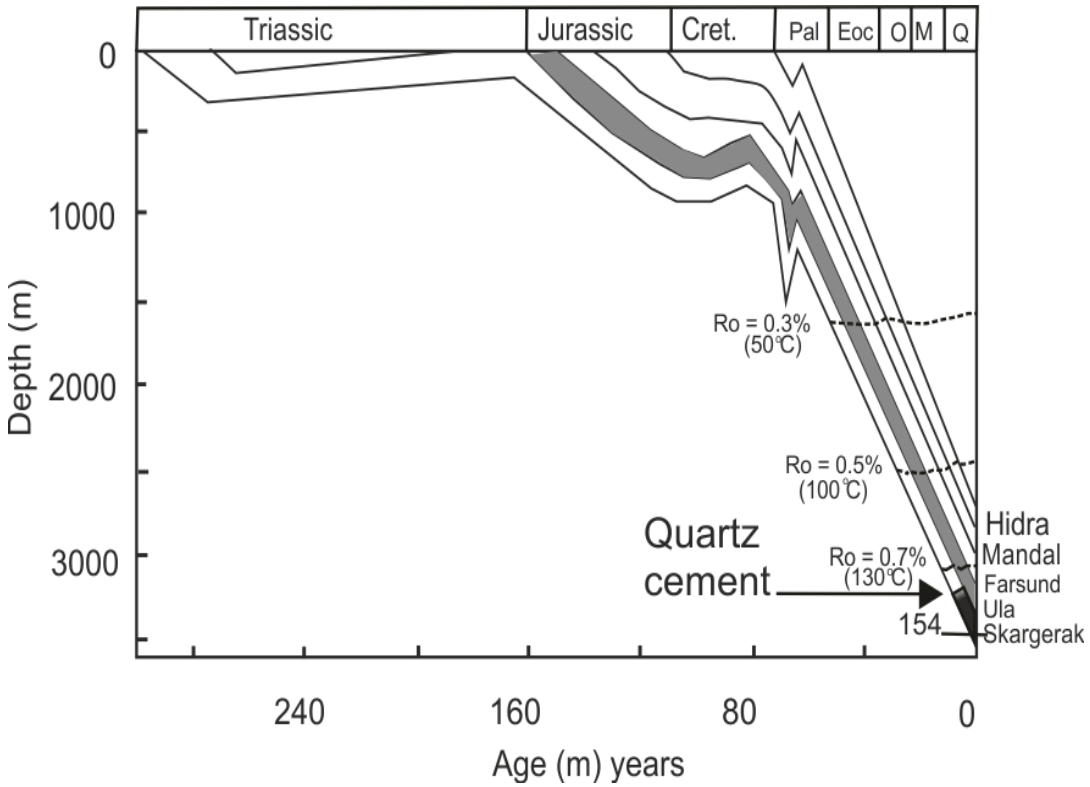

Figure 3. 3 Burial history curve for the Ula field showing related tectonics and temperatures modelled using Thermomodel for windows. Assumed constant thermal gradient of 40^{O}C/1000m

3.4 Methods and material

One hundred and fifteen samples of conventional core materials from five wells were obtained from the BP core store in Reslab laboratories in Stavanger, Norway. In addition core analysis data, wireline log data (gamma, sonic, density, resistivity, neutron porosity), well reports and maps were also available for this study. The core samples cover the range of present subsurface depth 3350 m to 4100 m true vertical depth (TVD), and they span the thickness of the reservoir. Individual sandstones were studied using a combination of techniques including; petrography, scanning electron microscopy (SEM), cathodoluminescence microscopy (CL), X-ray diffraction (XRD), fluid inclusion micro-thermometry and stable isotope analysis.

Polished thin sections were made from the core samples. The polished sections were impregnated with blue resin in order to highlight porosity and stop samples disaggregating during sample preparation. Sandstone modal compositions were

obtained by detailed point counting (400 counts per section) of all thin sections. Grain sizes were measured and grain coatings were determined using a Meiji 9000 transmitted light microscope fitted with an Infinity 1.5 digital camera. Images were collected and long axes of 100 grains were measured using Infinity Analyser software. No correction was carried out for cut effect. Fifty grains per section were measured for percentage grain coverage using visual estimate. Grain areas with coatings mainly by microcrystalline quartz, bitumen and clay materials were measured. Only surfaces where quartz could grow, or would grow, if not because of the occurrence of thin, grain rims material were considered. Surfaces in contact with neighbouring grains, detrital matrix, pore-filling cements that predates quartz cementation were excluded.

Scanning electron microscope examination was made using a Philips XL 30 SEM fitted with a tungsten filament at an accelerating voltage of 20 kV, and 8 nA beam current for both secondary electron imaging (SEI) and backscattered electron microscopy (BSEM). The SEM was fitted with a cathodoluminscence (CL) detector. BSEM was carried out on polished sections and SEI on freshly fractured, stub-mounted samples coated with carbon and gold respectively. Energy dispersive analysis of X-rays (EDAX) provided qualitative compositional analyses of individual points (approximately 5 μm spot size). Some of the broken core samples of sandstone samples had to be soaked, washed and rinsed in acetone for three nights to remove the oil staining (which caused problems for the gold coater and SEI imaging). The CL images were collected at 10 kV and spot size 7. They were collected by integrating the signal of 16 frames using a slow scanning raster which takes about 8 minutes to collect.

A PANalytical X'pert pro MPD X-Ray diffractometer was used for X-ray diffraction (XRD) analyses. Samples for XRD were cut from the core samples and then crushed using a McCrone micromill and distilled water for ten minutes. Samples were then dried overnight in a low temperature oven and powdered using an agate pestle and mortar. A copper X-ray source operating at 40kv and 40ma was used. Powdered samples were loaded into cavity holders and rotated continuously during the scan, completing one rotation every 2 seconds. Programmable anti-

scatter slits and a fixed mass maintained in an irradiated sample area of 10 x 15 mm, with an additional 2^o incident beam antiscatter slit producing a flat background in raw data 360^o. The X' Celerator detector was set to scan in continuous mode with full length active pulse-height discrimination levels set to 45 to 80%. Operation of the X-ray diffractometer and software to process the data was achieved using "HighScore Plus®" analysis software and automated Rietveld refinement methods with reference patterns from the International Centre for Diffraction Data; Powder Diffraction File-2 Release 2008.

Carbonate stable isotope analysis was carried out on 12 samples. These were the only samples that yielded sufficient carbon dioxide, following acid digestion of the dolomite in the samples that could be reliably used for analysis. Bulk samples were powdered and reacted with 100% phosphoric acid after 1 hour at 50^oC. The liberated CO_2 gas was analysed for carbon and oxygen isotope on a SIRA 12 mass spectrometer. The carbonate isotope data are presented in the normal δ notation relative to V-PDB (Craig, 1957). Stable isotope fractionation curves were used to calculate the temperature of $\delta^{18}O$ of the pore waters, which led to the precipitation of the dolomite cements (Land, 1983; O'Neil and Epstein, 1966) using the following equation.

$$1000 \ln \alpha_{\text{dolomite – water}} = (3.34 \times 10^6 \times T^2) - 3.34$$

Where,

$1000 \ln \alpha_{\text{mineral water-water}}$ = oxygen-isotope mineral water fractionation factor

T = Temperature in degrees Kelvin

Fluid inclusions microthermometric studies were carried out on selected samples. Fluid inclusion wafers were prepared from the core samples in the University of Birmingham. An Olympus BX-60 petrographic microscope equipped with heating and cooling stages which enables the temperature of phase transitions between -60^o to 600^0C to be observed with an accuracy of between ± 0.1 and $\pm 1.0^o$. Observations were made with different objective lens magnifications (10x, 20x, 50x and 100x). Inclusions were photographed with Digital Camera Olympus DP71 for the purpose

of the fast mapping of inclusion locations. Thermometric study was performed on a Linkam THMSG 600 Stage. All samples were studied for UV-luminescence using a UV source on the fluid inclusion microscope. The purpose of this was to check for the possible presence of liquid hydrocarbon (oil) inclusions. Fluorescence of fluid inclusions is typically caused by the presence of cyclic and aromatic hydrocarbons possessing benzene rings (which are C6 and higher). The majority of the inclusions observed were two-phase (liquid and vapour phase) aqueous inclusions. However, a population of hydrocarbon-bearing inclusions was recorded in two wells. Fluid inclusion last ice melting temperatures (Tm) were also determined and ultimately expressed as salinity (NaCl weight %) of the pore fluids from which the quartz cements precipitated. Fluid inclusion last melting temperatures were converted to corresponding weight percentage salinities using (Bodnar, 1993) conversion table derived from (Hall et al., 1988) with the assumption that effectively all the salinity is due to NaCl. The coolant used during freezing of the inclusion was liquid nitrogen.

Chinese version of Thermomodel for windows was used in modelling the burial history curve. Assumed surface seafloor temperature used was 5^{o}C and constant present geothermal gradient of 40^{o}C/km (Nedkvitne et al. 1993).

3.5 Sedimentology

The Ula Formation is best described as a shallow marine storm dominated sand sheet which has been subdivided into progradational and retrogradational depositional units (Bowman, 1981). The lithofacies classification for the Ula Formation sandstone is based on the one proposed by Caruthers (1992) which comprises of 1. Graded and structureless sandstones and shell coquinas ranging from fine to coarse grain without bioturbations. 2. Bioturbated sandstones without any apparent primary structures dominated by centimetre scale horizontal burrows of *Ophiomorpha/paleophycus* ichnofabrics ranging from fine to medium grain. 3. Very fine to fine grained, locally glauconitic sandstones showing centimetre scale laminated vertical and sub-horizontal burrows which are tentatively referred to Teichichnus*/Rhizocorallum* ichnofabric. 4. Cross stratified sandstones comprising of fine to medium decimetre

scale cross-beds which have not been included in this study. Summary of gamma logs of all the wells used and depth ranges of the core samples is given in Figure 3.4.

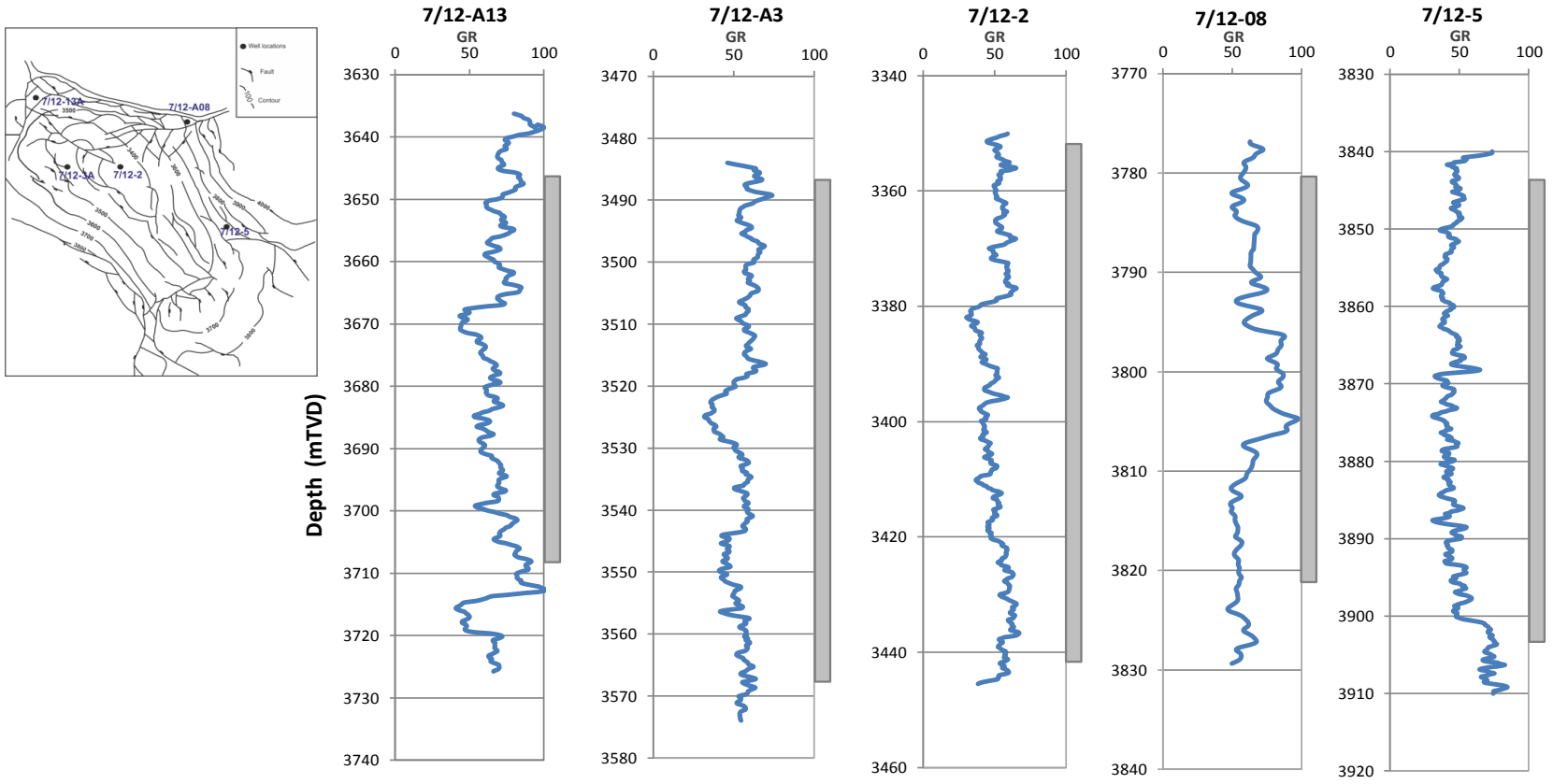

Figure 3. 4 Summary gamma logs of the wells used in this research work. Grey bars show the depth ranges of the core samples used. Left is a structural map of the Ula field showing the well locations.

3.5 Results

3.5.1 Petrography

3.5.1.1 Detrital mineralogy

The Ula Formation sandstone predominantly consists of very fine to coarse-grained, moderately sorted to poorly sorted, sub angular to sub rounded arkoses (Fig. 3.5) according to the classification of McBride (1963). It is texturally and mineralogically immature to sub-mature (19-25% feldspar). Detrital quartz grains, determined by point counting are comprised of monocrystalline quartz (av. 34 ± 2.5%); and poly crystalline quartz (av. 3.4 ± 0.7%) grains. Detrital feldspar is made up of plagioclase feldspar (11.6 ± 1.8%) and potassium feldspars (av. 11.2 ± 1.6%). The dominant types of lithic fragments are metamorphic and igneous (av. 2.5 ± 0.3%). Deformed mud intraclast is (av. 3.8 ± 0.8%). The proportion of K-feldspar and plagioclase are approximately equal in most samples with plagioclase slightly in excess of K-feldspar in samples from shallow depths.

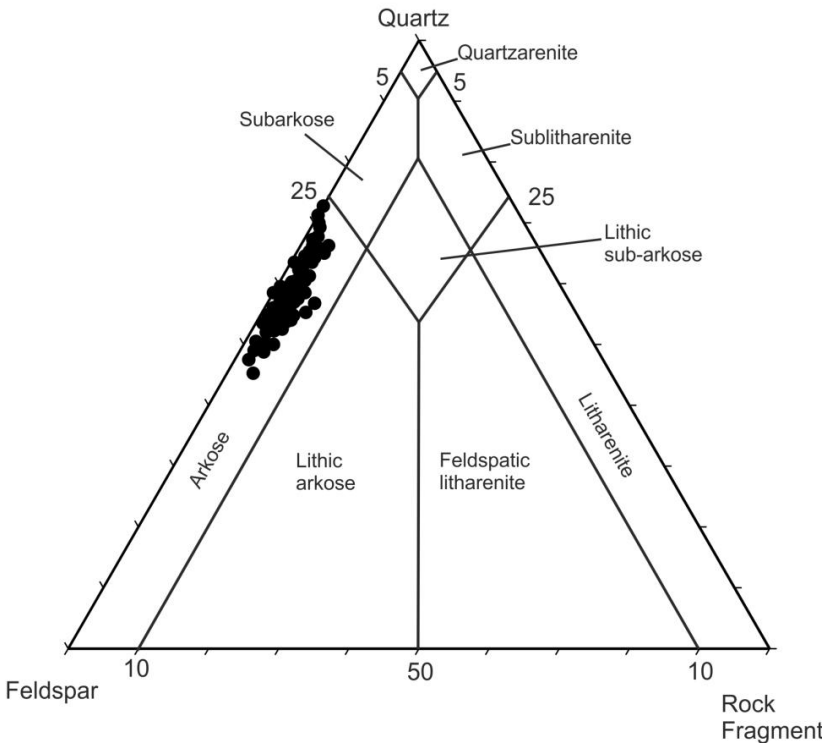

Figure 3. 5 Ternary diagram showing the Ula Formation sands classification (after McBride, 1963).

In some cases feldspar grains have been partially replaced by calcite or dolomite. Some detrital feldspar grains are coated with K-feldspar or albite cements while some have dissolved along cleavage planes. The lithic fragments are hard to identify since they have been extensively altered during diagenesis and deformed by compaction.

Detrital clays are present as patches and layers and they are more abundant in the very fine to fine-grained units (Fig.3. 10A). The highest clay content of 26% are found in the fine grained highly bioturbated facies with abundant microcrystalline quartz and the lowest clay of <1% are found in the coarse-grained graded sandstone with no evidence of bioturbation. Detrital clays are dispersed and commonly stylolitised. From the SEM observation and XRD analysis, the clay mineralogy is now dominated by illite and chlorite (Fig3.15). Bioclastic fossil fragments occur in small but variable amounts and are, but dominated by oyster and bivalve shell fragments (Fig. 3.11D). Glauconite (Fig. 3.10C) is more abundant in finer grained layers with relics of sponge spicule dissolution round holes (Fig. 3.9B) than other coarser grains.

Additional minor detrital components include shale fragments and heavy minerals (zircon, garnet and tourmaline, <1%). Mica (av. 1.5 ± 0.2%) is more abundant in finer grained, poorly sorted units. The mica flakes are not significantly deformed by compaction (Fig. 3.9B and 3.10B).

Bioturbation is widespread in the very fine to fine-grained units with higher proportions of bioclastic fragments. The bioclasts are locally replaced by framboid pyrite and sphalerite. Grain contacts range from point-long to sutured from matrix rich to matrix poor sandstones. Bitumen (Fig.3.7C) coating authigenic quartz are common in the samples from the oil leg but are not common in samples from the water leg and the transition zone.

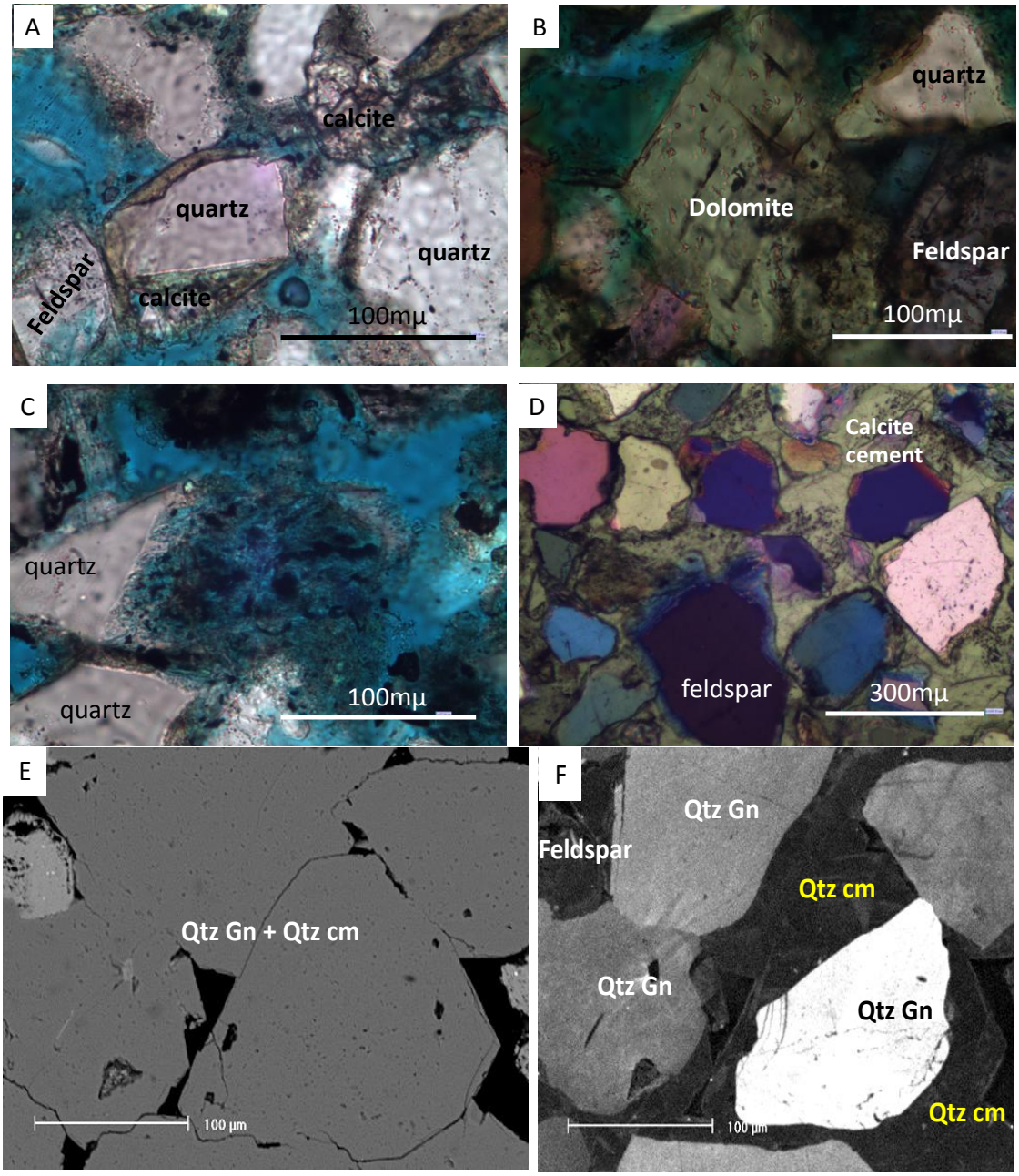

Figure 3. 6 Thin section images of sandstones of the Ula Formation (A) quartz grain with some evidence of calcite replacement at their edges (7/12-A3 3486.1mTVD) (B) early formed dolomite (7/12-A3 3489.66m TVD) (C) partially dissolved feldspar grain resulting in clay minerals and secondary porosity(7/12-A3 3509.66m TVD) (D) early formed calcite cement totally occluding porosity (7/12-A3 3524.1m TVD) (E) SEM-BSE quartz cemented sandstone (F) SEM-CL image of quartz cemented sandstone (same area as 5E) (7/12-A8 3800.2m TVD). The pair of BS and CL images clearly shows the amount of quartz cement.

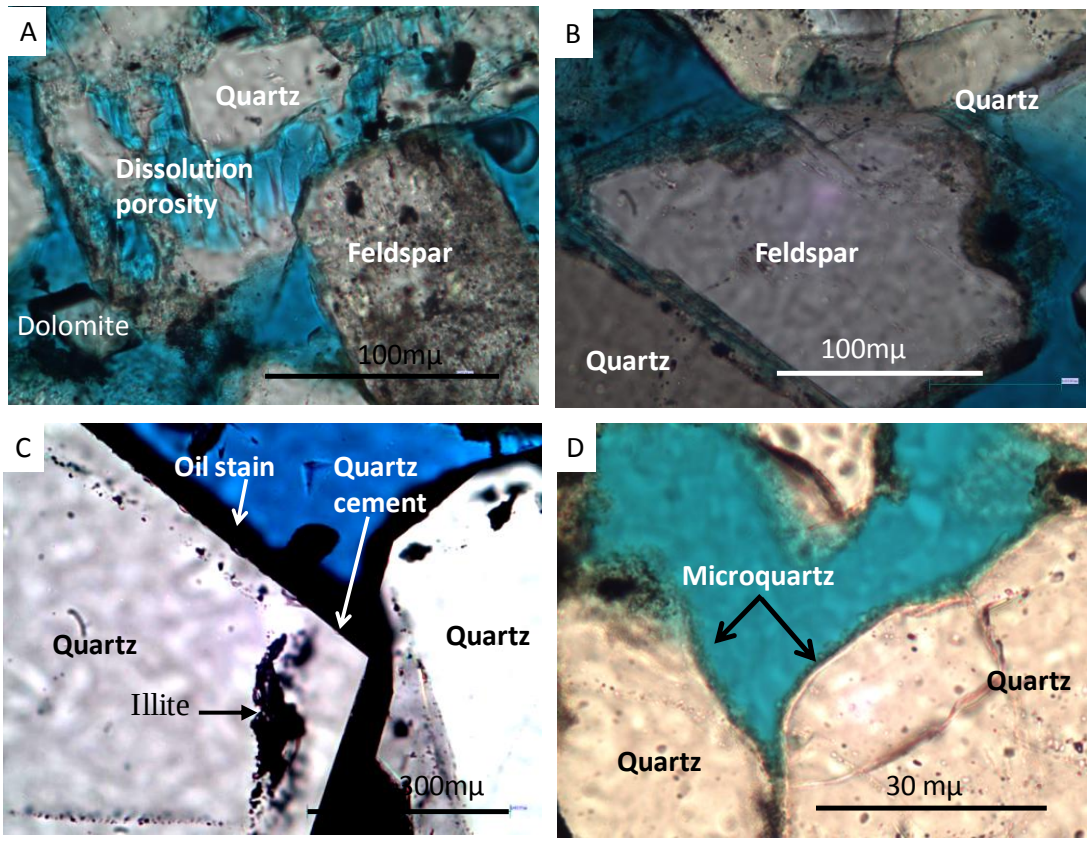

Figure 3. 7 Thin section images of Ula Formation sandstone (A) intragranular porosity from the dissolution of feldspar grains, plus an altered feldspar grain and pore-filling micro-rhombic dolomite (7/12-A3 3552.1m TVD) (B) partially-dissolved K-feldspar cement around the edges of detrital K-feldspar grain (7/12-A3 3489.66m TVD) (C) euhedral quartz overgrowth around detrital quartz grain covered by bitumen (7/12-A3 3571.9m TVD) (D) microcrystalline quartz coating detrital grain with preserved intergranular porosity (7/12-2 3387.4m TVD).

3.5.2 Authigenic mineralogy

The mineralogy and petropysical properties of the Ula Formation sandstone have undergone significant diagenetic modifications. Authigenic mineral cements, dissolution of unstable grains and compaction have modified the entire porosity and permeability of this reservoir rock. Authigenic minerals observed in thin sections and SEM microscopy are quartz cement, microcrystalline quartz, K-feldspar cement, albite cement, illite, chlorite, dolomite, calcite, dawsonite, halite framboidal pyrite, phosphate and sphalerite.

3.5.2.1 Quartz cements

Quartz cement (>10 µm – 50µm) thick is the most abundant authigenic mineral ranging from 0 to 18% in the Ula Formation sandstone. Quartz cement appear as overgrowths which is distinguished from the detrital grains in petrographic examination by the presence of dust rims and trains of fluid inclusions at the grain boundary. They are characteristically developed as incipient to large, well developed euhedral (Fig. 3.7C), pore-filling and pore-blocking syntaxial overgrowth. In some cases only the euhedral crystal outlines indicate the presence of quartz overgrowth. In such cases SEM-CL is employed to see the quantity of quartz overgrowth (e.g. Fig. 3.6E and F). Quartz overgrowths are more abundant and well developed in cleaner and coarser sandstones. In most wells it slightly increases in abundance with depth. The wells at the crest of the reservoir (7/12-A3 and 7/12-2) show lesser quartz cement (maximum of 7%) than wells at the flank (which show up to 18%). The early carbonate cemented horizons are notably quartz cement-free. The finer grain units, where microcrystalline quartz coats the detrital grains, show zero or negligible quartz cement. Quartz overgrowths envelop pyrite, dissolved feldspar, feldspar overgrowth and early formed microdolomite. Conversely, ferroan dolomite and late calcite cements crosscut (and seemingly post-date) quartz overgrowth (Fig. 3.8C and D). Zone with high oil saturation and no microquartz coating show low quartz cement volumes (av. 2 ± 0.2% high of 7%) compared to up to 18% in the water leg. Quartz cement volume might have been somewhat underestimated because of difficulty in defining the boundary with detrital grains in some samples.

3.5.2.2 Microcrystalline quartz

Microcrystalline quartz occurs as grain coating layers that grows into open pore space. They either directly grow on the host grain (Fig. 3.7D) or separated from the host grain by thin layer of cryptocrystalline silica (possibly chalcedony) which cannot be indexed by electron backscattered diffraction (EBSD). There are two forms of microcrystalline quartz in the Ula Formation sandstone; (i) fine (0.5-3.0 µm) and (ii) and coarser (>5 µm) (Fig. 3. 12C and D). The fine, forms are more associated with quartz cement. The amount of point counted microcrystalline quartz varies from 0-9%, but, it might have been underestimated considering its small size and difficulty in recognising it under petrographic microscope (Fig 3.7D). The distribution of microcrystalline quartz is related to facies and tends to be restricted to the very fine to fine-grained, highly bioturbated units with abundant detrital clay.

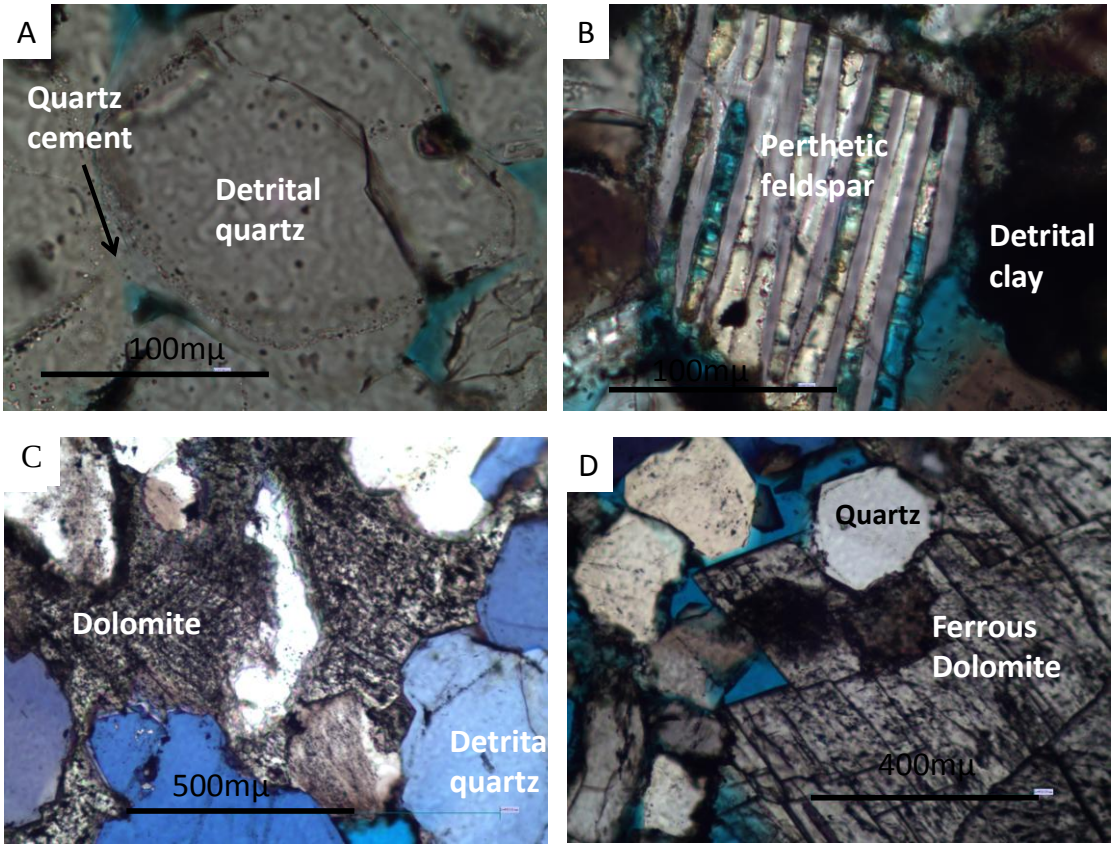

Figure 3. 8 Thin section photomicrograph of Ula Formation sandstone (A) quartz cemented sandstone in which bulk of the porosity is destroyed (7/12-A8 3792.63m TVD) (B) perthite undergoing dissolution along compositional planes of detrital grain (7/12-A8 3799.78m TVD) (C) late dolomite replacing all mineral grains (7/12-A8 3809.78m TVD) (D) late dolomite

enclosing quartz overgrowth showing that dolomite post-dated quartz cement precipitation (7/12-A8 3812.7m TVD) .

3.5.2.3 Carbonate cements

Dolomite, calcite, siderite and dawsonite occur as carbonate cements in the Ula Formation sandstone. The average volume of point counted dolomite is 5 ± 0.5%, calcite is 3%, while dawsonite is very rare. Dolomite occurs as rhombic micro-dolomite (Fig. 3.13C) and ferroan blocky spar which is both cementing and replacive in habit (Fig. 3.8D), replacing mainly feldspars, lithic fragments and matrix. Ferroan dolomite overlies and crosscuts quartz cement and is the most abundant carbonate cement in the Ula field. The rhombic microdolomite is seen at many locations being enveloped by quartz overgrowth. SEM-CL images reveal zoning in the microrhombic dolomites (Fig. 3.14B).

Calcite is less common than the dolomite cement in the Ula Formation sandstones except for two stratigraphic marker beds which are completely cemented by early calcite which is recognised in all the wells (Fig. 3.6D). Calcite occurs as early cement completely occluding porosity and is poikilotopic. Some calcite crystals show relics of the replaced bioclast (Fig 3.11A). XRD analysis (Figs. 3.15A and B) confirms the abundance of the carbonate cements in the Ula field. XRD results reveal the presence of minor amount of ankerite but it has not been distinguished from dolomite during the point counting as sections were not stained for carbonates.

Dawsonite ($NaAlCO_3(OH)_2$) a not a common carbonate mineral in sedimentary rocks, is found in one well in the Ula Formation sandstone reservoirs (Fig. 3.14A). All sandstones where dawsonite occurrence was reported are closely related to marine mud rock (Baker, 1991; Worden, 2006). Dawsonite crystals have acicular or tabular habit. It was not easy to identify from the optical microscope. The SEM was used in identification and confirmed by X-ray diffraction. The time relationship between dawsonite and quartz cement or dolomite is not clearly understood in these samples.

Siderite is found in trace amounts mainly occurring adjacent to clay matrix.

3.5.2.4 Feldspar cement

Both authigenic K-feldspar and albite were recognised in the Ula Formation sandstones. K-feldspar cement seems to dominate but their distribution is not uniform. Authigenic feldspars cement abundance range from 0 to 6 %. The control on the feldspar cement distribution is not certain. Both of the feldspar cement types are engulfed by quartz overgrowths that have developed on adjacent quartz grains. K-feldspar cements are commonly dissolved and replaced by ferroan dolomite.

3.5.2.5 Clay minerals

Authigenic clay minerals in the Ula Formation sandstone include illite and minor amounts of chlorite.

3.5.2.6 Illite

Illite occurs as fibrous, hair-like, radially dispersed crystals and filamentous crystals. Illite varies from few per cent to as much as 18%. There are two generations of illite; an early grain riming which is overgrown by authigenic quartz cement (Fig.3.7C) and often marks the boundary between detrital and authigenic quartz and a later generation of fibrous and filamentous pore-filling type (Fig. 3.12A). Locally it fills secondary dissolution pores from the decomposition of plagioclase feldspars. Pressure solution is observed in some samples where thin clay layer is found compressed by detrital quartz (Fig. 3.11C). Quartz cement is either interwoven or envelops illite (Fig. 3.13B). Illite is more abundant where there are more altered detrital feldspar grains. The abundance of illite seems to be related to feldspar alterations.

3.5.2.7 Chlorite

Chlorite is recognised in minor abundance in all the wells studied. Chlorite is found in wide variety of morphologies in the SEM. It occurs mainly as pore-filling rosettes and, rarely, as grain-rimming clay (Fig. 3.12B). It has also replaced unstable grains, mainly feldspar and rock fragments, and can be seen growing on decomposed feldspar grain or mica. The presence of chlorite is confirmed from the XRD results by its 14Å, 7Å, 4.7Å, 3.5Å and 2.83Å defractions (Fig .3. 15A and B).

Note that kaolinite and smectite are conspicuously absent in all the studied wells of the Ula field.

3.5.2.8 Other cements

Other diagenetic cements, which occur in minor amounts, include: pyrite, apatite, halite and sphalerite. Pyrite occurs as framboids of about 10μm composed of individual octahedral crystallites (Fig. 3.13B and C) associated mainly with fossil fragments (Fig. 3.11D). Sphalerite occurs in trace amount and it envelopes quartz cement and the ferroan dolomite. Sphalerite may be very late digenetic cement postdating all the other cements because it encloses both quartz cement and dolomite. Phosphate occurs as grain coating cements in wells 7/12-A3 and 7/12-5. Its relationship with other diagenetic minerals is not clear.

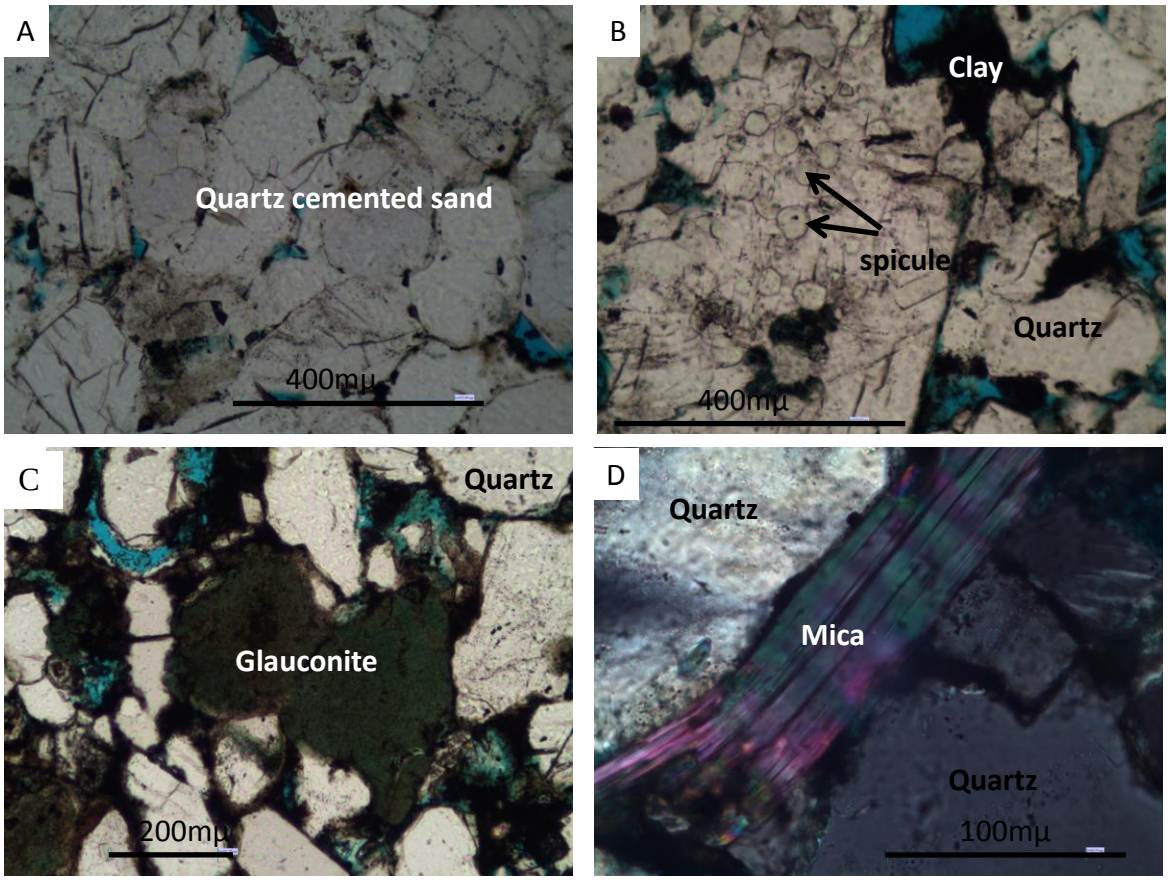

Figure 3. 9 Thin section photomicrograph (A) porosity occluded by quartz cementation in a clean sand (7/12-A8 3792.63m TVD) (B) round pores resulting from dissolution and re-precipitation of sponge spicules on quartz grains (7/12-A8 3792.63m TVD) (C) glauconite slightly deformed by compaction (7/12-A3 3492.7m TVD) (D) undeformed mica flake showing that compaction is not intensive (7/12-5 3479.3m TVD).

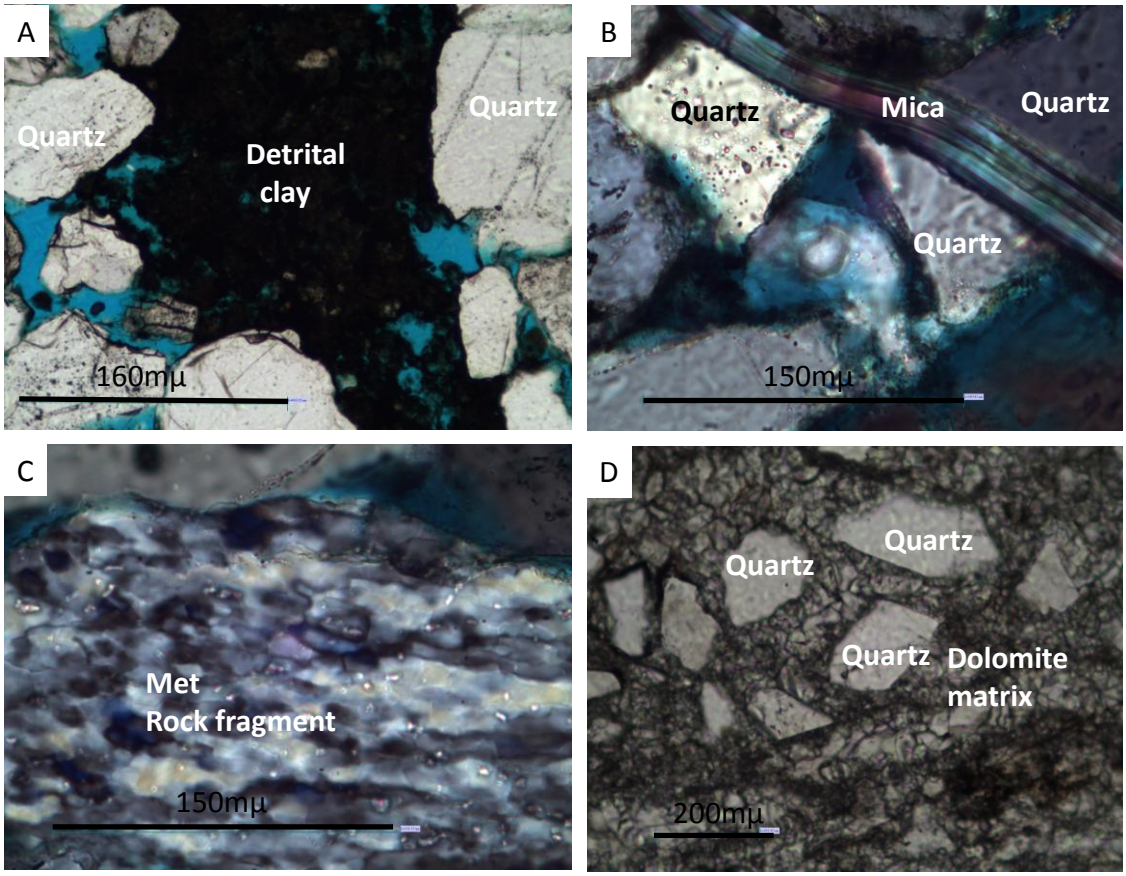

Figure 3. 10 Thin section photomicrograph of the Ula Formation sandstones (A) detrital clay in the fine-grained bioturbated sandstone (7/12-2 3360.54m TVD) (B) mica flakes cross having long contacts with quartz grain (7/12-2 3612.4m TVD) (C) metamorphic rock fragment (D) dolomite matrix completely filling the pore space(7/12-A8 3792.63m TVD).

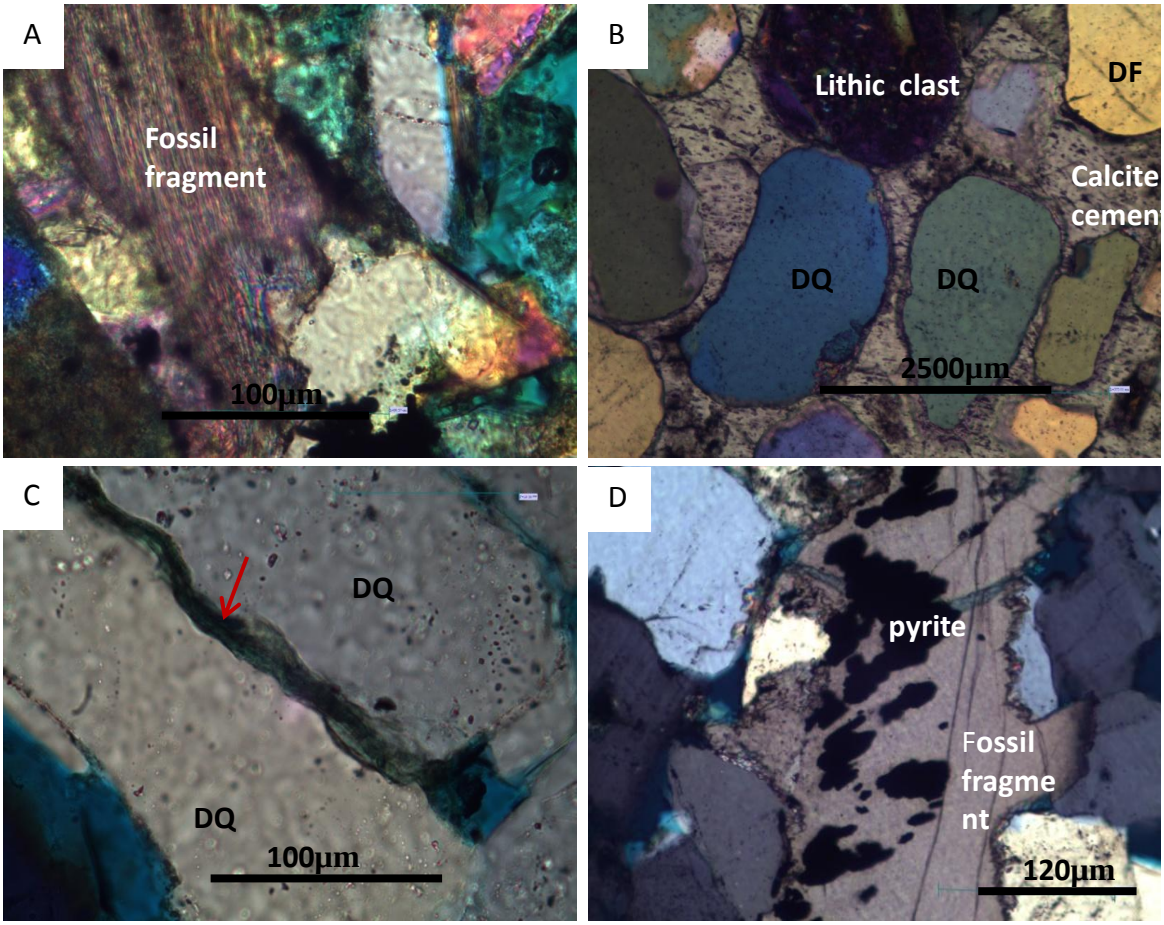

Figure 3. 11 Thin section photomicrograph of the Ula Formation sandstones (A) oyster bioclast fragment transformed to calcite (7/12-A3 3509.5m TVD) (B) unaltered by dissolution grains enclosed by early formed calcite cement (7/12-A3 3524.1m TVD) (C) detrital quartz grains undergoing pressure dissolution along layer of compressed clay (arrow) (7/12-A3 3509.5m TVD) (D) pyrite associated with bioclast (7/12-5 3868.4m TVD). DF=detrital feldspsr, DQ= detrital quartz.

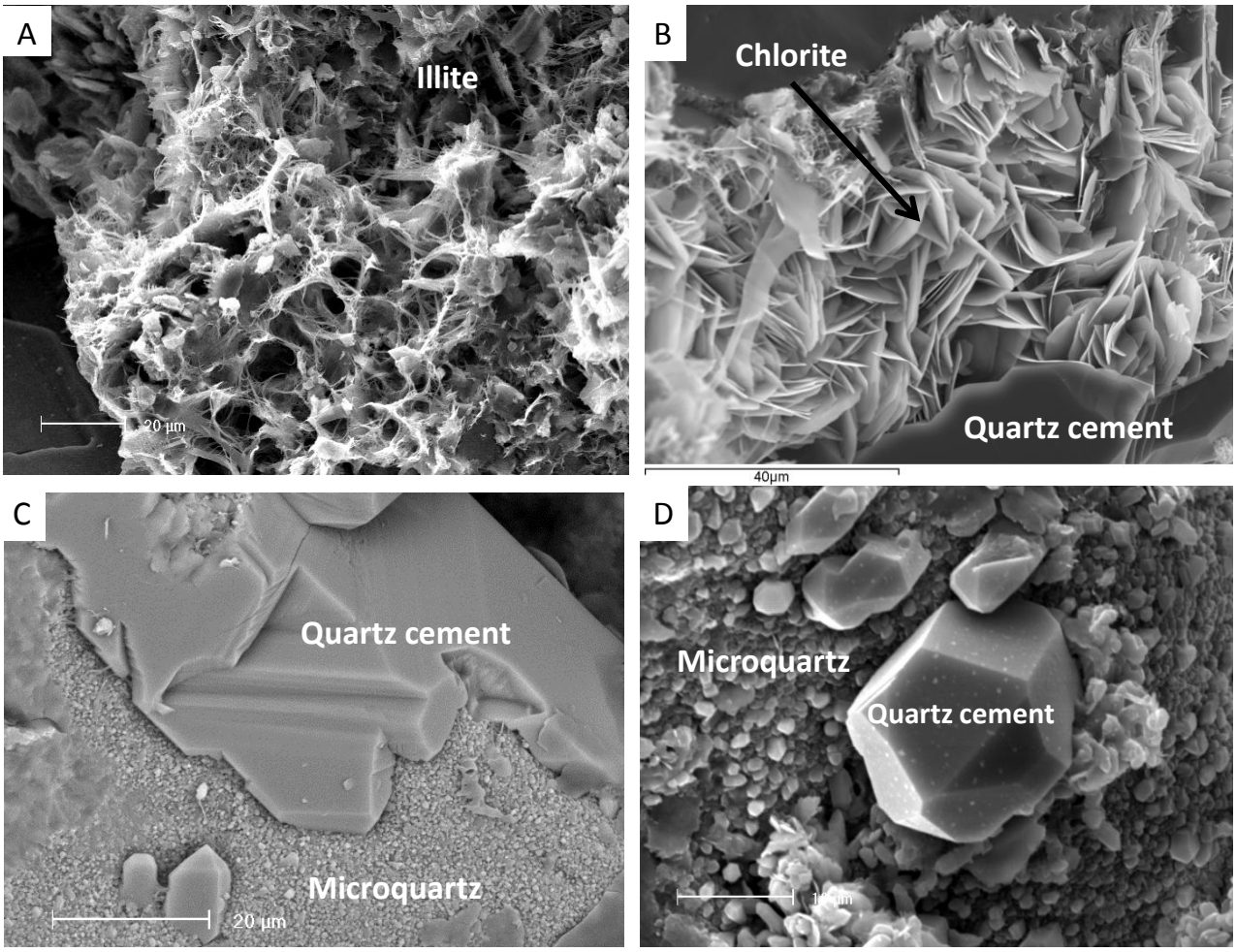

Figure 3. 12 SEM-SE image (A) fibrous illite (7/12-A8 3807.4m TVD) (B) showing authigenic 'rosette' type chlorite overgrown by authigenic quartz (7/12-A3 3509.5m TVD) (C) quartz cement growing over very fine microcrystalline quartz (7/12-A3 3534.9m TVD) (D) BSEM image microcrystalline and quartz cement (7/12-3 3444.0m TVD).

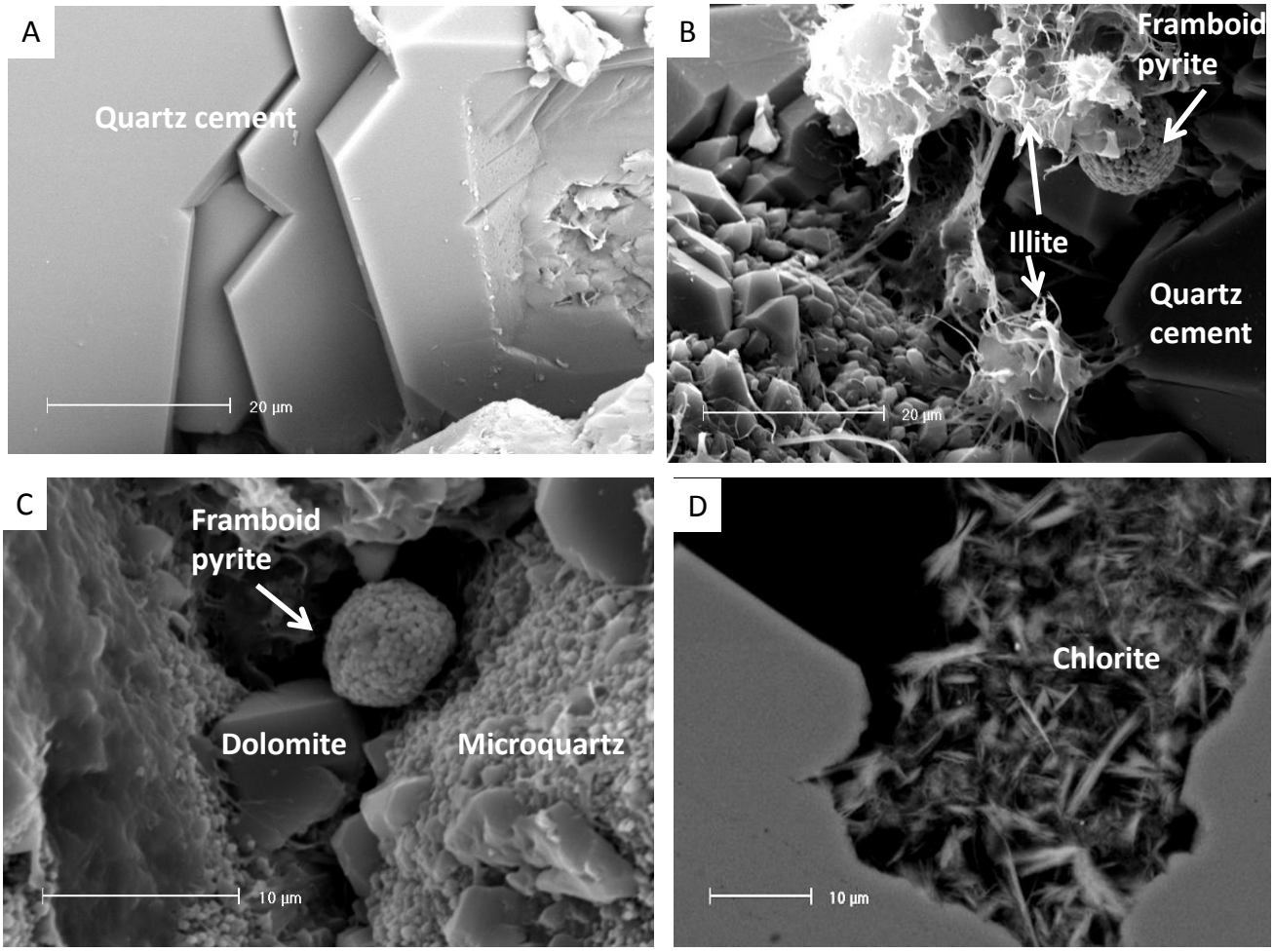

Figure 3. 13 SEM-SE (A) showing different stages of euhedral quartz cement growth (7/12-A3 3555.0m TVD) (B) hairy illite overgrowing framboidal pyrite and microcrystalline quartz and quartz cement overgrowing the illite (7/12-A3 3555.0m TVD) (C) microquartz growing along with microdolomite and framboidal pyrite in a pore space (7/12-3 3444.0m TVD). (D) pore-filling chlorite (7/12-A8 3807.4m TVD).

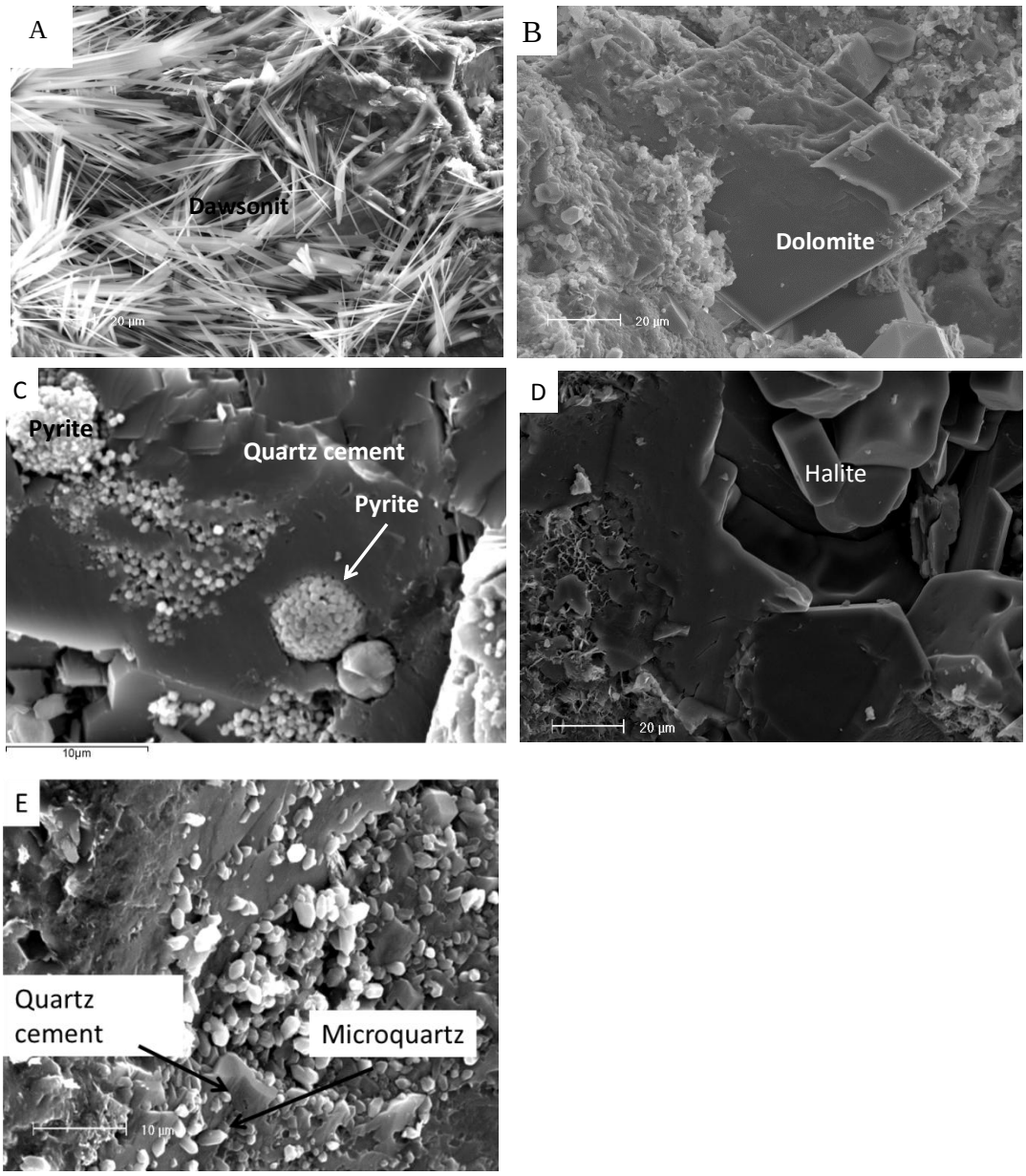

Figure 3.14 SEM-SE images of authigenic minerals of Ula Formation sandstone (A) dawsonite cement (7/12-A3 3486.1mTVD) (B) zoned micro dolomite (7/12-A3 3486.1mTVD) (C) quartz cement enclosing framboid pyrite (D) halite cement following drying of the core and precipitated from saline formation water (7/12-A8 3789.1mTVD) (E) microquartz on quartz cement (7/12-A3 3492.7m TVD).

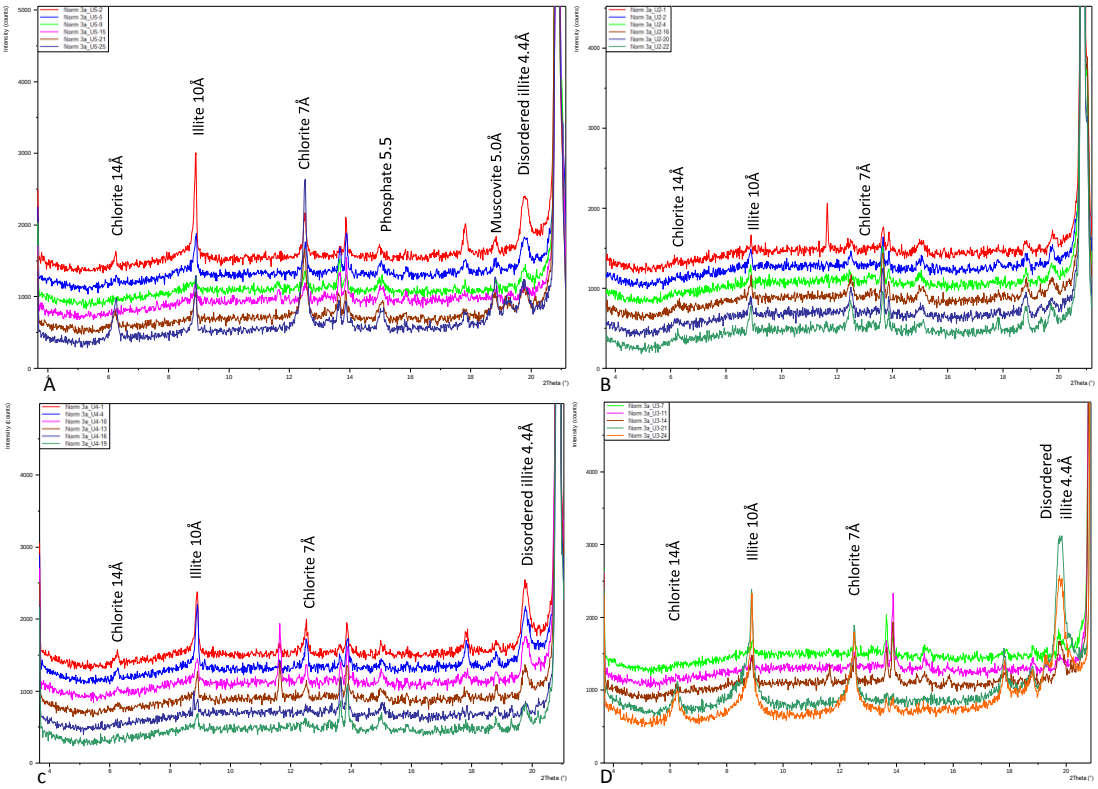

Figure 3.15 X-ray diffraction of <2µm samples from 4 wells studied in the Ula field. XRD patterns at different depths (top trace shallowest depth) for different wells. (A) well 7/12-2 (depths from above 3364.7, 3378.0, 3393.5, 3429.0, 3444.1, 3648.0) (B) well 7/12-5 (depth from above 3844.5, 3853.5, 3872.6, 3881.0, 3895.7, 3904.3) (C) well 7/12-3A (depths from above 3636.5, 3638.5, 3650.75, 3680.9 3720.3, 3722.3) (D) well 7/12-A08 (depths from above 3781.7, 3789.2, 3798.7, 4317.3, 4822.5). Depths in TVD. All the wells show illite and chlorite as common clay mineral but no trace of smectite or kaolinite.

3.5.4 Fluid inclusion analysis

Fluid inclusion microthermometric data for quartz cements have been acquired for 12 samples. All homogenization temperatures measured are from inclusions within the quartz cement or at grain cement boundary. Both aqueous and petroleum inclusions were measured. All aqueous inclusions are unimodal and homogenised between 120 and 170°C with modes between 140 and 150°C, while petroleum inclusions homogenised between 95 and 142°C with modes between 90 and 110°C (Fig. 3.16). The highest homogenization temperatures measured in these samples are higher than

present day temperature of 154^{o}C (e.g. measured in well 7/12-A3). Pressure corrections have not been made as the samples are likely to contain methane gas since they are from a working petroleum system and a producing field (Hanor, 1980). Measured homogenization temperatures of the aqueous inclusions are therefore considered to be true representatives of the actual temperatures of entrapment for the inclusions.

Salinity measurements could not be performed for many of the inclusion because of their small size. The measured salinity show that quartz cement precipitated in formation water with salinity of 0 to 11 weight % NaCl (Fig. 3.17). The low salinity formation water must have been trapped when there was some sort of meteoric flushing. Present day formation water salinity is 25 weight % NaCl (Oxtoby 1994).

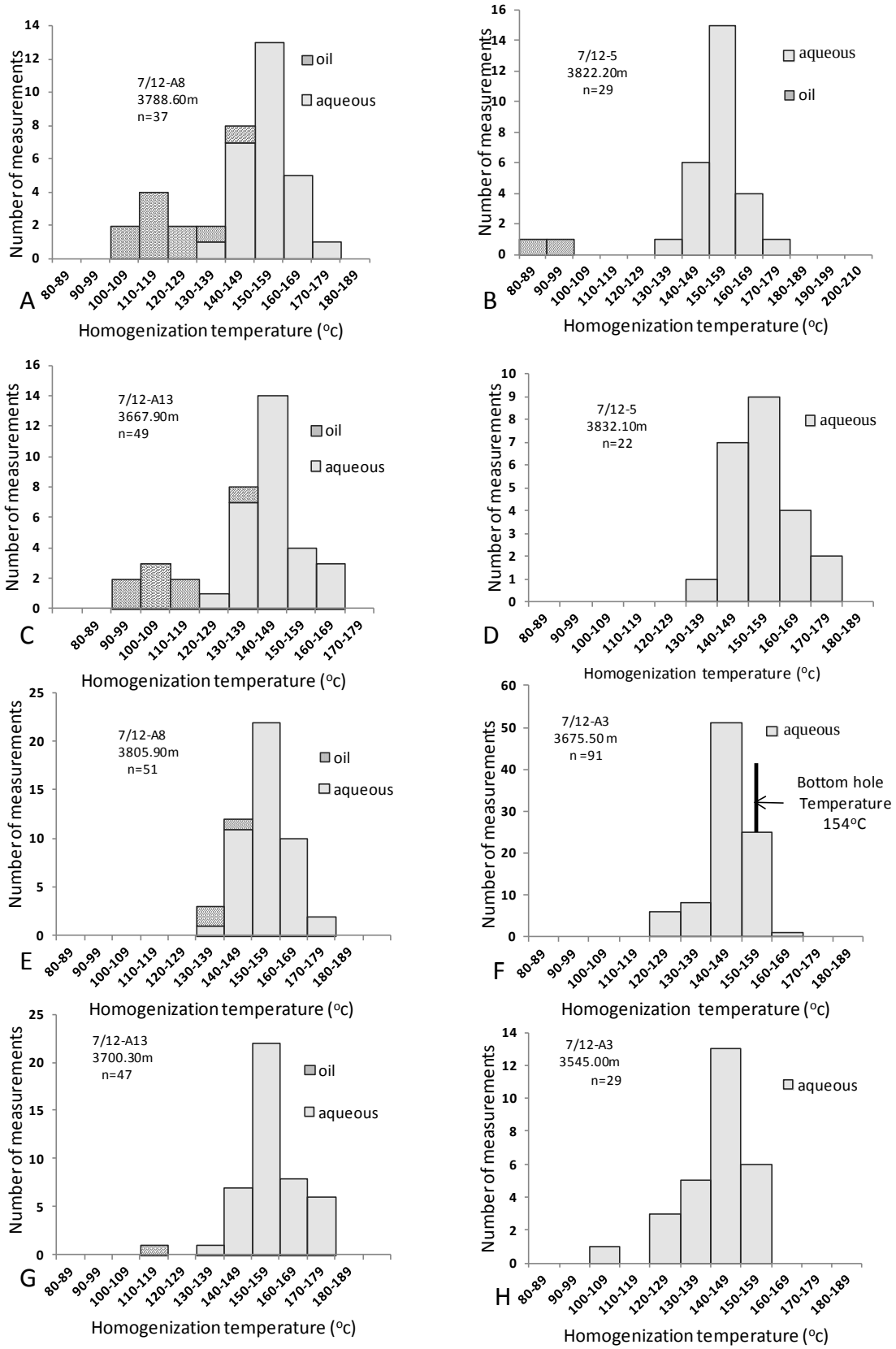

Figure 3.16 Histograms of homogenization temperatures of aqueous and petroleum fluid inclusion of the Ula field. True vertical depths and number of samples measured shown.

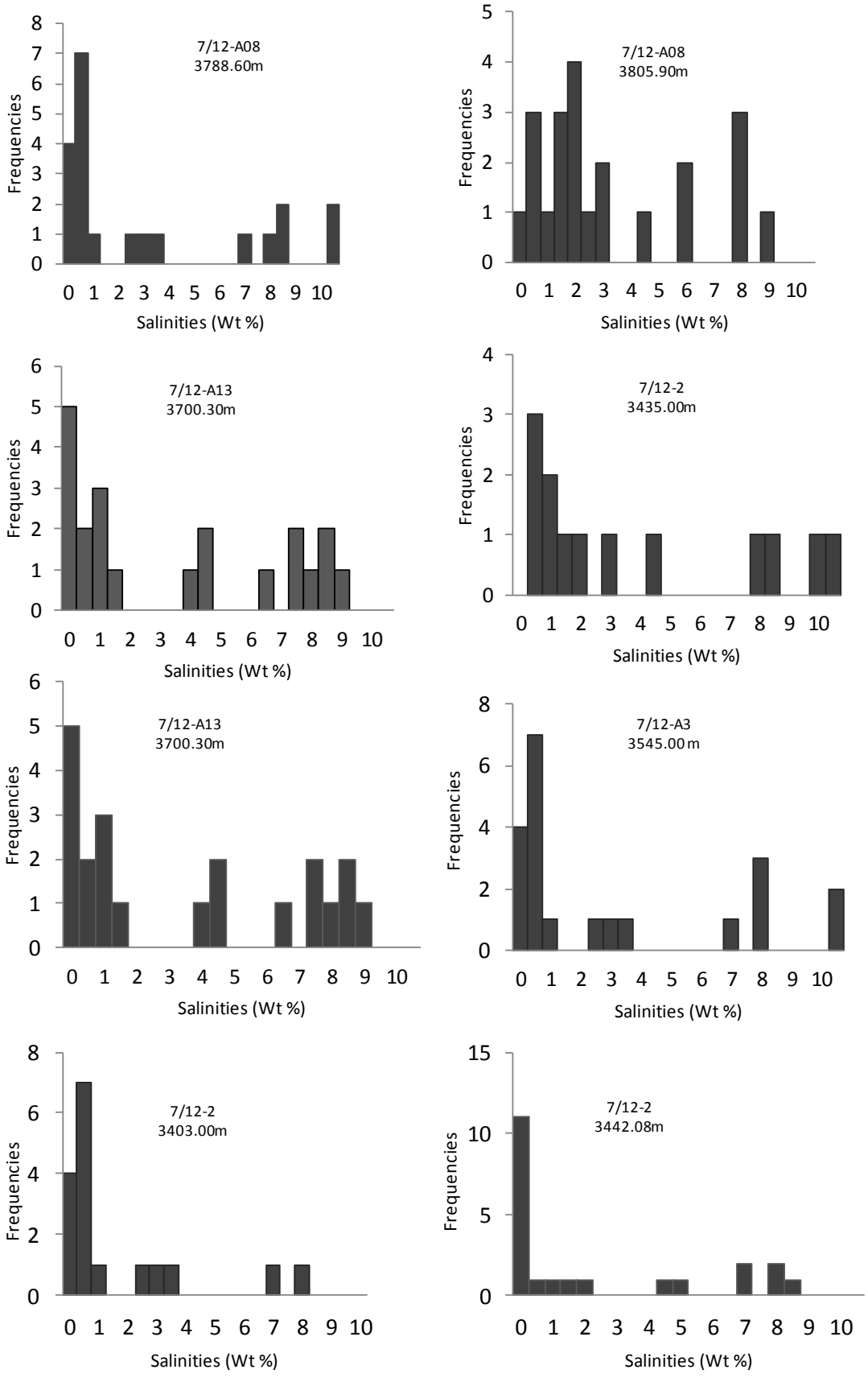

Figure 3.17 Histogram showing fluid inclusion salinity of the Ula wells.

3.5.5 Stable isotope geochemistry

Carbonate stable isotope analysis was carried out on 13 samples. As most of the dolomite consist of small crystals (<200mμ) which are intergrown with other minerals, pure dolomite could not be micro-sampled (e.g. by drilling). Instead samples with greatest amount of dolomite cement were selected and subject to bulk leaching. The oxygen and carbon isotope data therefore relate to bulk dolomite C and O isotope compositions. The analysis could not be completed for many of the samples selected, as they do not liberate enough CO_2 due to the small amount of dolomite cement in the bulk rock samples. The $\delta^{18}O$ values of the dolomite cement in the Ula Formation range from -12.40 to -5.48‰ PDB. The $\delta^{18}O$ values for samples in the water leg range from (-5.48 to -12.4‰ PDB) average -10.5 and the oil leg values range from (-5.50 to -6.52‰ PDB) average -6.17‰ PDB. The $\delta^{13}C$ values of the dolomite range from -7.40 to - 0.69‰ PDB (Table 3.2).

Table 3. 1 Oxygen and carbon isotope composition of dolomite cement of the Ula Formation

Wells	Depth (m TVD)	$\delta^{18}O$ Dol v-PDB	$\delta^{18}O$ Dol v-SMOW	$\delta^{18}O$ water v-SMOW	T oK	T oC	$\delta^{13}C$ v-PDB	Fluid zone
7/12.2	3372.8	-6.52	24.1	3.26	378.1	105.1 ± 8	-2.57	oil
7/12.2	3362.1	-6.5	24.2	3.26	378.0	105.0 ± 8	-2.5	oil
7/12-A3	3642.0	-5.5	25.2	3.26	369.6	96.6 ± 8	-0.8	oil
7/12-.2	3822.0	-6.89	23.8	3.26	381.4	108.4 ± 8	-2.61	transition
7/12-A13	3700.2	-12.4	18.1	3.26	442.8	169.8 ± 8	-7.4	water
7/12-A13	3702.7	-12.2	18.3	3.26	440.1	167.1 ± 8	-7.4	water
7/12-A08	3877.0	-12.06	18.4	3.26	438.2	165.2 ± 8	-6.19	water
7/12-A08	3912.0	-12.05	18.4	3.26	438.0	165.0 ± 8	-5.75	water
7/12-A13	3637.8	-10.9	19.6	3.26	423.2	150.2 ± 8	-5.18	water
7/12-A3	3708.5	-8.48	22.1	3.26	396.5	123.5 ± 8	-0.69	water
7/12-A3	3696.5	-5.48	25.2	3.26	369.4	96.4 ± 8	-3.55	water

Present the formation water assumed to be 3.26 V-SMOW. If we assume the formation water has slightly changed over the years rising to 4.26 or reducing to 2.26 changes the temperature by ± 8^{o}C.

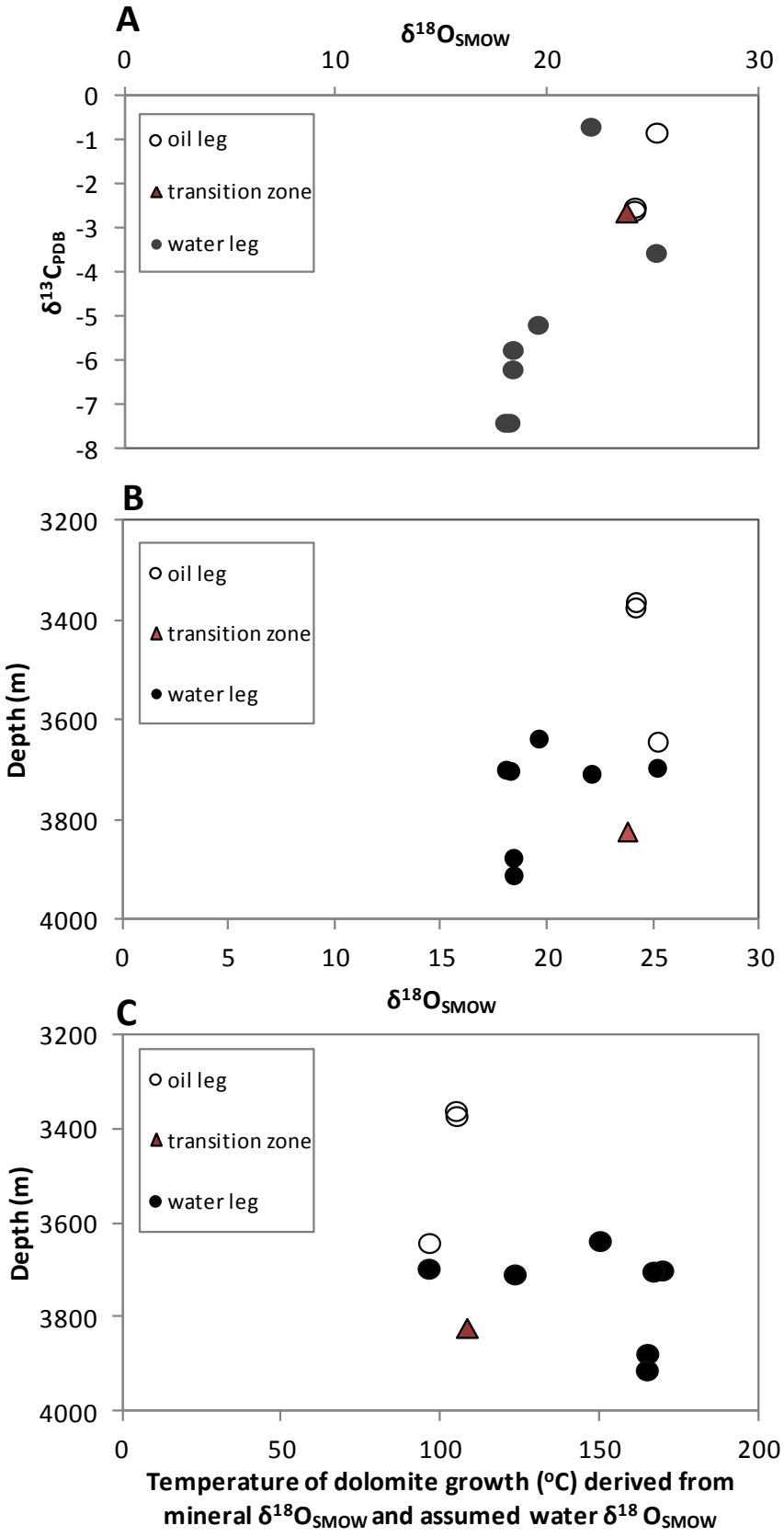

Figure 3.18 Stable isotope geochemistry plots (A) $\delta^{13}C$ plot versus $\delta^{18}O_{SMOW}$ (B) $\delta^{18}O$ plot versus depth (C) Temperature of dolomite growth derived from $\delta^{18}O$ versus depth.

Because the carbonate isotope values are for the whole rock, the isotopic composition of the carbon tends to be dominated by the average composition of the bulk dolomite which grew in equilibrium with the pore waters present at that time. Isotopic composition showed that pore water was stratified with more negative values of $\delta^{13}C$ for wells at the flank (-2.61 to -11.13‰ PDB) than wells at the crest (-3.55 to -0.8‰ PDB) of the reservoir (Fig. 3.18). Analysis of whole rock $\delta^{13}C$ signature suggests a carbon sourced from dissolution and precipitation of carbonate during burial diagenesis from wells at the crest (7/12-2 and 7/12-A3), and more lighter carbon sourced from thermal maturation of organic matter (Irwin et al. 1977; Surdam et al. 1984), with some influx from waters expelled from evaporites for wells at deeper (7/12-5, 7/12-A08, 7/12-A13). The correlation values between $\delta^{18}O$ and is weak (r^2 = 0.66 Fig. 3.19) precludes systematic increase in the input of dissolved carbon from thermal maturation of organic matter during progressive burial depth and increase in temperature (Mansurbeg et al., 2008). Temperature of dolomite cementation is lower for the oil leg (av. 102.2 ± 8°C) compared to water leg (av. 148.1 ± 8°C). This suggests that dolomite cementation was retarded in the oil leg at certain high oil saturation while cementation continued in the water leg.

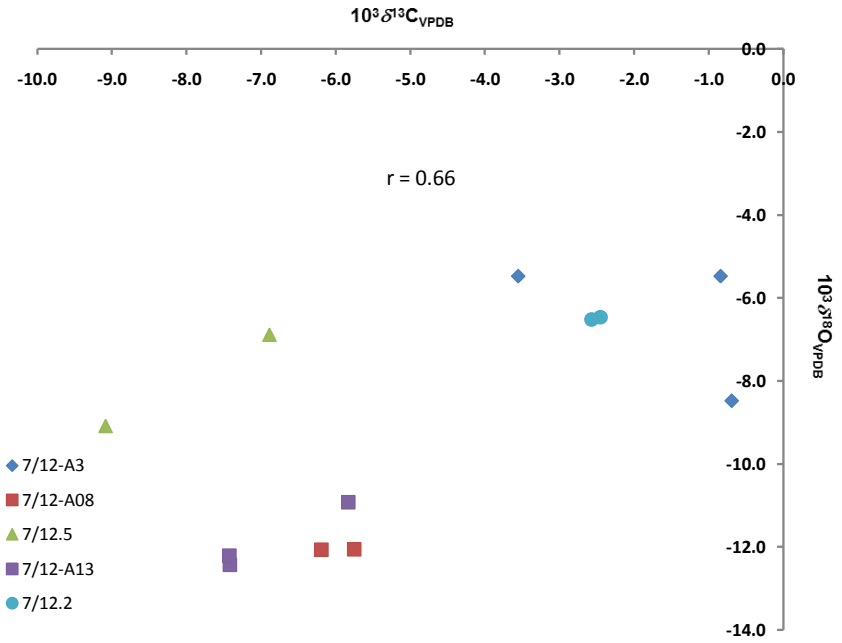

Figure 3.19 Oxygen versus carbon stable isotopes for dolomites in the Ula Formation sandstone split into different wells.

3.6 Discussion

3.6.1 Paragenetic sequence

The paragenetic sequence was determined on the basis of thin section and SEM observations. The inferred diagenetic sequence for the Ula Formation sandstones is shown in Figure 3.20. The earliest diagenetic events are the precipitation of framboidal pyrites (Figs. 3.13B and C, Fig. 3.14B) and microdolomite (Fig. 3.14B). Pyrite was formed during the sulphate reduction phase. Pyrite and microdolomite are of minor volumetric importance and are both enclosed by relatively early, poikilotopic calcite cement derived from decomposition of organic matter. Early calcite cementation was the first major diagenetic cement after the framboidal pyrite and microdolomite. This is supported by the calcite cement filling large intergranular pore space and enclosing all the feldspars and lithic clast without significant alterations (Fig. 3.11B). This event was followed by dissolution and re-precipitation of biogenic silica as randomly oriented microcrystalline quartz which probably precipitated following dissolution of sponge spicules (Fig. 3.9B). However, the precipitation of microcrystalline quartz seems to have lasted for a long time since some are grown over quartz cement (Fig. 3.14E). Thin section images show well rounded dissolution macropores which was probably formed from sponge spicules (Fig. 3.9B). At this time progressive burial led to mechanical compaction of the rocks. This was followed by dissolution of unstable grains such as feldspars possibly due to influx of meteoric water (Fig. 3.7A). This was followed by precipitation of feldspar cement (Fig. 3.7B and 3.8B). Illite began to precipitate from the decomposing feldspar grains (Fig. 3.21C) and probably unstable clay mineral smectite probably the same time with illitization of smectite and kaolinite from the detrital clay. Relationship between illite and chlorite is not clear. Both illite and chlorite occur within many feldspar dissolution pores (Fig. 3.21C).

Quartz overgrowths, which are common in all wells and increase in quantity with depth, formed syntaxially at the late stage of diagenetic events. Quartz overgrowth developed into open pores and formed euhedral crystal outlines (Fig 3.7C). From cross cutting relations and mineral entrapments, the minerals that are formed later

than quartz overgrowth are: replacive dolomite (Fig. 3.8C and D), the nodular calcite, and sphalerite. Because chemical compaction was active at that time pressure solution may be the main source of silica for the precipitation of quartz cement. Dolomite commonly overlies and cross cut quartz cement but is enveloped by nodular calcite. Calcite cementation took place in two stages. In addition to the early formed calcite cement (Fig. 3.11B) there is a phase that post-dates quartz cement (Fig. 3.11D). The late stage, like the early stage, filled pore spaces and replaced detrital grains indiscriminately.

The latest diagenetic event was the fracturing of grains and indiscriminate dissolution of grains and cements. Grain fracturing may be related in time to uplift or oil emplacement into the reservoir. Rhombic micro dolomite framboid pyrites and illite are commonly enveloped by quartz overgrowth. The relationship of quartz overgrowth and feldspar cements is not clear bit it is likely that quartz cement post-date feldspar cement.

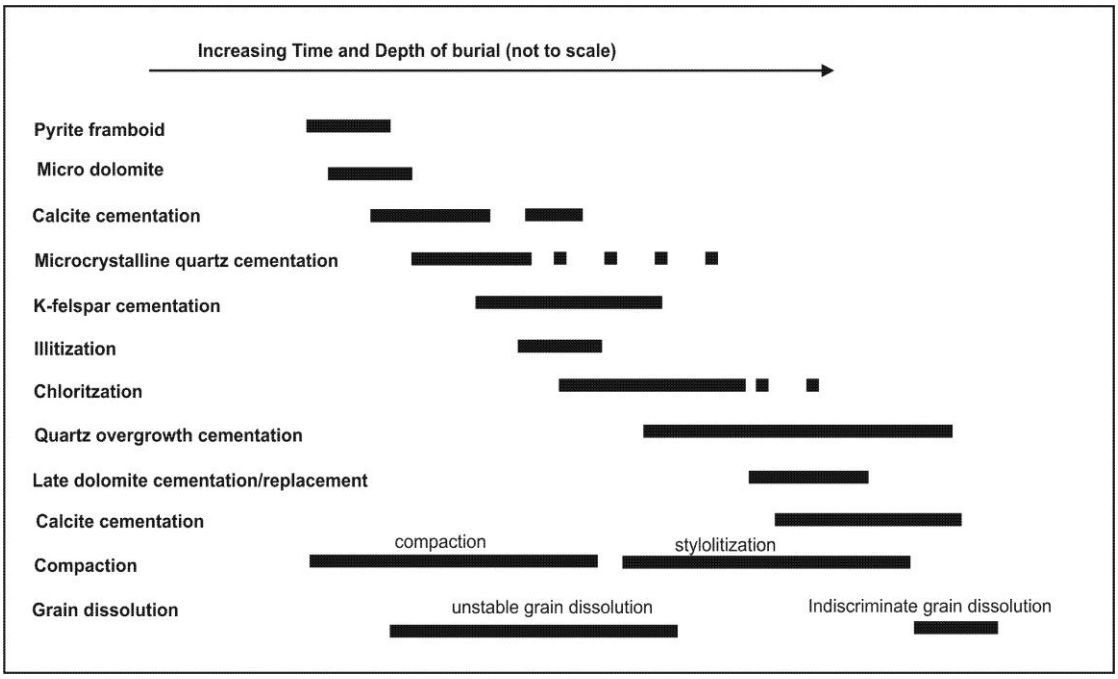

Figure 3.20 Paragenetic sequences of the Ula field sandstones. Dotted line implies inferred period.

3.6.2.1 Quartz cement sources

The source of silica cement in sandstones has been keenly debated in the recent years with fundamental arguments about external and internal source. Some investigations have suggested that huge volumes of water, released through compaction, could provide the silica precipitated as quartz cement in sandstones (Baccar and Fritz, 1993; Land and Dutton, 1979; McBride, 1989; Robinson and Gluyas, 1992; Siever, 1959). Chemical mass balance calculations and fluid flow modelling, however, indicate significant transport of silica by advection from thick sandstones would require orders of magnitude higher pore water fluxes than are likely in compactional regimes of sedimentary basins (Bjørlykke, 1983, 1994; Bjørlykke and Egeberg, 1993b; de Caritat, 1989). As a result it is likely that the bulk of the silica originates within the sandstone body. Various internal origin of silica has been envisaged including illitization and chloritization of smectite, feldspar-dissolution reactions, K-feldspar-kaolinite reaction, chemical compaction (pressure solution and stylolites) and dissolution of amorphous silica (Barclay and Worden, 2000; Worden and Morad, 2000).

In the Ula Formation sandstone, the sources of the silica in solution are likely to include numerous internal, depth-related sources: some silica may have been derived from dissolution of feldspar (Fig. 3.20C), smectite to illite transformation (McKinley et al., 2003) since no traces of smectite are found in the Ula Formation sandstone, and some coming from pressure solution and stylolites (Fig. 3.20A and B).

The tetrahedral substitution of Al for Si during the smectite to illite reaction results in surplus silica (Towe, 1962) which can be used for silica cementation. Smectite to illite conversion during burial diagenesis has been described by many authors (Bjørlykke and Egeberg, 1993a; McKinley et al., 2003; Worden and Morad, 2000). The transformation of smectite to illite starts at temperature, of about 60^{o}C producing smectite-illite mixed layers, around 90^{o}C, the products are illite-dominated mixed layers and at temperature >110^{o}C, nearly pure illite is formed (Worden and Morad, 2000). The burial depth of over 3000m and fluid inclusion (FI) temperature averaging temperature of 145^{o}C, the absence of smectite in the Ula Formation sandstone is understandable. Chloritization of smectite is likely to have the same role as in illitization of smectite in supplying the silica cement (Uuoa, 1991).

A reaction between kaolinite and K-feldspar (Wilkinson et al., 1997) might have contributed to the supply of silica in the Ula Formation sandstone since there is a total lack of kaolinite. At temperatures above 130^{o}C kaolinite reacts with K-feldspars to produce illite and silica. This transformation is an isochemical and pH-neutral process (Bjorkum and Gjelsvik, 1988). In arkosic sandstone that were little affected by eogenetic K-feldspar leaching (Bertieret et al., 2008), all kaolinite would be consumed before the K-feldspar was exhausted (Bertieret et al., 2008) thus explaining the absence of kaolinite in the Ula Formation sandstones. In contrast to the Ula Formation, in sandstones that had undergone excessive meteoric leaching of K-feldspar during early burial diagenesis, all K-feldspar would be consumed in the illitization reaction, during deep burial. Illitization of K-feldspar can proceed in the

absence of kaolinite. This reaction consumes the K-feldspar and acid, and produces illite and quartz. In the Ula Formation sandstone the presence of illite within altered detrital K-feldspar relics supports this assertion.

Part of the silica cement for quartz cementation in the Ula Formation sandstones must have been from stylolization (Fig. 3.21A). Stylolites, a localised dissolution surfaces abundantly found in sandstones and carbonate rocks is reported to have sometimes account for dissolution of more than 50% of the original rock volume (Alvarez et al., 1978; Stockdale, 1922) which goes into solution. Stylolites (Fig. 3.21) can be a significant quartz cement source (Wong and Oldershaw, 1981). It has been noticed (Oelkers et al., 1996) that the distribution of silica cement in some sedimentary basins is a function of distance from stylolite which indicates that much of the cement in those basins originate from stylolite. In the Ula sandstone the distribution of stylolites is significant enough to be a major source of silica.

Pressure solution is a source of silica supply for quartz cementation in the Ula sandstone reservoirs as occurrence of pressure solutions are recorded (Fig. 3. 21B). Experimental investigations of quartz pressure solution indicate that under certain conditions, substantial quartz dissolution can occur at quartz/quartz interface (De Boer, 1977; Maxwell, 1960; Sathar et al., 2012). However, mechanism of pressure solution was rejected as source of quartz dissolution by some authors e.g. (Maast et al., 2011; Sheldon et al., 2003).

3.5.6.2 Microcrystalline quartz source

The distribution of microcrystalline quartz is controlled by depositional facies (Fig. 3.24D). The source is related to early dissolution and re-precipitation of biogenic silica from sponge spicules. The presence of the relics of sponge spicules (Fig. 3.9B) in the microquartz-abundant units may be considered as evidence. The occurrence of microquartz in spicule-rich sandstones has been reported in many sedimentary basins (Aase et al., 1996; Goldstein and Rossi, 2002; Warren and Pulham, 2001; Worden et al., 2012).

3.5.6.3 Clay cement sources

The common clay minerals in Ula Formation sandstones are illite and chlorite. Potassium for the illite could have been derived from dissolution of orthoclase feldspar. Another most probable source of the illite is the reaction of K-feldspar and kaolinite (which might have been present at the early stage of mesogenesis) with solution from the dissolution of K-feldspar and dissolution of volcanic rocks.

Iron in the chlorite may have been derived from the transformation of smectite to illite or thermal reduction of iron compounds (Woronick and Land, 1985). Siderite and pyrite crystals are found scattered in the sandstones of the reservoir which may supply iron upon thermal reduction. Previously precipitated illite can also be altered to chlorite with abundant reduced iron. Some detrital component may have also acted as precursor and changed to chlorite during burial diagenesis (Aagaard et al., 2000).

3.5.6.4 Carbonate cement sources

The ^{13}C values show a range of sources for the carbonate. From the relics of bioclasts (Fig. 3.11A and D) associated with calcite, biogenic sources are envisaged to be the main contributor to the carbonate cements in Ula reservoir (Bjorkum and Walderhaug, 1990; Walderhaug, 1990). The increasingly negative $\delta^{13}C$ values in the water leg (Fig. 3.18A) relative to the oil leg suggest that a later stage source of carbonate was supplied by organic matter (e.g. CO_2 from source rocks).

It has been suggested that diagenetic dawsonite is the result of Na^+-rich alkaline waters reacting with an influx of CO_2 and an indigenous source of aluminium (Worden, 2006). Dawsonite is confined solely to sandstones of marine affinity and represents stagnation of aquifer (Baker, 1991). External source of sodium and aluminate ions associated with high pH waters and an excess of CO_2 was envisaged to be needed to produce authigenic dawsonite (Goldberry and Loughnan, 1977). In the Ula Formation sandstone which also has marine affinity CO_2 could be from thermal de-caboxylation of organic matter and, sodium and aluminium ions could easily be supplied by the alteration of the abundant detrital feldspars. The presence of CO_2 and source of aluminium as prerequisite for authigenic dawsonite

precipitation has been stated by many authors (Milton and Fahey, 1960; Smith and Milton, 1966; Worden, 2006).

The isotopic compositions show that pore water responsible for dolomite growth was stratified with more negative values of $\delta^{13}C$ for samples in the water leg (-0.1 to -7 average -5.1) than samples in the oil leg (-2.57 to -0.80) average -1.9‰ PDB (Fig. 3.18 Table 3.1). Thus the differences in $\delta^{13}C$ between the water leg dolomite and oil leg dolomite values can be explained in terms of the input of an external, isotopically light carbon source derived from organic matter (e.g. source rocks).

3.5.6.5 Feldspar cement sources

K-feldspar cements on detrital feldspar grains are common in all samples. The crystallization of authigenic K-feldspar requires an interstitial environment supplied with K, Al, and Si (Bertier et al., 2008). The alteration of intrastitial labile silicates, especially detrital K-feldspar, can be an important source of K (Ali and Tuner, 1982). Because authigenic feldspar is chemically more stable than (typically igneous sourced) detrital feldspar, it is feasible for feldspar overgrowth to precipitate concurrently with the dissolution of the detrital grain (De Ros et al., 1994; Rossi et al., 2002). In the Ula Formation, K-feldspar with compositional variation is commonly seen undergoing preferential dissolution and providing K for the authigenic feldspar (Fig. 3.8B).

Influences of meteoric water flushing in general in the North Sea have been documented by Bjorlyyke et al. (1992) and specifically in the Brent Group by Egberg and Aagard (1989). Numerous leached feldspars observed in thin section and SEM may be related to the early influx of meteoric water flushing. The high salinity inclusions reflect expulsion of high salinity water from Zechstein salt beneath the underlying Haugesund Formation as a result of compaction of underlying formations. First depositional sea water was flushed by meteoric water with zero salinity then followed by the expulsion of high salinity water from the dissolution of the underlying late Permian salt which resulted in the present salinity.

3.5.6.6 Pyrite cement sources

Framboidal pyrite is the result of bacterial sulphate reduction in marine environments with the sulphate coming from sea water and the iron supplied by reduction of detrital ferric detritus. Fisher and Hudson (1987) stated four conditions for pyrite formation: 1) Anoxic conditions in which the bacteria may function, 2) Sulphate supply – chiefly sea water sulphate, 3) Appropriate organic material as a substrate for the sulphate reducing bacteria, and 4) Iron for the conversion of H_2S to iron sulphide. The shallow marine sandstones of the Ula Formation satisfy all these conditions during deposition and shallow burial.

3.5.6.7 Other cement sources

Sphalerite might have been formed from zinc supplied from external sources through faults from the overlying Mandal Formation (Baines and Burley, 1991). Phosphate which is regarded as representative of hard ground (Kennedy and Garrison, 1955) might have been from teeth of some organisms (Fig. 3.21E).

Gypsum was found in one well. It might have replaced anhydrite nodules. It may have been formed at shallower depth than its present depth of >3000m. The formation water salinity is high (up to 13% weight NaCl). Therefore the gypsum must have been formed when meteoric water saturated with $CaSO_4$ extended down deep but shallower than the present depth (Woronick and Land, 1985).

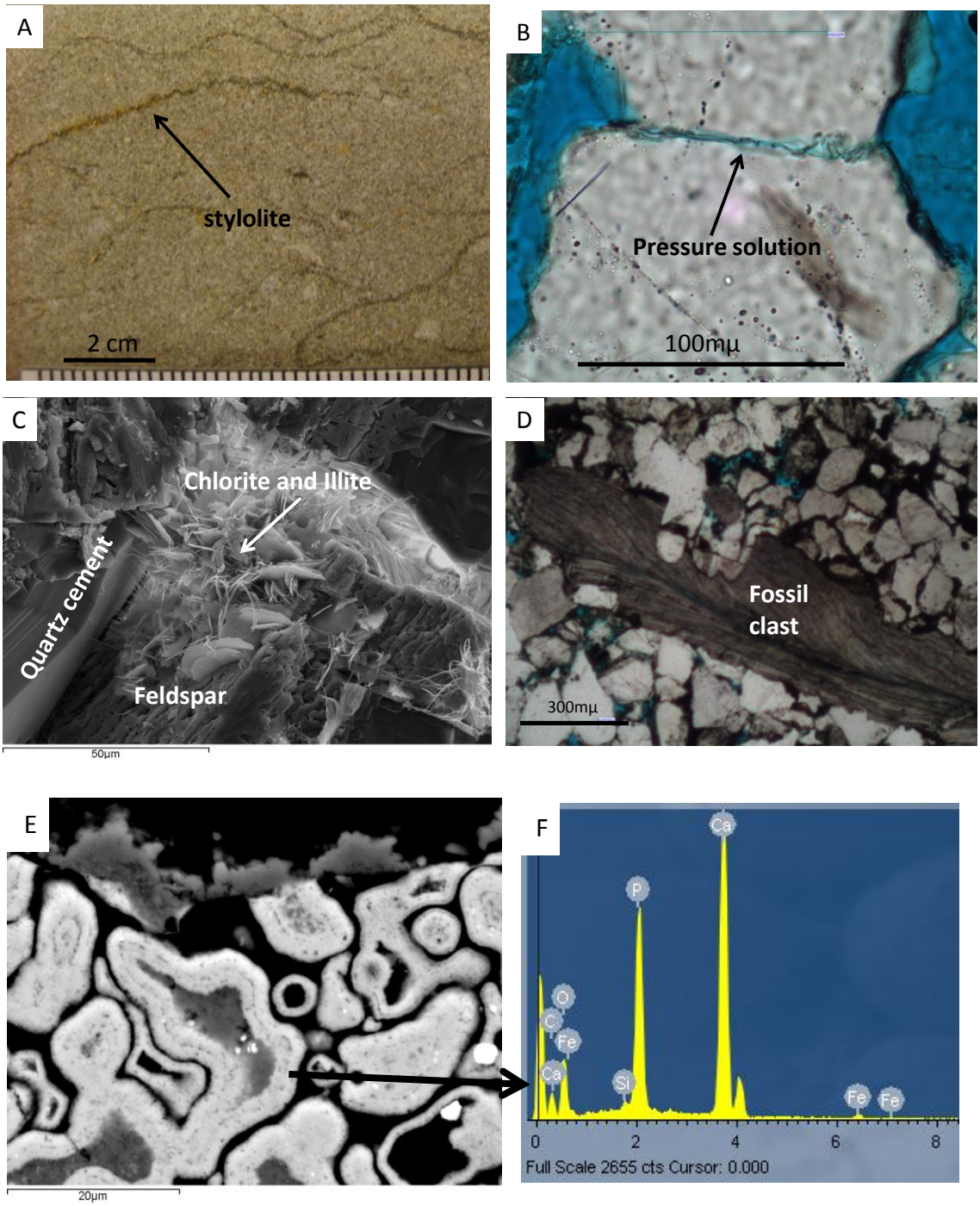

Figure 3.21 (A) Core photograph of Ula Formation sandstones showing stylolites (7/12-A13 3680.95m TDV) (B) Thin section photomicrographs showing localised pressure solution (7/12-2 3599.1m TVD) (C) SEM-BSE image of the Ula Formation sandstone showing alteration of detrital feldspar grain and precipitation of illite and chlorite (7/12-A3 3555.0m TVD) (D) photomicrograph image showing oyster fossil fragment (E) SEM image showing teeth of some organism (F) SEM EDAX showing composition of a teeth (shark?) probable source of phosphate (7/12-A3 3555.0m TVD).

3.7 Reservoir quality

3.7.1 Primary depositional controls on reservoir quality

Reservoir quality of the Ula Formation sandstone is related to the primary depositional environment. The primary depositional factors that have caused variation in composition are; grain size, sorting, sponge spicule abundance and clay content of the reservoir rocks in Ula. Plots of porosity versus permeability for different facies (Fig. 4.7) show that the very fine to fine grained glauconitic sandstone with high amount of argillaceous material showed low porosity and permeability. Graded, structureless coarse-grained, well sorted facies showed the best overall porosity and permeability where such sandstone is not cemented by quartz overgrowth.

3.7.2 Diagenetic controls on reservoir quality

Deterioration and enhancement of reservoir quality in the Ula Formation sandstones has been mainly controlled by cementation, chemical and mechanical compaction, early oil emplacement and early microcrystalline coating of the detrital grains. The two major controls on reservoir quality in the Ula Formation sandstones are: (1) authigenic quartz cement and other mineral cements (2) mechanical and chemical compaction (Fig. 3.22).

The extent of quartz cement precipitation in the Ula Formation sandstones have, in turn, been controlled by a range of factors including (1) primary depositional facies (amount of detrital clay), (2) early oil emplacement and (3) grain coating microquartz which is likely to affect silica supply coming from pressure solution. It is suggested that the displacement of aqueous pore fluids by hydrocarbon can inhibit diagenetic activities (Worden and Morad, 2000). Initial oil charge into the Ula Formation sandstone reservoir commenced when the reservoir was 50^{o}C and the main charge reportedly took place when the reservoir temperature was about 100^{o}C (Nedkvitne et al., 1993). Quartz cementation has taken place when there is oil in the reservoir, as shown by presence of petroleum inclusions and aqueous inclusions having homogenization temperatures greater than 100^{o}C in high oil saturation zones (Fig. 3.16). However, higher porosity and permeability values and

the small amount of quartz cement in low water saturation zones compared to high water saturation zones, of the same facies with no microquartz coatings, can only be attributed to early oil emplacement having inhibited quartz cementation at elevated oil saturation. Fluid inclusion homogenization temperatures measured from quartz cement in water leg samples (Fig. 3.16F) show that quartz cementation is presently taking place since the maximum fluid inclusion temperature recorded is close to present day bottom hole temperature. Quartz cement from the high water saturation zones contains rare petroleum inclusions.

The only grain coating mineral is the microcrystalline quartz (Fig. 3. 7D). Chlorite occurs as a pore-filling rather than grain-coating mineral in the Ula sandstones (Fig. 3.12B and 3.13D). The occurrence of microcrystalline quartz coating on detrital quartz grain has been described as a potentially effective mechanism for inhibiting quartz overgrowths. SEM results showed prismatic microquartz (Fig. 3.12C and D). This morphology is thought to be a result of rapid crystallization from silica-supersaturated solution (Taylor et al., 2010). An inverse relationship exists between quartz cement volume and the percentage of microcrystalline coatings on detrital grains (Fig.3. 24C). However a scatter exists which might be due to natural variations in composition and texture of the sandstone. The mechanism for inhibiting quartz overgrowth is explained by Enusten and Turkevich (1906) that; solubility of a given mineral is function of its crystal size. At a given temperature the degree of super saturation required for small crystal like microquartz to grow is higher than the amount of dissolved silica from stylolite dissolution surfaces, which are very sensitive to silica saturation (Oelkers et al., 1996). Pressure solution is rare in sandstones coated with microcrystalline quartz. Aase et al (1996) stated that as higher degree of super saturation is required to grow small crystals , the formation of microquartz crystal could allow pore water silica activities to increase to a level at which release of silica from stylolite would be inhibited. However, recent work of Worden et al (2012) revealed that microquartz unlike quartz cement grow with different crystallographic orientation to the detrital quartz grains. The inhibition of quartz cement growth is due to microquartz coating the clean surface of detrital quartz and porosity is preserved by the growth direction of microquartz which is parallel to the grain surface, preventing any significant growth into the pore.

Carbonate cement have no significant effect on the reservoir quality in the Ula Formation sandstone. Total carbonate cement versus porosity and permeability plots did not show any clear relationship between reservoir quality and carbonate cement (Fig.3. 24A and B). The effect of carbonate cement on reservoir quality is generally negligible apart from the nodular units where early calcite has filled all the pore spaces and led to non-reservoir. Pore filling illite (Fig. 3.12A) and chlorite (matrix clay) have affected the permeability of the Ula Formation sandstone reservoir (Fig.3. 25B), but their effect on porosity is insignificant.

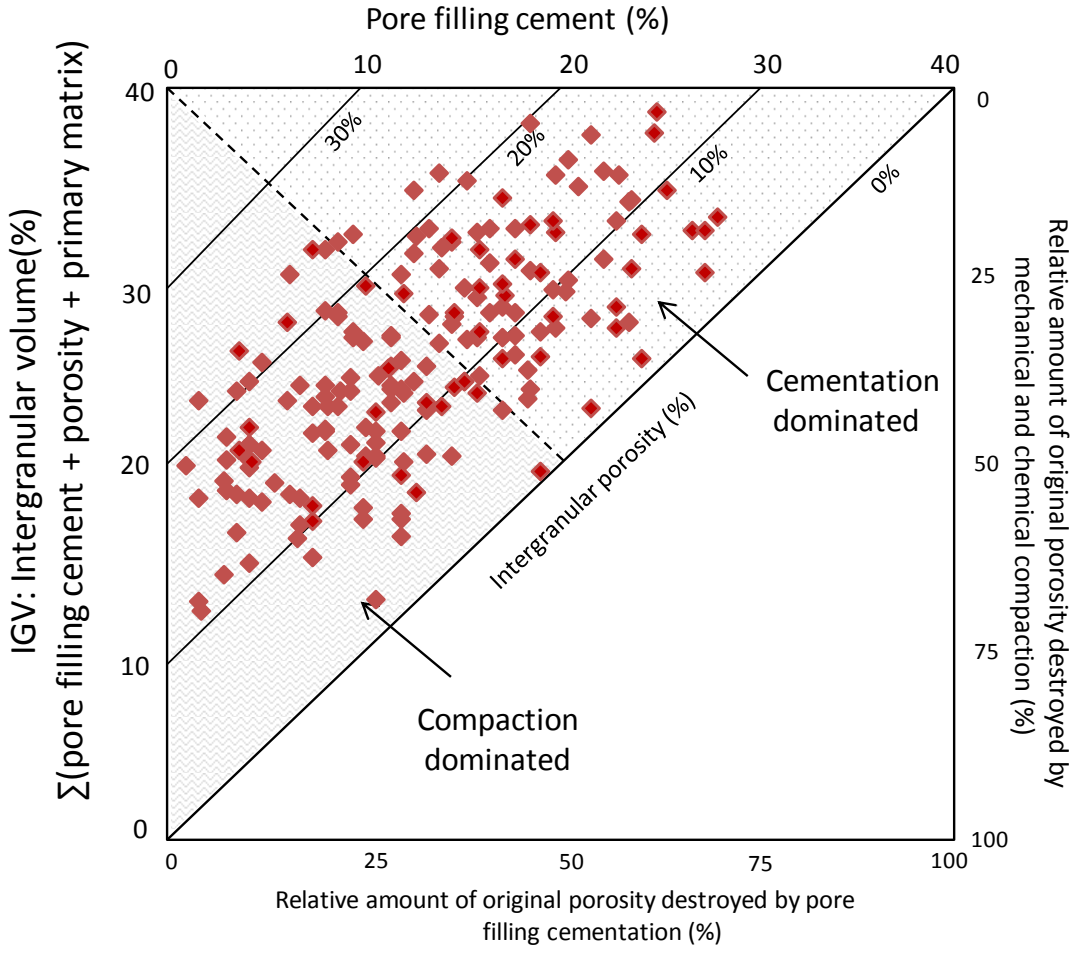

Figure 3.22 Plot of intergranular volume (IGV) versus volume of cement (Housenecht, 1988) for the Ula Formation sandstones showing that both cementation and compaction have reduced porosity in the Ula Formation sandstone.

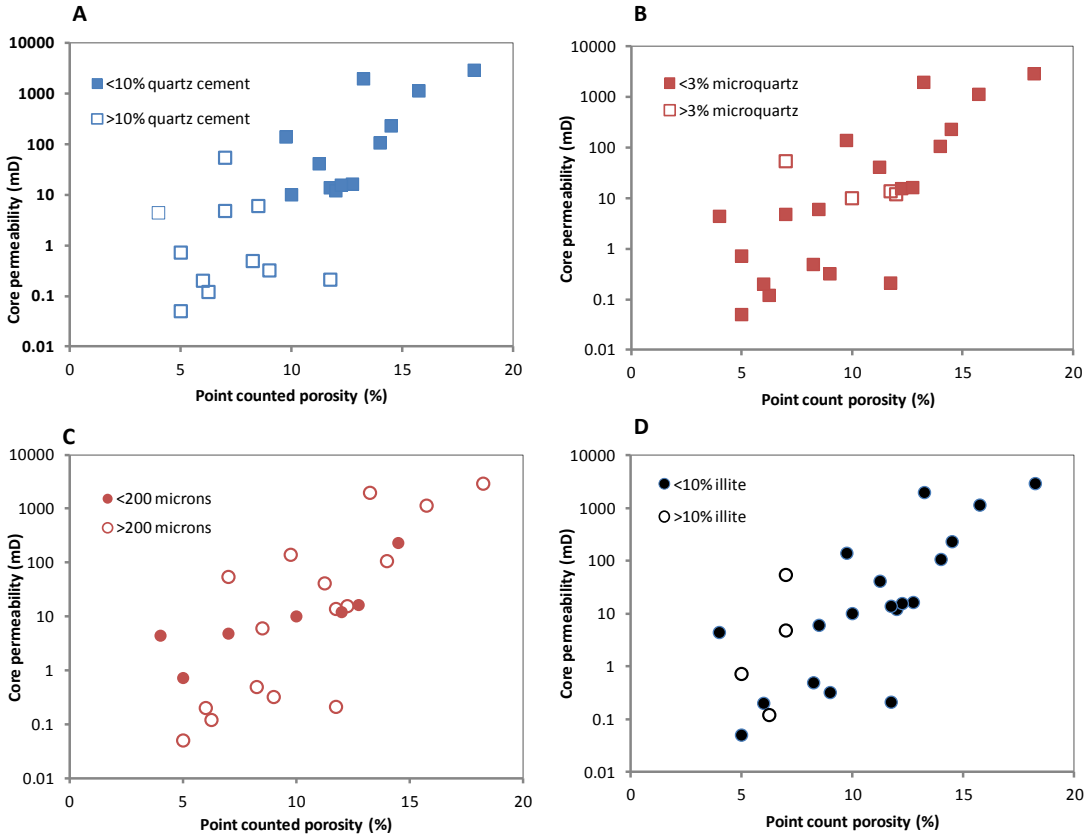

Figure 3.23 Plot of porosity and permeability for the coarse-grained sandstone facies split by different controlling parameters. The result show that quartz cements is the key control of the reservoir quality in the coarse-grained sandstones.

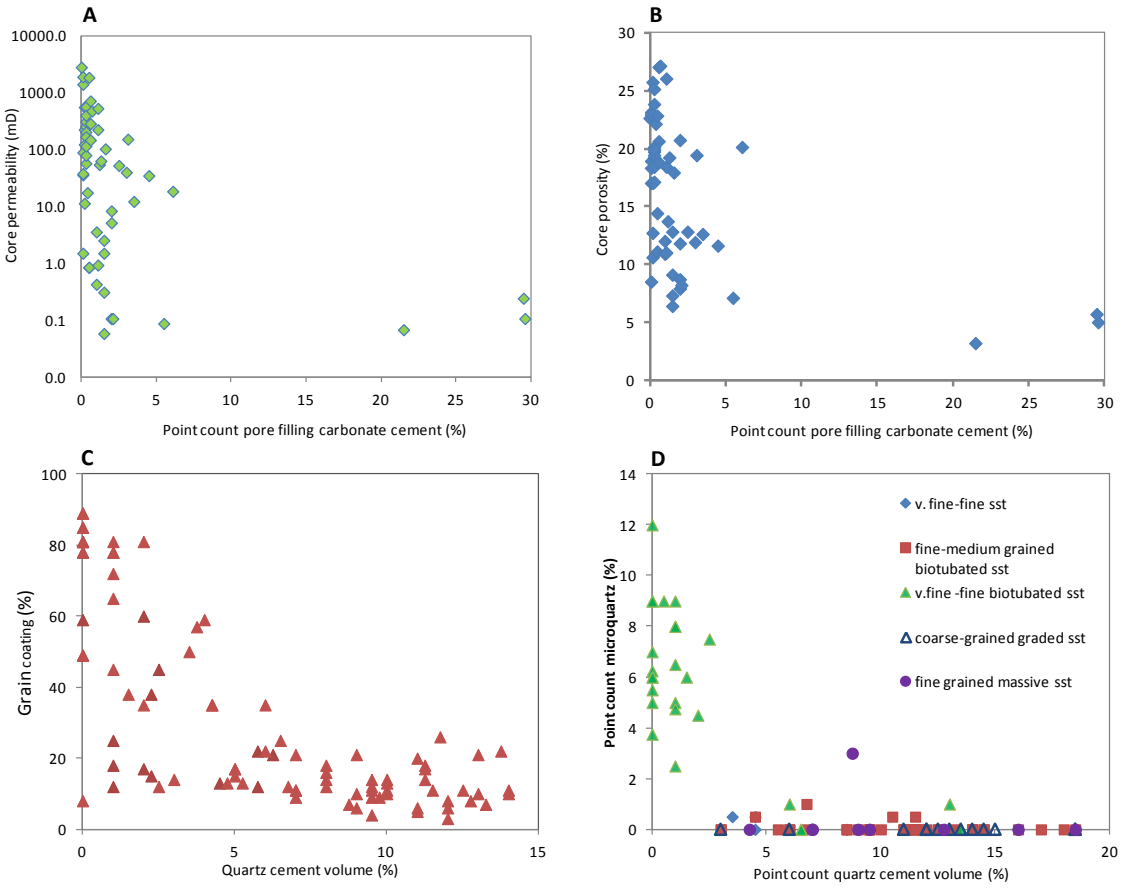

Figure 3.24 Plots of reservoir properties of the Ula Formation sandstone (A) carbonate versus core permeability (B) carbonate cement versus core porosity (C) quartz cement versus microcrystalline quartz coating (D) point count quartz cement versus microquartz volume for different lithofacies showing that distribution of microquartz is mainly controlled by facies.

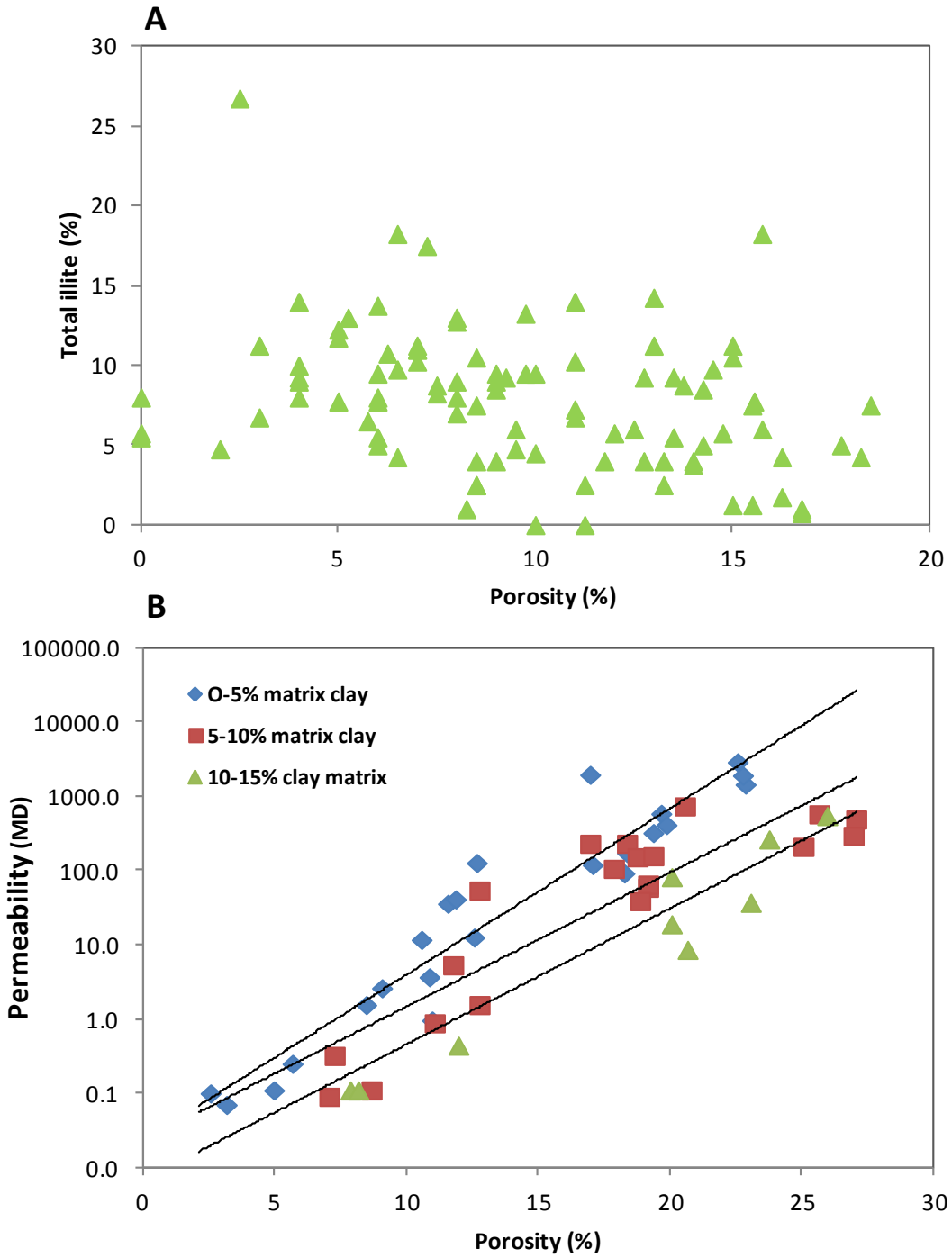

Figure 3.25 Effect of clay content on reservoir quality (A) porosity versus total illite plot (B) core porosity versus permeability plot for different clay matrix percentages. The figure shows that increase in clay content has no significant effect on porosity but reduces permeability.

3.8 Compactional controls on reservoir quality

Mechanical compaction led to rearrangement of grains leading to reduction in pore space. This process has led to deformation of ductile grains smearing it in between grains reducing pore space. Conspicuous evidence of mechanical compaction include grain fracturing, sutured contacts between grains are more conspicuous in the less cemented sandstone.

Chemical compaction and mechanical compaction have both reduced the reservoir quality of the Ula Formation sandstones. Chemical compaction seems to play an important role as stylolite and sutured quartz grain-grain contacts are common. Chemical compaction processes led to dissolution of detrital grains at grain contacts (pressure solution) realising silica solution for the precipitation of authigenic quartz (Fig. 3.21B). This process which is temperature, pH and effective stress, fluid pressure and composition of pore water controlled (Sheldon et al., 2003) becomes effective mainly at temperatures higher than 70^{o}C when rocks are deeply buried (Bjorkum, 1996; Giles et al., 2000; Oelkers et al., 2000). Though it is difficult to estimate the contribution of pressure solution to the amount of quartz cement, it is likely that bulk of the quartz cement in the Ula field has been sourced from pressure solution. The volume of quartz cement is greater in clean and coarse grained samples where grains have clean contacts compared to finer grain samples with abundant pseudomatrix sitting between grains (if all other factors are the same). Chemical compaction is inhibited in the pseudomatrix-rich sandstone because pressure dissolution is minimal and detrital quartz surfaces are often covered with clay that was squeezed between grains, thereby limiting the supply of silica.

Despite the great depth of burial, the oil zone of the Ula reservoir sandstones has not been intensely affected by mechanical and chemical compaction during its progressive burial as evidenced from un-deformed mica grains, and lack of concavo–convex sutured contacts.

3.9 Exploration significance

It is very important to understand the geological process controlling the evolution of pore systems in the Ula reservoirs. Depositional system which controls the initial distribution of lithofacies (especially grain size and clay content) should be understood as they influence the post depositional diagenetic activities of the sandstones. The main post depositional mechanisms of porosity preservation in the Ula field are early oil emplacement and microcrystalline quartz rims that inhibit the precipitation of quartz cement. Occurrence of microcrystalline quartz is associated with sponge spicules which upon dissolution precipitates grain coating microquartz. The main problems to reservoir quality prediction in the Ula field are: lack of depositional model to predict distribution and abundance of sponge spicules, timing of oil charge and distribution of detrital clay.

3.10 Conclusion

The Ula Formation sandstones are composed dominantly of very fine to coarse-grained, moderately sorted arkoses. The detrital framework is dominated by monocrystalline quartz, feldspars and subordinate lithic fragments.

Authigenic minerals include quartz overgrowth, microcrystalline quartz, feldspar overgrowth, dolomite, illite, calcite, chlorite and pyrite. Authigenic quartz is by far the most dominant cement which increases with depth.

Early diagenetic events are precipitation of calcite, micro-dolomite, pyrite and microcrystalline quartz derived from biogenic silica. Late diagenetic events are labile grain dissolution, precipitation of quartz cement, illitization and chloritization of detrital clay and ferroan dolomite. Chlorite and illite occur as pore-filling cements.

Quartz cement is mainly sourced internally through, stylolites, pressure solution, alteration of detrital feldspar, illitization and chloritization of smectite and feldspar. Carbonates are sourced from biogenic related organic matter.

Fluid inclusion evidence shows that quartz cementation is a continuous process and is still taking place in the field. Stable isotope data show that the carbonate cements

in the oil leg grew at about 100 ± 8°C, before oil emplacement, and were largely sourced from dissolved and precipitated bioclastic debris.

Precipitation temperature for carbonate cement in the oil leg stopped at 104 ± 8°C but carbonate cements in the water carried on growing to higher temperature (150 ± 8°C) and show progressive input of source-rock derived CO_2 (as the carbon isotopes get progressively lighter).

Porosity was decreased by compaction and cementation mainly by quartz overgrowth. Permeability is high in clean coarse-grained sand and very low in fine-grained sand with bioturbation and microquartz coating because of high detrital clay content.

3.11 References

Aagaard, P., Jahren, J. S., Harstad, A. O., Nilsen, O., and Ramm, M., 2000, Formation of grain-coating chlorite in sandstones. Laboratory synthesized vs. natural occurrences: Clay Minerals, v. 35, no. 1, p. 261-269.

Aase, N. E., Bjorkum, P. A., and Nadeau, P. H., 1996, The effect of grain-coating microquartz on preservation of reservoir porosity: American Association of Petroleum Geologists Bulletin, v. 80, no. 10, p. 1654-1673.

Ali, A. D., and Tuner, P., 1982, Authigenic K-feldspar in the Bromsgrove Sandstone Formation (Triassic) of ccntral England: Journal of Sedimentary Research, v. 52, no. 1, p. 187-197.

Alvarez, W., Engelder, T., and Geiser, P. A., 1978, Classification of solution cleavage in pelagic limestones: Geology, v. 6, no. 5, p. 263-266.

Baccar, M. B., and Fritz, B., 1993, Geochemical modelling of sandstone diagenesis and its consequences on the evolution of porosity: Applied Geochemistry, v. 8, no. 3, p. 285-295.

Baines, S. J., and Burley, S. D., 1991, Sphalerite mineralization and hydrocarbon migration in North Sea oil fields.

Baker, J. C., 1991, Diagenesis and reservoir quality of the Aldebaran Sandstone, Denison Trough, east-central Queensland, Australia: Sedimentology, v. 38, no. 5, p. 819-838.

Barclay, S. A., and Worden, R. H., 2000, Effects of reservoir wettability on quartz cementation in oil fields, *in* Worden, R. H., and Morad, S., eds., Quartz cementation in sandstones, Volume 29, Special Publication of the International Association of Sedimentologists, p. 103-117.

Bergan, M., Tørudbakken, B., and Wandås, B., 1989, Lithostratigraphic correlation of Upper Jurassic sandstones within the Norwegian Central Graben: sedimentological and tectonic implications, *in* Collinson, J. D., ed., Correlation in hydrocarbon exploration, Norwegian Petroleum Society, Graham and Trotman, London, p. 243-251.

Bjorkum, P. A., 1996, How important is pressure in causing dissolution of quartz in sandstones?: Journal of Sedimentary Research, v. 66, no. 1, p. 147-154.

Bjorkum, P. A., and Gjelsvik, N., 1988, An isochemical model for formation of authigenic kaolinite, K-feldspar and illite in sediments: Journal of Sedimentary Research, v. 58, no. 3, p. 506-511.

Bjorkum, P. A., and Walderhaug, O., 1990, Geometrical arrangement of calcite cementation within shallow marine sandstones: Earth-Science Reviews, v. 29, no. 1-4, p. 145-161.

Bjørlykke, K., 1983, Diagenetic reactions in sandstones: Sediment Diagenesis: Reading, UK, Reidel Publishing, p. 169-213.

-, 1994, Pore-water flow and mass transfer of solids in solution in sedimentary basins: Natural Resources Research, v. 453, p. 189-189.

Bjørlykke, K., and Egeberg, P., 1993a, Quartz cementation in sedimentary basins: Aapg Bulletin, v. 77, p. 1538-1538.

Bjørlykke, K., and Egeberg, P. K., 1993b, Quartz cementation in sedimentary basins: American Association of Petroleum Geologists Bulletin, v. 77, p. 1538-1538.

Bodnar, R. J., 1993, Revised equation and table for determining the freezing point depression of H [sub 2] O-NaCl solutions: Geochimica et Cosmochimica Acta, v. 57, no. 3.

Brown, A., Mitchell, A. W., Nilssen, I. R., Stewart, I. J., and Svela, P. T., 1992, Ula field: relationship between structure and hydrocarbon distribution: Structural and tectonic modelling and its application to petroleum geology: Norwegian Petroleum Society Special Publication, v. 1, p. 409-420.

Bowman, M. B. J., 1981, The sedimentary and reservoir geology of the upper Jurassic Ula Formation and its relationship with other 7/12 Block wells., p. (OC18236)

Caruthers, R. A. and Payne, D. F. 1992 A sedimentological and resrvoir quality evaluation of the Ula Formation (Jurassic) and Skagerrak Formation (Triassic) in well 7/12-10. Badley Ashton report (9167).

Craig, H., 1957, Isotopic standards for carbon and oxygen correction factors for mass spectrometric analysis of carbon dioxide: Geochimeca et Cosmochemica Acta, v. 12.

De Boer, R. B., 1977, On the thermodynamics of pressure solution—interaction between chemical and mechanical forces: Geochimica et Cosmochimica Acta, v. 41, no. 2, p. 249-256.

de Caritat, P., 1989, Note on the maximum upward migration of pore water in response to sediment compaction: Sedimentary Geology, v. 65, no. 3, p. 371-377.

De Ros, L. F., Sgarbi, G. N. C., and Morad, S., 1994, Multiple authigenesis of K-feldspar in sandstones; evidence from the Cretaceous Areado Formation, Sao Francisco Basin, central Brazil: Journal of Sedimentary Research, v. 64, no. 4a, p. 778-787.

Enusten, B. V., and Turkevich, J., 1960, Solubility of fine particles of strontium sulphate: Journal of the American Chemical Society, v. 82, p. 4502-4509.

Giles, M., Indrelid, S., Beynon, G., and Amthor, J., 2000, The origin of large scale quartz cementation: Evidence from large data sets and coupled heat–fluid mass transport modelling: Quartz cementation in sandstones, p. 21-38.

Gluyas, J. G., 1997, Poroperm predictions for reserves growth exploration: Ula trend Norwegian North Sea, *in* Kupecz, J. A., Gluyas, J. G., and Bloch, S., eds., Reservoir quality pr, Volume 69: edictions in sandstones and carbonates, American Association of Petroleum Geologist Memoir, p. 201-210.

Goldberry, R., and Loughnan, F. C., 1977, Dawsonite, aluminohydrocalcite and nordstrandite and geoceixite in Permian marine strata of Sydney Basin, Australia: Sedimentology, v. 24, p. 565-579.

Goldstein, R. H., and Rossi, C., 2002, Recrystallization in quartz overgrowths: Journal of Sedimentary Research, v. 72, no. 3, p. 432-440.

Hall, D. L., Sterner, S. M., and Bodnar, R. J., 1988, Freezing point depression of NaCl-KCl-H 2 O solutions: Economic Geology, v. 83, no. 1, p. 197-202.

Hanor, J. S., 1980, Dissolved methane in sedimentary brines; potential effect on the PVT properties of fluid inclusions: Economic Geology, v. 75, no. 4, p. 603-609.

Harris, N. B., 2006, Low-porosity haloes at stylolites in the feldspathic Upper Jurassic Ula sandstone, Norwegian North Sea: An integrated petrographic and chemical mass-balance approach: Journal of Sedimentary Research, v. 76, no. 3-4, p. 444-459.

Home, P. C., 1987, Ula, *in* Spencer, A. M., Holter, E., Campbell, C. J., Hanslein, S. H., Nelsen, P. H. H., Nysteacher, E., and Ormaasen, E. G., eds., Geology of the Norwegian oil and gas fields: London, Graham and Trotman, p. 143-151.

Karlsen, D. A., Nedkvitne, T., Larter, S. R., and Bjørlykke, K., 1993, Hydrocarbon composition of authigenic inclusions: application to elucidation of petroleum reservoir filling history: Geochimica et cosmochimica acta, v. 57, no. 15, p. 3641-3659.

Land, L. S., and Dutton, S. P., 1979, Cementation of sandstones, reply: Journal of Sedimentary Petrology, v. 49, p. 1359-1361.

Maast, T. E., Jahren, J., and Bjørlykke, K., 2011, Diagenetic controls on reservoir quality in Middle to Upper Jurassic sandstones in the South Viking Graben, North Sea: Americam Association of Petroleum Geologists Bulletin, v. 95, no. 11, p. 1883-1905.

Mansurbeg, H., Morad, S., Salem, A., Marfil, R., El-Ghali, M. A. K., Nystuen, J. P., Caja, M. A., Amorosi, A., Garcia, D., and La Iglesia, A., 2008, Diagenesis and reservoir quality evolution of palaeocene deep-water, marine sandstones, the Shetland-Faroes Basin, British continental shelf: Marine and Petroleum Geology, v. 25, no. 6, p. 514-543.

Maxwell, J. C., 1960, Experiments on compaction and cementation of sand: Rock Deformation: Geological Society of America, Memoir, v. 79, p. 105-132.

McBride, E. F., 1989, Quartz cement in sandstones: a review: Earth-Science Reviews, v. 26, no. 1, p. 69-112.

McKinley, J., Worden, R., and Ruffell, A., 2003, Smectite in sandstones: a review of the controls on occurrence and behaviour during diagenesis: Clay mineral cements in sandstones, p. 109-128.

Milton, C., and Fahey, J. J., 1960, Classification and association of the carbonate minerals of the Green River Formation: Am. J. Sci, p. 242-246.

Nedkvitne, T., Karlsen, D. A., Bjorlykke, K., and Larter, S. R., 1993, Relationship between reservoir diagenetic evolution and petroleum emplacement in the Ula Field, North Sea: Marine and Petroleum Geology, v. 10, no. 3, p. 255-270.

O'Connor, S., Rasmussen, H., Swarbrick, R., and Wood, J., 2001, Integrating a hydrodynamically-titled OWC and a salt-withdrawal depositional model to explore the Ula Trend: Geofluids, v. 11.

Oelkers, E. H., Bjorkum, P. A., and Murphy, W. M., 1996, A petrographic and computational investigation of quartz cementation and porosity reduction in North Sea sandstones: American Journal of Science, v. 296, no. 4, p. 420-452.

Oelkers, E. H., Bjorkum, P. A., Walderhaug, O., Nadeau, P. H., and Murphy, W. M., 2000, Making diagenesis obey thermodynamics and kinetics: the case of quartz cementation in sandstones from offshore mid-Norway: Applied Geochemistry, v. 15, no. 3, p. 295-309.

Partington, M. A., Mitchener, B. C., Milton, N. J., and Fraser, A. J., 1993, Genetic sequence stratigraphy for the North Sea Late Jurassic and Early Cretaceous: distribution and prediction of Kimmeridgian–Late Ryazanian reservoirs in the North Sea and adjacent areas: Geological Society of London, v. 4, p. 347-370.

Robinson, A., and Gluyas, J., 1992, Duration of quartz cementation in sandstones, North Sea and Haltenbanken Basins: Marine and Petroleum Geology, v. 9, no. 3, p. 324-327.

Rossi, C., Kalin, O., Arribas, J., and Tortosa, A., 2002, Diagenesis, provenance and reservoir quality of Triassic TAGI sandstones from Ourhoud field, Berkine (Ghadames) Basin, Algeria: Marine and Petroleum Geology, v. 19, no. 2, p. 117-142.

Sathar, S., Worden, R. H., Faulkner, D. R., and Smalley, P. C., 2012, The Effect of Oil Saturation On the Mechanism of Compaction In Granular Materials: Higher Oil Saturations Lead To More Grain Fracturing and Less Pressure Solution: Journal of Sedimentary Research, v. 82, no. 8, p. 571-584.

Sheldon, H. A., Wheeler, J., Worden, R. H., and Cheadle, M. J., 2003, An analysis of the roles of stress, temperature, and pH in chemical compaction of sandstones: Journal of Sedimentary Research, v. 73, no. 1, p. 64-71.

Siever, R., 1959, Petrology and geochemistry of silica cementation in some Pennsylvanian sandstones, *in* Ireland, H. A., ed., Silica in sediments: Society for Sedimentary Geolgist Spececial Publication, Volume 7, p. 55-79.

Smith, J. W., and Milton, C., 1966, Dawsonite in the Green river formation of Colorado: Economic Geology, v. 61, no. 6, p. 1029-1042.

Stockdale, P. B., 1922, Stylolites: Their nature and origin, Indiana University press, v. 55, 97 p.:

Taylor, M. S. G., LeROY, A., and Førland, M., 1999, Hydrocarbon systems modelling of the Norwegian Central Graben fairway trend, v. 5, p. 1325-1338.

Taylor, T. R., Giles, M. R., Hathon, L. A., Diggs, T. N., Braunsdorf, N. R., Birbiglia, G. V., Kittridge, M. G., Macaulay, C. I., and Espejo, I. S., 2010, Sandstone diagenesis and reservoir quality prediction: Models, myths, and reality: American Association of Petroleum Geologists Bulletin, v. 94, no. 8, p. 1093-1132.

Towe, K. M., 1962, Clay mineral diagenesis as a possible source of silica cement in sedimentary rocks: Journal of Sedimentary Research, v. 32, no. 1, p. 26-28.

Underhill, J. R., 1998, Jurassic, *in* Glennie, K. W., ed., Petroleum Geology of the North Sea:Basic Concepts and Recent Advances, Blackwell Science, p. 656.

Uuoa, M. N., 1991, Smectite-to-chlorite transformation in thermally metamorphosed yolcanoclastic rocks in the Kamikita area, northern Honshu, Japan Arsuyuxr lNour: American Mineralogist Journal, v. 76, p. 628-640.

Walderhaug, O., 1990, A fluid inclusion study of quartz cemented sandstones from offshore mid-Norway - possible evidence for continued quartz cementation during oil emplacement: Journal of Sedimentary Petrology, v. 60, no. 2, p. 203-210.

Warren, E. A., and Pulham, A. J., 2001, Anomalous porosity and permeability preservation in deeply buried Tertiary and Mesozoic sandstones in the Cusiana field, Ilanos foothills, Colombia: Journal of Sedimentary Research, v. 71, no. 1, p. 2-14.

Wilhelms, A., and Larter, S. R., 1994, Origin of tar mats in petroleum reservoirs. Part II: formation mechanisms for tar mats: Marine and Petroleum Geology, v. 11, no. 4, p. 442-456.

Wilkinson, M., Darby, D., Haszeldine, R. S., and Couples, G. D., 1997, Secondary porosity generation during deep burial associated with overpressure leak-off: Fulmar Formation, United Kingdom Central Graben: American Association of Petroleum Geologists Bulletin, v. 81, no. 5, p. 803-813.

Wong, P. K., and Oldershaw, A., 1981, Burial cementation in the Devonian, Kaybob reef complex, Alberta, Canada: Journal of Sedimentary Research, v. 51, no. 2, p. 507-520.

Worden, R. H., 2006, Dawsonite cement in the Triassic Lam Formation, Shabwa Basin, Yemen: A natural analogue for a potential mineral product of subsurface CO2 storage for greenhouse gas reduction: Marine and Petroleum Geology, v. 23, no. 1, p. 61-77.

Worden, R. H., and Barclay, S. A., 2003, The effect of oil emplacement on diagenetic clay mineralogy: The Upper Jurassic Magnus Sandstone Member, North Sea: In: Clay mineral cements in sandstones (eds. Worden, R.H. and Morad, S.) International Association of Sedimentologists Special Publications, v. 34, p. 453-469.

Worden, R. H., French, M. W., and Mariani, E., 2012, Amorphous silica nanofilms result in growth of misoriented microcrystalline quartz cement maintaining porosity in deeply buried sandstones: Geology, v. 40, no. 2, p. 179-182.

Worden, R. H., and Morad, S., 2000, Quartz cementation in oil field sandstones: a review of the key controversies, Wiley Online Library.

Woronick, R., and Land, L., 1985, Late burial diagenesis, Lower Cretaceous Pearsall and Lower Glen Rose Formations, South Texas.

CHAPTER 4

4. Does oil emplacement stop quartz cementation in deeply buried sandstone reservoirs? Evidences from the Upper Jurassic Ula Formation, Ula field, North Sea

4.1 Abstract

Quartz cement is an important porosity-occluding cement in sandstone reservoirs that are exposed to elevated temperature and effective stress for a significant period of time. The effect of oil emplacement is controversial with some concluding that early oil emplacement inhibits quartz cementation and preserves porosity in deeply buried reservoirs while others claim that quartz cementation continues unabated whether oil is present or not. In this work, shallow marine, Upper Jurassic sandstones from the Ula field in the Norwegian North Sea have been studied in an attempt to determine the effect of oil emplacement on diagenesis with particular attention to the distribution of quartz cements relative water saturation.

Core samples collected from the oil and water legs and the transition zone were studied using a range of techniques: core analysis, core logging, downhole wireline log analysis, light optics, scanning electron microscope (SEM), cathodoluminescence (CL), X-ray diffraction (XRD), fluid inclusion UV-petrology and thermometry. The distributions of all potential controls on porosity and permeability have been quantified so that it has been possible to assess the influence of all possible controls on quartz cement as well as fluid type. Thus the roles of depositional facies, grain size, sorting, chlorite coats and microcrystalline quartz coats have all been assessed. Using published burial and thermal histories, fluid inclusion studies have revealed that oil emplacement into the Ula reservoir commenced prior to the onset of quartz cementation. The results show that there is a consistent difference in the amount of quartz cement and thus porosity and permeability between the oil and water legs that cannot be explained by difference in facies, grain size, sorting, chlorite or grain-coating microcrystalline quartz coats. It must therefore be concluded that oil

emplacement has significantly inhibited the rate of quartz cementation. Early emplacement of oil into the Upper Jurassic Ula Formation sandstones seems to be an important control on reservoir quality.

4.2 Introduction

The Ula field is an offshore oil field located in the southern Norwegian sector of the North Sea (Fig. 4.1) along with Gyda, Tambar and Tambar East fields, making up the Ula-Gyda-Tambar (UGT) area (O'Connor et al., 2011). The Ula field is a very good site to study diagenesis because there is much core and supporting downhole data covering the whole field. The Ula Formation is the main reservoir rock in the Ula field. Accurate prediction of reservoir quality is ideally needed throughout the entire "life cycle" of a reservoir (Sneider, 1990). The accurate prediction of reservoir quality is, and will continue to be, a key challenge for hydrocarbon exploration and development. Assessing reservoir quality risk is important in plays and prospects where target sandstones have been exposed to elevated temperatures (>100°C) and/or high effective stress for significant period of time (Taylor et al., 2010).

Quartz cement is the most volumetrically important cement in deeply buried sandstones; being able to predict areas or sandstone units where quartz cement has been anomalously inhibited could lead to improved reservoir quality prediction. The concept that oil emplacement could inhibit quartz cementation and influence preservation of porosity in sandstone reservoirs became known to many geologists in R. H. Johnson's (1920) publication "The cementation process" and later from the works of Hawkins, (1978); Lowry, (1956); Scholle, (1977); and Scholle and Halley, 1985).

All diagenetic reactions take place, through an aqueous phase, by dissolution and re-precipitation. There is no possibility of significant solid state reactions at diagenetic temperatures, as solid state diffusion is too slow, even on geological time scales (Wilkinson and Haszeldine, 2011). Hence, for diagenetic reaction to occur there must be water to dissolve the mineral grains, an aqueous fluid pathway from the site of mineral dissolution to the site of precipitation and water at the site of mineral precipitation. In an oil or gas field, displacing the aqueous pore fluid by petroleum disrupts the pathway between the reactants and points of precipitation. If the oil saturation becomes high; (i) the residual (irreducible) water becomes isolated within a continuous hydrocarbon phase or (ii) the aqueous pathway becomes tortuous and

diffusion becomes slow or (iii) grain surfaces become coated by oil if the sandstone is oil wet (Barclay and Worden, 2000). Hence it was initially assumed that cementation is halted and porosity is preserved due to early oil emplacement.

Over the years there have been many publications that used the concept that early oil emplacement is a mechanism for porosity preservation in sandstone reservoirs (Bjørnseth and Gluyas, 1995; Dixon et al., 1989; Emery et al., 1993; England et al., 2003; Gluyas and Cade, 1997; Gluyas et al., 1993; Haszeldine et al., 2003; Higgs et al., 2007; Marchand et al., 2000; Marchand et al., 2001; Marchand et al., 2002; Robinson and Gluyas, 1992; Saigal et al., 1992; Wilkinson and Haszeldine, 2011; Wilkinson et al., 2004; Wilkinson et al., 2006) and in carbonate reservoirs (Feazel and Schatzinger, 1985; Hardman, 1982; Heasley et al., 2000; Neilson et al., 1998; Rothwell et al., 1993; Scholle, 1977; Scholle and Halley, 1985).

When quartz cement volume and albitized K-feldspar grains in the oil leg was compared to the water leg in Fulmar reservoir sandstones of the North Sea Saigal et al., (1992), found lower volumes of both quartz cement and albitized K-feldspar in the oil leg. Despite the similarity in homogenization temperature of fluid inclusions in quartz cement between oil leg and water leg they concluded that oil emplacement had retarded quartz cementation. From petrographic data and porosity measurements of the deeply buried invariably homogeneous, overpressured, sandstones of the Fulmar Formation, North Sea (Wilkinson and Haszeldine, 2011) concluded that early oil charge has preserved exceptional porosity.

In Brae Formation sandstones of the Miller and Kingfisher fields United Kingdom North Sea it was reported that there was a significant difference in quartz cement volume abundance between the oil leg and the water leg (Marchand et al., 2002). Quartz cementation rates were said to have been reduced by at least two orders of magnitude in the oil legs relative to water legs. The average volume of quartz cement increases from 6% in the oil bearing zones at the structural crest to 13.3% in the water bearing sands along the structural flank.

Studies of outcrop and subsurface samples of chalks from the North Sea, onshore Europe, the Scotian Shelf, Gulf Coast, and the U.S. Western Interior have shown that early introduction of oil into the rock also may preserve initial porosity through the exclusion of water (Scholle, 1977). Specifically, studies of chalk reservoirs have shown that replacement of oil with water during enhanced oil recovery by water-flooding results in collapse of the overlying rock column (De Gennaro et al., 2004; Hickman et al., 2008). The collapse is not due to overpressure-release since it occurs even when fluid pressure was maintained (De Gennaro et al., 2004). Much work has been undertaken to understand this phenomenon and it has been concluded that pressure solution is the key mechanism for compacting the increasingly water-filled chalk reservoirs (Risnes et al., 2005). By inference, this suggests that oil emplacement had significantly inhibited pressure solution over geological timescales but once water was put back into the chalk, then pressure solution could resume. The interpretation that rock column collapse during water-flooding was due to enhanced pressure solution has been supported by experimental approaches (De Gennaro et al., 2003; De Gennaro et al., 2004; Risnes et al., 2003; Risnes et al., 2005). Experimental studies of the effect of oil emplacement on compaction in granular halite have also shown that addition of oil significantly impedes pressure solution and the subsequent cementation (Sathar et al., 2012).

In contrast to these experiments on pressure solution, an experiment conducted on quartz-water-oil-gas system under elevated temperature and pressure (up to 350°C and 400 bar) using supersaturated silica to try to grow quartz cement in the presence of oil, the trapping of fluid inclusions and the formation of quartz cement were not suppressed under conditions of high oil saturation (Teinturier and Pironon, 2004). These experiments did not mimic pressure solution and were performed at very high temperature and pressure.

In recent years, several other workers have reported that quartz cement can continue to grow unhindered in oil fields after oil emplacement (Aase and Walderhaug, 2005; Bjørkum and Nadeau, 1998; Ehrenberg, 1990, 1993; Giles et al., 1992; Midtbø et al., 2000; Molenaar et al., 2008; Ramm and Bjorlykke, 1994). To explain this rather

different interpretation of diagenetic processes, it was assumed that the combined dissolution-diffusion-precipitation processes utilize the residual water that clings to grain surfaces and that this film of water apparently permits diagenesis to continue unhindered.

The occurrence of oil-bearing fluid inclusions trapped in quartz cement has also been used as evidence that quartz cement can continue to grow in the presence of oil (Ramm, 1992; Saigal et al., 1992; Teinturier and Pironon, 2004; Walderhaug, 1996). Using the presence of petroleum inclusion in authigenic quartz and homogenization temperatures as evidence (Nedkvitne et al., 1993) concluded that quartz cementation has continued to grow in the in the oil leg after oil charge in the Ula Field. However, it must be noted that the significance of petroleum inclusions remains unknown, there being no proven link between the occurrence of oil inclusions and oil saturation. Oil inclusions could become trapped in mineral cements even at low oil saturations (Worden et al., 1998).

In contrast to the work by Marchand et al. (2002), for the same field, a later separate study claimed that, when all data were taken into account, no discernible relationship between quartz cement volume and pore-fluid type was apparent in the Miller field (Aase and Walderhaug, 2005). They regarded the interpretation of porosity preservation due to hydrocarbon emplacement as being erroneous and instead assigned quartz cement inhibition as being due to microquartz coatings on sand grains. This assertion was further developed by some more selective and not fully-published petrographic work (Bonnell et al., 2006).

Using broad range of data from different geographical regions covering wide range of temperatures and burial depths (Giles et al., 1992) reported they found no systematic difference in porosity between the oil zone and the water zone.

Similarly, a regional review of Upper Jurassic sandstones of the south Viking Graben, North Sea, (Maast et al., 2011) claimed that there is no correlation between hydrocarbon saturation in sandstones and high porosity. On the contrary, they

reported that hydrocarbon saturated sandstones are found in the high, the normal, and the low-porosity sandstone. The water leg and the oil leg display similar amount of quartz cement.

Volumes of quartz cement and porosity in oil-filled sandstones, dry structures as well as water filled sandstones in Cambrian reservoirs sandstones from the Palaeozoic Baltic Basin were compared (Molenaar et al., 2008) and it was concluded that oil emplacement has no noticeable effect on porosity and quartz cement precipitation.

Comprehensive overviews of the empirical and theoretical arguments for and against oil emplacement inhibiting quartz cementation (Worden and Morad, 2000; Worden et al., 1998) concluded that quartz cementation that is synchronous with, or after, oil emplacement in sandstone is probably slow down relative to quartz cementation in the underlying aquifer. Quartz cementation will be strongly inhibited if the system is mixed or oil-wet, if the silica is externally supplied or if advection is an important part of the transport process. However, even in internally-sourced silica systems with diffusion as the transport control, quartz cementation will be slowed down due to added tortuosity of the diffusion pathway once oil is in the pore system. The question of the inhibiting effect of oil on quartz cementation remains open and is highly contentious (Sathar et al., 2012; Taylor et al., 2010) .

The key elements of risk in exploration and production within the Ula trend is the presence and effectiveness of reservoir (Bjørnseth and Gluyas, 1995), thus success in managing the Ula field depends on the ability to map out the extent of porosity in the trend and its distribution. The aim of this paper is to view whether oil charge has stopped or retarded quartz cementation and consequently preserved porosity in the Ula Formation. Understanding this phenomenon will help in predicting porosity and permeability distribution in an oil field and enhance more accurate volumetric reserve estimate in prospects and well performance (such as aquifer influx) during production.

One of the main difficulties in addressing the question of oil inhibition of quartz cement is the large number of potential controls on quartz cementation, over and above the question of fluid type. The main variables include the important question of the timing of oil emplacement relative to quartz cementation, primary sedimentary facies (and the associated variables: grain size, sorting and detrital clay), primary depositional mineralogy, presence, type and extent of grain coating materials (such as chlorite or microcrystalline quartz), occurrence of (typically early diagenetic) pore-filling cements before quartz cementation commenced, wettability and tortuosity, the source of quartz cement and the exact degree of oil saturation. It is possible that previous studies have compared fundamentally different rocks when trying to prove or disprove the effect of oil emplacement on quartz cementation. In this paper, we have defined oil saturation for each sample and we have been careful to compare sandstones from the same facies. We have also carefully quantified the presence, type and extent of grain coating materials and taken account of pore-filling cements and only made comparison between rocks that are the same in every other way (apart from oil saturation). Key questions to be addressed are;

1. Was oil present during quartz cementation in the Ula Formation?
2. Is there a difference in the quartz cement content above and below the oil-water contact for rocks of the same pre-oil filling characteristics?
3. What other influences are there on quartz cementation in the Ula Formation?
4. How much quartz would we expect if no oil were present in the Ula Formation?
5. Has oil slowed down or stopped quartz diagenesis in the Ula Formation?

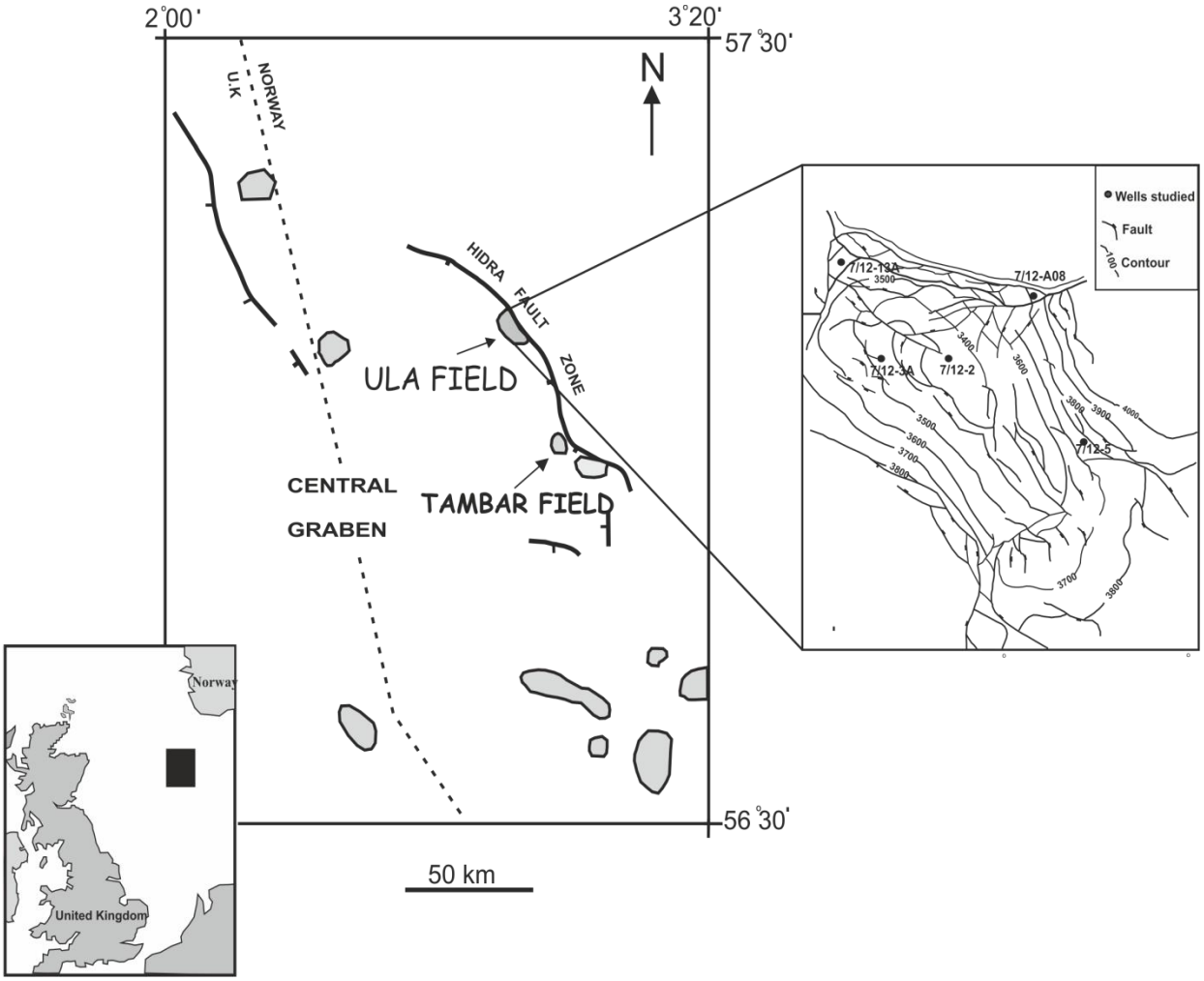

Figure 4. 1 Location map of the Central Graben showing the Ula field with insert map of the North Sea region (lower left) showing study area in black square and insert structural map right showing structures and well locations (Modified from Nedkevitne et al., 1993).

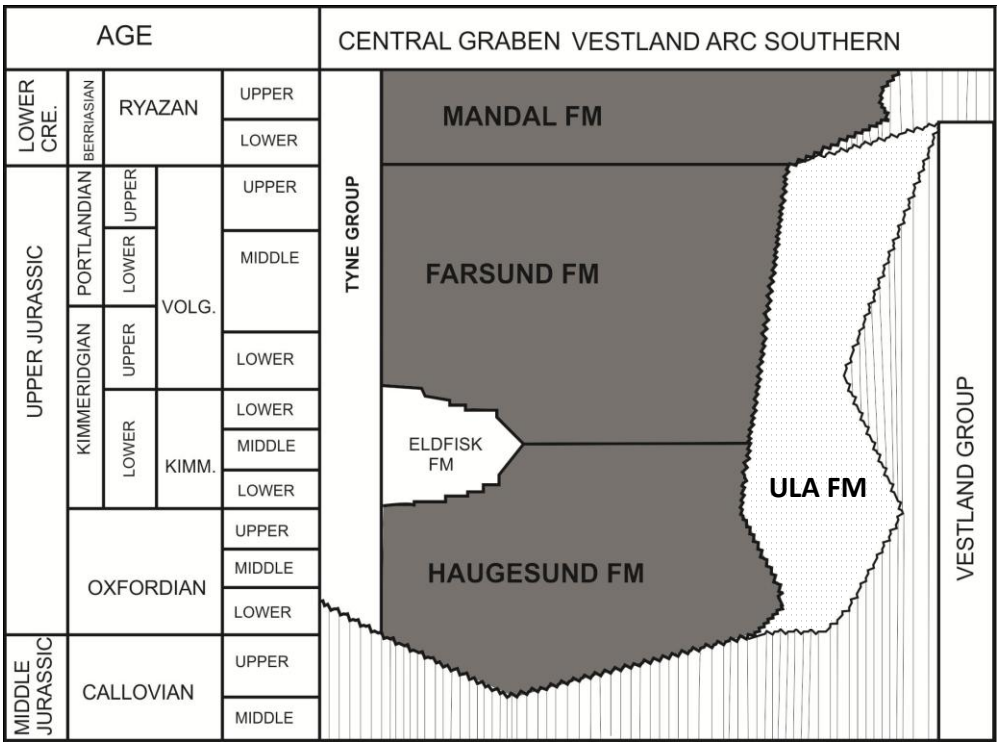

Figure 4. 2 Generalised stratigraphy of the Ula field modified from (Fraser et al., 2002). The Mandal Formation is the main regional source rock, the Ula Formation is the reservoir in question.

4.3 Geological background

The Ula field is located 280 km south-west of Stavanger at the eastern margin of the Central Graben along Hidra Fault zone (Fig. 4.1) (Nedkvitne et al., 1993). The field consists of Upper Triassic to Upper Jurassic sandstones in an anticlinal structure. The structure is a result of late Jurassic rifting followed by inversion in the Cretaceous and Tertiary (Brown et al., 1992). Oil was generated from the Upper Jurassic Mandal Formation beginning in the late Cretaceous from the deeper parts of the Central Graben and is currently being generated in the Ula trend (Taylor et al., 1999). The reservoir rock is the Upper Jurassic Ula Formation (Fig. 4.2) (Bergan et al., 1989; Karlsen et al., 1993; Partington et al., 1993; Underhill, 1998).

Ula Formation underwent more than 2000m of subsidence after the early Oligocene and is overpressured possibly as a result of the rapid late Tertiary subsidence (Harris, 2006; O'Connor et al., 2011). Multiple pressure measurement by repeat formation

tester is equivalent to an average gradient of 0.703 psi/foot (15.9 Mpa/km), equivalent to an excess over normal pressure in Jurassic sandstones of the Central Graben to hydrocarbon generation in the overlying Farsund Formation. The Ula reservoir has a tilted oil water contact (O'Connor et al., 2011) thus obviating the sense in simply plotting reservoir characteristics versus depth when assessing the influence of pore fluid type. Porosities in the Ula Formation range mostly between 14 to 28%, with permeabilities mostly between 650 to 850 mD in the better reservoir units (extremes 0.2 to 2800 mD)(Karlsen et al., 1993). Reservoir temperature at 3450 m is 143 to 145 ^{o}C (Home, 1987). Within the Ula trend, the Mandal Formation provides seal for the underlying Jurassic sandstones (Bjørnseth and Gluyas, 1995).

This unit is a marine sandstone, up to 200m thick, that prograded across outer-shelf mudstones, following a sea level drop in the Kimmeridgian (Harris, 2006). The Ula Formation is typically fine, well sorted, variably bioturbated and locally glauconitic with some beds rich in shale fragments. The Ula Formation has been intensively burrowed, and even where no burrows are evident, physical sedimentary structures are nonetheless absent, suggesting that the unit has been completely bioturbated. Trace fossils are limited to *Ophiomorpha*, suggesting a shallow marine origin for the sandstone (Bowman, 1981). The key element of risk in exploration within the Ula trend is the presence and effectiveness of reservoir (Bjørnseth and Gluyas, 1995), thus exploration success in the Ula field depends on the ability to map out the extent of porosity in the trend and its distribution.

The Ula Formation sandstones have been described as arkorsic and interpreted as having been sourced from nearby Triassic sandstone outcrop (Gluyas, 1997). He also stated that they are significantly affected by quartz cementation, with quartz cement volume ranging from as little as 3% to as much as 19%. He attributed the variation in quartz cement volume, which occurs over a very narrow range of burial depth, to the timing of cementation relative to oil emplacement. However, the Ula Formation sandstones in Ula and Gyda fields have also been described as being high porosity sandstones due to the presence of grain coating microcrystalline quartz, seen using

SEM examination, due to the original presence of detrital sponge spicules in the sandstone (Aase et al., 1996).

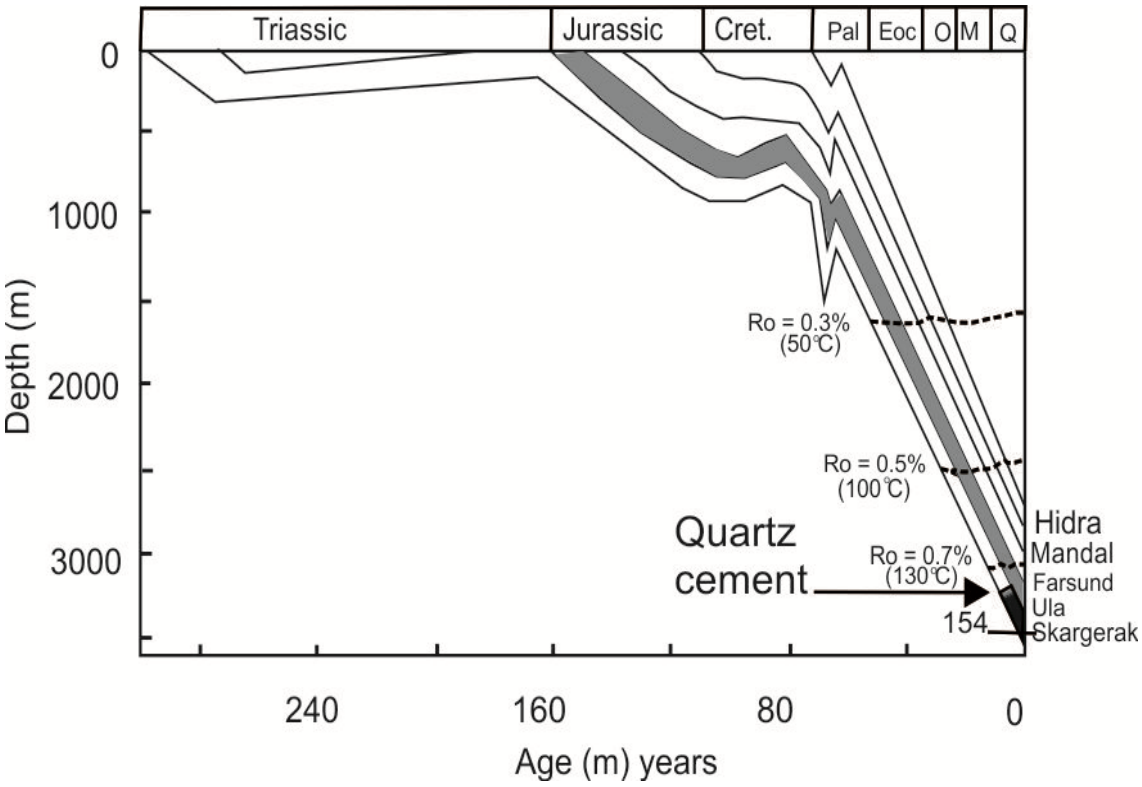

Figure 4. 3 Burial history curve of the Ula field from well 7/12-6, grey is the reservoir rock. Burial history curve modelled using the Chinese version of Thermodel for Windows software.

4.4 Methods and material

Wireline and conventional core analysis data were made available by BP Norway. Core plugs were taken at 30cm-spacings with porosity and permeability measured using industry-standard methods. The downhole wireline logs available were: caliper, bulk density, neutron porosity, sonic transit time, bulk gamma, shallow resistivity and deep resistivity. Wireline data were reported every 10cm from the Ula Formation from each well. Porosity was calculated for each of the logs using the density log and the following relationship:

Fractional porosity = $(\rho_{mbd} - \rho_{amd})/(\rho_{fd} - \rho_{amd})$ (eq 1)

Where:

ρ_{mbd} = measured bulk density (from wireline logs)

ρ_{amd} = average mineral density

ρ_{fd} = fluid density

The average mineral density employed was 2.66 g/cm^3. The average fluid density was taken as 1.00 g/cm^3 since the fluid in the zone next to the well bore will be aqueous due to the water-based drilling fluids replacing the initial pore fluid. The results of the wireline calculation of porosity were compared to the core analysis porosity to check credibility (Fig. 4.4).

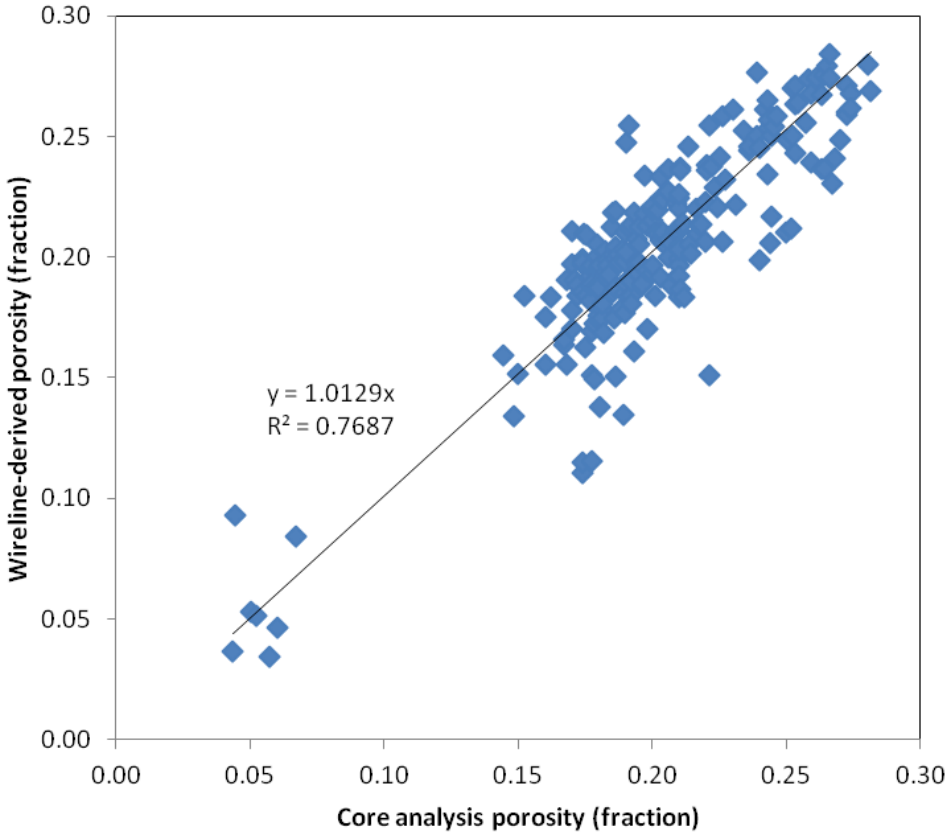

Figure 4. 4 Comparison of core analysis porosity and wireline-derived porosity for well 7/12-A13.

Water saturation was calculated from the wireline data for each depth using the Archie equation:

$S_w = [(a/Ø^m)/(R_w/R_t)]^{(1/n)}$ (eq 2)

Where:

Sw = fractional water saturation

n = saturation exponent

a = tortuosity constant

R_w =formation water resistivity (determined at reservoir temperature)

R_t = formation resistivity (obtained from deep resistivity log to reduce any effect of drilling mud).

Ø = density log-derived fractional porosity (see equation 1)

m = cementation exponent

Values of n, a, and m were fixed at 2.5, 0.82 and 2.0 respectively as used by the field development geoscientists. Only deep induction resistivity measurements were used in the formula, as these are the only resistivity measurements that give true formation resistivity, unaffected by invasion of the formation by drilling fluids (Asquith and Gibson, 1982). Water resistivity was taken to be 0.025 ohm/m (Oxtoby, 1994).

One hundred and fifteen samples of conventional core plugs from five wells were obtained from the BP core store at Reslab laboratories in Stavanger, Norway. The core sample suite covers the range of present subsurface measured depths between 3350m and 4100m, and spans the thickness of the whole reservoir. Individual sandstones were studied using a combination of techniques, including petrography, scanning electron microscopy (SEM), cathodoluminescence microscopy (CL), X-ray diffraction (XRD) and fluid inclusion micro-thermometry.

Polished thin sections were made from the core samples. The polished sections were impregnated with blue resin in order to highlight porosity. Sandstone modal composition was obtained by detail point counts (400 counts per section) of all thin sections. Grain sizes and grain coating were measured using Meiji 9000 microscope fitted with an Infinity 1.5 digital camera. Images were snapped and long axes of 100 grains were measured using Infinity Analyser software. No corrections for grain cut effect were applied. Fifty grains per section was measured for percentage of grain-coating microcrystalline quartz coverage using visual estimates. Only potential sites for quartz cementation (i.e. facing pores, not coated with dead-oil or with clay

matrix) that were coated with microcrystalline quartz were measured and expressed as a percentage of all potential sites for quartz cementation.

SEM examinations were made using a Philips XL 30 SEM with tungsten filament with an accelerating voltage of 20 kV, and 8 nA beam current for both SE and BSEM. The SEM was carried out on polished sections and freshly fractured, stub-mounted samples coated with carbon and gold respectively. Energy dispersive X-ray analysis (EDAX) provided qualitative compositional analysis of clay minerals, carbonate cements and feldspars. Some of the sandstone samples were soaked in acetone to remove the oil stains which caused problems for the vacuum system in the gold coater. The CL images were collected at 10 Kv and spot size 7. They were collected by integrating the signal of 16 frames using a slow scanning raster which takes about 8 minutes to collect. Samples for XRD were cut from the core samples.

PANalytical X'pert pro MPD X-ray diffractometer was used for the XRD analysis. Samples were crushed using micromill and distilled water for 10 minutes. They were then dried overnight in a low temperature oven and powdered using agate pestle and mortar. A copper X-ray source operating at 40kV and 40mA was used. Powder samples were loaded into cavity holders and rotated continuously during the scan, completing one rotation every 2 seconds. Programmable anti-scatter slits and a fixed mask maintained in an irradiated sample area of 10 x 15 mm, with an additional 2^{o} incident beam antiscatter slit producing a flat background for raw data down to a 2theta angle of 3^{o}. The X'Celerator detector was set to scan in continuous mode with full length active pulse-height discrimination levels set to 45 to 80%. Operation of X-ray Diffractometer and Software was set using "HighScore Plus ®" analysis software and automated Rietveld refinement methods with reference patterns from the International Centre for Diffraction Data; Powder Diffraction File-2 Release 2008.

Fluid inclusions microthermometric studies were carried out on selected samples. Doubly polished fluid inclusion wafers were prepared from the core samples at the University of Birmingham. An Olympus BX-60 petrographic microscope was used for thermometry and was equipped with a Linkam THMSG 600 heating and cooling

stage which enabled the measurement of the temperature of phase transition from -180^0 to 600^{0}C with an accuracy of ± 0.1 to ± 1.0. Observations were made with different magnifications (objectives 10x, 20x, 50x and 100x). Inclusions were photographed with Digital Camera Olympus DP71 for the purpose of the fast mapping of inclusion locations. Homogenisation temperature measurements were made on each inclusion in each small piece of fluid inclusion wafer and then freezing point depression measurements were made on each inclusion to prevent modification of the homogenisation temperature (Worden et al., 1995). All fluid inclusion samples were also studied using UV-luminescence using Olympus BX-60 microscope. A super high pressure mercury lamp was used to provide the light. The purpose of this was to check for the possible presence of the oil inclusions. Chinese version of Thermomodel for windows was used in modelling the burial history curve. Assumed surface seafloor temperature used was 5^{o}C and constant present geothermal gradient of 40^{o}C/km (Nedkvitne et al. 1993).

4.5 Results

4.5.1 Wireline and core analysis data

The density derived porosity and water saturation values for each 10cm interval from each well, derived using the density and resistivity logs and the Archie equation are illustrated in Figure 4.5. The wireline-porosity correlate well with the core analysis porosity (Fig. 4.4). There are a wide range of water saturations revealed for the Ula reservoir with well 7/12-2 having low water saturation, 7/12-a13 having very high water saturation and 7/12-a3 somewhere in between. Wells 7/12-5 and 7/12-a-08 seem to represent the transition zone from oil leg to water leg. The very low porosity and high water saturation "spikes" (e.g. for well 7/12-2) represent carbonate cemented intervals. The water saturation from each sample (including those with core analysis and petrological data) was determined using this approach.

The core analysis data have been split between the three main lithofacies (see following section) and data for each lithofacies have been divided by water saturation calculated using the Archie approach (see Fig.4. 5). For all facies, it

seems that the samples with the lowest water saturations (highest oil saturations) have the highest porosities and permeabilities (Figs. 4.6a-c). The very fine to fine grained sandstones have the lowest porosity and permeability values.

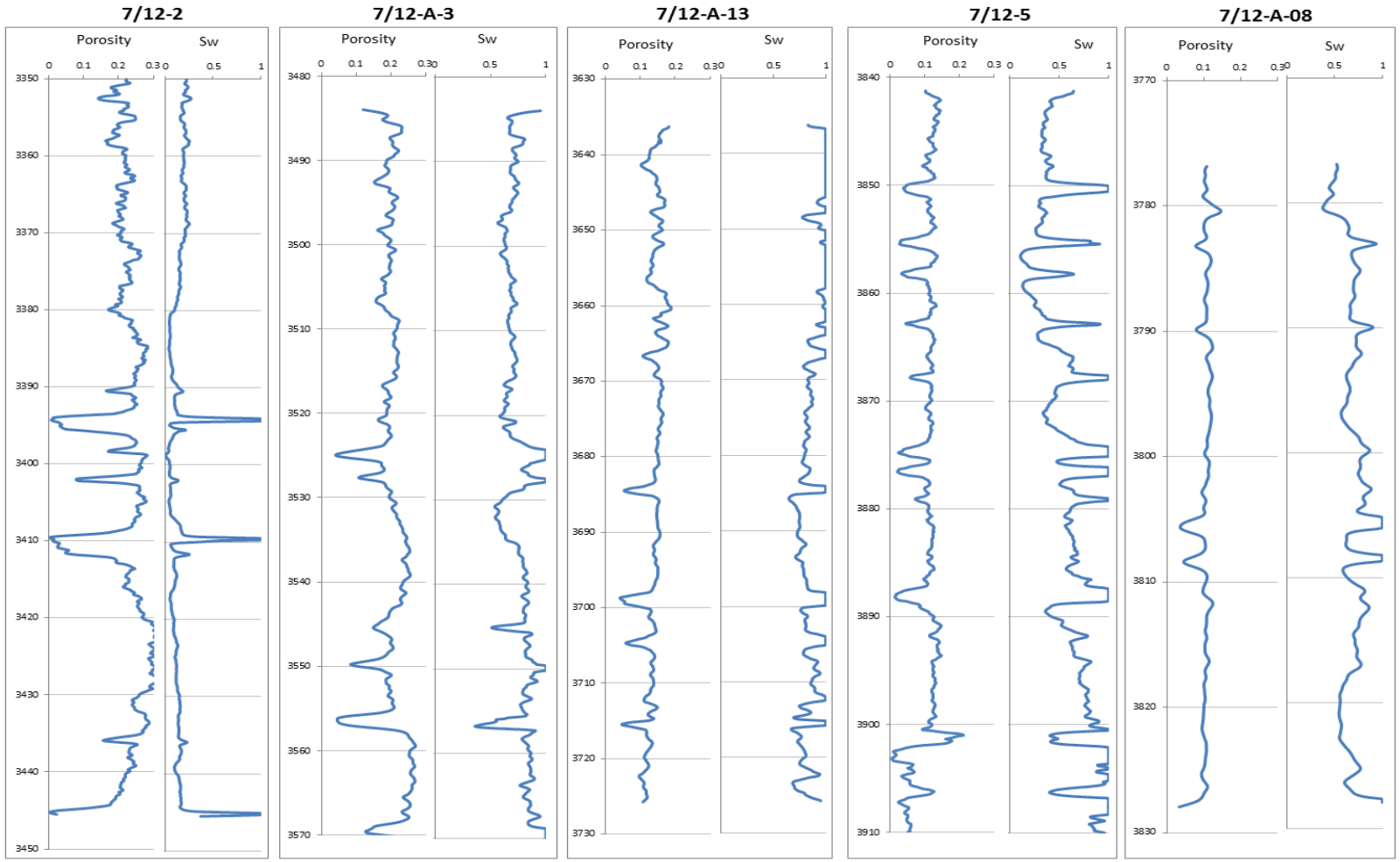

Figure 4. 5 Plots of density-derived porosity and Archie-derived water saturation (Sw) from the five wells from the Ula field used in this study.

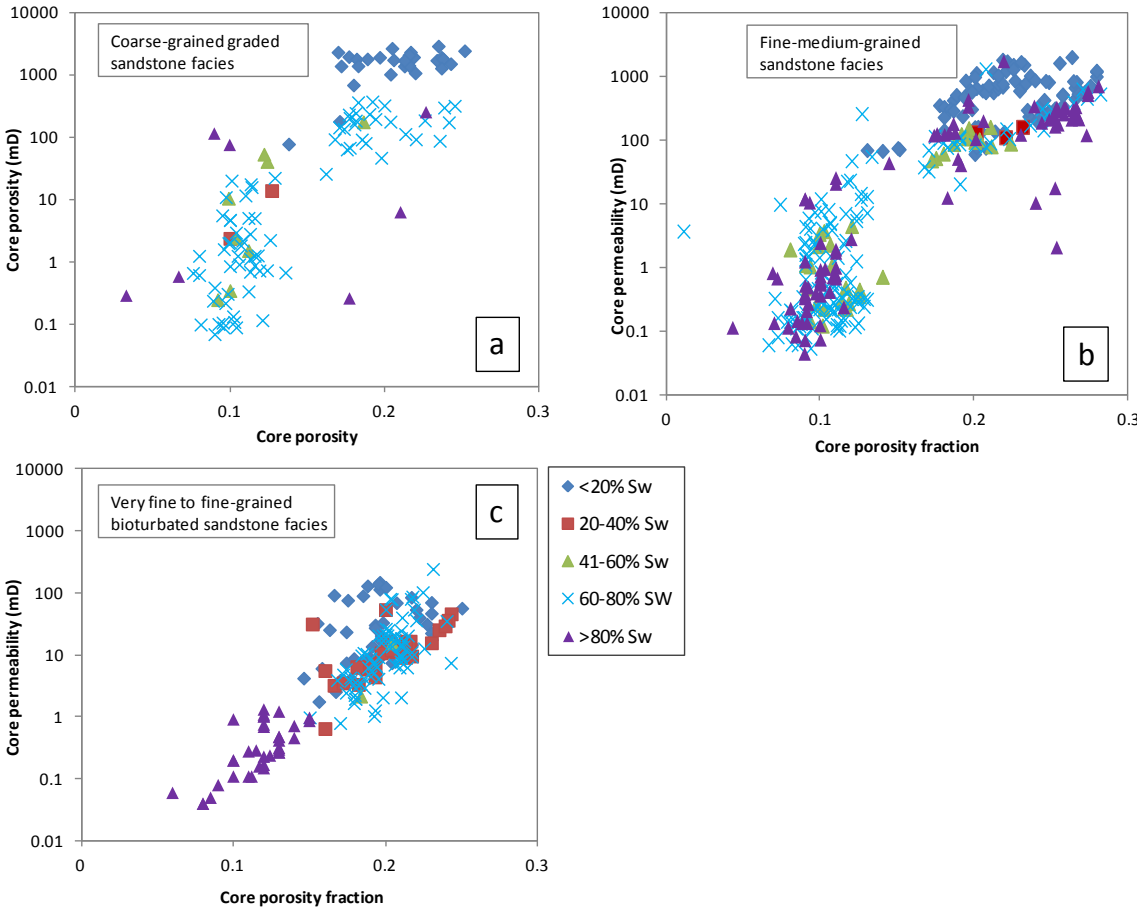

Figure 4. 6 Plots of reservoir parameters for different water saturations for clean different lithofacies (a) Core porosity versus core permeability for fine-medium grained biotubated sandstone facies (b) Core porosity versus core permeability for coarse-grained graded sandstone facies (c) Core porosity versus core permeability for very fine to fine grained biotubated sandstone facies.

4.5.2 Petrographic data

The Ula Formation reservoir is an arkosic sandstone (Fig. 4.7) (Bowman, 1981). Petrographic variations in the Ula Formation are related to depositional lithofacies. The main variations in different lithofacies are in terms of: grain size, clay content and degree of bioturbation.

The three main lithofacies are:

1. Coarse-grained, graded sandstone facies medium to coarse-grained, moderately well-sorted (0.52ø), with low detrital clay content (av. 3.3 ± 0.3%) and no direct sign

of bioturbation. Point counting result shows that the most dominant detrital mineral is monocrystalline quartz (av. 34 ± 2%), followed by K-feldspar (av. 11 ± 0.3%) and plagioclase (14 ± 0.3%). Polycrystalline quartz and traces of rock fragments are also present in this facies.

2. Fine-medium grained, bioturbated sandstone facies, fine-medium grained, moderately- to well-sorted (0.62ø), with variable detrital clay content ranging from (3-15%). Dominant detrital mineral grains are monocrystalline quartz (av. 28 ± 2%), K-feldspar (av. 9 ± 0.6%), plagioclase (av. 15 ± 0.8%) and rock fragments (<3%).

3. Bioturbated, very fine to fine-grained sandstone facies, intensively bioturbated, moderately-sorted (0.83ø) with a high detrital clay content ranging from 9 to 27%. The dominant detrital mineral grains are monocrystalline quartz (av. 27 ± 2%), K-feldspar (av. 7 ± 0.2%), and plagioclase (av. 11 ± 0.3%). This facies has an abundance of shell fragments, mica flakes, glauconite and siderite but only small amounts of rock fragments. XRD and SEM (Chapter 3 Figs. 3.11A, B and 3.14 A - D) revealed that the detrital clay in all facies is dominantly illitized with minor chlorite.

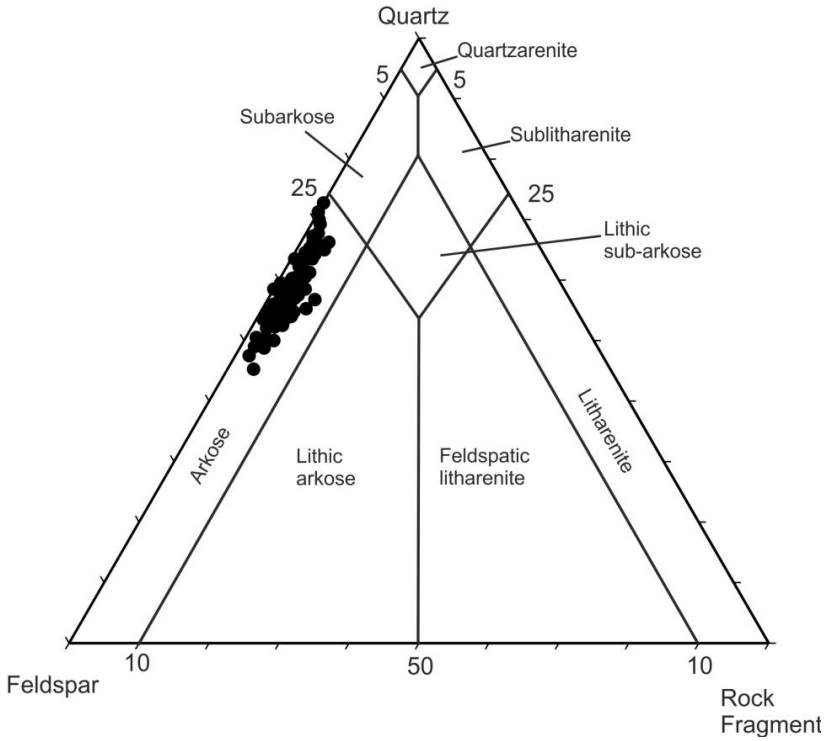

Figure 4. 7 Ternary diagram showing the Ula Formation sandstone classification (after McBride, 1963).

4.5.3 Authigenic minerals

The Ula Formation varies from porous with small amounts of cement (Fig. 4.8a) to highly cement in which the porosity is almost completely occluded by quartz cement (Fig. 4.8b). The most important authigenic minerals are quartz overgrowths, grain-coating microcrystalline quartz, illite and ferroan dolomite cements.

Authigenic quartz overgrowths are mainly euhedral (Fig. 4.9a) in thin sections. The boundary between detrital quartz grain and quartz overgrowth are characterized by rim of clay minerals or fluid inclusions (Fig. 4.9a black arrow). Quartz overgrowth range in thickness from <10µm to >50µm, sometimes occluding porosity completely where overgrowths in neighbouring grains interlock. Quartz overgrowth is more abundant in cleaner coarse-grained sandstone units than clay rich finer grain units (Table 1). SEM-CL observation revealed that the cement does not show zoning (Fig. 4.8d). SEM-CL confirms the volumetric importance of quartz cement in the Ula Formation. It is particularly abundant in well 7/2-A08 (18%). It increases with depth if all other factors are the same. The euhedral edges of quartz overgrowth are often stained by "dead" petroleum/bitumen (Fig. 4.9a).

SEM observation on polished sections and freshly fractured rock samples show that some of the samples contain microquartz (Fig. 4.10 a & b, Table 4.1). The microquartz occurs in two forms; <5µm more regularly oriented crystals that nucleate on quartz and other grains, and 5 to >10 µm crystal that nucleate mainly on quartz grains. The occurrence is more restricted to particular facies (very fine to fine bioturbated sandstone) in all the studied wells. Thin film of amorphous silica probably chalcedony is commonly seen coating the grains and sometimes underneath the microquartz. The point-counted volume of microcrystalline quartz range from 0 to the very high value of 9 %. It can be difficult to quantify the volume of microquartz from point counting because of their small size in light microscope; so, the volume here may be underestimated. It was decided to compliment point counting by measuring the percentage of quartz grains coated with microcrystalline quartz.

Dolomite in the Ula Formation occurs as non ferroan, ferroan and microrhombic forms. The most volumetrically important carbonate cement is rhombic ferroan dolomite with the rare rhombs sitting in pores and having a minor effect on the flow properties of their hosts. The mean point count volume for total dolomite is 4%. Ferroan dolomite is most abundant in the more argillaceous units (finer grained facies; Table 4.1). The ferroan dolomite replaces or crosscuts quartz cement. A few layers are completely cemented with early diagenetic calcite and so have zero porosity (Fig. 4.5). These nodular or bedded calcite-cement samples have been excluded from the dataset since they clearly do not inform the discussion about the effect of oil emplacement on quartz cementation.

Chlorite predominantly occurs as minor pore-filling rosettes and rarely as a grain rimming clay. Volumetrically chlorite is less <3% and appears to be facies related with the majority occurring the finer grained bioturbated facies. Grain-coating chlorite is not present as an important aspect of the Ula Formation reservoir.

A comparison of the effects of cementation and compaction using a Houseknecht type plot (Fig. 4.11) shows that there is a subtle difference in the control on porosity-loss as a function of position in the oil field. On average, the oil leg samples show 48 % porosity lost to compaction and 52% lost to cementation. In comparison, the water leg samples show 36% lost to compaction and 64 % lost to cementation. It seems that quartz cement, the dominant diagenetic mineral, dominates in the high water saturation zone leg while there has been less cement and relatively more compaction in the high oil saturation zones (Fig. 4.11).

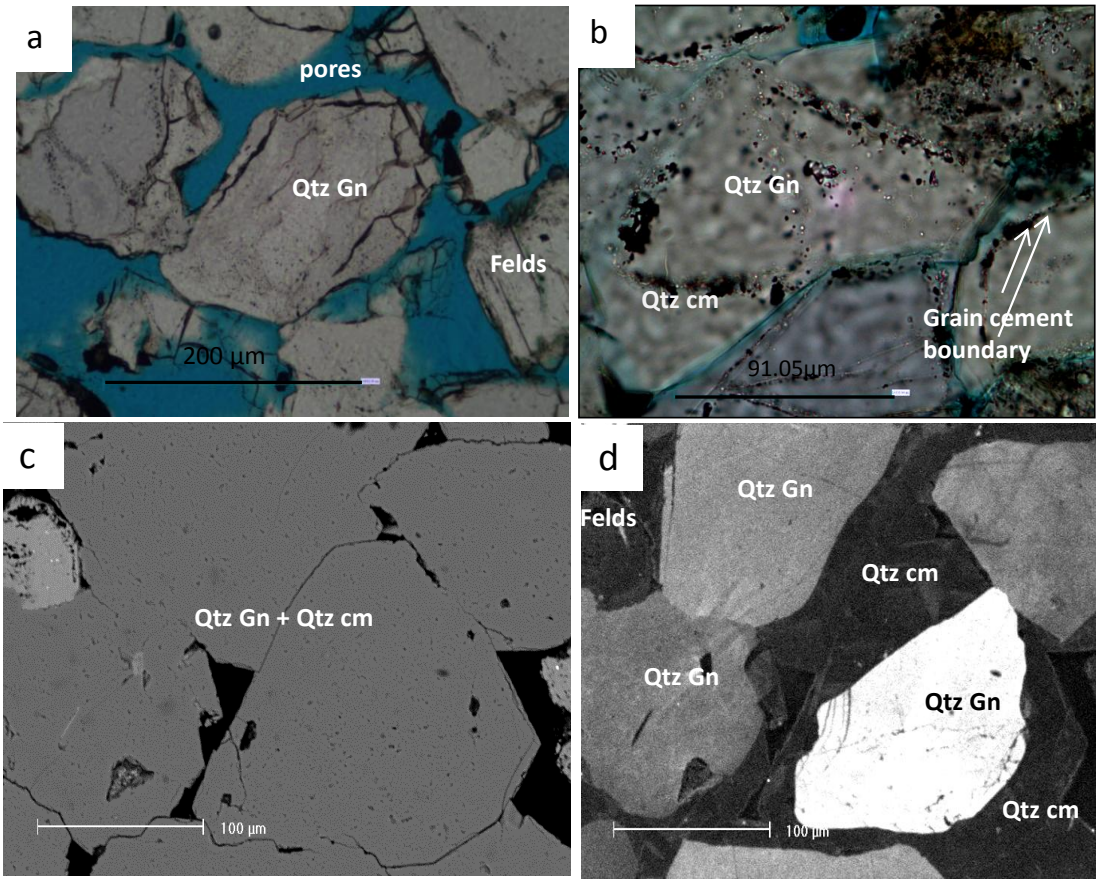

Figure 4. 8 Thin section photomicrograph of Ula Formation (a) plane polarized thin section of porous quartz cement free sandstone in oil leg (7/12-2 3393.54m TVD) (b) plane polarized thin section image of quartz cemented sandstone in water. Dust rim (arrow) shows the boundary between detrital quartz and the quartz cement (7/12-A13 3725.05m TVD) (c) SEM-BSE of cemented sandstone 7/12-A8 3800.2m TVD) (d) CL image of same location as in (c). Quartz cement is clearly distinguishable from the detrital quartz grain in the CL image.

Table 4. 1 Average values of horizontal permeability, core porosity, point count quartz cement volume, detrital clay volume, microquartz and ferroan dolomite for the different lithofacies within oil leg, transition zone and water leg.

Parameter	Fluid type	Coarse-grained graded facies	Medium to fine-grained bioturbated facies	Very fine to fine bioturbated facies
Horizontal permeability mD	oil leg	1113.9	413.4	23.1
	transition zone	29.8	33.2	8.6
	water leg	86.1	130.3	16.7
Core porosity %	oil leg	18.5	19.1	17.2
	transition zone	12.1	10.9	20.7
	water leg	15.3	16.9	13.8
Quartz cement %	oil leg	6.5	6.6	3.8
	transition zone	15.6	16.3	2
	water leg	13.4	9.6	4.45
Point count detrital clay %	oil leg	3.2	5.3	14.7
	transition zone	4	4	14.5
	water leg	2.6	6.8	12
Microcrystalline quartz %	oil leg	0.3	0.6	3.8
	transition zone	0	0	4.5
	water leg	0	0.1	3.3
Ferroan dolomite %	oil leg	0.1	0.7	2.2
	transition zone	4.2	1.2	5.5
	water leg	0.4	1.6	3.3

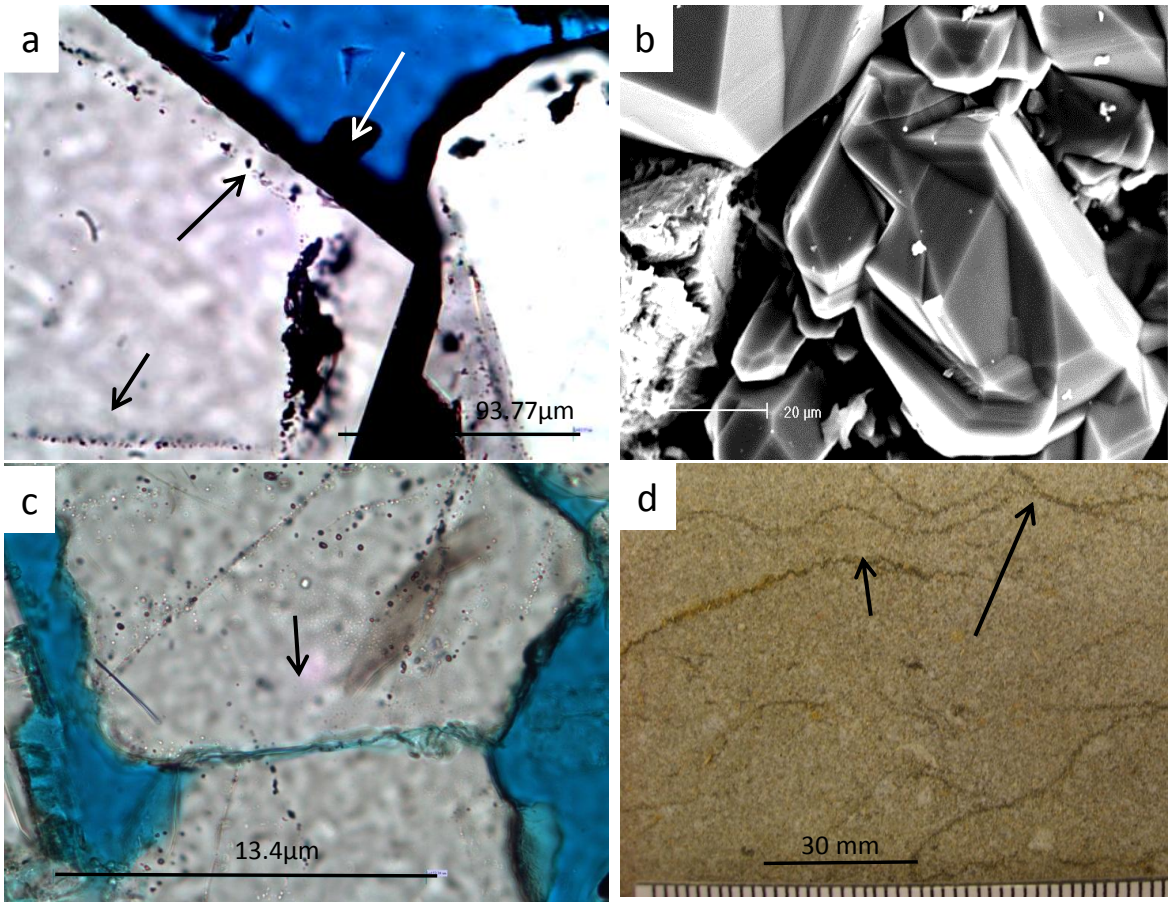

Figure 4. 9 Thin section photomicrographs (a) showing oil stain (white arrow) on euhedral quartz cement (black arrow) showing the boundary between detrital quartz and quartz cement (7/12-A3 3571.9m TVD) (b) SEM image showing cluster of quartz cement (7/12-A13 3680.95m TVD). (c) SEM image showing pressure solution (arrow) (7/12-2 3599.1m TVD) (d) core photograph showing stylolite (arrow) plane polar photomicrograph showing pressure solution (7/12-A13 3680.95m TVD).

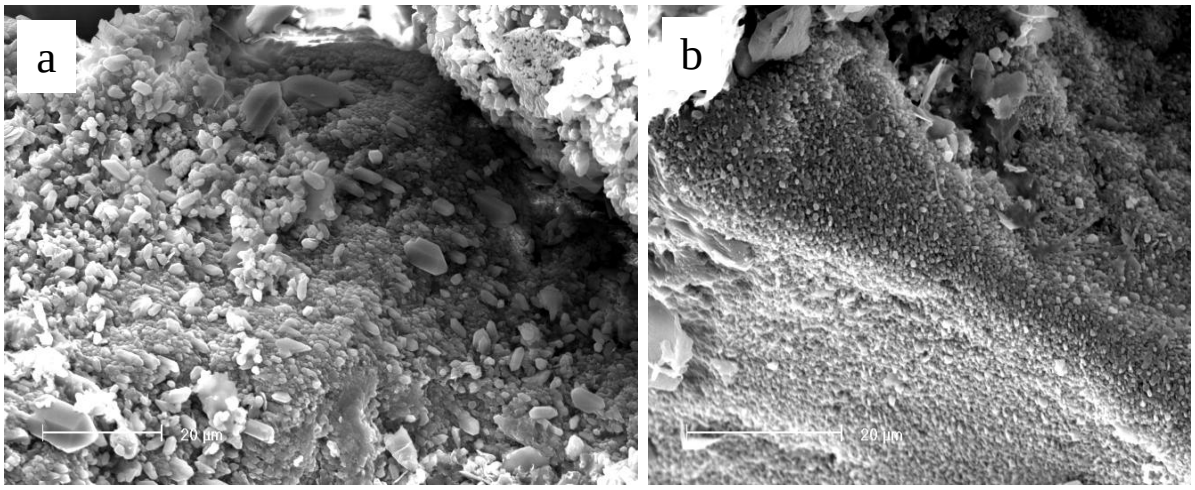

Figure 4. 10 SEM (images of microcrystalline quartz cement in the Ula Formation very fine to fine-grained facies (7/12-2 3387.4m TVD).

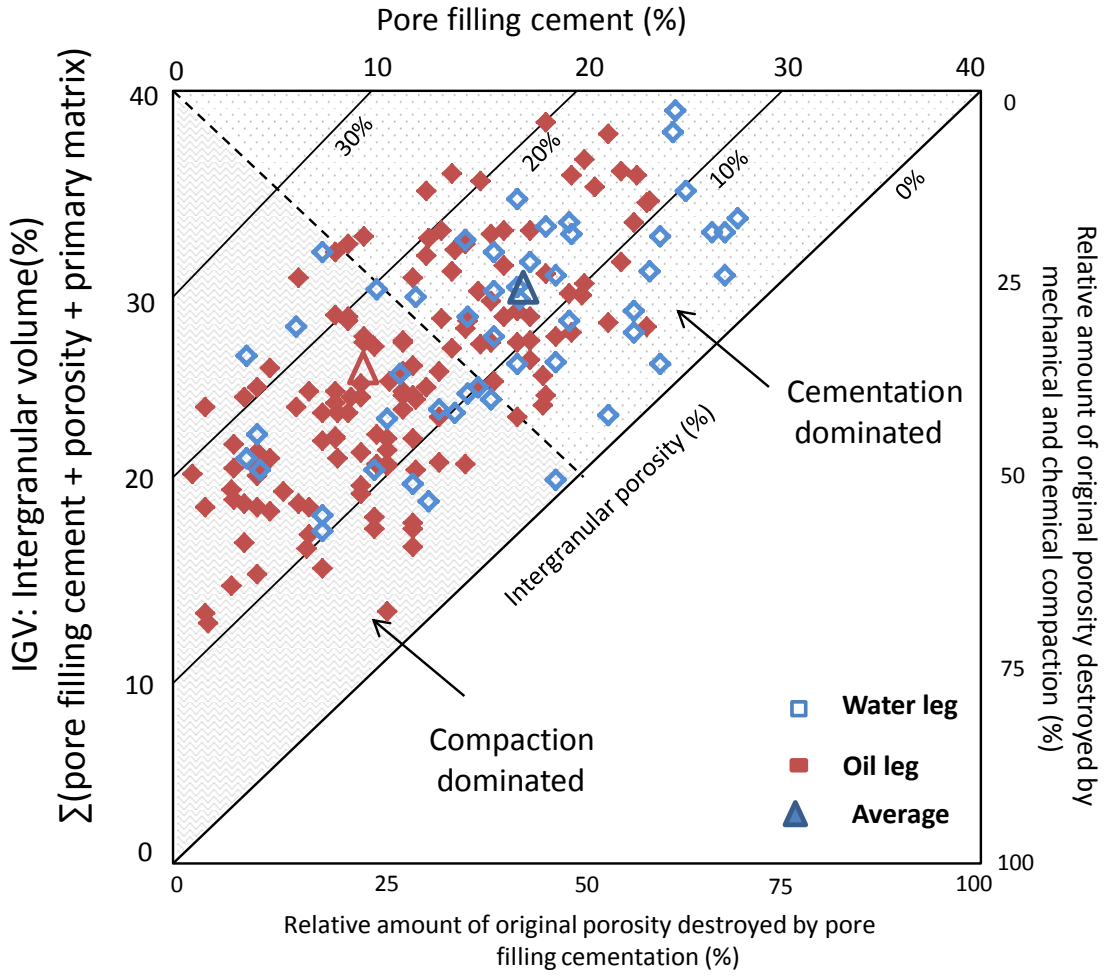

Figure 4. 11 Diagram illustrating styles of porosity loss in the Ula Formation (Houseknecht, 1984). The open squares are samples within the water leg and the filled squares are samples

within the oil leg. The oil leg samples show 48 % porosity lost to compaction and 52% lost to cementation. The water samples show 36% lost to compaction and 64 % lost to cementation.

4.5.4 Fluid inclusions

Sample for fluid inclusion study were selected from both oil and water legs. Homogenization temperatures were measured for aqueous inclusions and petroleum inclusions in 12 samples of the Ula Formation. Petroleum inclusions are generally larger in size (Fig. 4.12 a-d) and have bigger bubbles than aqueous inclusions and therefore were easier to work with. All the homogenization temperatures measured are from inclusions within the quartz overgrowth or between the edges of the detrital grain and the quartz overgrowth. The aqueous inclusions range in diameter from 1 to 17 µm. The petroleum inclusions range in diameter from 7 to 38 µm. Only homogenization temperatures that were reproducible within (<5ºC) were recorded. The liquid to vapour ratio for aqueous fluid inclusion was consistently about 8:1 and for petroleum inclusion was about 5:1. All inclusions homogenized to liquid upon heating. The distribution of aqueous inclusion is unimodal and homogenized between 120 and 174ºC, and hydrocarbon inclusions homogenized between 95 and 142ºC. Histograms in Figure 4.13 show the homogenization temperatures for four representative samples, the details of which are given in Table 4.2. The present day formation temperature, determined by drill stem test, is only available for well 7/12-A3. The highest homogenization temperature measured in this wells are close to the present day formation temperature. Pressure corrections were not made to the aqueous inclusion homogenisation temperatures as the water is very likely to have been saturated with methane at the time of trapping (Hanor, 1980). Measured homogenization temperatures are therefore considered to represent the actual entrapment temperature for the aqueous inclusions. Homogenization temperatures of inclusions trapped in quartz are not likely to be re-equilibrated (Worden and Matray, 1995; Worden et al., 1995). The oil inclusions cannot easily be used to reveal the conditions of trapping since the precise PVT properties of the trapped petroleum are not known.

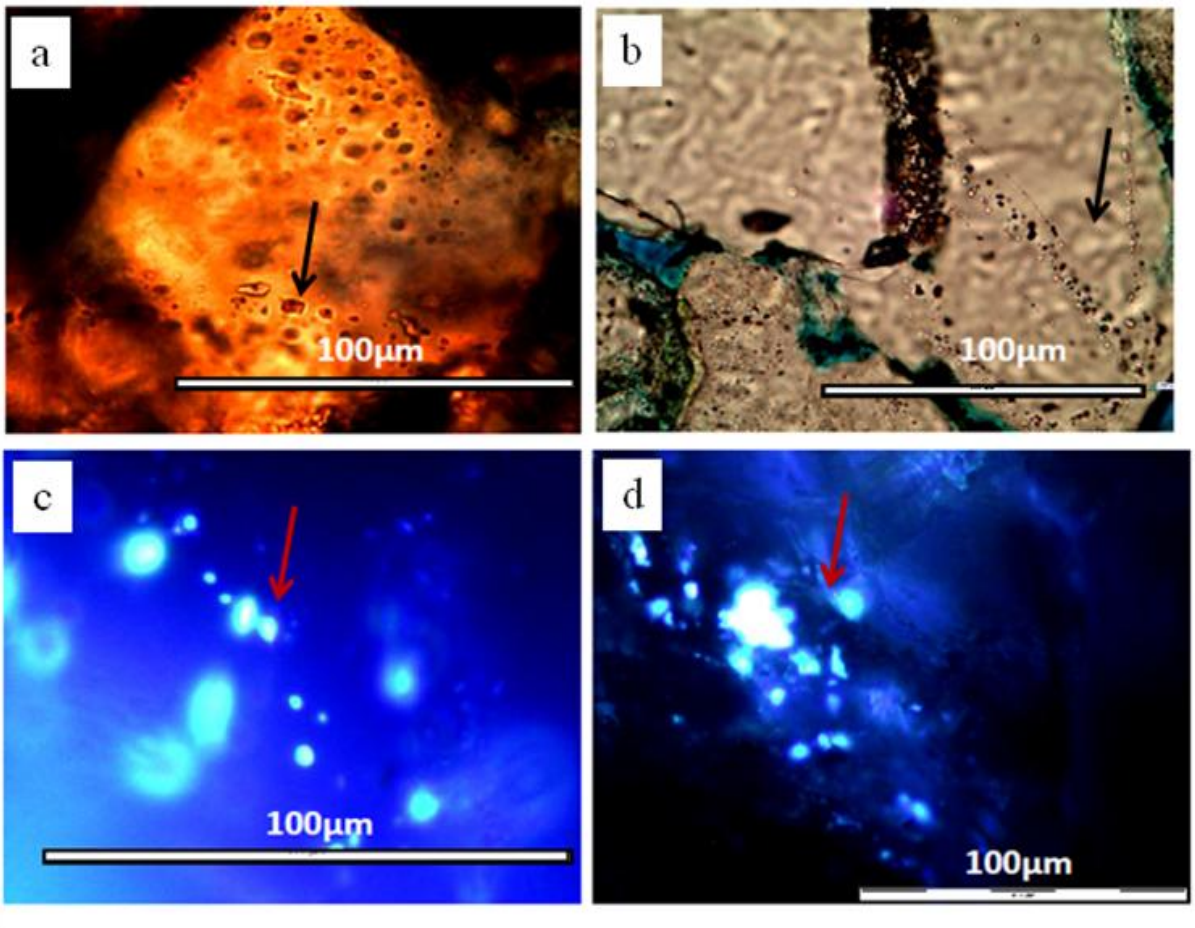

Figure 4. 12 Thin section photomicrograph showing fluid inclusions (a) Plane polar showing fluid inclusion assemblage in quartz cement. (b) plane polar photomicrograph showing fluid inclusion rim at the boundary between detrital quartz grain and quartz cement samples from water zone well 7/12-A3. (c and d) petroleum inclusion under fluorescence light samples from oil leg of 7/12-2

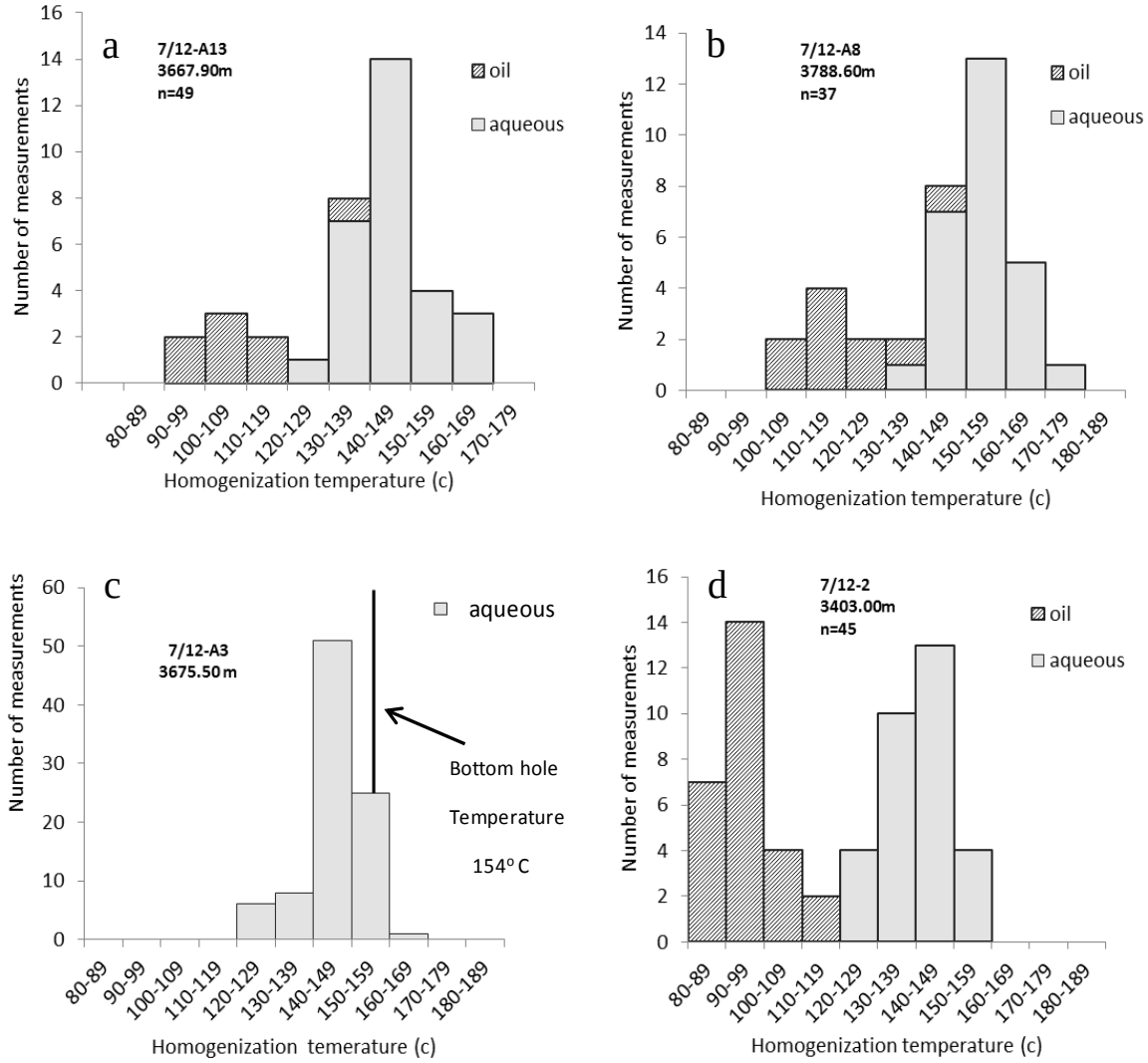

Figure 4. 13 Homogenization temperature measurements for aqueous and petroleum inclusions in selected samples of the Ula Formation. Note present day reservoir temperature is only available for well 7/12-A3.

Table 4. 2 Showing properties of fluid inclusion located in different wells of the Ula field.

well	7/12-A13	7/12-A8	7/12-A3	07/12-.2
depth TVD m	3667.90	3788.60	3675.50	3403.00
Inclusion	A	B	C	D
Facies	Coarse-grained graded	Medium to fine-grained bioturbated	Coarse-grained graded	Coarse-grained graded
Water saturation %	88	70	62	5
Porosity %	11	13	20	20.4
Permeability (mD)	3.65	7.06	332	1024
Qtz Cement %	15	15	12	7

4.6 Discussion

4.6.1 Quartz cementation in the presence of oil

The very presence of primary oil inclusions in quartz cement shows that oil was present in the reservoir when this authigenic mineral was growing. The onset of oil generation from the overlying source rock will have started when the Mandal Formation was at about 100ºC, with the underlying Ula Formation being deeper and thus slightly hotter. This occurred during the Miocene (Fig. 4.3). It is, of course, possible that oil generation occurred off structure with migration updip. This may have allowed oil to be present in the reservoir at slightly lower temperatures. The lowest homogenisation temperatures for the aqueous inclusions are about 120°C which is rather higher than the threshold of 80°C widely asserted as the temperature above which quartz cement grows (Walderhaug, 1996). These cements contain oil inclusions confirming that oil was present when the reservoir was at 120°C. It is not known what the oil saturation was at the time of trapping by the growing quartz cement although it is noteworthy that the fluid inclusion sample with highest oil saturation at the present day (7/12-2, 3403.00m) has the smallest amount of quartz cement (Table 4.2) and the greatest number of petroleum inclusions (Fig. 4.13). Having some oil in the pore network clearly does not automatically proves that quartz cementation is not affected by oil emplacement but the abundance of petroleum inclusions increases as the amount of quartz cement decreases suggesting that greater oil saturation has resulted in less quartz cement.

4.6.2 Is there a difference in the quartz cement content above and below the oil-water contact for rocks of the same pre-oil filling characteristics?

The characteristics of the three different primary lithofacies above and below the oil-water contact (and in the transition zone) are summarized in Table 4.1. These three lithofacies (coarse grained graded sandtones, medium to fine bioturbated sandstones, very fine to fine bioturbated sandstones) have homogeneous grain size and sorting characteristics and have a narrow range of primary mineralogies (Fig. 4.7). They also have consistent quantities of detrital clay and grain-coating microcrystalline quartz. Samples cemented with poikilotopic calcite (i.e. with all pore space filled very soon after deposition) have been removed from the analysis. The amounts of ferroan dolomite sitting in the pores are also consistent. The outstanding conclusion from Table 4.1 is that in coarse-grained sandstones of identical detrital clay, ferroan dolomite, and grain-coating microquartz, the oil-filled rocks have less quartz cement, higher porosity and higher permeability than water-filled rocks. The same is true for medium-grained bioturbated rocks.

Raw porosity-permeability data for each lithofacies, split by water saturation, are also displayed in Figure 4.6 showing that the coarse-grained lithofacies and medium-grained bioturbated lithofacies have the highest porosity and permeability in samples with lowest water saturations. At >80% S_w quartz cementation is almost completely halted. The quantity of quartz cement has been plotted against specific water saturation for each lithofacies (Fig. 4.14) showing that low water saturations (high oil saturations) equate to less quartz cement especially for the coarse-grained sandstones, but also for the medium-grained bioturbated facies. There is no relationship between water saturation and quartz cement content in the very fine- to fine-grained bioturbated facies (Fig. 4.14c).

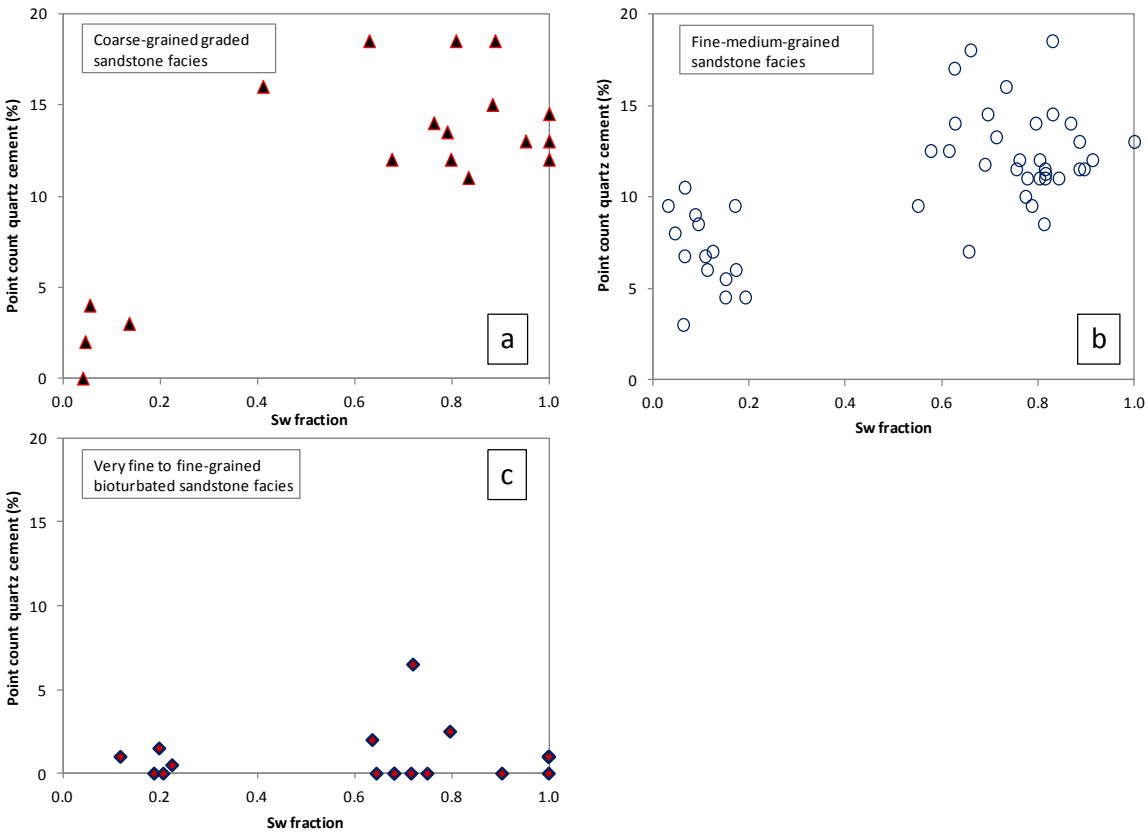

Figure 4. 14 Point counted quartz cement volume versus Archie derived water saturation (a) fine to medium-grained bioturbated sandstone facies (b) coarse-grained graded sandstone facies (c) very fine to fine bioturbated facies.

The assessment of compaction versus cementation (Fig. 4.11) shows that oil-filled samples tend to be slightly more compaction-dominated than water-filled samples. It is not that the oil-leg has undergone absolutely more compaction; rather it is that the water-filled samples basically have *more* quartz cement.

In summary, it seems that for rocks of otherwise similar characteristics (grain size, detrital clay, extent of microquartz coating), having oil in the pore network has inhibited quartz cement growth. The effect of oil emplacement seems to be more extreme for coarser-than medium-grained sandstones.

4.6.3 The role of grain size, detrital clay and grain-coating microcrystalline quartz on quartz cementation

In some oil fields, anomalously high porosity has been explained by the presence of microquartz-coated sand grains (Aase et al., 1996; Aase and Walderhaug, 2005; Bloch et al., 2002; Jahren and Ramm, 2000; Ramm and Bjorlykke, 1994). Microquartz is certainly present in the Ula Formation (Fig. 4.10, Table 4.1). However, it is not particularly abundant in the coarse-grained or medium-grained bioturbated facies and seems unlikely to be a controlling factor. When grain-coating microquartz percentage and the degree of grain-coating by microquartz are plotted against quartz cement (Fig. 4.15) it is apparent that samples from the coarse-grained or medium-grained bioturbated facies show a large range of quartz cement volumes. This suggests that a control other than microquartz is controlling the amount of quartz cement; from Table 4.1 and Figure 4.14, it seems that the fluid type (oil versus water) is what controls the amount of quartz cement.

Where microquartz is abundant and grain-coating by microquartz is prevalent, in the very fine- to fine-grained bioturbated facies, then quartz cementation has certainly been inhibited (Figs. 4.15a and b). This effect has previously been reported (Aase et al., 1996; French et al., 2010; Hendry and Trewin, 1995; Ramm et al., 1997; Weibel et al., 2010; Worden et al., 2012). However, grain-coating microquartz is limited to this very fine to fine-grained bioturbated facies, presumably since this is the facies in which the source of the microquartz (sponge spicules) was preferentially deposited. Microcrystalline quartz cannot be held to be responsible for the distribution of quartz cement in sandstones in which it is not dominant (the coarse-grained graded and medium-grained bioturbated facies).

In the water leg, quartz cement is most abundant in the coarse-grained, with less in the medium-grained bioturbated facies and least of all in the very fine- to fine-grained bioturbated facies (Table 4.1, Fig. 4.14). For the three facies types in the water leg samples, there is a well-developed inverse correlation between the amount of detrital clay and the amount of quartz cement. This suggests that the more clay-

rich finer-grained, more bioturbated samples have some degree of inhibition of the quartz cement. Ferroan dolomite is not a major mineral cement but it too correlates with primary lithofacies and detrital clay content possibly (Table 4.1).

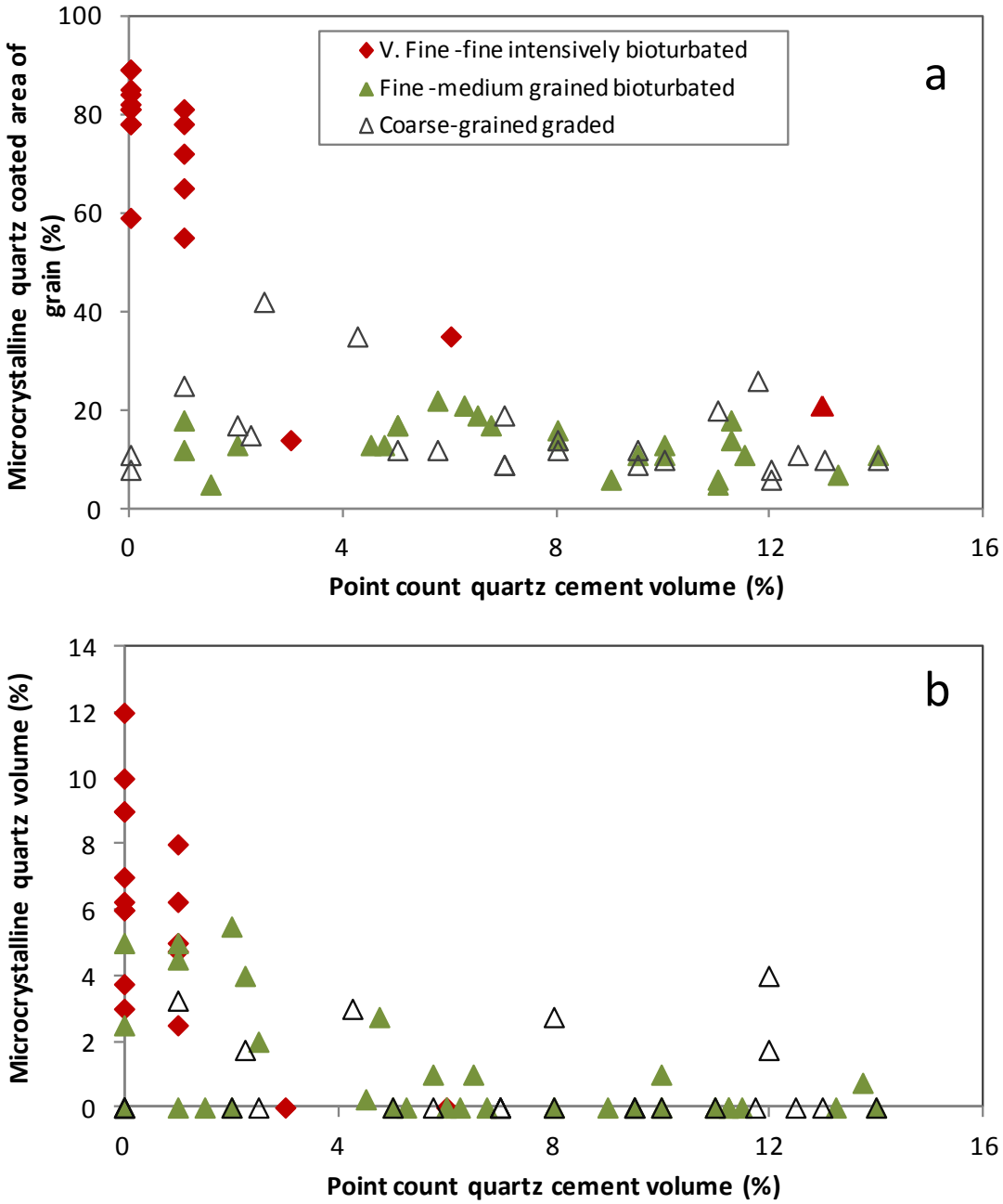

Figure 4. 15 Point count quartz cements volume versus grain coating. Grain coating microquartz inhibited quartz cement only in the very fine to fine-grained bioturbated facies.

4.6.4 How much quartz cement would be expected in the oil saturated sandstones?

There is necessarily a depth (and therefore temperature) difference between the oil leg and the water leg of the Ula Reservoir although the dipping oil-water contact (O'Connor et al., 2011) means the boundary between the two varies across the field. In recent years simple modeling approaches have been developed to try to link quartz cement quantities to time-temperature histories (Bjørkum et al., 1998; Lander and Walderhaug, 1999; Walderhaug, 1990, 1994a, b, 1996; Walderhaug et al., 2000). These models were calibrated by examining quartz cement quantities in different Norwegian sandstones and relating them to the time-temperature history. The models employ the assumption that quartz cement is internally derived and that the overall process is ubiquitously controlled by the quartz precipitation step. The timing of quartz cementation in each well (sample) was derived by using aqueous fluid inclusion temperatures and the assumption that quartz cementation was continuous from the lowest recorded aqueous inclusion homogenization temperature onwards (despite there being punctuated fluid inclusion records reported). The models were also calibrated assuming that addition of oil did not inhibit quartz cementation. Geometric characteristics were accounted for by examining grain size (and relating this to available surface area) and the fraction of grains that are quartz (as opposed to feldspars, lithics etc). The models were thus calibrated using a wide range of primary assumptions that may not be correct or valid in all cases.

Nonetheless, with an awareness of the assumptions and limitations of the models, they can be used to test the effect of the depth (temperature) differences on the expected quantity of quartz at the crest of the field and the flank of the field. For thermal histories (Fig. 4.16a) that reflect the different T_{max} revealed by fluid inclusions (Fig. 4.11) the amount of quartz cement was modelled using the algorithm outlined previously (Walderhaug, 1994a). The amounts of quartz at the crest, flank and an intermediate position have been calculated for coarse grained sandstone (300 μm) with 20% grain coating (Fig. 4.15a) and that contained 65% quartz grains (Fig. 4.7) and that had 25% porosity at the time that quartz cementation started. Note that

these models assume that quartz cementation is continuous and that oil does not inhibit quartz cementation; indeed they were calibrated form datasets in which it was initially assumed that oil does not inhibit quartz cementation.

The models show that, given the elevated temperatures and textural constraints, the pore space should be fully cemented with quartz at all positions in the field. The simple models also show that the small difference in temperature between flank and crest is insufficient to explain the difference in quartz cement volume revealed in Table 4.1.

The models (Fig. 4.16a) and fluid inclusion temperatures (Fig. 4.13) highlight the issue that the Ula Formation sandstones are relatively high temperature and yet have high porosity and even relatively clean sandstones such as the coarse-grained graded sandstones, do not have much quartz (or any other type of) cement.

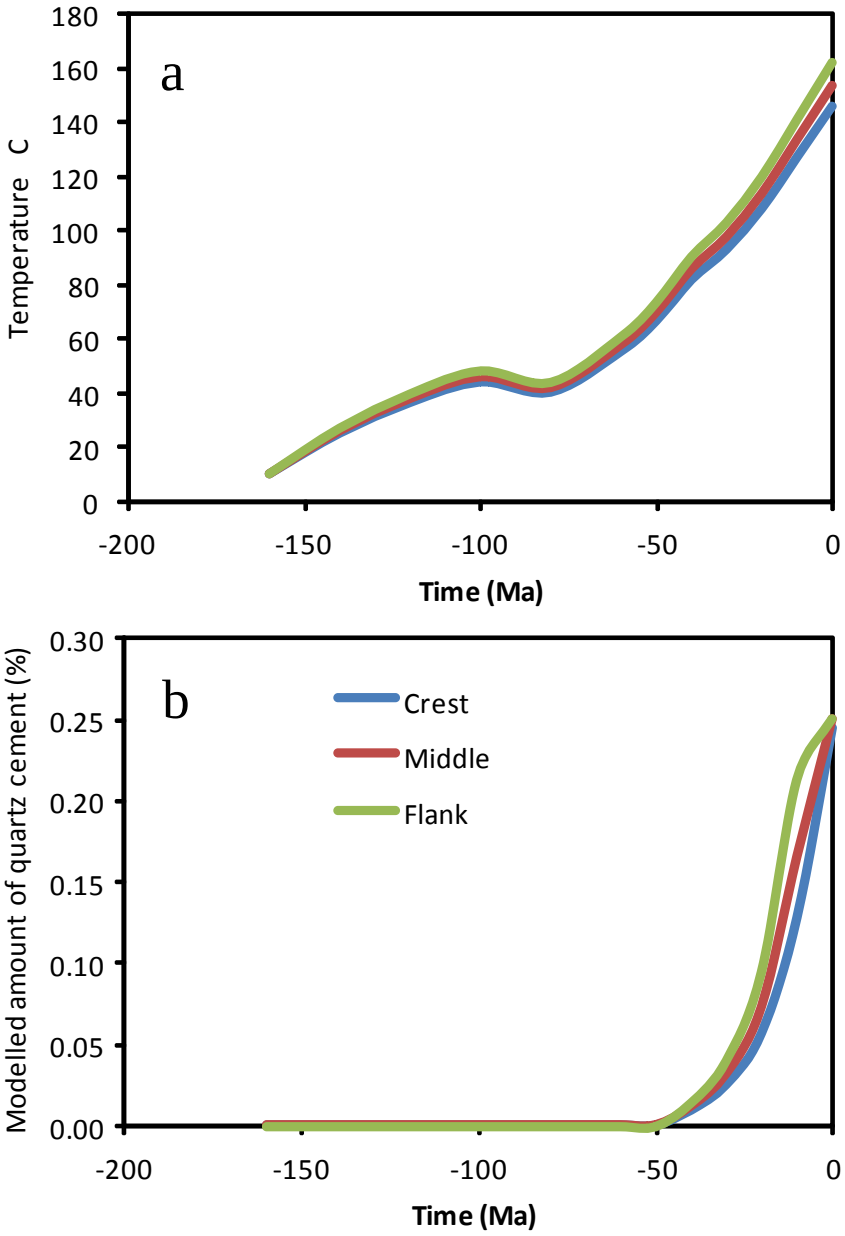

Figure 4. 16 Different positions in the field with their (a) modelled temperature (b) modelled amount of quartz cement that could be expected for 20% grain coating (Fig.4 14a), 300 μm grain size sand (Table 4.1) with 65% quartz grains (Fig.4. 7) and the assumptions that (i) quartz cementation is continuous, (ii) oil does not stop quartz cementation, (iii) quartz cement is not controlled by supply (e.g. from external sources). Temperatures, in Fig 4.16a, were adjusted to match aqueous fluid inclusion temperatures at different parts of the field (Fig. 4.11).

4.6.5 Synthesis: has oil slowed quartz cementation and preserved porosity?

The key question is has emplacement of oil inhibited quartz cementation in the Ula Formation in the Ula reservoir. The oil leg has higher porosity and less quartz cement than the water leg for the coarse-grained graded sandstones and the medium-grained bioturbated sandstone (Table 4.1). The difference cannot be explained by differential degrees of microcrystalline quartz coating, grain-coating chlorite, other pore-filling cements (e.g. ferroan dolomite), grain size or any other primary lithofacies influence. The difference can be attributed to the specific pore fluid. Having oil in the sandstone during quartz cementation (as shown by oil inclusions in quartz cement; Fig.4.12) has led to a slower rate of quartz precipitation and less quartz cement. The reduce rate of quartz cementation could be the result of reduced rates of silica supply (presumably from internal, stylolite-related, sources; Figs. 4. 9c and d), reduced rates of transport (either advection due to relative permeability effects or diffusion due to tortuosity effects (Worden et al., 1998).

4.6 Conclusion

1. Oil was present during quartz cementation in the Ula Formation in the Ula field as revealed by the presence of oil inclusion and geochemical modelling that suggested that oil filling started when the reservoir was at 100°C. Quartz cementation seems to have started at 120°C if the minimum homogenisation temperatures for aqueous inclusions in quartz are to be held as representative of minimum growth temperature.

2. For sandstones of the same facies, with the same grain, same detrital clay content, same low quantity of grain coating microquartz and same low quantity of ferroan dolomite, there is less quartz cement in the oil leg than water leg for coarse-grained graded sandstones and medium-grained bioturbated sandstones.

3. For fine- to very fine-grained sandstones there is little quartz cement whether oil is present or not due to the amount of grain-coating microquartz associated with this facies and the amount of detrital clay.
4. Conventional modelling of quartz cementation (admittedly with a large number of uncertain assumption employed) shows that, given the thermal history, small amount of grain-coating microquartz and geometric characteristics of these sandstones, quartz cement should be much more abundant in the oil leg than has been found.

6. Emplacement of oil before, and during, quartz cementation has inhibited the growth of quartz in the Ula Formation.

4.7 References

Aase, N. E., Bjorkum, P. A., and Nadeau, P. H., 1996, The effect of grain-coating microquartz on preservation of reservoir porosity: American Association of Petroleum Geologists Bulletin, v. 80, no. 10, p. 1654-1673.

Aase, N. E., and Walderhaug, A., 2005, The effect of hydrocarbons on quartz cementation: diagenesis in the Upper Jurassic sandstones of the Miller Field, North Sea, revisited: Petroleum Geoscience, v. 11, no. 3, p. 215-223.

Asquith, G. B., and Gibson, C. R., 1982, Basic well log analysis for geologists: American Association of Petroleum Geologists Methods in Exploration, no. 3, p. 216.

Barclay, S. A., and Worden, R. H., 2000, Effects of reservoir wettability on quartz cementation in oil fields, *in* Worden, R. H., and Morad, S., eds., Quartz cementation in sandstones, Volume 29, Special Publication of the International Association of Sedimentologists, p. 103-117.

Bergan, M., Tørudbakken, B., and Wandås, B., 1989, Lithostratigraphic correlation of Upper Jurassic sandstones within the Norwegian Central Graben: sedimentological and tectonic implications, *in* Collinson, J. D., ed., Correlation in hydrocarbon exploration, Norwegian Petroleum Society, Graham and Trotman, London, p. 243-251.

Bjørkum, P. A., and Nadeau, P. H., 1998, Temperature controlled porosity/permeability reduction, fluid migration, and petroleum exploration in sedimentary basins: Australian Petroleum Production and Exploration Association Journal, v. 38, p. 453-464.

Bjørkum, P. A., Oelkers, E. H., Nadeau, P. H., Walderhaug, O., and Murphy, W. M., 1998, Porosity prediction in quartzose sandstones as a function of time, temperature, depth, stylolite frequency, and hydrocarbon saturation: American Association of Petroleum Geologists Bulletin, v. 82, no. 4, p. 637-648.

Bjørnseth, H. M., and Gluyas, J., 1995, Petroleum exploration in the Ula Trend: Norwegian Petroleum Society Special Publications, v. 4, p. 85-96.

Bloch, S., Lander, R. H., and Bonnell, L., 2002, Anomalously high porosity and permeability in deeply buried sandstone reservoirs: Origin and predictability: Americam Association of Petroleum Geologists Bulletin, v. 86, no. 2, p. 301-328.

Bonnell, L., Larese, R. E., and Lander, R. H., 2006, Hydrocarbon versus microquartz inhibition of quartz cementation in North Sea sandstones: Empirical and experimental evidence American Association of Mineralogist Journal Convention Abstract, Volume 15.

Bowman, M. B. J., 1981, The sedimentary and reservoir geology of the upper Jurassic Ula Formation and its relationship with other 7/12 Block wells., p. (OC18236).

Brown, A., Mitchell, A. W., Nilssen, I. R., Stewart, I. J., and Svela, P. T., 1992, Ula field: relationship between structure and hydrocarbon distribution: Structural and tectonic modelling and its application to petroleum geology: Norwegian Petroleum Society Special Publication, v. 1, p. 409-420.

De Gennaro, V., Delage, P., Cui, Y. J., Schroeder, C., and Collin, F., 2003, Time-dependent behaviour of oil reservoir chalk: A multiphase approach: Soils and Foundations, v. 43, no. 4, p. 131-147.

De Gennaro, V., Delage, P., Priol, G., Collin, F., and Cui, Y.-J., 2004, On the collapse behaviour of oil reservoir chalk: Geotechnique, v. 54, p. 415-420.

Dixon, S. A., Summers, D. M., and Surdam, R. C., 1989, Diagenesis and preservation of porosity in Norphlet Formation (Upper Jurassic), southern Alabama: Americam Association of Petroleum Geologists Bulletin, v. 73, no. 6, p. 707-728.

Ehrenberg, S. N., 1990, Relationship between diagenesis and reservoir quality in sandstones of the Garn Formation, Haltenbanken, mid-Norwegian continental shelf: American Association of Petroleum Geologists Bulletin, v. 74, no. 10, p. 1538-1558.

-, 1993, Preservation of anomalously high porosity in deeply buried sandstones by grain-coating chlorite: examples from the Norwegian continental shelf: American Association of Petroleum Geologists Bulletin, v. 77, p. 1260-1260.

Emery, D., Smalley, P. C., Oxtoby, N. H., Ragnarsdottir, K. V., Aagaard, P., Halliday, A., Coleman, M. L., and Petrovich, R., 1993, Synchronous oil migration and cementation in sandstone reservoirs demonstrated by quantitative description of diagenesis [and discussion]: Philosophical Transactions of the Royal Society of London. Series A: Physical and Engineering Sciences, v. 344, no. 1670, p. 115-125.

England, G. L., Haszeldine, R. S., Cleverley, J., Barclay, S. A., Yardley, B. W. D., Fisher, Q. J., Graham, C., and Fallick, A., 2003, Applying Ion-Microprobe Technology in Reconstructing Quartz Cement History in an Upper Jurassic Sandstone Reservoir of the Outer Moray Firth Basin, North Sea, United Kingdom: Americam Association of Petroleum Geologists Annual meeting south lake Tulsa, OK.

Feazel, C. T., and Schatzinger, R. A., 1985, Prevention of carbonate cementation in petroleum reservoirs, , *in* Schnedermann, N., and Harris, P. M., eds., Carbonate cements: Society for Sedimentary Geology Special Publication, Volume 36, p. 97-106.

Fraser, S. I., Robinson, A. M., Johnson, H. D., Underhill, J. R., Kadolsky, D. G. A., Connell, R., Johannessen, P., and Ravnas, R., 2002, Upper Jurassic, *in* Evans, D., Armour, A., and Bathurst, P., eds., *Millennium Atlas: petroleum geology of the central and northern North Sea*: London, The Geological Society of London.

French, M. W., Worden, R. H., Mariani, E., Horn, W. C., Kliewer, C. E., Lamberti, W. A., Mueller, R. R., and Fischer, C., 2010, Low temperature porosity preserving microquartz from Upper Cretaceous sandstones of the Subhercynian Basin (Germany): Geochimica et Cosmochimica Acta, v. 74, no. 12, p. A305-A305.

Giles, M. R., Stevenson, S., Martin, S. V., Cannon, S. J. C., Hamilton, P. J., Marshall, J. D., and Samways, G. M., 1992, The reservoir properties and diagenesis of the Brent Group: a regional perspective, *in* Morton, A. C., Haszeldine, R. S., Giles, M. R., and Brown, S., eds., Geology of the Brent Group, Geological Society, London, Special Publications, v. 61, p. 329-350.

Gluyas, J., and Cade, C. A., 1997, Prediction of porosity in compacted sands: In: Reservoir quality prediction in sandstones and carbonates (eds. Kupecz, J.A., Gluyas, J. and Bloch, S.) AAPG Memoir, v. 69, p. 19-28.

Gluyas, J. G., Robinson, A. G., Emery, D., Grant, S. M., and Oxtoby, N. H., 1993, The link between petroleum emplacement and sandstone cementation, *in* Parker, J., ed., Petroleum Geology of the North west Europe, Geological Society of London, v. 4, p. 1395-1402.

Hanor, J. S., 1980, Dissolved methane in sedimentary brines; potential effect on the PVT properties of fluid inclusions: Economic Geology, v. 75, no. 4, p. 603-609.

Hardman, R. F. P., 1982, Chalk reservoirs of the North Sea: Bulletin of the geological Society of Denmark, v. 30, no. 3-4, p. 119-137.

Harris, N. B., 2006, Low-porosity haloes at stylolites in the feldspathic Upper Jurassic Ula sandstone, Norwegian North Sea: An integrated petrographic and chemical mass-balance approach: Journal of Sedimentary Research, v. 76, no. 3-4, p. 444-459.

Haszeldine, R. S., Cavanagh, A. J., and England, G. L., 2003, Effects of oil charge on illite dates and stopping quartz cement: calibration of basin models: Journal of Geochemical Exploration, v. 78-9, p. 373-376.

Hawkins, P. J., 1978, Relationship between diagenesis, porosity reduction, and oil emplacement in late Carboniferous sandstone reservoirs, Bothamsall Oilfield, E Midlands: Journal of the Geological Society, v. 135, no. 1, p. 7-24.

Heasley, E. C., Worden, R. H., and Hendry, J. P., 2000, Cement distribution in a carbonate reservoir: recognition of a palaeo oil–water contact and its relationship to reservoir quality in the Humbly Grove field, onshore, UK: Marine and Petroleum Geology, v. 17, no. 5, p. 639-654.

Hendry, J. P., and Trewin, N. H., 1995, Authigenic quartz microfabrics in Cretaceous turbidites - evidence for silica transfer processes in sandstones: Journal of Sedimentary Research Section a-Sedimentary Petrology and Processes, v. 65, no. 2, p. 380-392.

Hickman, R. J., Gutierrez, M. S., De Gennaro, V., and Delage, P., 2008, A model for pore-fluid-sensitive rock behavior using a weathering state parameter: International Journal for Numerical and Analytical Methods in Geomechanics, v. 32, no. 16, p. 1927-1953.

Higgs, K. E., Zwingmann, H., Reyes, A. G., and Funnell, R. H., 2007, Diagenesis, porosity evolution, and petroleum emplacement in tight gas reservoirs, Taranaki Basin, New Zealand: Journal of Sedimentary Research, v. 77, no. 11-12, p. 1003-1025.

Home, P. C., 1987, Ula, *in* Spencer, A. M., Holter, E., Campbell, C. J., Hanslein, S. H., Nelsen, P. H. H., Nysteacher, E., and Ormaasen, E. G., eds., Geology of the Norwegian oil and gas fields: London, Graham and Trotman, p. 143-151.

Houseknecht, D. W., 1984, Influence of grain size and temperature on intergranular pressure solution, quartz cementation, and porosity in a quartzose sandstone: Journal of Sedimentary Research, v. 54, no. 2, p. 348-361.

Jahren, J., and Ramm, M., 2000, The Porosity preserving effects of microcrystalline quartz coatings in arenitic sandstones: Examples from the Norwegian Continental Shelf, *in* Worde, R. H., and Morad, S., eds., Quartz cementation

in sandstones, Volume 29, International Association of Sedimentologists Special edition. Blackwell Science, p. 271-280.

Karlsen, D. A., Nedkvitne, T., Larter, S. R., and Bjørlykke, K., 1993, Hydrocarbon composition of authigenic inclusions: application to elucidation of petroleum reservoir filling history: Geochimica et Cosmochimica Acta, v. 57, no. 15, p. 3641-3659.

Lander, R. H., and Walderhaug, O., 1999, Predicting porosity through simulating sandstone compaction and quartz cementation: American Association of Petroleum Geologists Bulletin, v. 83, no. 3, p. 433-449.

Lowry, W. D., 1956, Factors in loss of porosity by quartzose sandstones of Virginia: American Association of Petroleum Geologists Bulletin, v. 40, no. 3, p. 489-500.

Maast, T. E., Jahren, J., and Bjørlykke, K., 2011, Diagenetic controls on reservoir quality in Middle to Upper Jurassic sandstones in the South Viking Graben, North Sea: Americam Association of Petroleum Geologists Bulletin, v. 95, no. 11, p. 1883-1905.

Marchand, A. M. E., Haszeldine, R. S., Macaulay, C. I., Swennen, R., and Fallick, A. E., 2000, Quartz cementation inhibited by crestal oil charge: Miller deep water sandstone, UK North Sea: Clay Minerals, v. 35, no. 1, p. 201-210.

Marchand, A. M. E., Haszeldine, R. S., Smalley, P. C., Macaulay, C. I., and Fallick, A. E., 2001, Evidence for reduced quartz-cementation rates in oil-filled sandstones: Geology, v. 29, no. 10, p. 915-918.

Marchand, A. M. E., Smalley, P. C., Haszeldine, R. S., and Fallick, A. E., 2002, Note on the importance of hydrocarbon fill for reservoir quality prediction in sandstones: American Association of Petroleum Geologists Bulletin, v. 86, no. 9, p. 1561-1571.

Midtbø, R. E. A., Rykkje, J. M., and Ramm, M., 2000, Deep burial diagenesis and reservoir quality along the eastern flank of the Viking Graben. Evidence for illitization and quartz cementation after hydrocarbon emplacement: Clay Minerals, v. 35, no. 1, p. 227-237.

Molenaar, N., Cyziene, J., Sliaupa, S., and Craven, J., 2008, Lack of inhibiting effect of oil emplacement on quartz cementation: Evidence from Cambrian reservoir sandstones, Paleozoic Baltic Basin: Geological Society of America Bulletin, v. 120, no. 9-10, p. 1280-1295.

Nedkvitne, T., Karlsen, D. A., Bjorlykke, K., and Larter, S. R., 1993, Relationship between reservoir diagenetic evolution and petroleum emplacement in the Ula Field, North Sea: Marine and Petroleum Geology, v. 10, no. 3, p. 255-270.

Neilson, J. E., Oxtoby, N. H., Simmons, M. D., Simpson, I. R., and Fortunatova, N. K., 1998, The relationship between petroleum emplacement and carbonate reservoir quality: examples from Abu Dhabi and the Amu Darya Basin: Marine and Petroleum Geology, v. 15, no. 1, p. 57-72.

O'Connor, S., Rasmussen, H., Swarbrick, R., and Wood, J., 2011, Integrating a hydrodynamically-titled OWC and a salt-withdrawal depositional model to explore the Ula Trend: Geofluids, v. 11, no. 4, p. 388-400.

Oxtoby, N. H., 1994, The Ula field, *in* Warren, E. A., and Smalley, P. C., eds., North Sea Formation waters: London, The Geological Society London. Memoir No. 15, p. 74.

Partington, M. A., Mitchener, B. C., Milton, N. J., and Fraser, A. J., 1993, Genetic sequence stratigraphy for the North Sea Late Jurassic and Early Cretaceous: distribution and prediction of Kimmeridgian–Late Ryazanian reservoirs in the North Sea and adjacent areas, v. 4, p. 347-370.

Ramm, M., 1992, Porosity-depth trends in reservoir sandstones: theoretical models related to Jurassic sandstones offshore Norway: Marine and Petroleum Geology, v. 9, no. 5, p. 553-567.

Ramm, M., and Bjorlykke, K., 1994, Porosity depth trends in reservoir sandstones - assessing the quantitative effects of varying pore-pressure, temperature history and mineralogy, Norwegian shelf data: Clay Minerals, v. 29, no. 4, p. 475-490.

Ramm, M., Forsberg, A. W., and Jahren, J., 1997, Porosity-depth trends in deeply buried Upper Jurassic Reservoirs in the Norwegian Central Graben: an example of porosity preservation beneath the normal economic basement by grain coating microquartz: In: Reservoir quality prediction in sandstones and carbonates (eds. Kupecz, J.A., Gluyas, J. and Bloch, S.) AAPG Memoir, v. 69, p. 177-200.

Risnes, R., Haghighi, H., Korsnes, R. I., and Natvik, O., 2003, Chalk-fluid interactions with glycol and brines: Tectonophysics, v. 370, no. 1-4, p. 213-226.

Risnes, R., Madland, M. V., Hole, M., and Kwabiah, N. K., 2005, Water weakening of chalk - Mechanical effects of water-glycol mixtures: Journal of Petroleum Science and Engineering, v. 48, no. 1-2, p. 21-36.

Robinson, A., and Gluyas, J., 1992, Duration of quartz cementation in sandstones, North Sea and Haltenbanken Basins: Marine and Petroleum Geology, v. 9, no. 3, p. 324-327.

Rothwell, N. R., Sorensen, A., Peak, J. L., Byskov, K., and McKean, T. A. M., 1993, Gyda: Recovery of difficult reserves by flexible development and conventional reservoir management: Offshore Europe, v. SPE Proceedings of the 1992 0ffshore Europe Conference, p. 271-280.

Saigal, G. C., Bjorlykke, K., and Larter, S., 1992, The effects of oil emplacement on diagenetic processes; examples from the Fulmar reservoir sandstones, central North Sea: American Association of Petroleum Geologists Bulletin, v. 76, no. 7, p. 1024-1033.

Sathar, S., Worden, R. H., Faulkner, D. R., and Smalley, P. C., 2012, The Effect of Oil Saturation On the Mechanism of Compaction In Granular Materials: Higher Oil Saturations Lead To More Grain Fracturing and Less Pressure Solution: Journal of Sedimentary Research, v. 82, no. 8, p. 571-584.

Scholle, P. A., 1977, Chalk diagenesis and its relation to petroleum exploration: oil from chalks, a modern miracle: Americam Association of Petroleum Geologists Bulletin, v. 61, no. 7, p. 982-1009.

Scholle, P. A., and Halley, B., 1985, Burial diagenesis: out of sight, out of mind!, *in* Schneidermann, N., and Harris, P. M., eds., Out of sight, out of mind!, Society of Sedimentary Geology Special Publication, p. 309-334.

Sneider, R. M., 1990, Introduction: Reservoir description of sandstones, *in* Barwis, J. H., McPherson, J. G., and Studlick, J. R. J., eds., Sandstone petroleum reservoirs: New York, Springer-Verlag, p. 1-3.

Taylor, M. S. G., LeROY, A., and Førland, M., 1999, Hydrocarbon systems modelling of the Norwegian Central Graben fairway trend, v. 5, p. 1325-1338.

Taylor, T. R., Giles, M. R., Hathon, L. A., Diggs, T. N., Braunsdorf, N. R., Birbiglia, G. V., Kittridge, M. G., Macaulay, C. I., and Espejo, I. S., 2010, Sandstone diagenesis and reservoir quality prediction: Models, myths, and reality: American Association of Petroleum Geologists Bulletin, v. 94, no. 8, p. 1093-1132.

Teinturier, S., and Pironon, J., 2004, Experimental growth of quartz in petroleum environment. Part I: Procedures and fluid trapping: Geochimica et Cosmochimica Acta, v. 68, no. 11, p. 2495-2507.

Underhill, J. R., 1998, Jurassic, *in* Glennie, K. W., ed., Petroleum Geology of the North Sea:Basic Concepts and Recent Advances, Blackwell Science, p. 656.

Walderhaug, O., 1990, A fluid inclusion study of quartz cemented sandstones from offshore mid-Norway - possible evidence for continued quartz cementation during oil emplacement: Journal of Sedimentary Petrology, v. 60, no. 2, p. 203-210.

-, 1994a, Precipitation rates for quartz cement in sandstones determined by fluid inclusion microthermometry and temperature history modelling: Journal of Sedimentary Research Section a-Sedimentary Petrology and Processes, v. 64, no. 2, p. 324-333.

-, 1994b, Temperatures of quartz cementation in Jurassic sandstones from the Norwegian continental shelf - evidence from fluid inclusions: Journal of Sedimentary Research Section a-Sedimentary Petrology and Processes, v. 64, no. 2, p. 311-323.

-, 1996, Kinetic modeling of quartz cementation and porosity loss in deeply buried sandstone reservoirs: American Association of Petroleum Geologists Bulletin, v. 80, no. 5, p. 731-745.

Walderhaug, O., Lander, R. H., Bjorkum, P. A., Oelkers, E. H., Bjorlykke, K., and Nadeau, P. H., 2000, Modelling quartz cementation and porosity in reservoir sandstones: examples from the Norwegain continental shelf: In: Quartz cementation in sandstones (eds. Worden, R.H. and Morad, S.) International Association of Sedimentologists Special Publications, v. 29, p. 39-50.

Weibel, R., Friis, H., Kazerouni, A. M., Svendsen, J. B., Stokkendal, J., and Poulsen, M. L. K., 2010, Development of early diagenetic silica and quartz morphologies - Examples from the Siri Canyon, Danish North Sea: Sedimentary Geology, v. 228, no. 3-4, p. 151-170.

Wilkinson, M., and Haszeldine, R. S., 2011, Oil charge preserves exceptional porosity in deeply buried, overpressured, sandstones: Central North Sea, UK: Journal of the Geological Society, v. 168, no. 6, p. 1285-1295.

Wilkinson, M., Haszeldine, R. S., Ellam, R. M., and Fallick, A., 2004, Hydrocarbon filling history from diagenetic evidence: Brent Group, UK North Sea: Marine and Petroleum Geology, v. 21, no. 4, p. 443-455.

Wilkinson, M., Haszeldine, R. S., and Fallick, A. E., 2006, Hydrocarbon filling and leakage history of a deep geopressured sandstone, Fulmar Formation, United Kingdom: American Association of Petroleum Geologists Bulletin, v. 90, no. 12, p. 1945-1961.

Worden, R. H., French, M. W., and Mariani, E., 2012, Amorphous silica nanofilms result in growth of misoriented microcrystalline quartz cement maintaining porosity in deeply buried sandstones: Geology, v. 40, no. 2, p. 179-182.

Worden, R. H., and Matray, J. M., 1995, Cross formational flow in the Paris Basin: Basin Research, v. 7, no. 1, p. 53-66.

Worden, R. H., and Morad, S., 2000, Quartz cementation in sandstones: a review of the key controversies *in* Worden, R. H., and Morad., S., eds., Quartz cementation in sandstones International Association of Sedimentologists Special Publication v. 29, p. 1-20.

Worden, R. H., Oxtoby, N. H., and Smalley, P. C., 1998, Can oil emplacement prevent quartz cementation in sandstones?: Petroleum Geoscience, v. 4, no. 2, p. 129-137.

Worden, R. H., Warren, E. A., Smalley, P. C., Primmer, T. J., and Oxtoby, N. H., 1995, Evidence for resetting of fluid inclusions from quartz cements in oil fields - discussion: Marine and Petroleum Geology, v. 12, no. 5, p. 566-570.

CHAPTER 5

5. Diagenesis and controls on reservoir quality of the Tambar field, Norwegian North Sea

5.1 Abstract

This work was carried out on the Upper Jurassic reservoir sandstones of the Tambar field in the Norwegian North Sea to understand diagenesis and the reservoir quality. Core samples and set of wireline logs obtained from 3 wells were used to carry out petrographic, petrophysical, fluid inclusion, XRD and stable isotope studies. The Tambar reservoir sandstones range from siltstone to fine-grained sandstones, exclusively arkoses cemented by microquartz, quartz overgrowth, dolomite cement and clays. Early diagenetic minerals include calcite, pyrite and microcrystalline quartz and the late diagenetic minerals include quartz cement, dolomite, illite and chlorite. The reservoir quality is controlled mainly by texturally controlled early formed grain coating microquartz quartz that precipitated from dissolution of sponge spicules and to some extent by dolomite and feldspar cements. Oil emplacement did not show significant control on reservoir quality because significant quartz cementation has taken place before the onset of major oil charge. Only the coarse grains show correlation between quartz cement volume and water saturation. Understanding these controls on the reservoir quality will enhance exploration strategy in the Tambar field.

5.2 Introduction

The Tambar oil field is described as part of Ula trend because of its proximity to the main Ula oil field (16 kilometres to the north) (O'Connor et al., 2011). Considerable interest has been focussed over the last few decades on the reservoir potential of the Upper Jurassic sandstones of the Central Graben area of the North Sea (Home, 1987; Karlsen et al., 1993; Karlsen and Skeie, 2006; Knipe et al., 1991; Nedkvitne et al., 1993; Oxtoby et al., 1995; Stewart, 1993). Most studies have been performed at the regional level or on the Ula field; few studies have been carried out specifically on the reservoir properties and factors controlling the reservoir quality of the Tambar field. This present study has been performed to fill the gap and give account of how sandstone composition and diagenetic activity has affected reservoir quality of the Tambar field.

Sandstones buried to depths greater than 2500m and exposed to high lithostatic pressure tend to loose porosity mainly through a combination of compaction and cementation (Ehrenberg, 1990). Compaction includes mechanical compaction (rearrangement of grains, grain bending, grain fracturing) and chemical compaction (pressure solution at grain contacts or along stylolite seams). Cementation occurs when sediment-fluid systems are out of geochemical and textural equilibrium; they tend to interact progressively as the ambient environment evolves in terms of temperature, pressure and fluid chemistry during burial. The result is the precipitation of new mineral cements that is in, or approaching, equilibrium with new burial environment. The new cements tend to result in the blocking of pore throats reduce porosity. The most common cements are quartz (as overgrowths), pore-filling dolomite, and pore-throat blocking clays such as illite. However, porosity can be preserved in deeply buried sandstones by: (1) early diagenetic microquartz coating (Aase et al., 1996; Jahren and Ramm, 2000; Lima and De Ros, 2002), (2) the presence of early diagenetic chlorite coating (Ajdukiewicz et al., 2010; Bloch et al., 2002; Dixon et al., 1989), (3), over pressure (Osborne and Swarbrick, 1999; Ramm and Bjorlykke, 1994), (4) early oil emplacement (Gluyas et al., 1993; Marchand et al., 2001; Wilkinson and Haszeldine, 2011). Microquartz and chlorite coatings preserve porosity by inhibiting quartz cementation, whereas overpressure limits

compaction and potentially inhibits pressure solution (Sheldon et al., 2003). Early emplacement of oil into a reservoir potentially limits diagenetic activity thereby stopping precipitation of cements (Kraishan et al., 2000; Worden et al., 1998). Reservoir quality, to a great extent, is controlled by depositional characteristics and early diagenetic processes that the sandstone has undergone since these conditions affect rock's behaviour during burial diagenesis.

Porosity controls oil and gas reserve volumes and permeability controls flow rate of the produced oil to the surface. Thus understanding what controls porosity and permeability is crucial for predicting reservoir quality and so determining the economic viability and development strategy of a given oil or gas field. Although Tambar sits relatively close to Ula, it has been reported to have different, less good, reservoir quality although the reasons for this remain obscure. Therefore, a diagenetic analysis has here been undertaken to understand the diagenesis and its effect on the reservoir quality of the Tambar field. Specific questions to be addressed are:

What are the most significant diagenetic mineral cements in the Tambar field?
What was the sequence of diagenetic mineral growth?
What are the sources and processes that resulted in these minerals?
What controls porosity and permeability in the Tambar field?
Have any processes led to inhibition of quartz cement growth and preservation of porosity?

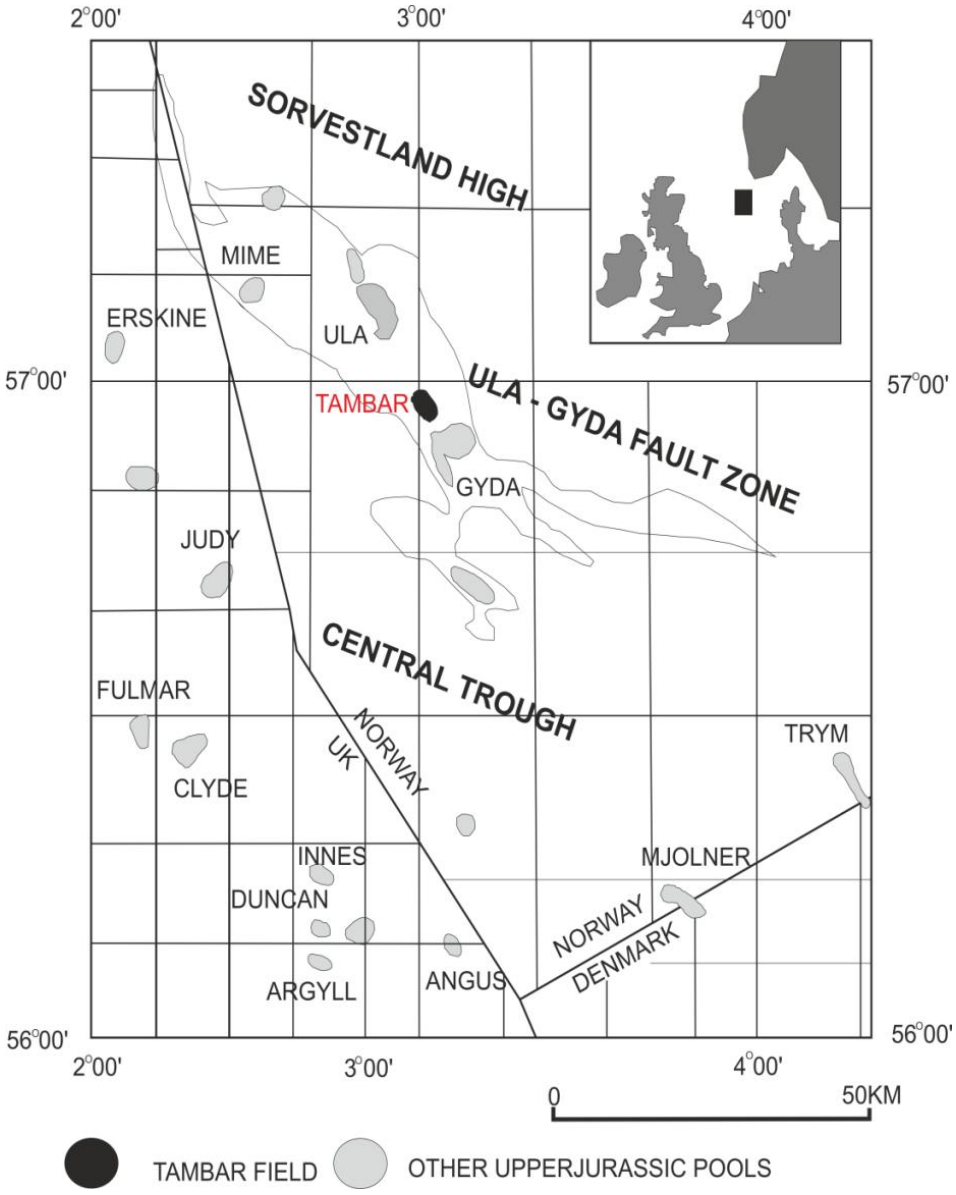

Figure 5. 1 Location map of the Tambar field in the Central Graben, in the North Sea Modified from (Bjørnseth and Gluyas, 1995)

5.3 Geological Background

Tambar (Norwegian: *Tambarfeltet*) is an offshore oil field located in the southern Norwegian section of North Sea, along with Ula and Gyda fields making up the UGT area (Fig. 5.1). It is a major geological structure that was tectonically active from the middle Jurassic through to the late Cretaceous probably due to collapse of the Zechstein salt. It forms part of the Central Graben where shallow marine Jurassic sands were deposited in salt-dissolution features separated by inverted Triassic pods (O'Connor et al., 2001). The Central Graben is characterized by several narrow,

discontinuous structural highs and lows (Skjerven et al., 1983), with a very complicated tectonic history.

The formations encountered in the Tambar field consist of the Vestland Group, Tyne Group, Cromer Knoll Group, Shetland Group, Rogaland Group and the Hordland Group (Fig. 5.2). The Vestland group consist of the Ula Formation which was deposited on the Triassic Skaggarak Formation. The Ula Formation consists of very fine to medium-grained, moderately to well sorted sandstone and mudstone toward the lower part. The Tyne Group is made up of the Farsund and Mandal Formations. The Farsund Formation is composed of a lower Gyda Sandstone Member and an Upper Mudstone Member. In some company reports (Completion Logs etc.), the Gyda Sandstone member is considered to be part of the Ula Formation. The Mandal Formation is the local stratigraphic name for the Kimmeridge Clay Formation, which is more typically used by authors in the Central Graben area (Hamar et al., 1983). Mudstones and argillaceous limestone of the Lower Cretaceous Cromer Knoll Goup overlie the Upper Jurassic of the Mandal Formation. The Cromer Knoll is made up of Asgard, Tuxen, Sola and Rødby Formations which are dominantly mudstones. This is overlain by the late Cretaceous to early Tertiary, carbonate-dominated Shetland Group (also known as the Chalk) comprising of the Ekofisk, Tor and Hod Formations. The Eocene Rogaland Group comprising the Vale, Lower Lista, Vidar, Upper Lista, Sele and Balder Formations overlies the Shetland Group. The undifferentiated Hordland Group is the topmost sediments in the Tambar field.

The pay horizons in the Tambar field are confined to the Upper Jurassic Ula Formation and the Gyda Sandstone Member of the Farsund Formation (Fig. 5.2); (Bergan et al., 1989; Karlsen et al., 1993; Partington et al., 1993; Underhill, 1998). From the neighbouring Ula field, this unit has been described as a shallow marine sandstone up to 200m thick that prograded across outer-shelf mudstones, following a sea level fall in the Kimmeridgian (Harris, 2006). The Ula Formation sandstones are typically fine-grained, well sorted and highly bioturbated with beds rich in lithic shale fragments. The Ula Formation unconformably overlies the partly-eroded Middle Jurassic to

Triassic fluvial Skagerrak Formation (Fig. 5.2). This unit is in turn overlain by Late Jurassic mudstones, which include the Upper Jurassic source rock (Wilhelms and Larter, 1994). The shale member of the Farsund Formation and especially the overlying Mandal Formation are likely to be the local source rocks, as is the case of the adjacent Ula field and oil fields in the neighbouring Danish sector (Petersen et al., 2012).

The reservoir temperature recorded from bottom hole (4272m) measurements of well 1/3-3 was 179°C. The Tambar field seems to have had a relatively simple burial and thermal history with the Ula Formation being progressively buried, with no notable periods of uplift or cooling. The Ula Formation reached 90°C at about 60Ma, 130°C at about 25Ma and 160°C at about 2Ma (Fig. 5.3).

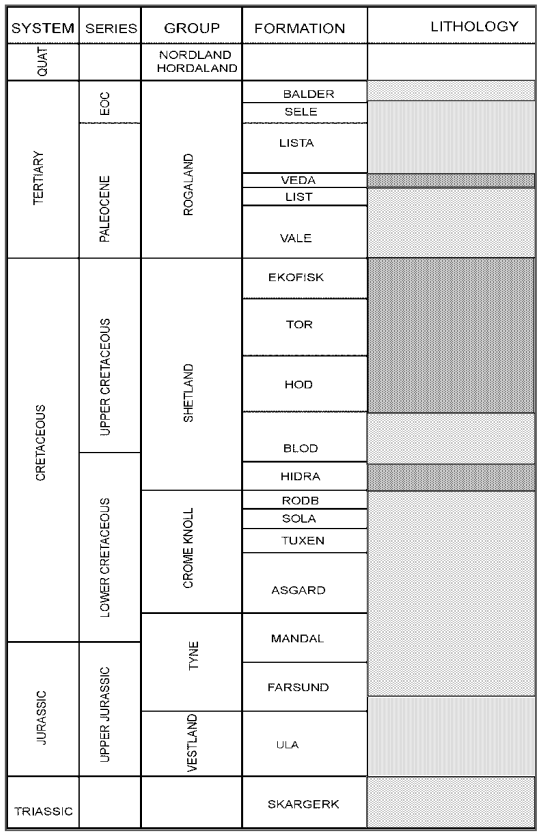

Figure 5.2 Simplified stratigraphy of the Tambar field produced from well 1/3-3. (Data used from BP well report).

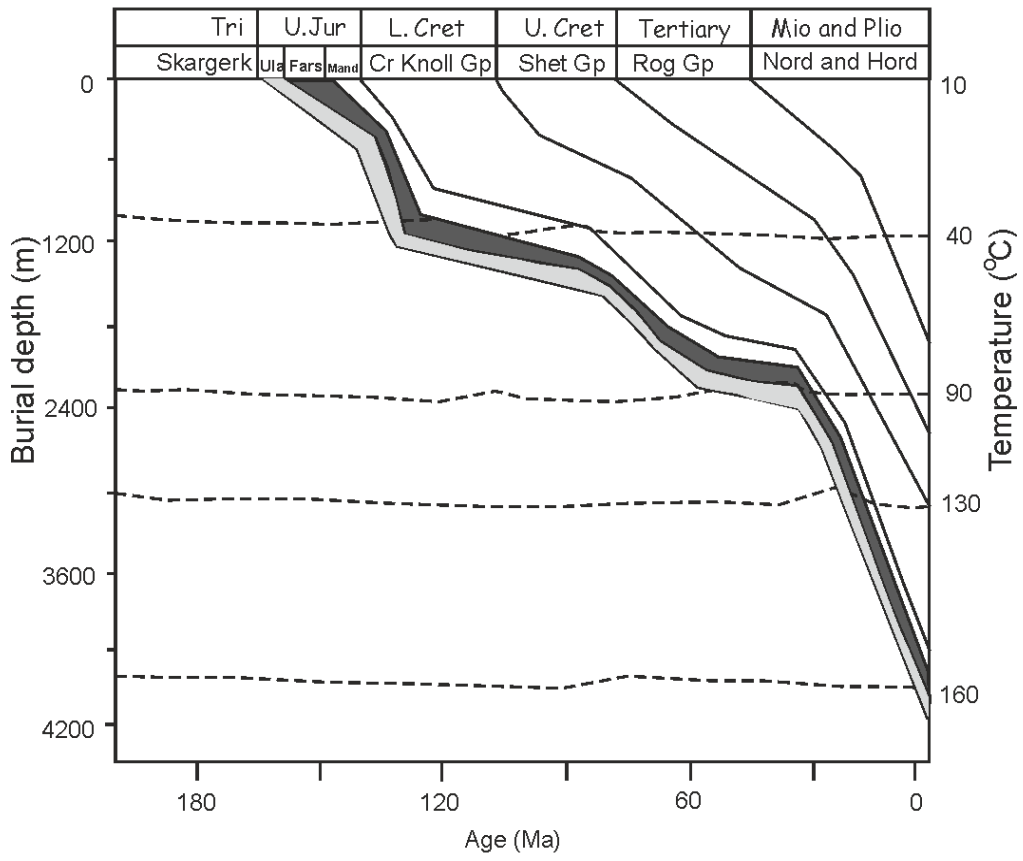

Figure 5.3 Burial history curve of the Tambar field showing related tectonic events and Temperatures, reservoir rocks in grey. Thermomodel for windows was used for modelling. (Data used from BP well report). Assumed constant thermal gradient of 40^{O}C/1000m

5.4 Material and methods

Wireline and conventional core analysis data from the Tambar field were made available by BP Norway. Core plugs were taken at 30cm-spacings with porosity and permeability measured using industry-standard methods. The downhole wireline logs available were: caliper, bulk density, neutron porosity, sonic transit time, bulk gamma, shallow resistivity and deep resistivity. Wireline data were reported every 10cm from the Ula Formation from each of the three wells sampled in the Tambar field. Porosity was calculated for each of the logs using the density log and the following relationship:

Fractional porosity = $(\rho_{mbd} - \rho_{amd})/(\rho_{fd} - \rho_{amd})$ (eq 1)

Where:

ρ_{mbd} = measured bulk density (from wireline logs)

ρ_{amd} = average mineral density

ρ_{fd} = fluid density

The average mineral density employed was 2.66 g/cm^3. The average fluid density was taken as 1.00 g/cm^3 since the fluid in the zone next to the well bore will be aqueous due to the water-based drilling fluids replacing the initial pore fluid (predominantly oil in the oil leg). The results of the wireline calculation of porosity were compared to the core analysis porosity to check credibility (Fig. 5.4). Conventional core analysis porosity and permeability data were provided by the operating oil company (BP) from the cored sections of the Ula Formation (Fig. 5.5).

Water saturation was calculated from the wireline data for each depth using the Archie equation:

$$S_w = [(a/Ø^m)/(R_w/R_t)]^{(1/n)} \qquad \text{(eq 2)}$$

Where:

S_w = fractional water saturation

n = saturation exponent

a = tortuosity constant

R_w =formation water resistivity (determined at reservoir temperature)

R_t = formation resistivity (obtained from deep resistivity log to reduce any effect of drilling mud).

Ø = density log-derived fractional porosity (see equation 1)

m = cementation exponent

Values of n, a, and m were fixed at 2.5, 0.82 and 2.0 respectively as used by the field development geoscientists. Only deep induction resistivity measurements were used in the formula, as these are the only resistivity measurements that give true formation

resistivity, unaffected by invasion of the formation by drilling fluids (Asquith and Gibson, 1982). Water resistivity was 0.025 ohm/m (Oxtoby, 1994).

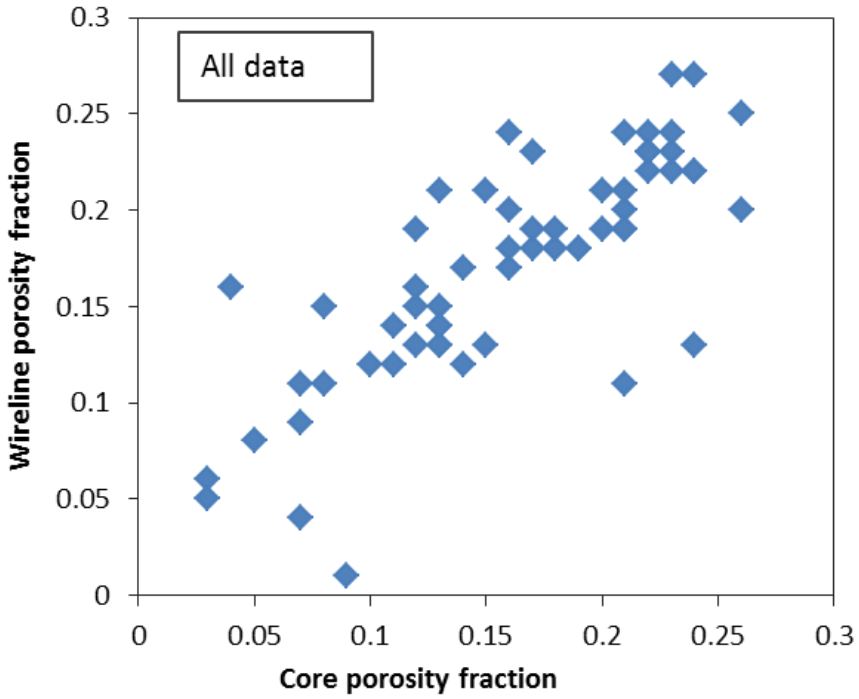

Figure 5.4 Calibration of wireline porosity against core analysis porosity from the Ula sandstones of the Tambar field. Wireline porosity was derived from the density log data.

Seventy seven samples of conventional core plugs from three wells were obtained from the BP core store at Reslab laboratories in Stavanger, Norway. The core sample suite covers the range of present subsurface measured depths between 4130m and 4373m, and spans the thickness of the whole reservoir. Individual sandstones were studied using a combination of techniques, including petrography, scanning electron microscopy (SEM), cathodoluminescence microscopy (CL), X-ray diffraction (XRD) and fluid inclusion micro-thermometry.

Polished thin sections were made from the core samples. The polished sections were impregnated with blue resin in order to highlight porosity. Sandstone modal composition was obtained by detail point counts (400 counts per section) of all thin sections. Grain sizes and grain coating were measured using Meiji 9000 microscope fitted with an Infinity 1.5 digital camera. Images were photograped and long axes of 100 grains were measured using Infinity Analyser software. Fifty grains per section

was measured for percentage of grain-coating microcrystalline quartz coverage using visual estimates. Only potential sites for quartz cementation (i.e. facing pores, not coated with dead-oil or with clay matrix) that were coated with microcrystalline quartz were measured and expressed as a percentage of all potential sites for quartz cementation.

SEM examinations were made using a Philips XL 30 SEM with tungsten filament with an accelerating voltage of 20 kV, and 8 nA beam current for both SE and BSEM. The SEM study was carried out on polished sections and freshly fractured, stub-mounted samples coated with carbon and gold respectively. Energy dispersive X-ray analysis (EDAX) provided qualitative compositional analysis of clay minerals, carbonate cements and feldspars. Some of the sandstone samples were soaked in acetone to remove the oil stains which caused problems for the vacuum system in the gold coater. The CL images were collected at 10 Kv and spot size 7. They were collected by integrating the signal of 16 frames using a slow scanning raster which takes about 8 minutes to collect. Samples for XRD were cut from the core samples.

PANalytical X'pert pro MPD X-ray diffractometer was used for the XRD analysis. Samples were crushed using micromill and distilled water for 10 minutes. They were then dried overnight in a low temperature oven and powdered using agate pestle and mortar. A copper X-ray source operating at 40kV and 40mA was used. Powder samples were loaded into cavity holders and rotated continuously during the scan, completing one rotation every 2 seconds. Programmable anti-scatter slits and a fixed mask maintained in an irradiated sample area of 10 x 15 mm, with an additional 2^{o} incident beam antiscatter slit producing a flat background for raw data down to a 2theta angle of 3^{o}. The X'Celerator detector was set to scan in continuous mode with full length active pulse-height discrimination levels set to 45 to 80%. Operation of X-ray Diffractometer and Software was set using "HighScore Plus ®" analysis software and automated Rietveld refinement methods with reference patterns from the International Centre for Diffraction Data; Powder Diffraction File-2 Release 2008.

Fluid inclusions microthermometric studies were carried out on selected samples. Doubly polished fluid inclusion wafers were prepared from the core samples at the

University of Birmingham. An Olympus BX-60 petrographic microscope was used for thermometry and was equipped with a Linkam THMSG 600 heating and cooling stage which enabled the measurement of the temperature of phase transition from

-180^0 to 600^0C with an accuracy of ± 0.1 to ± 1.0. Observations were made with different magnifications (objectives 10x, 20x, 50x and 100x). Inclusions were photographed with Digital Camera Olympus DP71 for the purpose of the fast mapping of inclusion locations. Homogenisation temperature measurements were made on each inclusion in each small piece of fluid inclusion wafer and then freezing point depression measurements were made on each inclusion to prevent modification of the homogenisation temperature (Worden et al., 1995). All fluid inclusion samples were also studied using UV-luminescence using Olympus BX-60 microscope. A super high pressure mercury lamp was used to provide the light. The purpose of this was to check for the possible presence of the oil inclusions.

For stable-isotope analysis of diagenetic carbonates, the bulk compositions of dolomite cemented samples were used. The powders were prepared and XRD was carried out in order to pre-select samples with only dolomite cements (no calcite). The dolomite samples were corrected for the effects of kinetic oxygen isotope fractionation associated with the production of CO_2 by reaction of dolomite with phosphoric acid at 50^oC using a fractionation factor of 1.01066 (Rosenbaum and Sheppard, 1986). Only a few of the selected dolomite samples were able to liberate enough CO_2 for reliable analysis. The carbon isotope data are presented in the normal δ notation relative to PDB (Craig, 1957), and oxygen isotope was converted to SMOW for comparison using (Friedman and O'Neil, 1977) equation. Stable isotope fractionation curves were used to calculate the temperature of $\delta^{18}O$ of the pore waters, which led to the precipitation of the dolomite cements (Land, 1983; O'Neil and Epstein, 1966) using the following equation.

$$1000 \ln \alpha_{dolomite-water} = (3.34 \times 10^6 \times T^2) - 3.34$$

Where,

$1000 \ln \alpha_{mineral\ water-water}$ = oxygen-isotope mineral water fractionation factor

T = Temperature in degrees Kelvin

Chinese version of Thermomodel for windows was used in modelling the burial history curve. Assumed surface seafloor temperature used was 5^{o}C and constant present geothermal gradient of 40^{o}C/km (Nedkvitne et al. 1993).

5.5 Results

5.5.1 Wireline analysis

For the studied sections in the three wells, density-derived porosity values range from as high as 27-28% to as low as 0% (Fig. 5.5). The interpreted water saturation varies from 100% to a minimum of about 10%.

In well 1/3-9-ST2, the Ula Formation has a water saturation approaching 100% at about 4245m true vertical depth (TVD) above which it progressively decreases to 10 to 20% right up to the top of the cored section at about 4135mTVD. There are variations of porosity with what can be interpreted to be two thick sequences of increasing reservoir quality up-stratigraphy.

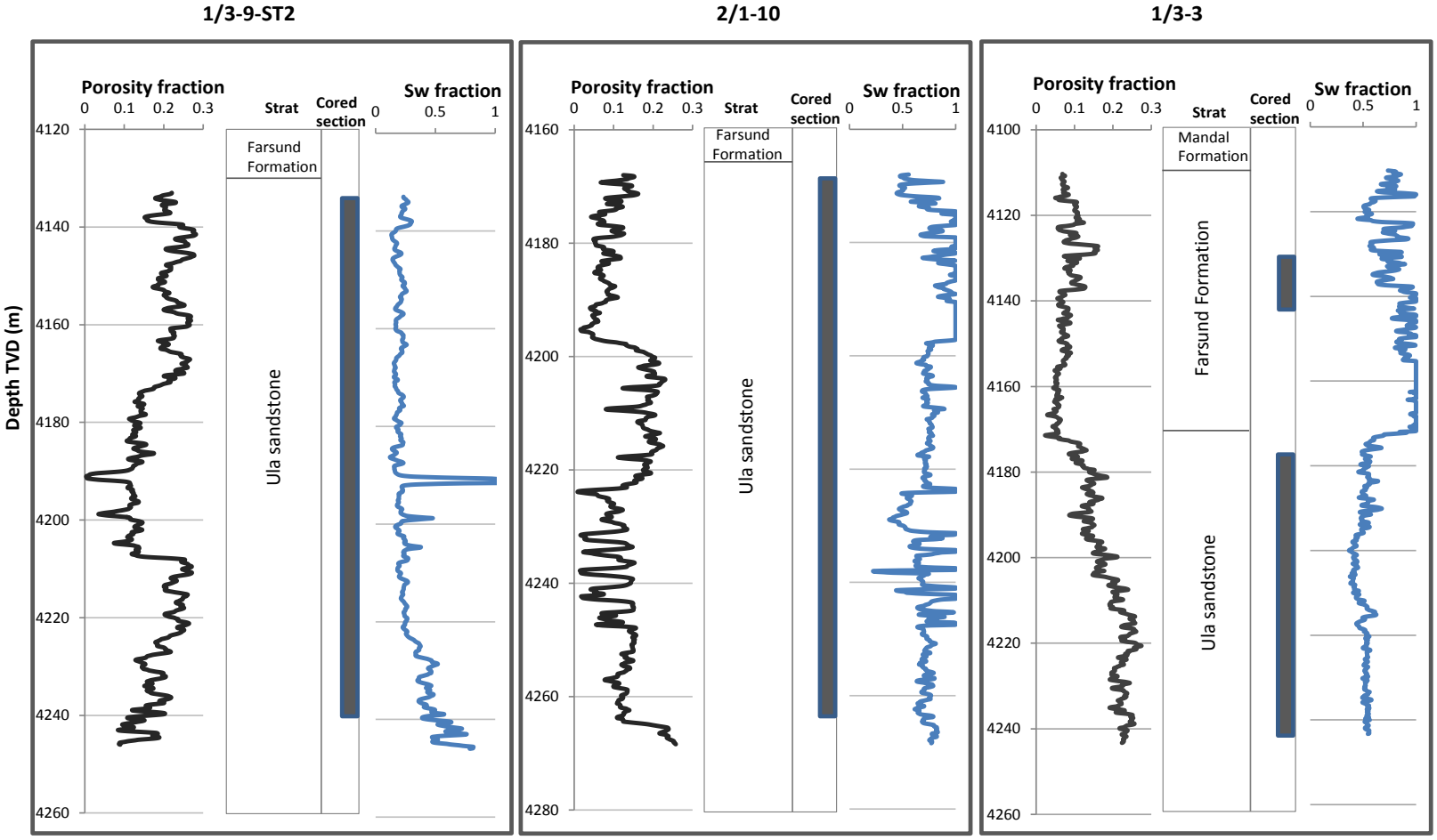

Figure 5.5 Interpreted porosity from the density log (see Figure 4) and interpreted water saturations calculated from the resistivity log and using the Archie equation; for the three wells from Tambar used in this study.

Two spikes of 100% water saturation and very low porosity represent two carbonate cemented intervals. This well is predominantly in the oil leg of Tambar.

In well 2/1-10, the Ula Formation has relatively high water saturations throughout much of the section and is conventionally considered to represent the water leg of the oil field. Porosity is fairly low throughout this well except for an interval between about 4220 and 4240mTVD where it approaches 20%.

In well 1/3-3, the Ula Formation has a water saturation as low as about 40% up to about 4180mTVD above which it suddenly increases to 100%. This depth matches a decrease in porosity from 25% down to a few percent and represents the stratigraphic top of the reservoir (the shale-rich Farsund Formation Fig. 5.5). The porous reservoir rocks largely sit within the oil leg in this well but have notably low maximum oil saturations.

5.5.2 Detrital grains, minerals and textures

Classification of the detrital mineralogy of the Tambar reservoir sandstones was performed using ternary plots (Folk, 1968); they fall into arkose class (Fig. 5.6) since they are relatively rich in detrital feldspars but contain few lithic fragments. Point count result show that the most abundant detrital grain is monocrystalline quartz (av. 34 ± 1.2%) of the rock volume, about 60% of the detrital grain mineralogy; Figs. 5.7 and 5.8, Table 1), with minor polycrystalline (av. 3 ± 0.2%). Feldspars represent about 25% of the rock volume and are volumetrically the second most important group of minerals. Tambar reservoir clastic rocks range from very fine - to fine-grained sandstones, and locally are silty. Grain sizes tend to be little above 250µm and have been divided into three classes (<125µm, 125-177µm and >177µm). They are moderately to well sorted (Figs. 5.7 and 5.8). The grains are dominantly sub-angular to sub-rounded.

The detrital feldspars include K-feldspar (av. 12 ± 0.2%) and plagioclase (av. 12 ± 0.2%) (Table 5.1). The majority of the K-feldspar and some plagioclase grains have undergone dissolution (Fig. 5.9). Locally total grain dissolution has occurred leaving traces of replacive illite (Fig. 5.9C). This has resulted in secondary porosity of up to

7% in some samples. Rock fragments are generally rare (< 3%) in all samples (Table 5.1). Detrital clay occurs in patches and thin lenses. There are no apparent systematic compositional variations in mineralogy between wells or at different depths within wells.

Mica, mainly muscovite, occurs in variable amounts (<1–3% volume). The muscovite grains are flat or platy but deformed when found between two detrital grains. Micas have apparently caused dissolution of quartz grains since they are flattened at quartz-mica grain contact (Fig. 5.7C).

Other detrital minerals that occur in small amounts (<1% volume) include glauconite, chalcedony, chert, carbonate or bioclasts, and heavy minerals (zircon, epidote, tourmaline, rutile, apatite, garnet and Fe–Ti oxides). The glauconite grains are greenish in colour. This mineral is typically strongly deformed by compaction.

Sponge spicules, common in Upper Jurassic marine sandstones in the North Sea (Aase et al., 1996; Vagle et al., 1994), have apparently dissolved away leaving sand-grain sized circular pores in some samples (Fig. 5.10). Secondary evidence for the former presence of abundant sponge spicules will be provided in the section on diagenetic cements (and see Fig. 5.11).

Table 5. 1 Average petrographic properties of the oil and water leg sandstones from the three wells studied in the Tambar field.

Detrital and diagenetic components	1/3-9-ST2 oil leg n=23	1/3-9-ST2 water leg n=8	1/3-3 oil leg n=5	1/3-3 water leg n=9	2/1-10 water leg n=20	Weighted Mean
Mono quartz	33.8 ± 0.8	32.5 ± 1.3	31.3 ± 1.6	30.2 ± 0.6	36.1 ± 1.2	33.9 ± 1.2
Poly quartz	3.6 ± 0.2	4.3 ± 0.2	2.8 ± 0.4	2.1 ± 0.2	2.8 ± 0.2	3.1 ± 0.3
K-feldspar	10.8 ± 0.4	13.6 ± 7.0	11.7 ± 0.8	11.7 ± 0.7	13.1 ± 0.5	12.1 ± 0.6
Plagioclase	12.9 ± 0.4	11.7 ± 0.4	12.2 ± 1.1	15.0 ± 0.4	11.1 ± 0.5	12.3 ± 0.3
Sedimentary RF	0.2 ± 0.1	0.0 ± 0.0	0.4 ± 0.2	0.3 ± 0.1	0.3 ± 0.1	0.3 ± 0.2
Igneous RF	0.5 ± 0.1	0.0 ± 0.0	0.6 ± 0.2	0.6 ± 0.1	0.9 ± 0.2	0.5 ± 0.1
Metamorphic RF	0.7 ± 0.1	0.5 ± 0.2	1.3 ± 0.2	1.0 ± 0.2	1.0 ± 0.1	0.9 ± 0.7
Muscovite	1.9 ± 0.3	2.1 ± 0.4	3.0 ± 0.8	1.3 ± 0.2	0.6 ± 0.1	1.8 ± 0.3
Heavy Minerals	0.1 ± 0.1	0.0 ± 0.0	0.2 ± 0.2	0.2 ± 0.3	0.0 ± 0.0	0.1 ± 0.1
Glauconite	0.1 ± 0.1	0.1 ± 0.1	0.1 ± 0.0	0.1 ± 0.1	0.1 ± 0.0	0.1 ± 0.1
Calcite PF	1.9 ± 2.0	0.3 ± 0.1	0.0 ± 0.0	0.0 ± 0.0	1.9 ± 0.3	0.8 ± 0.1
Calcite replacive	1.2 ± 0.3	2.3 ± 1.0	2.7 ± 0.7	2.0 ± 0.5	1.6 ± 1.5	2.0 ± 0.4
Dolomite PF	0.3 ± 0.1	0.7 ± 0.6	0.4 ± 0.2	1.3 ± 0.4	1.6 ± 0.1	0.8 ± 0.5
Dolomite replacive	2.6 ± 0.5	2.7 ± 0.5	4.0 ± 0.7	2.0 ± 0.4	1.9 ± 0.3	2.3 ± 0.4
Illite PF	2.6 ± 0.7	2.0 ± 0.3	0.8 ± 0.3	1.2 ± 0.4	0.7 ± 0.1	1.3 ± 0.4
Illite replacive	2.7 ± 0.4	4.1 ± 0.7	3.4 ± 0.9	2.3 ± 0.5	2.7 ± 0.4	3.0 ± 0.5
Chlorite PF	0.1 ± 01	0.0 ± 0.0	3.0 ± 0.8	1.9 ± 0.3	0.5 ± 0.2	2.3 ± 0.3
Chlorite replacive	0.3 ± 0.1	0.0 ± 0.0	0.4 ± 0.2	0.1 ± 0.1	0.6 ± 0.2	053 ± 0.1
Quartz cement	2.3 ± 0.6	0.8 ± 0.2	0.3 ± 0.2	1.4 ± 0.4	3.6 ± 0.8	3.2 ± 0.3
Microcrystalline quartz	5.2 ± 0.5	9.5 ± 1.1	8.0 ± 0.6	4.4 ± 0.6	2.6 ± 0.6	4.8 ± 0.5
K-feldspar cement	1.6 ± 0.3	0.5 ± 0.3	0.8 ± 0.3	3.5 ± 0.3	3.0 ± 0.3	2.1 ± 0.2
Albite cement	1.8 ± 0.3	0.5 ± 0.2	0.9 ± 0.4	3.0 ± 0.4	2.2 ± 0.3	1.7 ± 0.3
Pyrite	0.3 ± 0.1	0.1 ± 0.1	0.4 ± 0.1	0.3 ± 0.1	0.5 ± 0.1	0.3 ± 0.1
Hydrocarbon stain	0.3 ± 0.1	0.1 ± 0.1	0.1 ± 0.1	0.3 ± 0.1	0.1 ± 0.5	0.2 ± 0.1
Siderite	0.2 ± 0.1	0.0 ± 0.0	0.0 ± 0.0	0.3 ± 0.2	0.2 ± 0.1	0.1 ± 0.1
Intergranular porosity	9.5 ± 0.9	9.1 ± 1.0	9.8 ± 1.8	8.7 ± 6.5	6.8 ± 0.6	8.8 ± 0.2
Intragranular porosity	2.5 ± 0.9	2.4 ± 0.4	1.9 ± 0.6	5.0 ± 0.5	2.8 ± 0.3	3.7 ± 0.5
Total	100.0	100.0	100.0	100.0	100.0	100.0

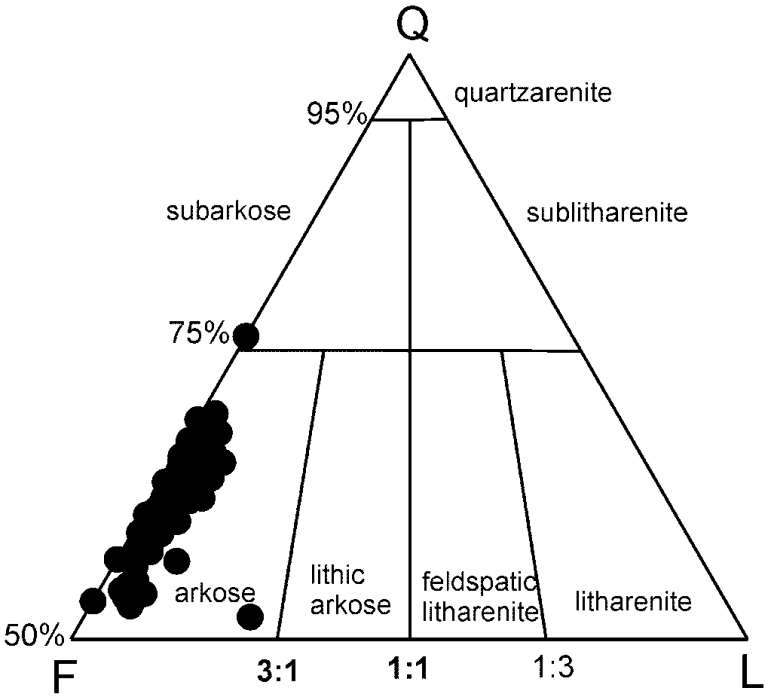

Figure 5.6 Detrital composition of the Tambar reservoir sandstone samples plotted on (Folk, 1968) classification diagram. The sandstones are exclusively arkoses. Q=quartz, F=feldspar and L=lithic fragments

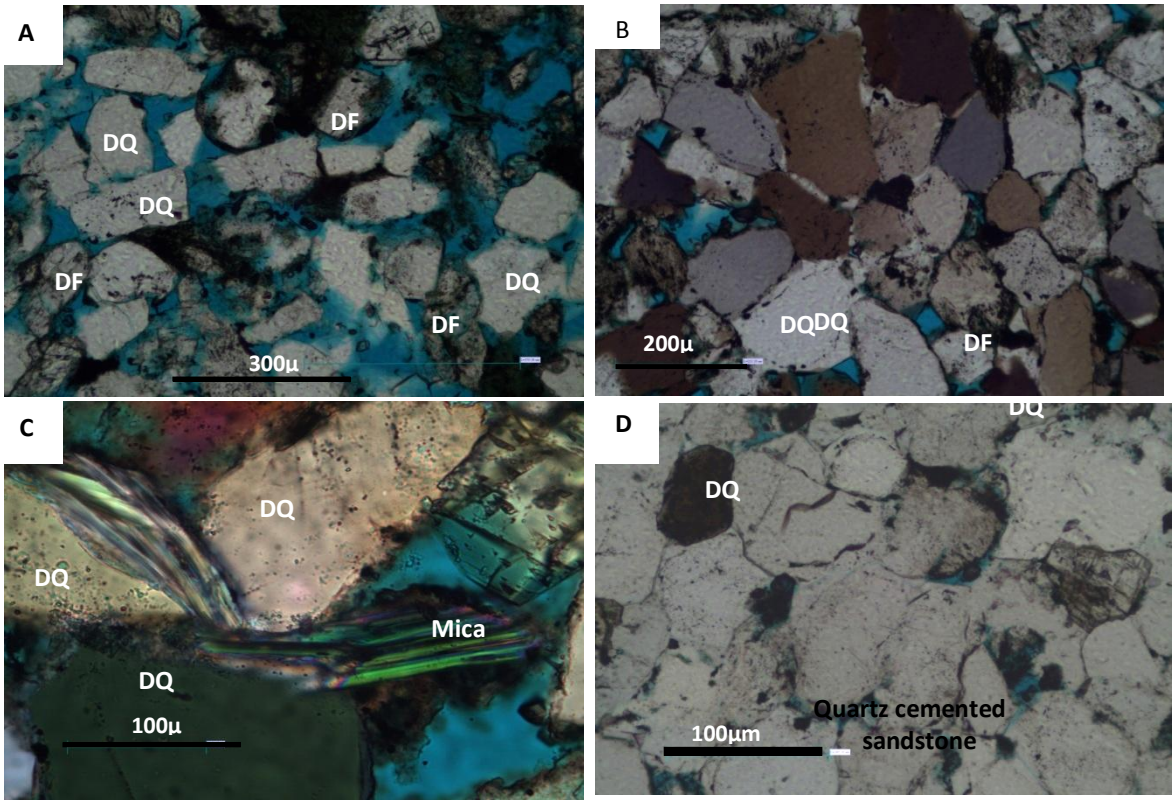

Figure 5.7 Thin section images of detrital mineralogy. (A and B) Plane polarized light showing fine and coarse-grain texture and composition of the Tambar reservoir sandstones well 1/3-3(4243mTVD) and well 2/1-10 (4238mTVD) (C) Crossed polarised quartz grains and mica deformed at grain contact well 1/3-9ST2 (4214mTVD) (D) plane polarized light image showing quartz cemented part of the sandstone well . Note: cement occluding porosity completely 2/1-10 (4225mTVD) . Key: detrital quartz (DQ) detrital feldspar (DF).

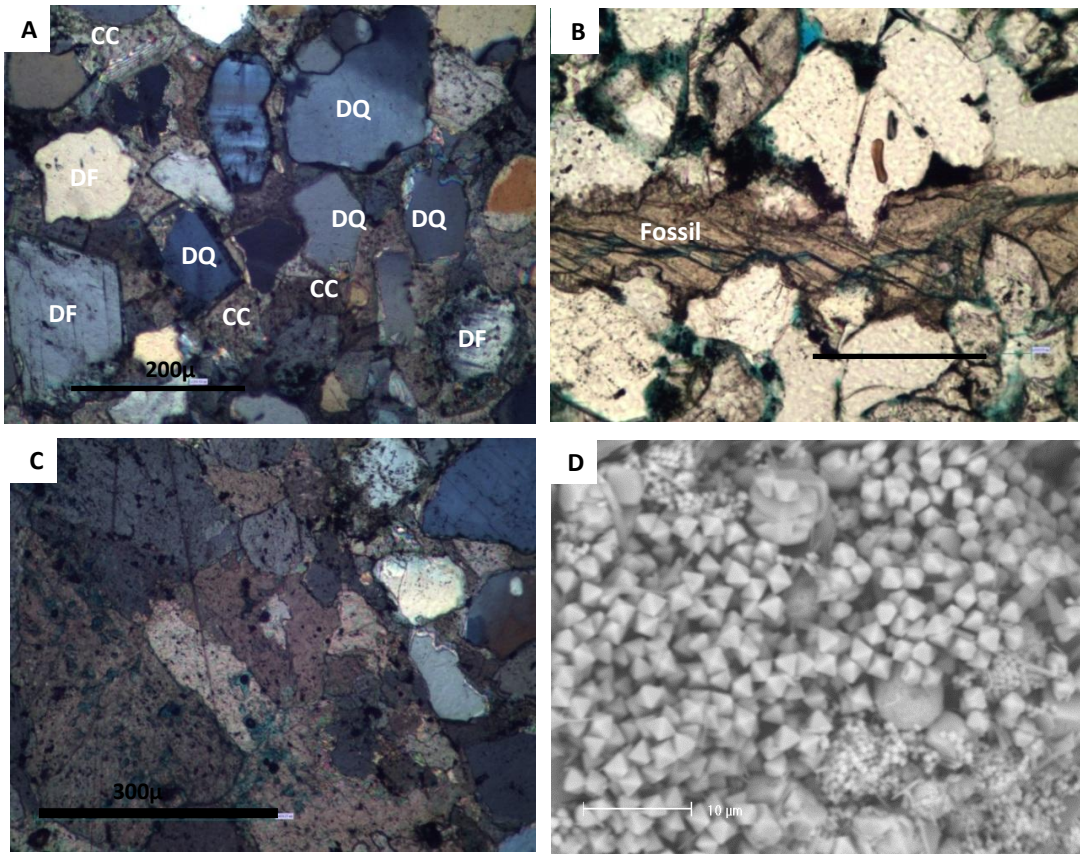

Figure 5.8 Thin section images of early diagenetic mineral cements (A) crossed polar image of early formed pore filling calcite 2/1-10 (4217mTVD) (B) plane-polar image showing calcified fossil fragment 1/3-3 (4231mTVD) (C) cross-polar image showing large crystal of early formed calcite cemented 2/1-10 (4252mTVD) (D) SEM image of pyrite crystals 2/1-10 (4217mTVD).

5.5.3 Diagenetic minerals

The most common diagenetic constituents of the Tambar reservoir rock found in these three wells are: microcrystalline quartz (Figs. 5.10 and 5.11), illite and chlorite (Fig. 5.12), quartz cement (Figs. 5.13 and 5.14), feldspar cements (Fig. 5.9), dolomite and calcite (Figs. 5.8 and 5.15), and pyrite (Fig. 5.8).

Calcite occurred in two forms. It appears as early-formed, pore-occluding cement and as corrosive replacement of other minerals in minor amounts (<5%). In the early formed calcite samples (Fig. 5.8A and C), porosity and permeability are insignificant and other detrital grains have not undergone major dissolution or other mineral cement precipitation. The detrital grains appear to float in the large intergranular

volume. The second type is replacive which occur in minor amounts replacing detrital grains and clays.

Traces to minor amounts of pyrite are widespread in occurrence, sitting in pores and on grain surfaces, associated with micas and mud intraclasts. Pyrite occur as aggregate of small cubic crystals <15µm (Fig. 5.8) or in the form of framboids.

Diagenetic feldspar occurs as K-feldspar or albite overgrowths. K-feldspar cement is a present authigenic mineral in most samples. It ranges from 0 to 5%; (av.2 ± 0.1%) of the rock volume. Though the thickness of the K-feldspar overgrowth reaches up to 15µm, it mainly has undergone etching due to partial dissolution leaving most of the detrital feldspar intact (Fig. 5.9B). The albite and K-feldspars cements have been overgrown by chlorite and illite and also are engulfed by quartz overgrowth (Fig. 5.9B and C) that have developed on adjacent quartz grains. Feldspar cements therefore predate these mineral cements.

Microcrystalline quartz is the most abundant diagenetic mineral in the Tamar field reservoir. It occurs in two forms; as isopachous rims covering the detrital grain and an intergranular pore-filling form. Generally euhedral microcrystalline quartz (2-5µm) range in volume from 0-13% (av. 4.8 ± 0.8%; Fig. 5.11). This amount of microcrystalline quartz is somewhat greater than has been reported previously from sandstones worldwide (Aase et al., 1996; Jahren and Ramm, 2000; Ramm, 1992). The pore filling form occur as aggregate of prismatic euhedral quartz crystals similar in size to the grain coating form and is locally associated with fibrous illite and framboidal pyrite. The microcrystalline quartz is associated with samples that contain sponge spicules (Fig. 5.10). In some places, there is some sort of coating between the sand grain surfaces and the microcrystalline quartz (Fig. 5.11D). This may be a layer of amorphous silica, analogous to that observed in the Heidelberg sandstone (French et al., 2012; Worden et al., 2012).

Illite is the most abundant clay mineral in the Tambar sandstone reservoir (0-16% with average of 4.3%). It is associated with highly altered feldspar and muscovite and can be interpreted to be a product of labile detrital grain alteration (e.g. detrital intraclast alteration: Fig. 5.12A). Illite occurs as fibrous, hair like radially-disposed

crystal and filamentous crystals bridging pore throats (Fig. 5.12B) or filling pores (Fig. 5.12C). Illite can be identified from XRD analysis by the typical prominent peaks (10Å; Figs. 5.13 A and B).

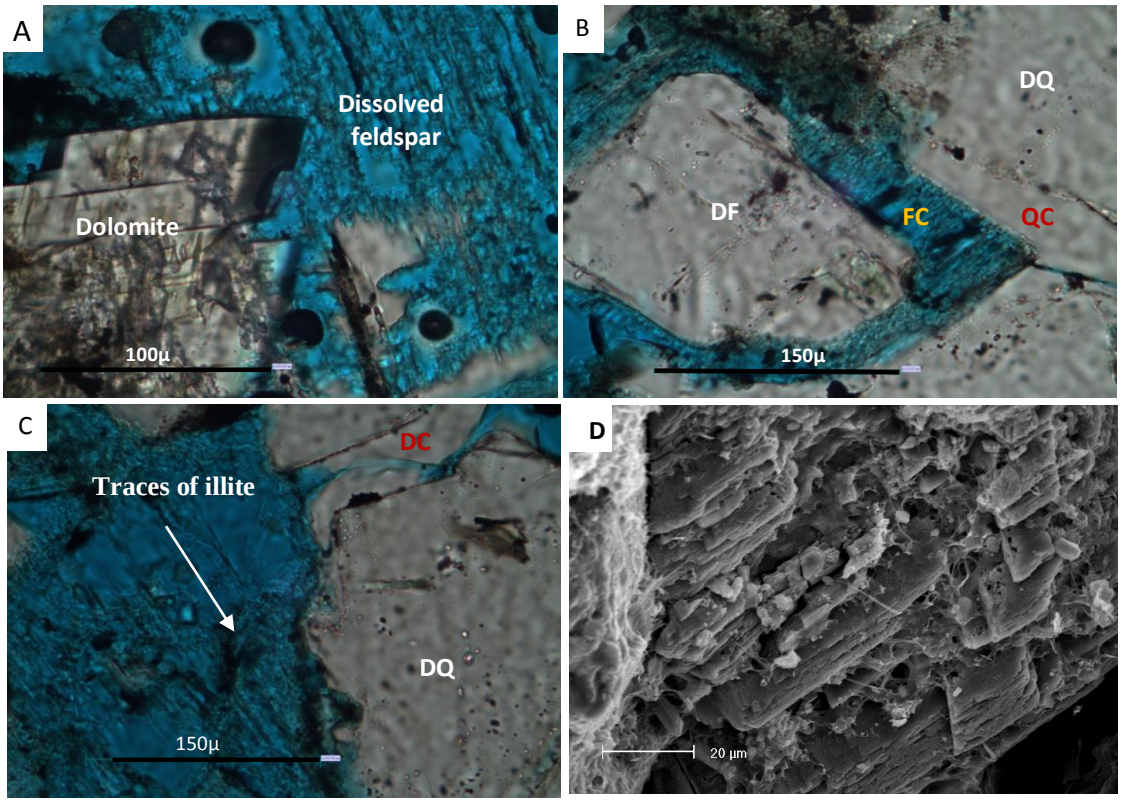

Figure 5.9 Thin section images showing partial feldspar dissolution and feldspar cement fabrics. (A) feldspar dissolution pore with dolomite crystal growing in the pore 2/1-10 (4241mTVD) (B) feldspar cement dissolution leaving unaltered detrital feldspar 2/1-10 (4241mTVD) (C) total detrital feldspar dissolution Feldspar-dissolution results in secondary porosity and formation of authigenic clays 2/1-10 (4221mTVD) . (D) SE image showing altered detrital feldspar 2/1-10 (4241mTVD) . Key: detrital quartz (DQ) detrital feldspar (DF) feldspar cement (FC) quartz cements (QC).

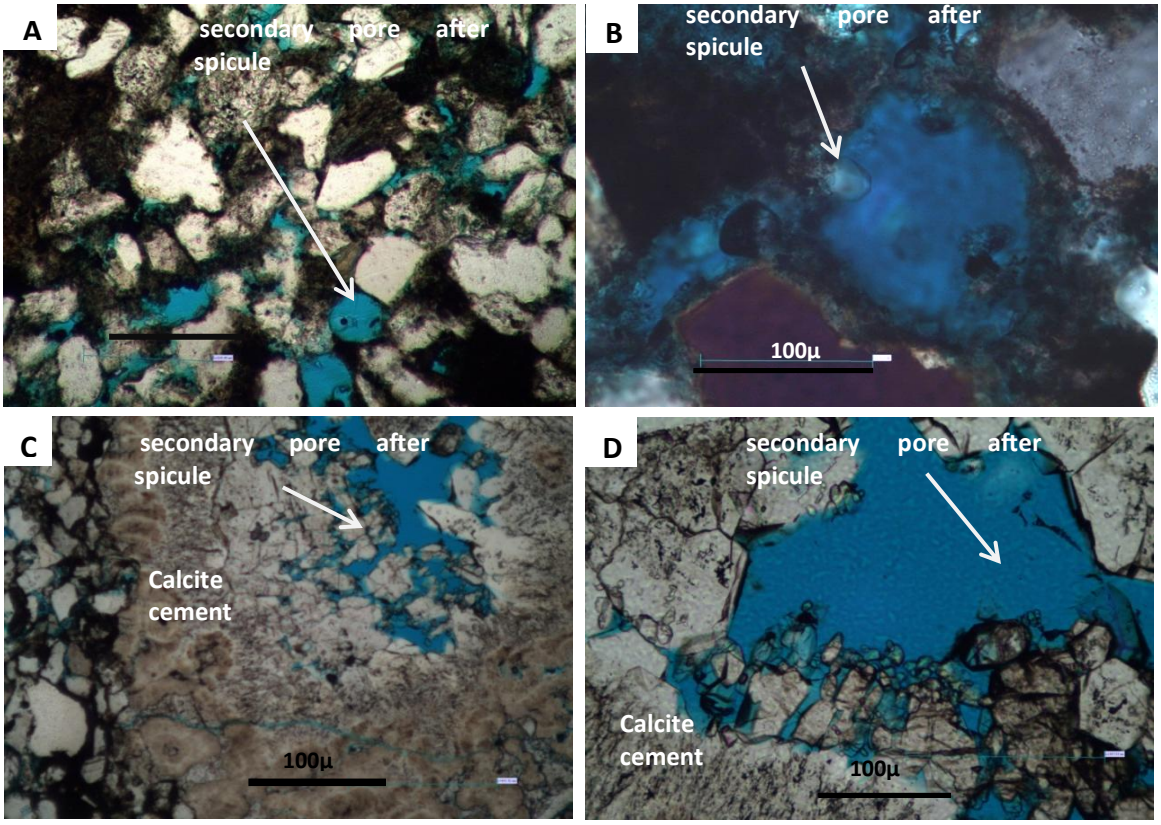

Figure 5.10 Thin section images of secondary pores after sponge spicules dissolution (arrows) (A) 1/3-9ST2 (4260mTVD), (B) 1/3-9ST2 (4241mTVD) and (C and D) 2/1-10 (4241mTVD). Note: A and B have the highest microquartz among the samples.

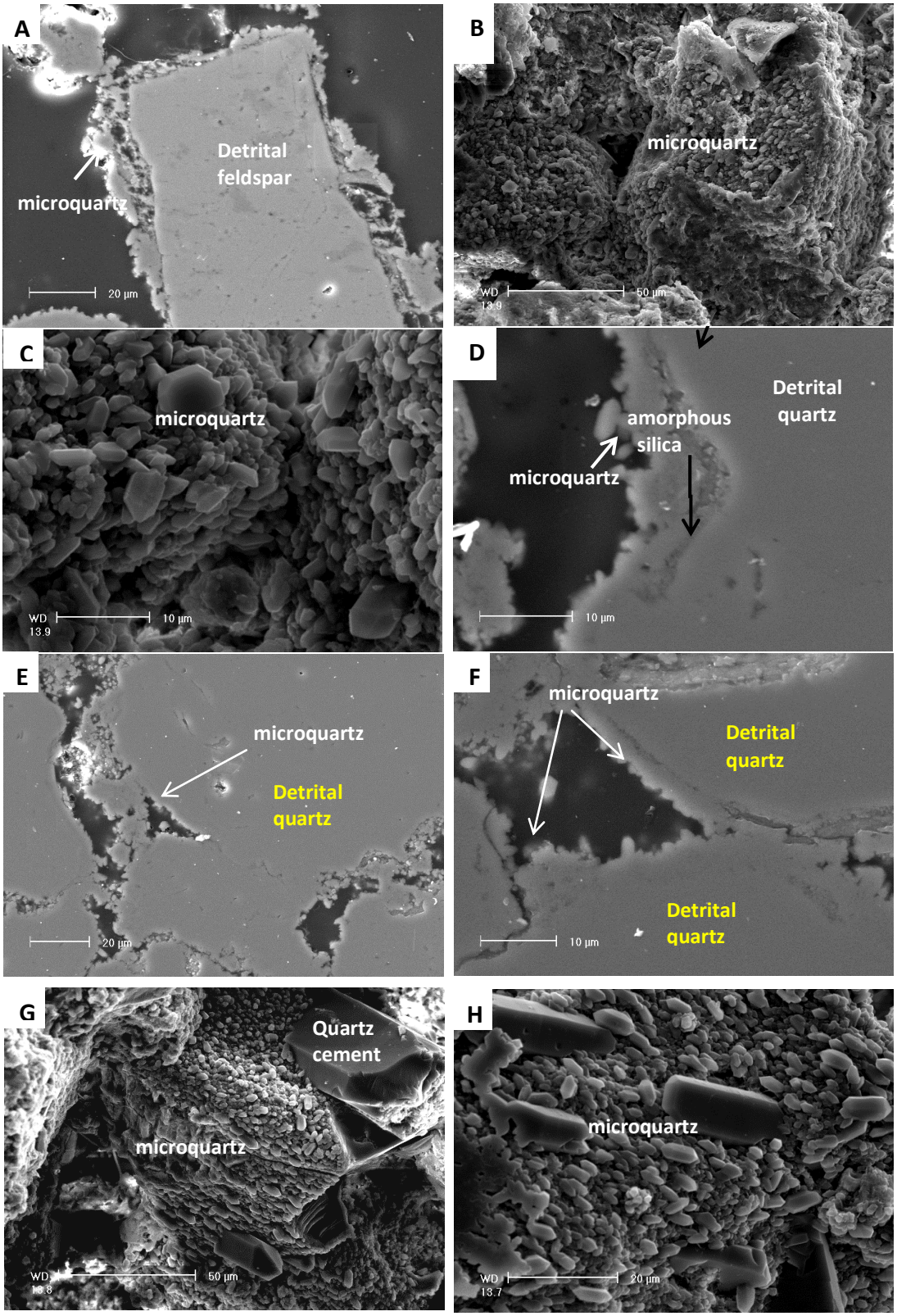

Figure 5. 11 SEM images of grain coating microcrystalline quartz cement (A) grain rimming microquartz around feldspar grain (1/9-3-ST2 4273.2) (B) thick grain coating microquartz (1/9-3-ST2 4278.45) (C) high magnification view of prismatic microquartz crystals coating grain surface in the highly porous units of the reservoir (1/9-3-ST2 4273.2) (D) grain rimming microquartz around detrital quartz grain within layer of amorphous silica (black arrow) between them (E) pore filling microquartz (1/9-3-ST2 4273.2) (F) grain rimming and pore filling microquartz 1/9-3-ST2 (G, H) high magnification view of microquartz with patch of quartz cement growing (1/9-3-ST2 4273.2). It is not known weather quartz cement is growing in areas with no microquartz or in a fracture.Note the lack of significant quartz overgrowth in all the microquartz coated samples.

Chlorite occurs as rare pore-filling aggregates. It consists of microcrystalline plates aligned perpendicular to the surface of detrital grains forming rosettes (Fig. 5.12D) often interwoven with illite and a flaky type filling pores. It is sometimes seen clearly associated with decomposing detrital feldspar and lithic grains. Chlorite is also identified from XRD analysis by the two typical prominent peaks (14Å and 7Å; Figs. 5.14A and B).

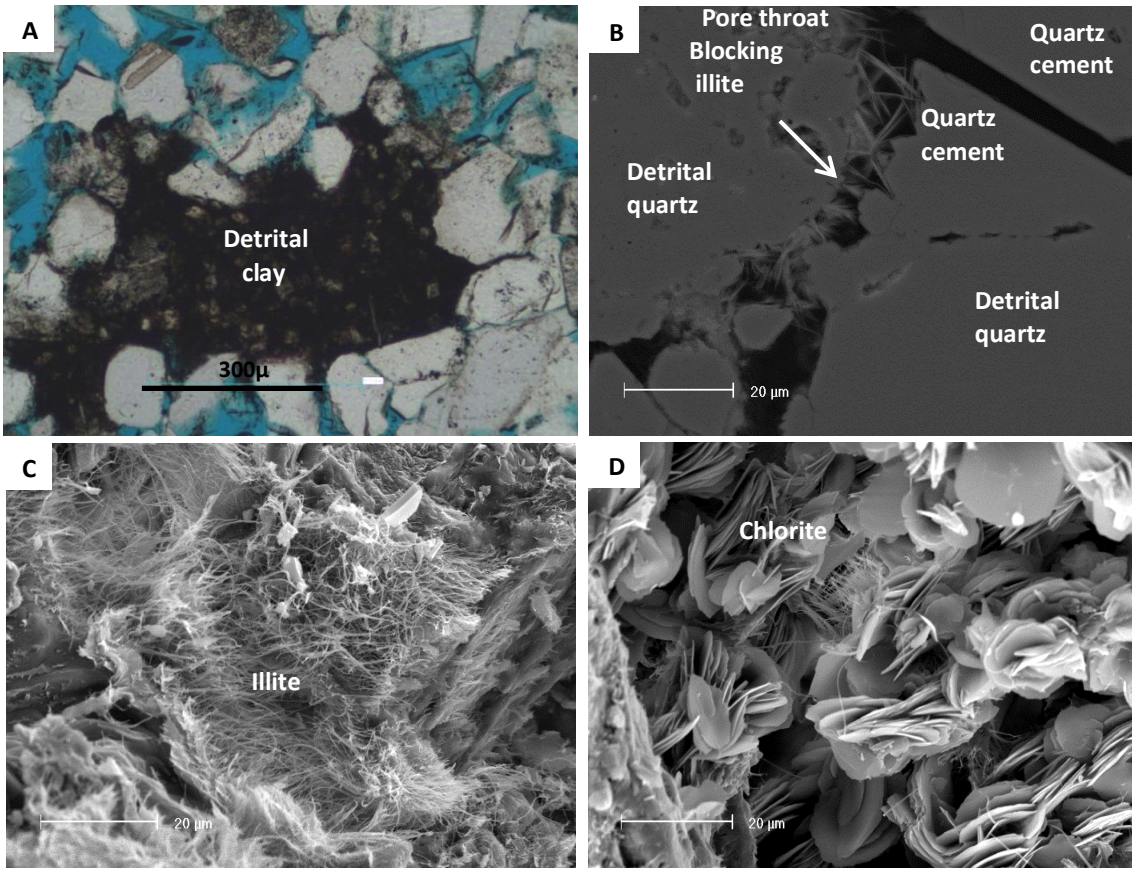

Figure 5.12 Thin section and SEM images of detrital clay and illite and chlorite cement1 (A) detrital clay matrix (well 1/3-3 3452m TVD) (B) SEM image showing pore throat blocking illite 1/3-9ST2 (4243) (C) SEM image showing high magnification view of pore filling fibrous illite 1/3-9ST2 (4260mTVD) (D) SEM image showing high magnification view pore filling chlorite 1/3-9ST2 (4260mTVD). The pore-filling clays have no significant effect on porosity but reduce permeability considerably.

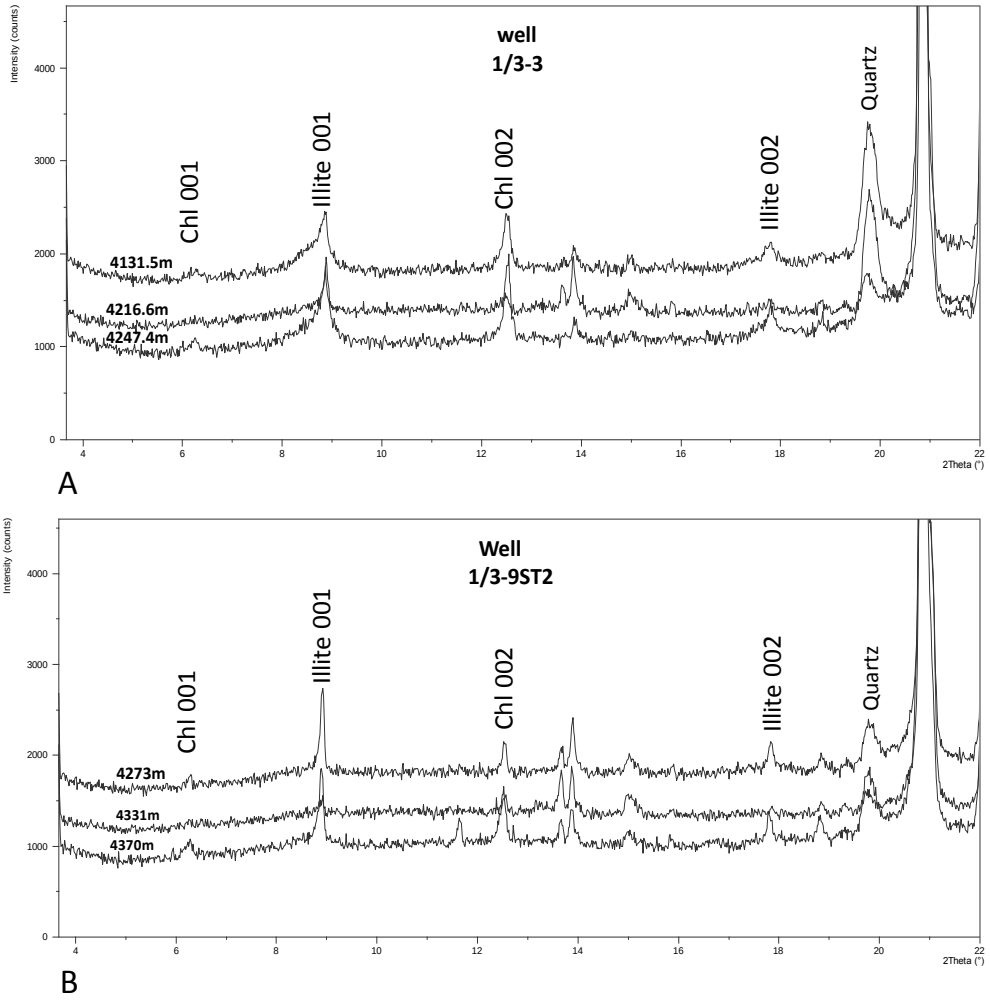

Figure 5.13 XRD patterns of whole rock samples from different wells at different depths. The signatures show that the dominant clay minerals are chlorite and illite.

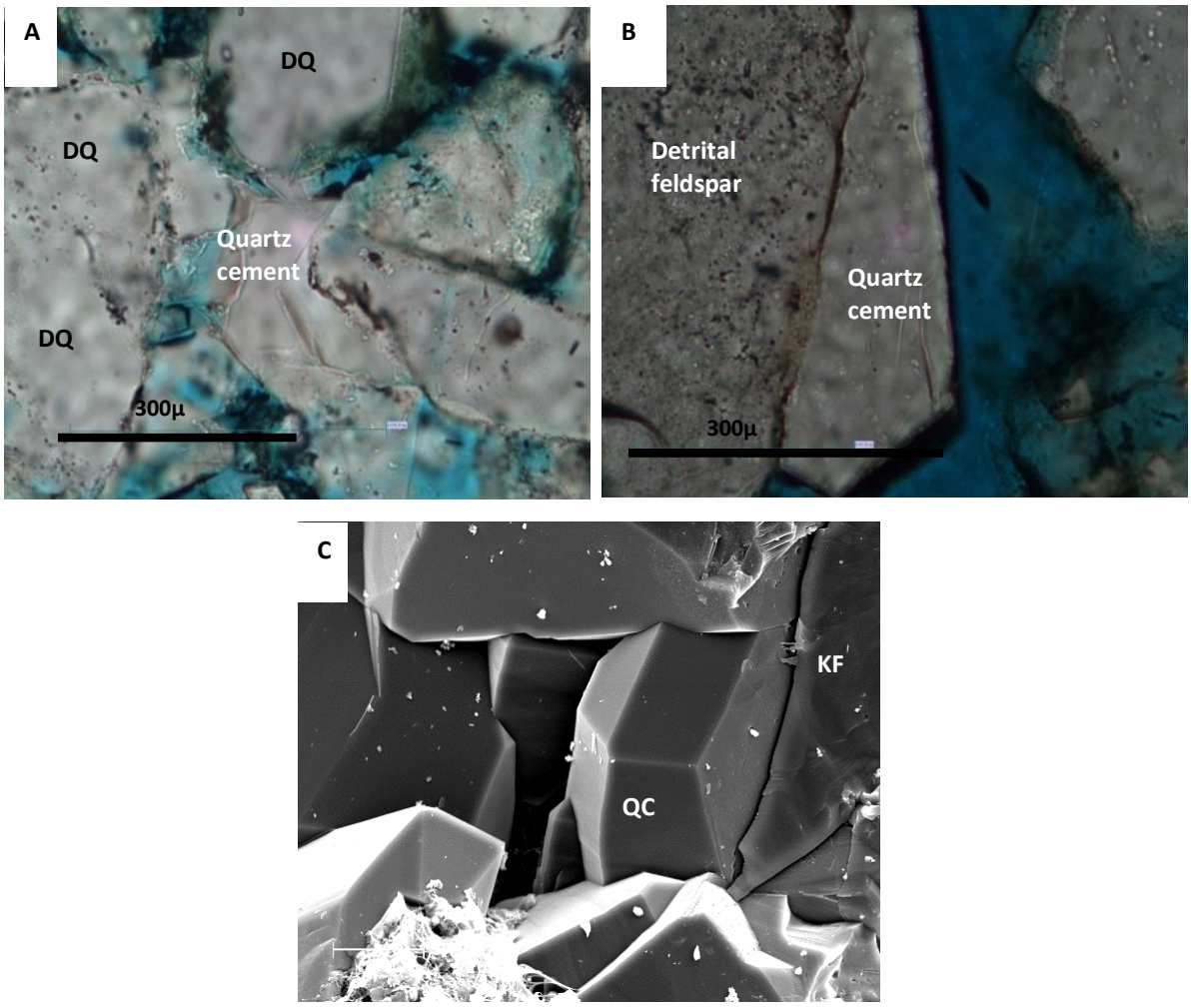

Figure 5.14 Thin section and SEM images of quartz cements (A) Plane polarized image showing quartz cements occluding pores well 2/1-10 (4226mTVD) (B) quartz cements with euhedral outlines growing around detrital feldspar grain 2/1-10 (4226mTVD) (C) SEM image of quartz cements 2/1-10 (4226mTVD). Note the lack of microquartz on the quartz cement. Key: Quartz cement (QC) K-feldspar cement (KF).

Quartz cement in the Tambar field occurs as overgrowth and, less commonly, as prismatic outgrowth (Fig. 5.11A). It has average of 2% by volume across the field but locally it is abundant and pervasive and completely block pores (Figs. 5.7B, 5.14, 5.15). It is largely absent in the microcrystalline quartz coated samples. However, patches of quartz cement (Fig. 5.13B) are locally found growing on top of the microcrystalline quartz. There is no clear relationship between quartz overgrowth abundance and depth where microquartz is not involved. The only substrate that authigenic quartz cement grows on in the Tambar field is detrital quartz and feldspar. Overgrowths are typically 15 to 30µm thick with euhedral terminations. SEM-CL was used to look for zonation of the quartz cement after (Hogg et al., 1992). No zonation was observed (Fig. 5.15) suggesting either continuous growth under constant water chemistry conditions and at a similar rate or one phase of growth. Quartz grain fracturing is apparent in some grains under CL examination (Fig 5.15B). Quartz overgrowths enclosed illite, chlorite and feldspar cements. Thin dust rims or fluid inclusions commonly separate the quartz overgrowth from the detrital grain.

Dolomite occurs as either 100 to 200µm long rhombs growing into pores space, clusters of rhombs that have grown together to fill the pore space (Fig. 5.16) or pervasively replacing other minerals. Dolomite cement is commonly observed enclosing quartz and feldspar cements. Dolomite crystals commonly have a non-ferroan core and become increasingly ferroan towards their outer margins (Fig. 5.16C). In some cases the non-ferroan cores look as if they are partially resorbed having rounded embayments. This suggests two distinct phases of dolomite separated by a dolomite partial dissolution event.

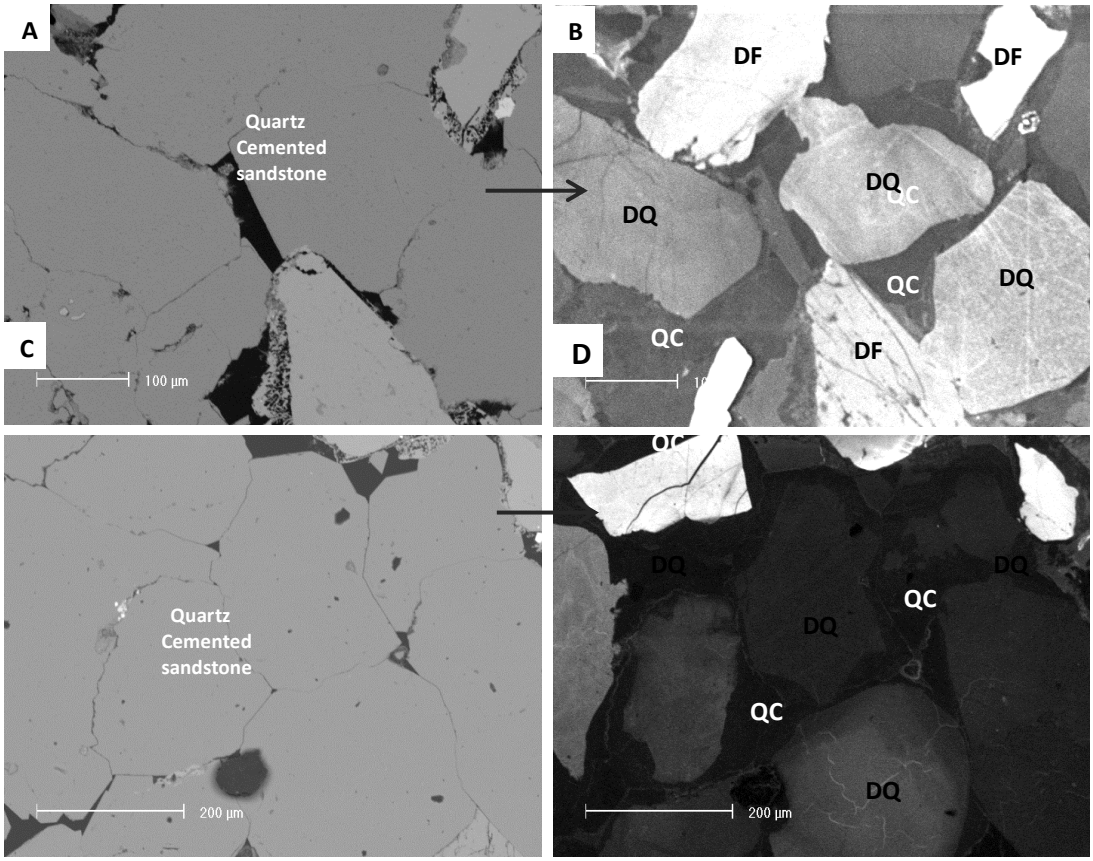

Figure 5.15 BSEM and SEM-CL images of quartz cemented sandstone (A 2/1-10 (4226mTVD and C) BSEM images of quartz cemented sandstone (B and D) CL images distinguishing detrital quartz and authigenic quartz cement (same as A and C). Key: detrital quartz (DQ) detrital feldspar (DF) feldspar cement (FC) quartz cements (QC) 2/1-10 (4226mTVD.

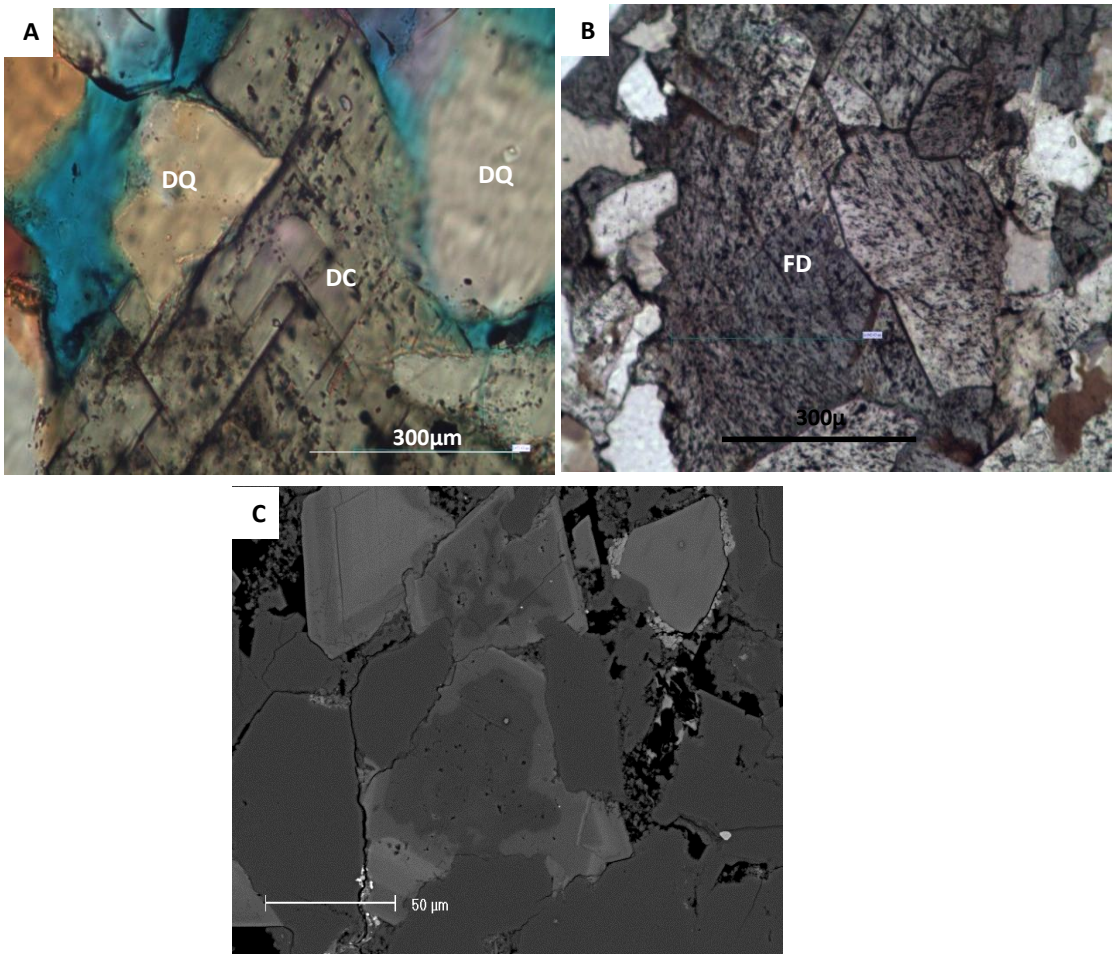

Figure 5.16 Thin section images of dolomite cements. (A) plane polar image of replacive dolomite cement 1/3-3 (4221mTVD) (B) late ferroan dolomite replacing grains and cements well 1/3-3 (4241mTVD) (C) SEM image showing zoning in dolomite cement becoming more ferroan toward the outer edge 1/3-3 (4221mTVD). DQ detrital quartz DC diagenetic dolomite FD ferroan dolomite.

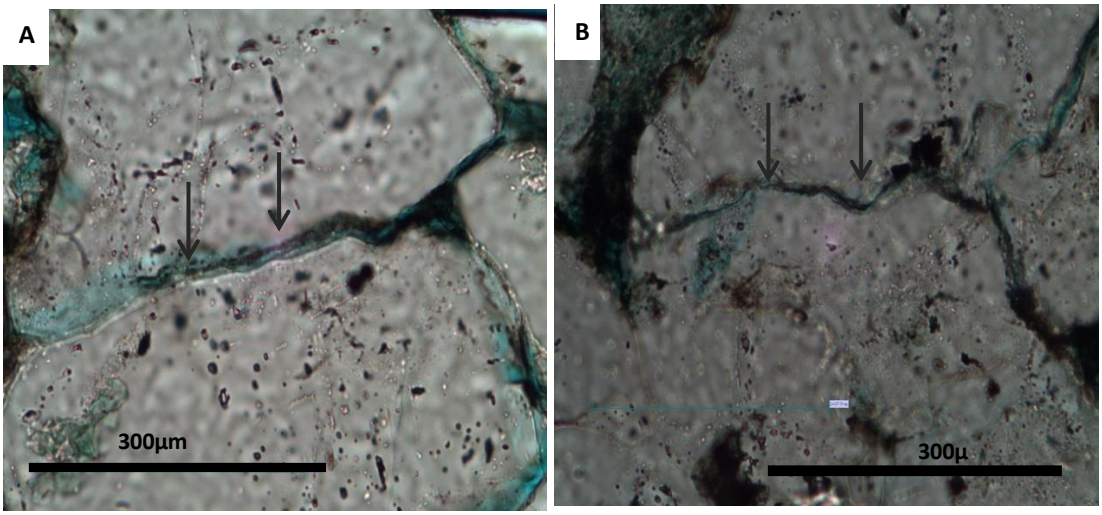

Figure 5.17 Thin section plane-polarized images of long sutured contact (arrow) between quartz grains illustrating the effects of pressure solution (A) well 1/3-9ST2 (4177mTVD).

5.5.4 Porosity and compaction

Porosity of the Tambar reservoir sandstone is both primary intergranular and secondary dissolution types of varying sizes. Core analysis (total) porosity varies from 5% to 26% with an average of 14 ± 1.5% for the Ula Formation from Tambar. Point count intergranular porosity is up to 16 ± 1.8% and the moldic porosity is up to 7%. Moldic porosity has developed by partial or total dissolution of coarse and fine grains of detrital feldspar, sponge spicules, rock fragments, detrital mud and feldspar cements. Dissolved mica grains locally show intragranular porosity and been expanded into open pores making pseudomatrix. The primary pores are affected by compaction and precipitation of authigenic quartz cements and clays. Evidence of mechanical compaction can be seen from bending of mica grains (Fig. 5.7C), deformation of mud intraclasts and grain re-arrangement with straight grain contacts.

Secondary porosity due to dissolution of feldspar grains and cements has contributed significantly to the overall porosity of the sandstone (Fig. 5.9). Pressure solution (chemical compaction) can be observed at long sutured contacts between sand grains (Fig. 5.17).

Reservoir quality includes porosity and permeability as defined by conventional core analysis techniques (Fig. 5.25). The range of helium-derived porosity values of these sandstones is good (av. of 16.1 ± 0.8% for all samples in the petrological study). The permeability values are less good (arithmetic mean of 38mD, geometric mean of 4mD).

5.5.5 Fluid inclusion thermometry and petrology

Fluid inclusion microthermometric studies were carried out on ten samples. The inclusions are generally small (Fig. 5.18) ranging from 4 to 15μm with vapour to liquid ratio of 1:10 to 1:4. Only fluid inclusions within quartz cement and at quartz cement-quartz grain boundaries were measured.

Both aqueous and petroleum inclusions (Fig. 5.18C) were found. All aqueous inclusions contained two phase (liquid and vapour) and displayed homogenization temperatures between 120 and 168°C (Fig. 5.19). The aqueous inclusions are unimodal with the vast majority of values between 150 and 160°C. Oil inclusions were found in three out of ten samples but were relatively rare even in these samples. The oil inclusions show lower homogenization temperature (120 to 145°C) than aqueous inclusions. The properties of the six samples illustrated in Figure 5.19 are given in Table 5.2.

From the last ice melting temperature, the formation water salinity for the Tambar reservoir sandstone range from 0.5 to 18 wt. % NaCl equivalent (Fig. 5.20) which is much higher than the salinity of the (marine) waters in which these were deposited (3.5 wt. % NaCl).

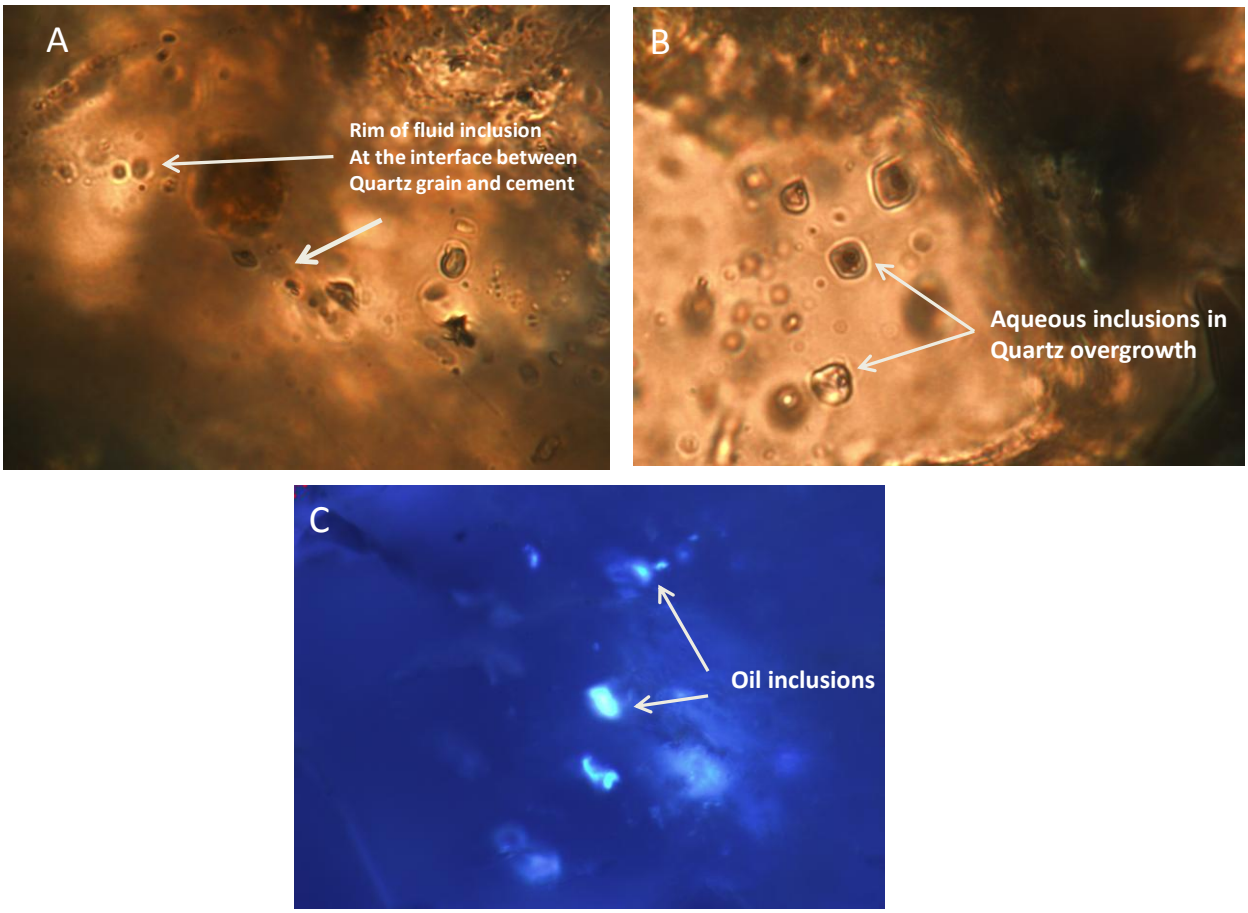

Figure 5.18 Photomicrograph of fluid inclusions (A) rim of fluid inclusions bounding detrital quartz grain and authigenic quartz overgrowth (B) fluid inclusions within quartz overgrowth (C) petroleum inclusion in quartz overgrowth.

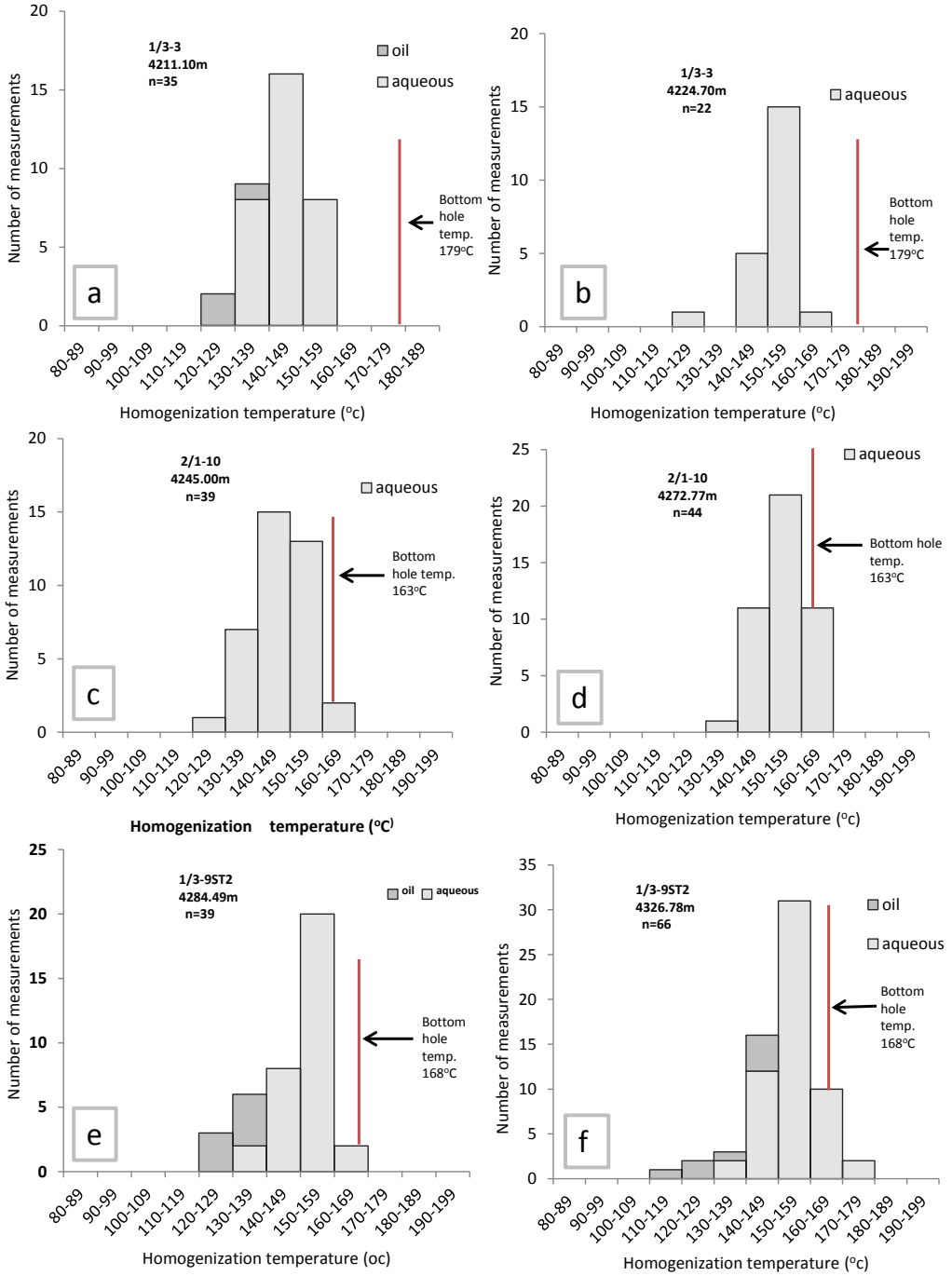

Figure 5.19 Histograms showing fluid inclusion homogenizarion temperatures measured at different depths for the oil and aquous inclusion in quartz cement and the interface between quartz grain and cement. The red vertical line show measured bottom hole temperatures. Well name, inclusion depth and number of measured inclusions are shown for each histogram.

Table 5. 2 Properties of the six fluid inclusion samples represented in Figure 20.

Well	1/3-3.	1/3-3.	2/1-10.	2/1-10.	1/3-9ST2	1/3-9ST2
Depth (m)	4211.1	4224.7	4245	4272.77	4284.49	4326.78
Inclusion	A	B	C	D	E	F
Mean grain size (µm)	119	131	229	203	117	199
Water saturation (%)	41.8	46.3	69.4	71.9	15.1	17.8
Porosity (%)	17	21	15	13	18	13
Permeability (mD)	3.33	33.5	0.09	8.8	5.3	5.7
Quartz cement (%)	1.0	3.5	4.0	7.0	<1.0	1.0

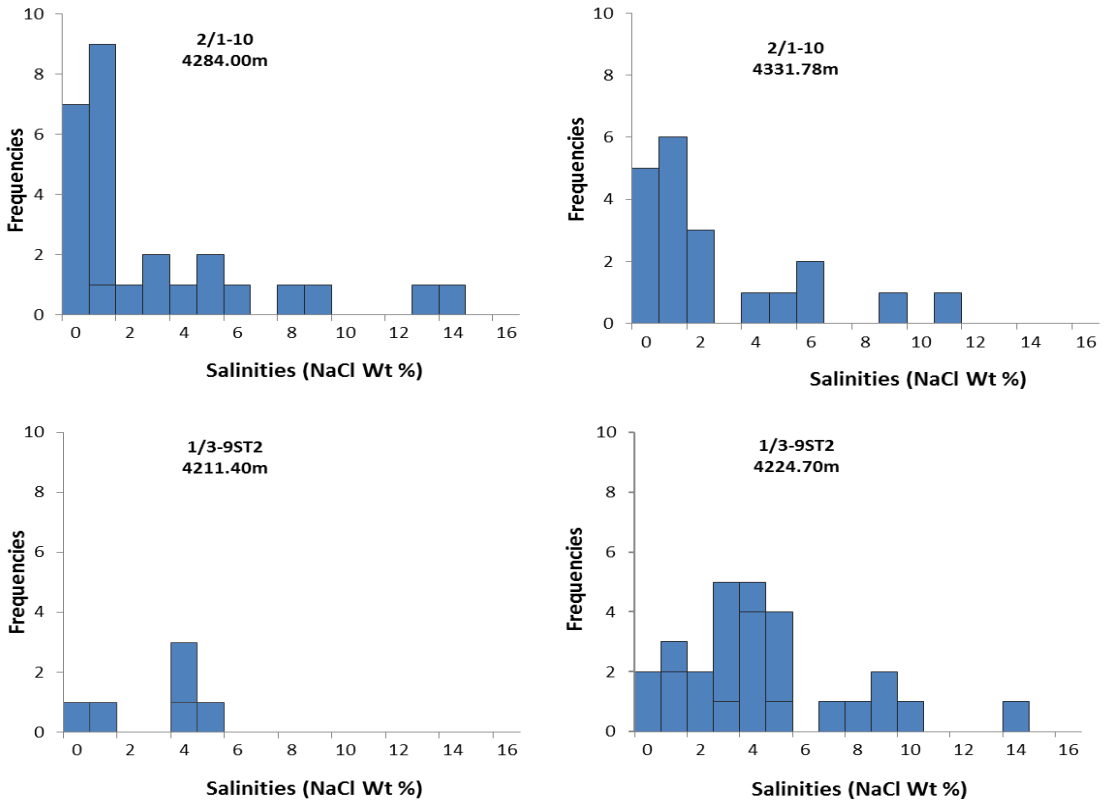

Figure 5.20 Fluid inclusion salinity plots with data derived from last ice melting temperatures from aqueous inclusions within quartz cement.

5.5.6 Stable isotope geochemistry

The $\delta^{18}O$ values of dolomite cement in the Tambar sandstone reservoir range from -11.77 to -3.57‰ PDB. There is a clear differentiation between oil and water leg samples, with the most depleted values in the water leg (Fig. 5.21A and B); Table 5.3).

The $\delta^{13}C$ values of the dolomite cement range from -5.07 to -1.12‰ PDB, with the most negative values from the high water saturations parts of the cored sections (Fig. 5.21A.

Table 5. 3 Dolomite isotopic composition of the Tambar field reservoir sandstones.

$\delta^{18}O_{dol}$ PDB	$\delta^{18}O_{dol}$ SMOW	Assumed $\delta^{18}O$water V- SMOW (after Warren and Smalley, 1994)	Interpreted temperature of growth T°K	Interpreted temperature of growth T° C	$\delta^{13}CV_{PDB}$	Depth (mDD)	fluid zone
-3.57	27.18	3.26	354.80	81.80 ± 8	-1.12	4131.5	oil
-4.72	26.00	3.26	363.36	90.36 ± 8	-1.61	4144.1	oil
-11.01	19.51	3.26	424.56	151.56 ± 8	-3.52	4224.1	water
-11.15	19.36	3.26	426.38	153.38 ± 8	-3.23	4229.7	water
-10.63	19.91	3.26	419.92	146.92 ± 8	-5.07	4215.0	water
-11.77	18.73	3.26	434.25	161.25 ±8	-3.16	4146.5	water
-11.66	18.84	3.26	432.87	159.87 ± 8	-3.96	4210.5	water
-10.35	20.19	3.26	416.66	143.66 ± 8	-3.63	4222.6	water

Present the formation water assumed to be 3.26 V-SMOW. If we assume the formation water has slightly changed over the years rising to 4.26 or reducing to 2.26 changes the temperature by ± 8^{o}C.

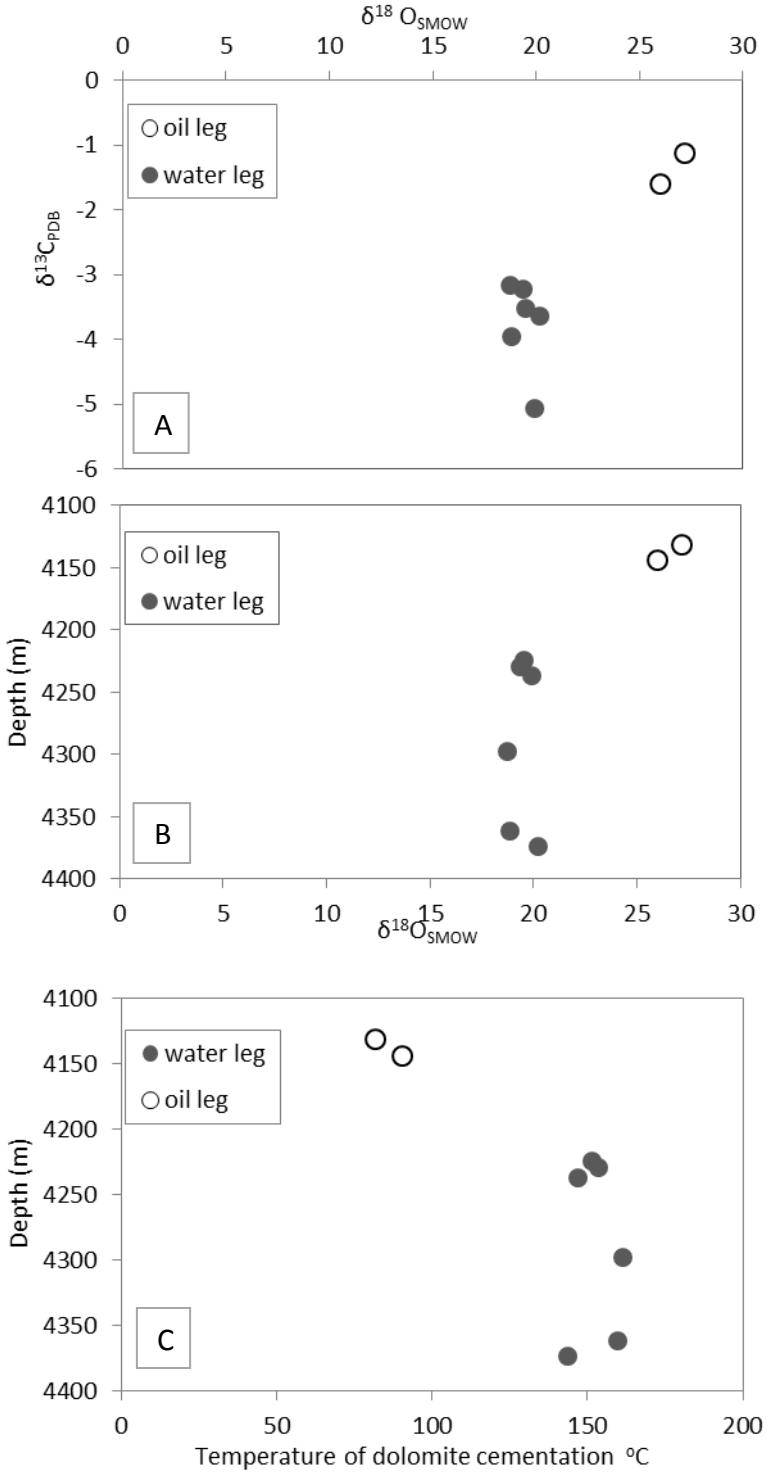

Figure 5.21 Carbon versus oxygen isotope plot for the dolomite in the Tambar rservoir sandstone (B) Oxygen isotope of the dolomite versus depth with data split by oil leg and water leg samples. (C) Interpreted temperature of growth for the dolomite in the oil leg and the water leg assuming that the formation water at the time had the same $\delta^{18}O$ as present day formation water (3.2‰ V-SMOW).

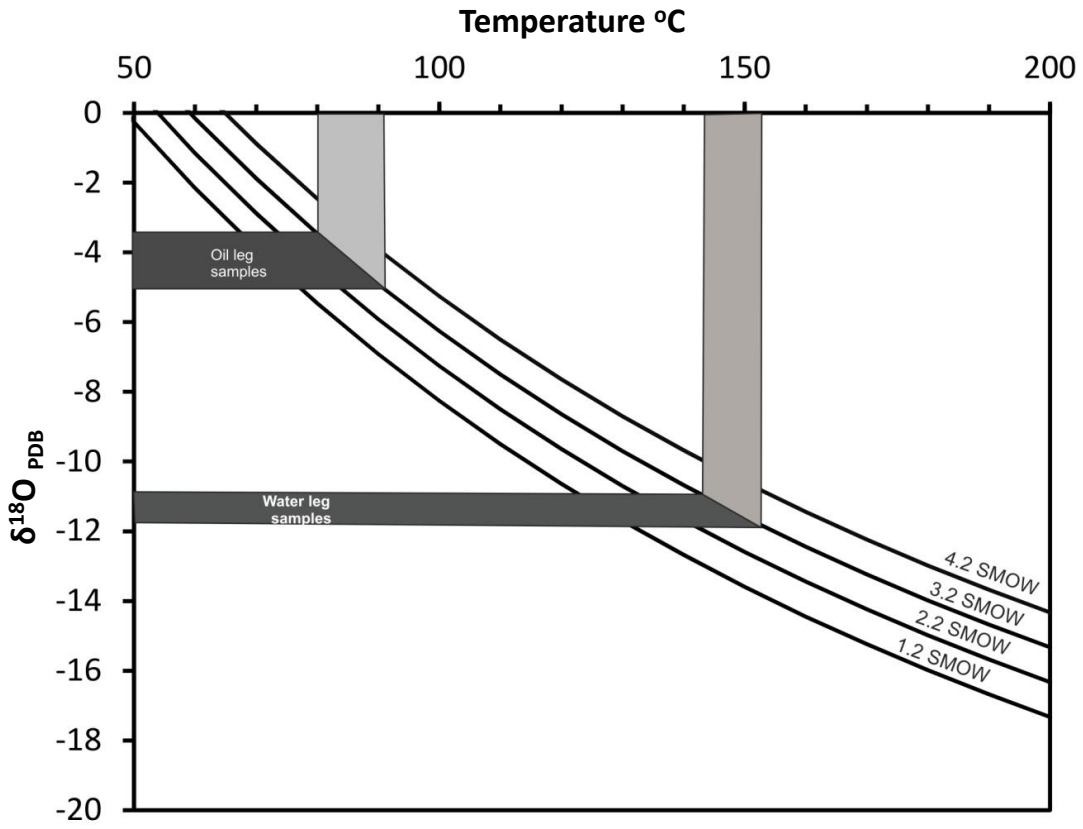

Figure 5. 22 Curves showing the relationship between the $\delta^{18}O$ of diagenetic dolomite showing possible temperatures of precipitation of the dolomites. The vertical bars the range of temperatures for samples in water leg and samples in oil leg. Estimated local marine water composition was 3.2‰ SMOW. The curves defined the range of possible water compositions from which the dolomite could have been precipitated.

5.6 Discussion

5.6.1 The most significant diagenetic mineral cements and processes in Tambar, Ula Formation

The petrographic (point count) data show that the most volumetrically-important cement is microcrystalline quartz (4.8%; Table 5.1). Quartz cement is the next most important minerals (3.2%). There are approximately equal average volumes (all close to an overall average value of 2%) of albite, K-feldspar and pore-filling illite cements. There are small but highly variable amounts of pore-filling dolomite (0.6%). Calcite either tends to be absent or totally occludes pores (representing 45% of the total rock volume). These average values mask a wide range in some of the

cements; especially quartz cement which can occupy up to 16% by volume. There are also trace quantities of chlorite and pyrite.

Intergranular volumes have been derived from the point count data and Houseknecht-type diagrams have been plotted with the data subdivided by grain size and water saturation. All samples, however, they are split, fall into the cementation-dominated portion of the diagram with cementation clearly dominating over compaction as the main control on porosity-loss (Fig. 5.23). There are no clear differences in the porosity-loss behaviour of the finest and the coarsest grained sandstones from the Ula Formation from Tambar (Fig. 5.23A). From the Houseknecht-type plots, there are also no clear differences in the porosity-loss behaviour of the most and least oil-filled sandstones (Fig. 5.23B).

The sandstones from Tambar are unusual in having such large volumes of microcrystalline quartz. In many Upper Jurassic sandstones from the North Sea Basins, micrquartz is present as a very thin grain-coating mineral representing a fraction of a percent of overall rock volume (Aase et al., 1996; Ramm et al., 1997). The mean of 4.8% from Tambar reported here is a clear exception.

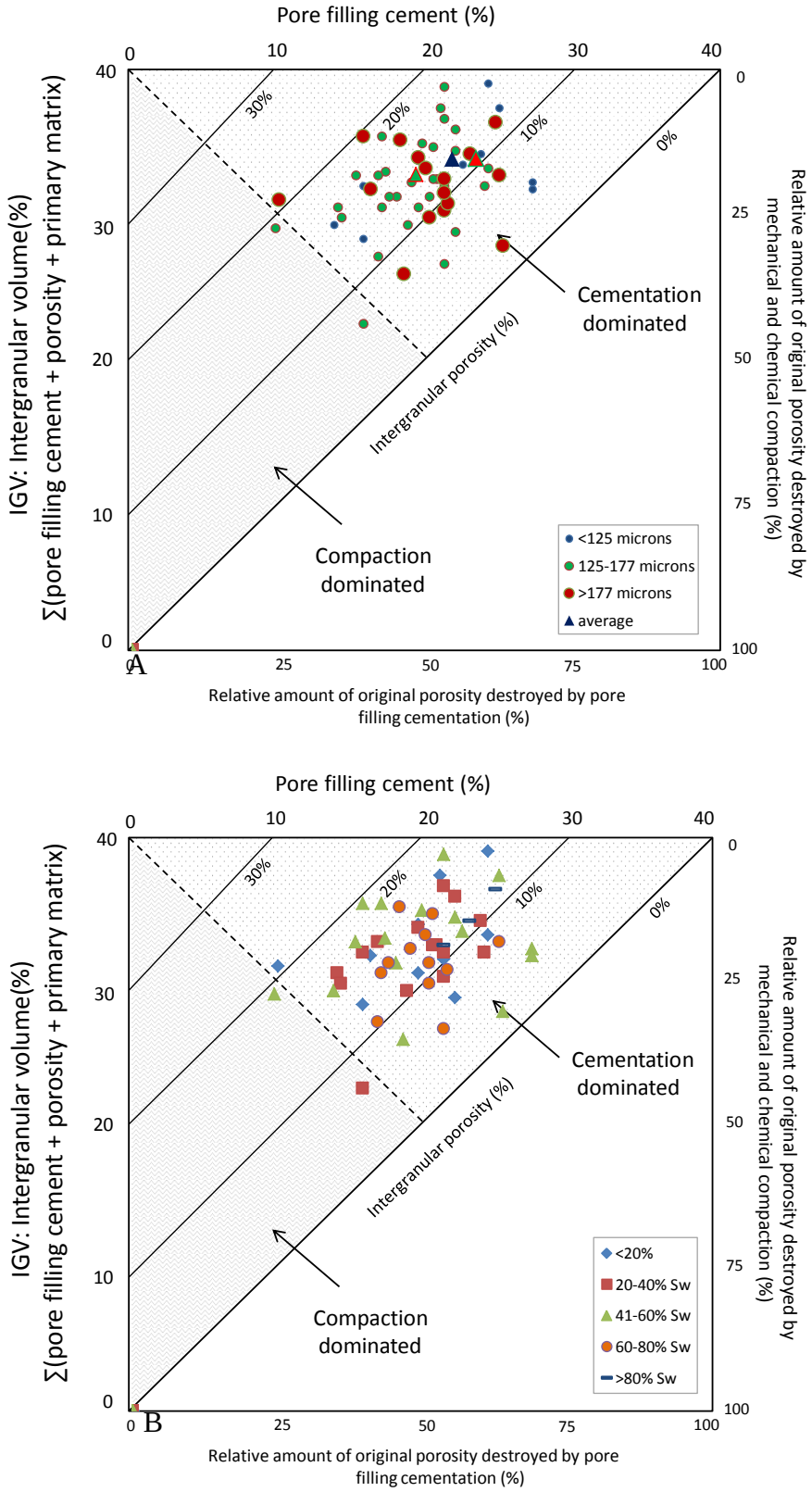

Figure 5.23 Houseknecht type plots data split by (A) grain size of sandstone (B) water saturation. There is no clear separation in porosity lost between samples of different grain size and different water saturation.

5.6.2 Sequence of mineral growth

By examining the petrographic images collected using light optics, SEI, BSEM and SEM-CL, it has been possible to deduce an overall order of mineral growth. This is represented in a paragenetic sequence (Fig. 5.24). .

A fall in relative sea level is likely to have led to a meteoric water influx with marine pore-waters flushed through the sandstone by low salinity water (Morad et al., 2010). This led to the onset of dissolution of feldspar grains evidenced by secondary intragranular pores. Microcrystalline quartz growth typically starts to happen during early diagenesis and is at an advanced stage by the time sandstones are buried to about 60°C. Microcrystalline quartz growth thus straddles the conventionally-assumed boundary between early and burial diagenesis (Worden and Burley, 2003).

Burial diagenesis involved the growth of the following cements in sequence: feldspar dissolution, K-feldspar and albite cementation, chlorite, illite, quartz and dolomite. There was almost certainly some degree of overlap between the growth of some of these cements although spatial separation of growth sites made unequivocal determination of the exact relative start and end times of cementation rather difficult. Feldspar cementation may have started in the early diagenesis regime (Bjorlykke et al., 1988) and possibly continued during the initial stages of burial diagenesis. Feldspar dissolution may also have started relatively early but continued through to burial diagenesis as revealed by the dissolution of K-feldspar cement after quartz cementation (Fig. 5.9C) as well as having secondary pores within feldspars containing illite cement (Fig. 5.9B). Illite and chlorite growth occurred at approximately the same time and overlapped with feldspar cementation and the development of microcrystalline quartz coatings. Dolomite seems to have had two growth episodes; one relatively earlier during burial diagenesis and one towards the end. The simple interpretation of the oxygen isotope data corroborate this (Fig. 5.21C) with the main growth of dolomite found in the oil leg occurring at about 80 ± 8 to 90 ± 8°C and the dominant phase of dolomite growth or recrystallization in the water leg occurring at about 145 ± 8 to 160 ± 8°C. Dolomite cement became increasingly Fe-rich as diagenesis progressed (Fig. 5.16C). The relative lack of oil inclusions within quartz cement suggests that much quartz cementation occurred

before oil-filling had started. The few oil inclusions found in the three out of ten fluid inclusion wafers (Fig. 5.18) suggests that oil-filling happened towards the end of quartz cementation. The differences in the carbon and oxygen isotope values of the dolomite above and below the oil-water contact (Table 5.3, Fig. 5.21) suggest that oil-filling had a major impact on dolomite diagenesis.

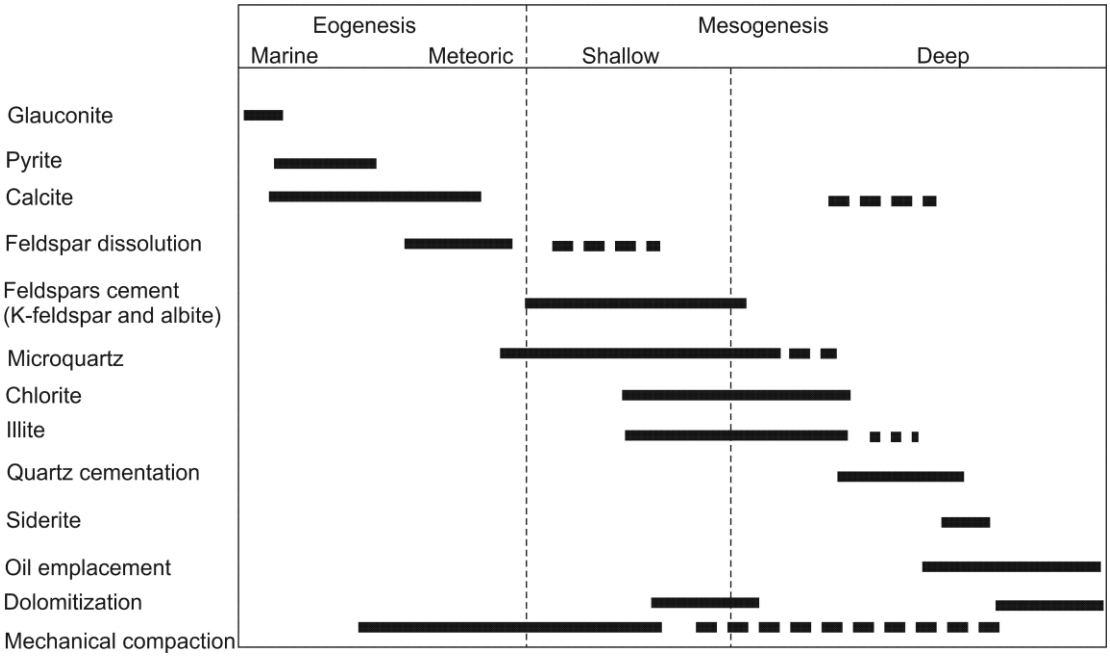

Figure 5.24 Simplified paragenetic sequence of the diagenetic processes in the Tambar reservoir sandstones. Eogenetic processes include formation of calcite, pyrite and dissolution of feldspars. Mesogenetic events include precipitation of microquartz, illite, chlorite quartz overgrowth and ferroan dolomite.

The aqueous inclusions from quartz cements show a minimum temperature of about 130°C with a mode of about 140 to 150°C (Fig. 5.19). This represents an unusually high minimum temperature for quartz cementation, conventionally assumed to commence at about 80 to 100°C and reach its peak at about 120°C (Walderhaug, 1994; Walderhaug et al., 2000). From the thermal history (Fig. 5.3), it is possible to conclude that quartz cementation started at about 30Ma. The high initiation temperature suggests something has inhibited quartz cement growth.

5.6.3 Sources of mineral cements

Eogenesis (early diagenesis) has been defined as those processes that occur when sediment is close to the surface and in communication with surface-supplied oxygenated water (Burley, 1984), equivalent to burial depth of <2000 m and temperature of <70^{o}C. Calcite and pyrite are early diagenetic cements in the Ula Formation at Tambar. Calcite tends to totally block porosity where present (45% by volume of the rock) and therefore grew before any significant compaction had occurred. Bioclastic fragments are present in a few samples (Fig. 5.8B) suggesting that the calcite cement was sourced by dissolution and reprecipitation of shelly material co-deposited with the sediment. Pyrite cement is very common in marine sandstones. It occurs as framboids, typically of a bacterial sulphate reduction origin but is also locally recrystallized into clusters of bipyramidal (euhedral) crystals (Fig 5.8D). The sulphide was probably sourced from reduced marine aqueous sulphate and the iron was probably supplied by the clastic sediments.

Microcrystalline quartz is a relatively early diagenetic mineral that coated sand grain surfaces (quartz grains and feldspar grains alike, Figs. 5.11A and 5.D) and was probably supplied by the dissolution of amorphous silica sponge spicules. Upper Jurassic sponges were siliceous (i.e. composed of amorphous opaline silica) and their bioclastic fragments tended to be composed of sand-grade material. Upper Jurassic marine sandstones in the North Sea basins commonly contained sponge spicules when they were deposited (Aase et al., 1996; Aase and Walderhaug, 2005; Jahren and Ramm, 2000; Ramm, 1992; Ramm et al., 1997; Stokkendal et al., 2009; Vagle et al., 1994; Weibel et al., 2010). There are sand grain-sized dissolution voids (secondary pores) in the Ula Formation at Tambar that are surrounded by microcrystalline quartz that are almost certainly the remnants of these spicules (Figs. 5.10A and B). There are also pores filled with clumps of microcrystalline quartz crystals (containing microporosity) that may represent the remnants of recrystallized sponge spicules (Fig. 5.11E). The generalised diagenetic sequence of amorphous silica diagenesis is: opal-A (biogenic silica) transforms to disordered opal-TC, which in turn transforms to ordered opal-CT and cryptocrystalline quartz or chalcedony which then finally is replaced by microcrystalline quartz (Williams and Crerar, 1985; Williams et al., 1985). The presence of a potentially amorphous silica film of <1µm

between microcrystalline quartz crystal and detrital quartz grains (Fig. 5.11D) suggests that the Tambar reservoir sandstone followed this processes with the amorphous silica being supplied by sponge spicule dissolution and local reprecipitation.

Feldspar cement was likely sourced by reactions involving the large volume (Fig. 5.6) of detrital feldspars. Feldspar-feldspar pressure solution may have occurred as might simple dissolution of metastable forms of feldspar (in terms of crystallography and/or mineral chemistry) followed by growth of more stable forms of feldspar (Schmid et al., 2004). Pore-filling and replacive illite cement, and the less volumetrically-significant chlorite, grew before quartz and overlapped with feldspar and microcrystalline quartz. Illite was probably sourced from feldspar alteration reactions (Barclay and Worden, 2000; Worden and Morad, 2003). The source of chlorite is not certain but it may have been generated by alteration of pre-existing Fe minerals (pyrite, glauconite).

Dolomite cement has a range of $\delta^{13}C$ values (Fig. 5.21A). The high values are similar to those of Jurassic marine bioclastic carbonates (Veizer et al., 1999) suggesting that the dolomite is at least partly the result of dissolution and precipitation of primary bioclastic grains. The low values suggest that there has been an influx of light carbon during diagenesis. Note that the high $\delta^{13}C$ values correspond to lower temperature growth than the low $\delta^{13}C$ values (Fig. 5.21C), as interpreted from the dolomite $\delta^{18}O$ values. The pattern of evolution to progressively lower $\delta^{13}C$ values at progressively higher diagenetic temperatures is commonly reported. There are a number of possible sources of isotopically light carbon during deep burial diagenesis with the most likely being CO_2 (or organic acid precursors) driven from petroleum source rocks (Macaulay et al., 1998). The distribution of $\delta^{13}C$ values (high in the oil leg, lower in the water leg) suggests that the supply of isotopically-distinct carbonate after oil emplacement was inhibited in the oil leg relative to the water leg. Table 5.1 also suggests that oil leg samples have less pore-filling dolomite than water leg samples.

The present day formation water from nearby Ula Field (same reservoir age, same detrital mineralogy, same stratigraphy, similar thermal and filling history) has a $\delta^{18}O$

value of 3.26‰ V-SMOW (Oxtoby, 1994). If Ula and Tambar are assumed to have the same type of formation water then it is possible to derive the temperature of dolomite growth using the appropriate isotope fractionation equations (Fig. 5.22) (Land, 1983; O'Neil and Epstein, 1966). Dolomite in the water leg grew, or recrystallized, at close to the present day temperature while dolomite in the oil leg appears to have grown at a significantly lower temperature, possibly before oil entered the reservoir (Fig. 5.21C).

Quartz cement, in many deeply buried sandstones the most volumetrically important cement, has a number of potential sources (Kraishan et al., 2000). The growth of quartz cement commenced at relatively high temperatures (Fig. 5.19) suggesting that sources such as smectite alteration reactions were not important. Some quartz cement may have been sourced by pressure solution, although note that intergranular volumes and porosity-loss is cementation controlled not compaction controlled (Fig. 5.23) and that stylolites are not common features of these sandstones but long and sutured interpenetrating grains (micro-stylolites) contacts are present (Fig. 5.17). Quartz grain have flattened margins against mica flakes suggesting minor local quartz dissolution (Oelkers et al., 1996). Feldspar decay reactions may have contributed to the supply of silica (Fig. 5.8). Quartz cement may have been sourced partly by the dissolution and reprecipitation of more fine-grained forms of quartz by an Ostwald ripening process (Chang and Yortsos, 1994); for example the spongey masses of microcrystalline quartz that are so common in these sandstones (Fig. 5.11D).

5.6.4 Main controls on reservoir quality

The diagrams of intergranular volume (IGV) versus the volume of pore-filling cements (also known as Houseknecht diagrams) (Fig. 5.23), demonstrate that the Ula Formation at Tambar is cementation, as opposed to compaction, dominated. These rocks have undergone relatively little compaction but much cementation by: microcrystalline quartz, quartz overgrowths, illite, dolomite, albite, K-feldspar etc.

In essence then, these sandstones have retained fairly good porosity even at a depth of burial >4000m and temperatures in excess of 160°C, they have undergone

relatively little compaction (Fig. 5.23) but they do not have especially good permeability. The controls on reservoir quality will now be examined in detail.

Grain size can have an important effect on permeability since small grains lead to narrow pore throats (Bryant et al., 1993; Cade et al., 1994; Evans et al., 1997). The data from Tambar have been subdivided by depositional grain size into three classes (<125 μm (very-fine), 125-177 μm (lower fine) and >177 μm (upper fine) and plotted on separate conventional linear porosity-log permeability diagrams (Fig. 5.25). The data have also been grouped together (Fig. 5.26) revealing that there is a subtle separation of the grain size classes. The coarser sandstones plot to the left of the finer grained sandstones and so seem to have slightly higher permeability for a given porosity than the finer grained sandstones. It is also noteworthy that the 125-177 μm grain size class (lower fine sand) has a cluster of points at >100mD suggesting that the very best reservoir quality is found in these lower fine sandstones. Sorting does not seem to play a major role in defining porosity-permeability variations in the Ula Formation at Tambar (Fig. 5.26B).

The total amount of clay minerals in sandstones can have a major effect on sandstone reservoir quality with more clay usually having a relatively small effect on porosity but a major detrimental effect on permeability (Worden and Morad, 2003). The core data have been subdivided on the basis of <4%, 4-8% and >8% total clay (Fig. 5.26C). Difference in the volume of clay content did not significantly affect the reservoir quality.

Quartz cement is volumetrically the second most important cement in Tambar. The porosity-permeability data have thus been divided on the basis of less than and greater than 5% quartz cement (Fig. 5.26D). The quartz cement-rich sandstones plot to the left of the diagram and so seem to have slightly higher permeability for a given porosity than the more quartz cement-poor sandstones.

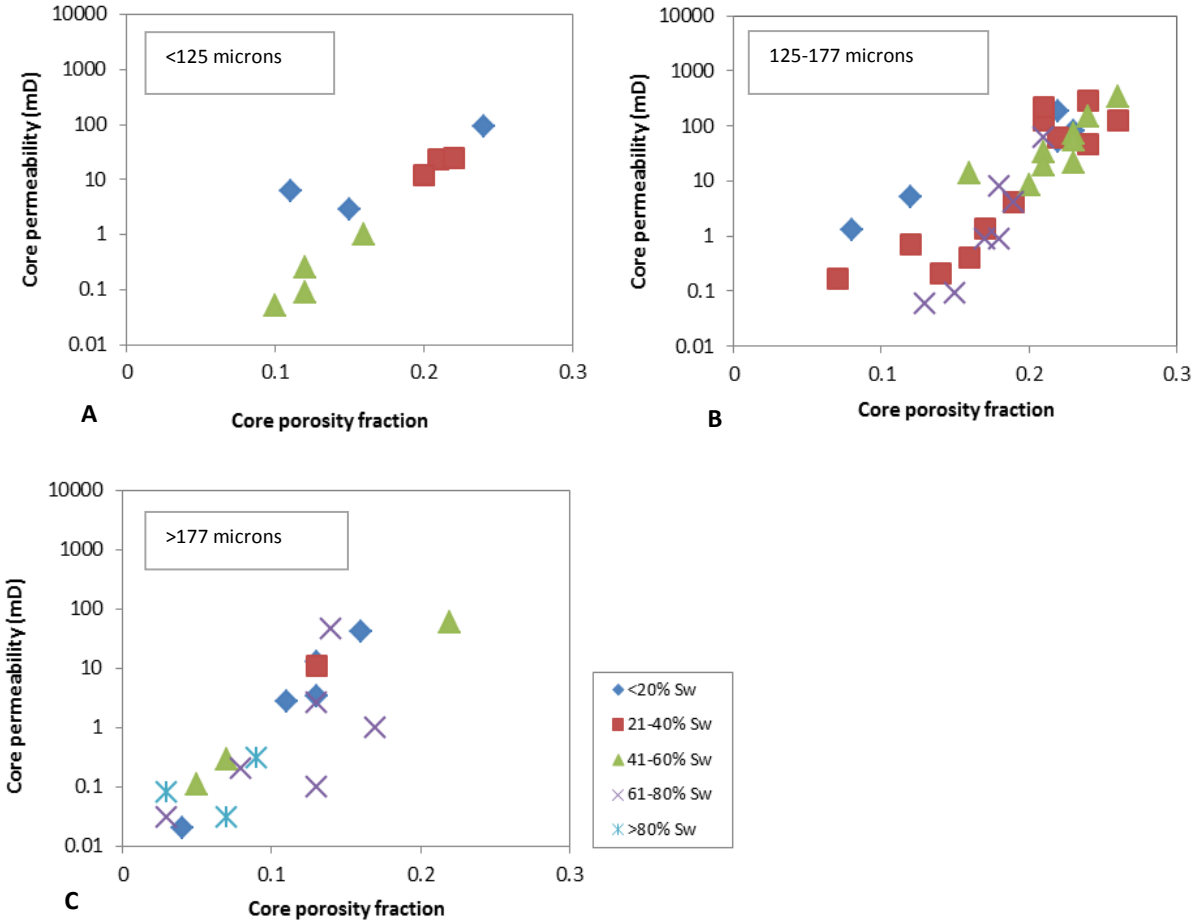

Figure 5.25 Core analysis porosity versus permeability for the three defined grain size ranges from the Ula Formation in the Tambar oil field split by water saturation. These show that 125 - 177µm grain size class show the higher porosity and permeability.

Dolomite cement is present in small amounts in most samples so that the core analysis data have been subdivided on the basis of <1%, between 1 and 3% and >3% dolomite cement (Fig. 5.27A). The samples with low and intermediate amounts of dolomite sit to the left of the data.

Microcrystalline quartz is the most volumetrically important of all the cements in Tambar. The core analysis data have been subdivided on the basis of <5 and >5% microcrystalline quartz cement (Fig. 5.27B). The core analysis data do not split in any discernible pattern on the basis of the amount of microcrystalline quartz.

The effect of the addition of oil on diagenesis remains controversial (Bjorkum et al., 1998; Bloch et al., 2002; Worden et al., 1998). The timing of oil emplacement relative to the time of diagenesis is crucially important though seldom recognized

(Molenaar et al., 2007). Nonetheless, the core analysis data have been split by water saturation (using wireline log derived Sw values) (Fig. 5.27C). The core analysis data do not split in any discernible pattern on the basis of the amount of oil versus water presently in the core. To test the role of oil and water saturation specifically on the amount of quartz cement, the petrographically determined amounts of quartz cement have been plotted against water saturation, split by grain size (Fig. 5.28). The very fine and lower fine sandstones show no systematic variation. The upper fine sands (>177μm) have the greatest amount of quartz cement (greater than 10%) only in samples with less than 30% oil saturation (Fig. 5.28C); samples with higher saturations tend to have less quartz cement. To further investigate the relationship between quartz cement and water saturation, the petrographic and wireline data have been combined plotting quartz cement volume versus microcrystalline cement volume with data split first by water saturation and then grain size (Figs. 5.29A and B). As well as the absolute amount of microcrystalline quartz it is possible to plot the average degree of grain coating by microcrystalline quartz (that is: what percentages of grains have a coating of microcrystalline quartz in each sample). Thus the petrographic and wireline data have been combined differently plotting quartz cement volume versus the degree by which grains are coated with microcrystalline quartz with the data again split first by water saturation and then grain size (Figs. 5.29C and D). Quartz cement is most abundant in the coarser sandstones (upper fine class) with the highest water saturations. Where sand grains have more than 50% coated with microcrystalline quartz, the quartz cement volume is <4%. The degree by which grains are coated with microcrystalline quartz looks as a better diagnostic of the amount of quartz cement than the absolute quantity of microcrystalline quartz.

The total amounts of clay and pore-filling dolomite have been separately plotted against porosity and permeability (Fig. 5.30). There are no clear or simple correlations, presumably because these are subordinate to other controls (grain size, microcrystalline quartz, quartz cement etc). The total amount of feldspar cement has also been plotted against porosity, split by well and by water saturation (Fig. 5.31). Feldspar cement volumes do not seem to have exerted a primary control on porosity

and the amount of feldspar cement does not seem to be reflected in the water saturation values.

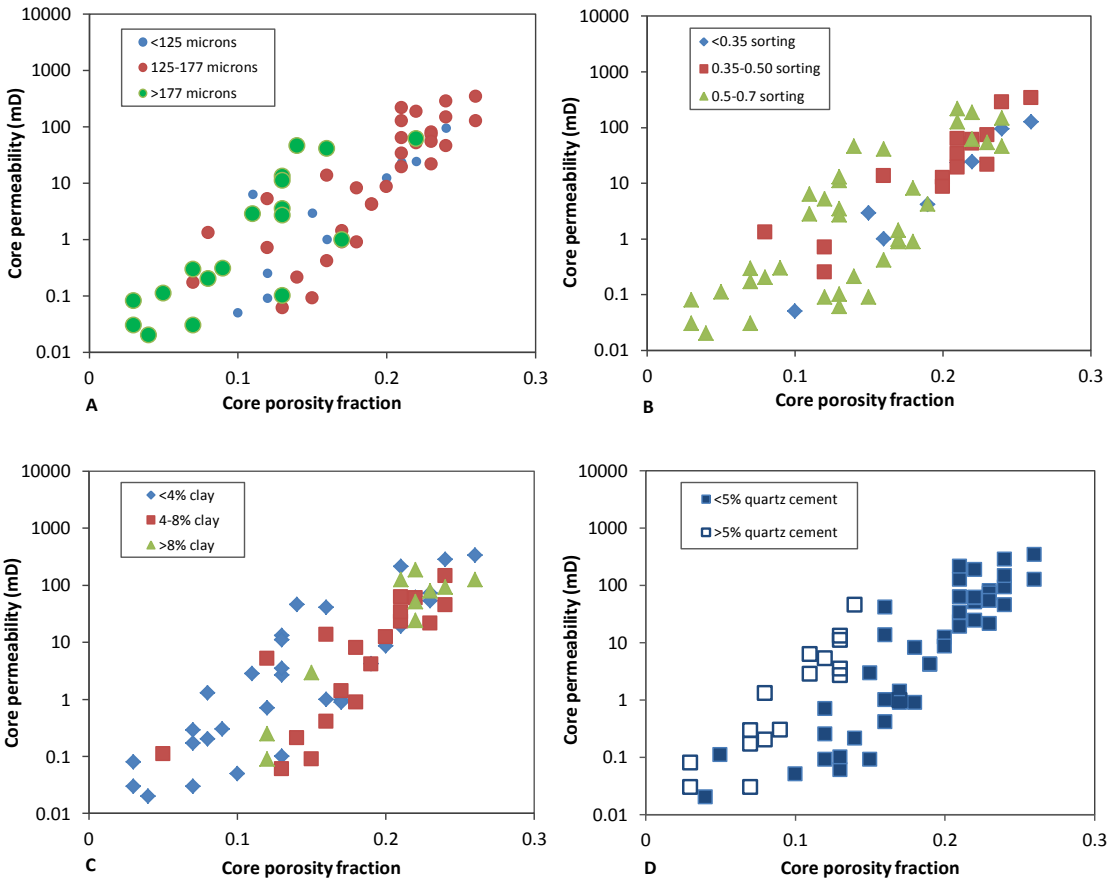

Figure 5.26 Core analysis porosity versus permeability with data split by (A) grain size, (B) the degree of sorting (C) the total amount of clay minerals, (D) the amount of quartz cement showing samples with higher quartz cements have lower porosity and permeability.

Early diagenetic cements, probably related to the marine environment of deposition, include pyrite, calcite and possibly glauconite. These tend to be volumetrically minor and do not play much of a role in controlling reservoir quality. However, calcite is dominant in some samples filling all intergranular volume and leaving a floating grain texture

5.6.5 Localised inhibition of quartz cementation

Quartz cement is the most common cause of porosity-loss in deeply buried sandstones (McBride, 1989). Quartz cementation has not been inhibited significantly in the Ula Formation at Tambar as shown by the late onset of quartz cementation (high minimum fluid inclusion homogenisation temperature, Fig. 5.19) and the small amount of quartz cement and the relatively high porosity (Fig. 5.26D) for the relatively high temperature these rocks have been exposed to (Figs. 5.3 and 5.19).

There are a finite range of factors that have been reported to inhibit quartz cementation. It is possible to exclude the possibility that there is little quartz cement due to the pervasive early filling of pores with an alternative cement; early pore-filling calcite cement is the exception rather than the rule in these sandstones (Figs. 5.5 and 5.8A). The remaining options are (Bloch et al., 2002): (i) microcrystalline quartz coatings, (ii) grain-coating chlorite coats, (iii) early emplacement of oil and (iv) overpressure preventing compaction and related pressure solution processes (Sheldon et al., 2003)

Grain coating microcrystalline quartz has certainly inhibited quartz cementation as revealed by the lack of quartz overgrowths on sand grains that are coated with the thick layers of microcrystalline quartz (Fig. 5.11). Samples with grains with well-developed coats of microcrystalline quartz have the least amounts of quartz cement (Figs. 5.29C and D). Microcrystalline quartz thus has had an important control on quartz cementation and reservoir quality in these sandstones.

Chlorite is present in these sandstones but it does not occur as well developed grain coatings. Rather it tends to be highly localised and occurs as pore-filling mats (Fig. 5.12D). Chlorite grain coats can be excluded as a primary control on quartz cement abundance.

For oil to inhibit diagenesis, its emplacement must occur before the diagenetic process under consideration. The relative few number of oil inclusions in quartz suggests that much or most quartz cementation happened before oil filling; i.e. oil filling was a relatively late process in these sandstones. The addition of oil seems to have had no direct effect on quartz cement abundance in all but the coarsest of the

sandstones (Fig. 5.28). Indeed, quartz cement is only abundant in the coarsest sandstones that have high water saturations. Oil emplacement seems to have had a role in controlling reservoir quality in some of the Ula Formation sandstones at Tambar.

It is not easy to establish whether overpressure development has had a role in limiting quartz cementation using the empirical data provided, the samples available and the techniques employed. However, these sandstones are reported not to have high fluid pressures (O'Connor et al., 2011) suggesting that overpressure has not been an important control on quartz cementation.

.

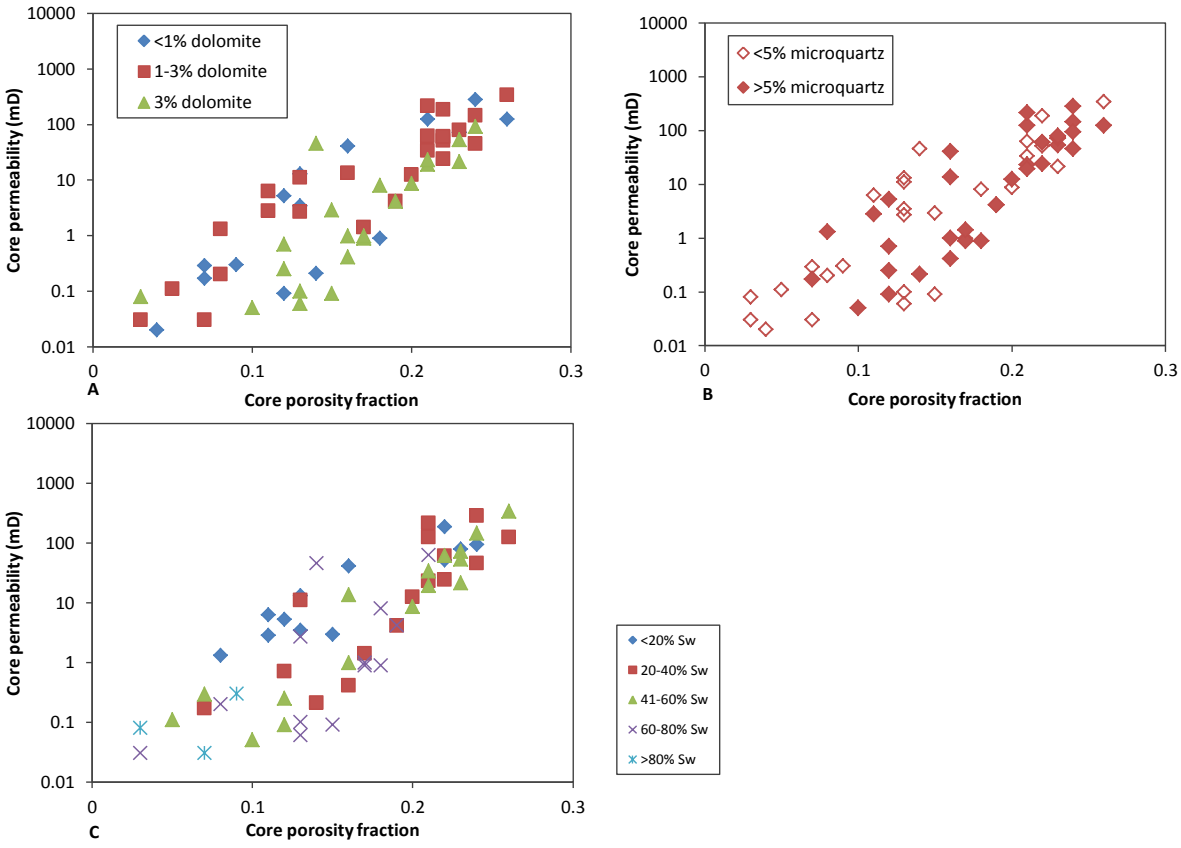

Figure 5.27 Core analysis porosity versus permeability with data split by (A) the amount of dolomite cement (B) the amount of microcrystalline quartz, (C) the water saturation. No single diagenetic cement or water saturation solely controlling porosity and permeability.

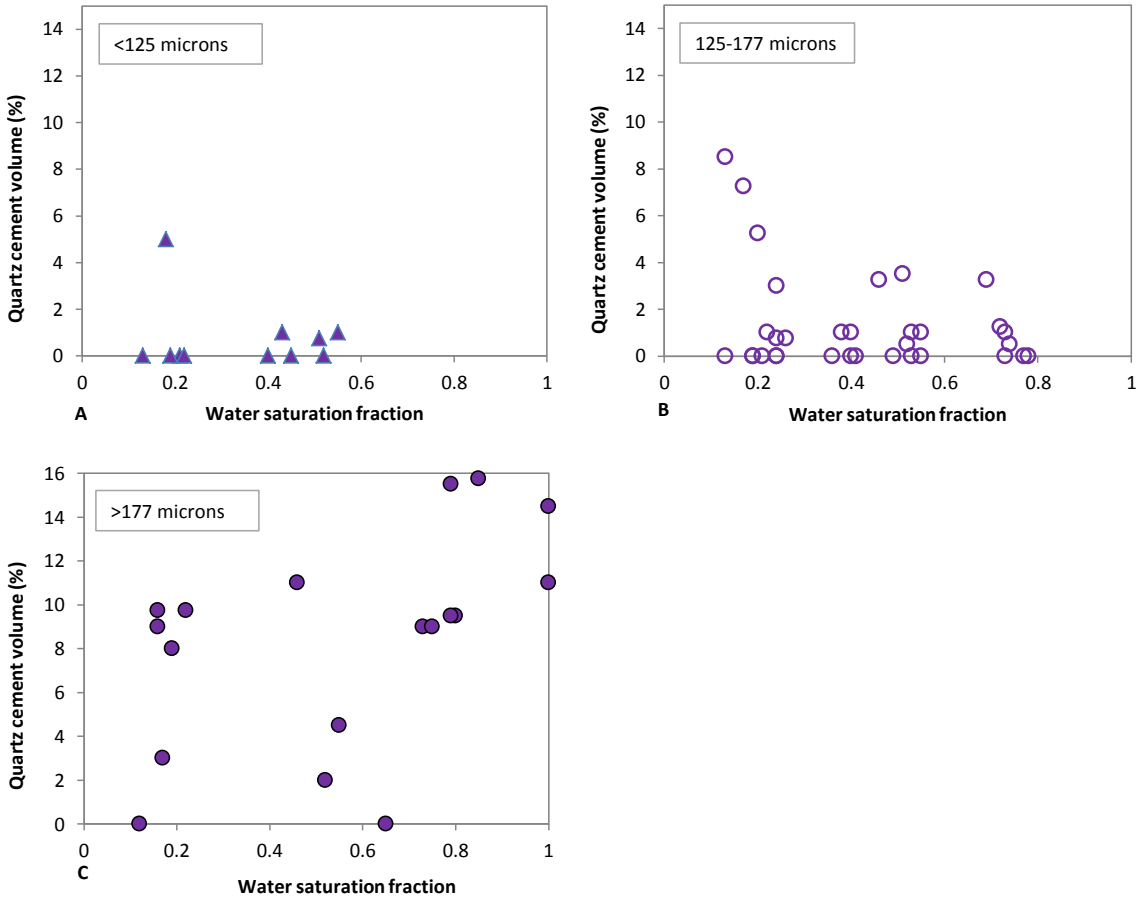

Figure 5.28 Water saturation versus the amount of quartz cement for the three different size fractions. Only the >177µm grain size class show correlation between high water saturation and high quartz cement volume.

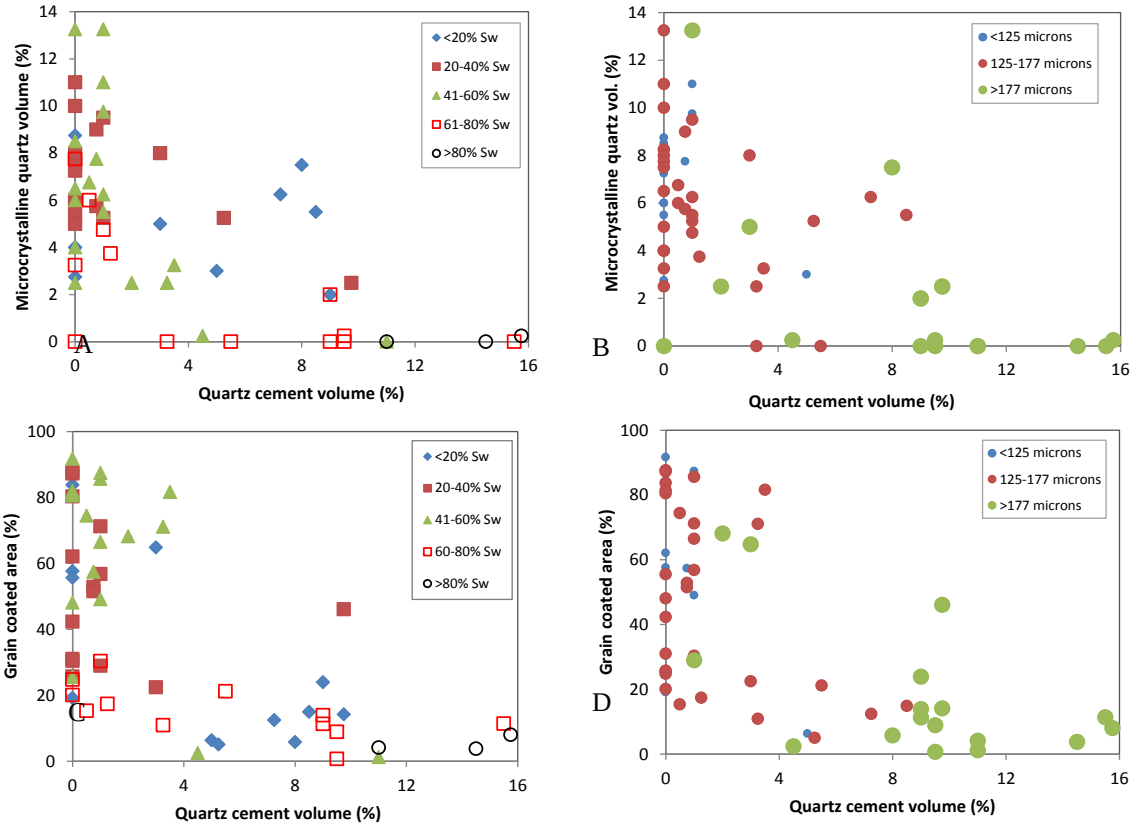

Figure 5.29 Quartz cement volume versus the amount of microcrystalline quartz split by (A) water saturation (G) grain size and quartz cement volume versus the average degree of grain coating split by (C) water saturation (D) grain size. Higher microquartz volume and grain coating show low quartz cement volume.

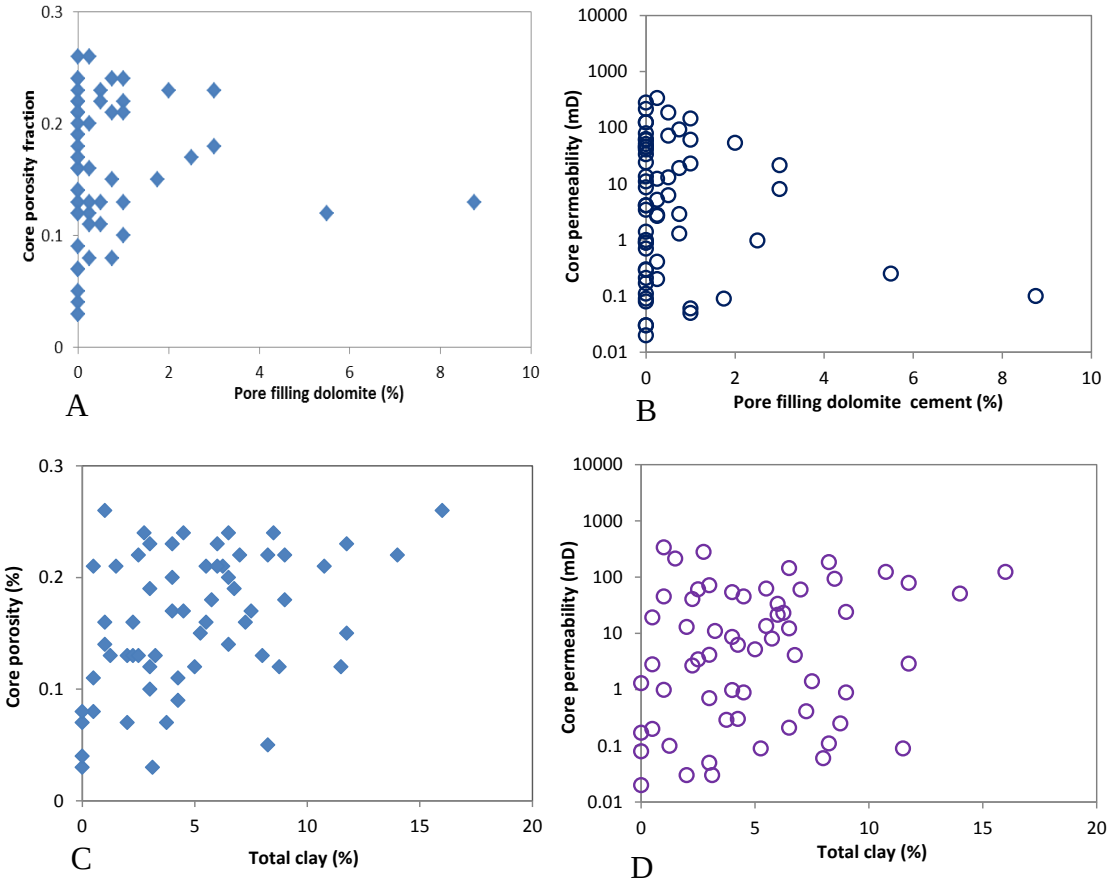

Figure 5.30 The amount of pore-filling dolomite versus (A) porosity and (B) permeability and the total amount of clay minerals versus (C) porosity and (D) permeability. Both dolomite and clay did not show significant control on porosity.

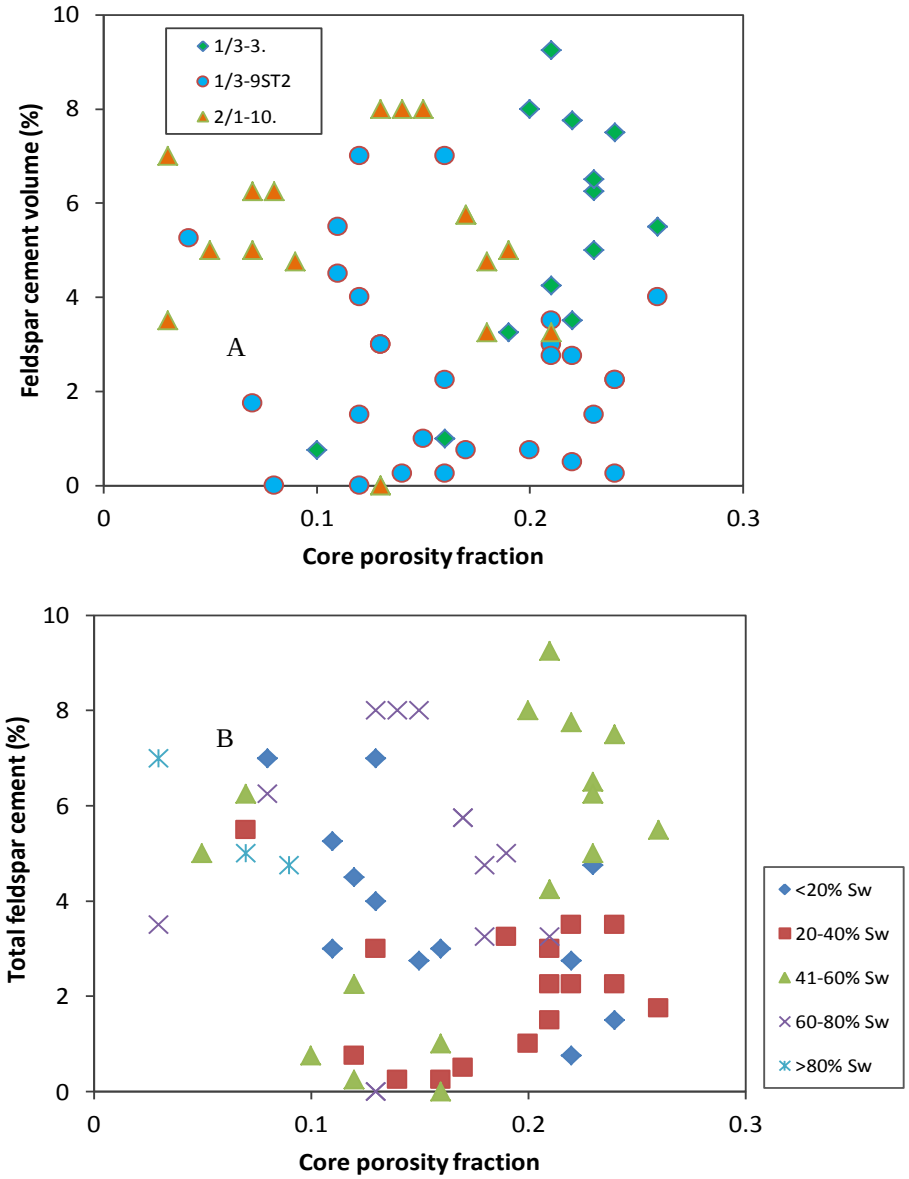

Figure 5.31 Core analysis porosity versus the total amount of feldspar cements split by (A) well and (B) degree of water saturation.

Table 5. 4 Summary of reservoir quality indicators and controls for the three different grain size classes split into oil and water leg. Number of samples for each grain size class: <125 µm oil (n=9) water (n=2) 125-177µm oil (n=13) water (n=20) >177µm oil (n=6) water (n=10).

Parameters	Fluid type	<125 µm grain size	125-177µm grain size	>177µm grain size
Core permeability (mD)	oil	26.0	92.9	10.9
	water	0.2	39.1	9.2
Core porosity (%)	oil	18.0	19.1	11.7
	water	13.0	18.7	9.0
Quartz cement (%)	oil	0.1	2.0	7.9
	water	0.8	0.9	9.2
Detrital clay (%)	oil	6.5	5.9	2.5
	water	7.6	4.9	1.8
Microcrystalline quartz (%)	oil	7.2	5.8	3.7
	water	8.5	5.8	0.4
Dolomite cement (%)	oil	4.7	1.3	0.6
	water	3.5	2.9	2.7
Feldspar cement (%)	oil	1.6	3.3	5.6
	water	1.25	4.2	6.4

5.6.6 Synthesis of the controls on reservoir quality in the Ula Formation at Tambar

The dominant controls on reservoir quality in the Ula Formation at Tambar are grain size, quartz cementation, and total quantity of clay minerals present, oil emplacement and dolomite cement content. These controls combine in different ways in different grain size classes (Table 5.4). In general, the lower fine-grained sandstones have the highest porosities and permeabilities and represent better reservoir than the very fine sandstones or the upper fine grained sandstones (Fig. 5.26A). Thus coarser grain size does not automatically equate to better reservoir in this case. The mean quartz cement content increases with increasing grain size (Table 5.4). The mean feldspar cement content mirrors the quartz cement and presumably was controlled by similar processes. In contrast the mean total clay, microcrystalline quartz and dolomite cement contents decrease with increasing grain size. For the very fine sandstones (<125µm), the quartz cement and feldspar cement abundance are very low for the

depth of burial and thermal history of these sandstones. Conversely, they have relatively high concentrations of microcrystalline quartz, clay and dolomite. These rocks have relatively high mean porosity but have low permeability due to the pore throat blocking behaviour of clay and dolomite and possibly the microcrystalline quartz given its unusually thick grain coats (Figs. 5.11E and F). The presence of oil has had little impact on the very fine sandstones since the later stages of diagenesis (quartz cementation) that occurred after oil filling had little effect on the reservoir quality.

For the upper fine sandstones (>177μm), the quartz cement and feldspar cement abundance are the highest for the Ula Formation at Tambar but still low for the depth of burial and thermal history of these sandstones. They have low concentrations of clay and dolomite and the lowest concentration of microcrystalline quartz (and least well developed grain coats) of all sandstones from Tambar (Table 5.4). These rocks have relatively low mean porosity and permeability due to the presence of quartz (and feldspar) cement. These rocks have the greatest amount of quartz cement in samples with the least well-developed microcrystalline quartz grain coats and that have high water saturations. The presence of oil has had some impact on the upper fine sandstones since the later stages of diagenesis (quartz cementation) that occurred after oil filling had a significant impact on reservoir quality.

The highest porosity and permeability sandstones from the Ula Formation at Tambar are the lower fine sandstones (125-177μm) since these have enough microcrystalline quartz to prevent much quartz cementation (and presumably feldspar cementation), but have less dolomite cement and clay than the very fine sandstones (Table 5.4). The presence of oil has had little impact on the lower fine sandstones since the later stages of diagenesis (quartz cementation) that occurred after oil filling had little effect on reservoir quality.

5.7 Conclusion

The Upper Jurassic Ula Formation at Tambar is a very fine- to fine-grained marine sandstones with an average porosity of 16% despite being buried to >4000m and experiencing temperatures >160°C.

The main diagenetic cements that had an impact on the reservoir quality of the Ula Formation at Tambar are microcrystalline quartz, quartz overgrowths, illite and dolomite.

Microcrystalline quartz is present as thick coatings on sand grains and is more abundant than in other marine sandstone reservoirs of the same age in the North Sea Basins. It was sourced from sponge spicules and had a major inhibiting effect on quartz cement growth.

Quartz cementation started at 130°C, a somewhat higher minimum temperature than many basins, presumably due to the inhibiting effect of microcrystalline quartz.

The coarsest grained sandstones (upper fine) have the least amount of microcrystalline quartz and commensurately the greatest amount of quartz cement. These sandstones have the greatest amount of quartz cement in sandstones with high water saturations suggesting that the relatively late addition of oil had an impact only on the cleanest and coarsest sandstones. These sandstones have relatively poor reservoir quality due to quartz and feldspar cement growth.

The finer sandstones have the greatest quantity of clay and dolomite cement as well as microcrystalline quartz and so have at best, moderate reservoir quality. It is possible that the extreme quantity of microcrystalline quartz has led to reduced permeability due to it blocking pore throats.

The intermediate sandstones (lower fine) have the best reservoir quality due to them having abundant microcrystalline quartz coating, thus inhibiting quartz cement, but also having less microcrystalline quartz, clay and dolomite than the very fine sandstones.

5.8 Reference

Aase, N. E., Bjorkum, P. A., and Nadeau, P. H., 1996, The effect of grain-coating microquartz on preservation of reservoir porosity: American Association of Petroleum Geologists Bulletin, v. 80, no. 10, p. 1654-1673.

Aase, N. E., and Walderhaug, A., 2005, The effect of hydrocarbons on quartz cementation: diagenesis in the Upper Jurassic sandstones of the Miller Field, North Sea, revisited: Petroleum Geoscience, v. 11, no. 3, p. 215-223.

Ajdukiewicz, J. M., Nicholson, P. H., and Esch, W. L., 2010, Prediction of deep reservoir quality using early diagenetic process models in the Jurassic Norphlet Formation, Gulf of Mexico: American Association of Petroleum Geologists Bulletin, v. 94, no. 8, p. 1189-1227.

Asquith, G. B., and Gibson, C. R., 1982, Basic well log analysis for geologists: American Association of Petroleum Geologists Methods in Exploration, no. 3, p. 216.

Barclay, S. A., and Worden, R. H., 2000, Geochemical modelling of diagenetic reactions in a sub-arkosic sandstone: Clay Minerals, v. 35, no. 1, p. 57-67.

Bergan, M., Tørudbakken, B., and Wandås, B., 1989, Lithostratigraphic correlation of Upper Jurassic sandstones within the Norwegian Central Graben: sedimentological and tectonic implications, *in* Collinson, J. D., ed., Correlation in hydrocarbon exploration, Norwegian Petroleum Society, Graham and Trotman, London, p. 243-251.

Bjorkum, P. A., Oelkers, E. H., Nadeau, P. H., Walderhaug, O., and Murphy, W. M., 1998, Porosity prediction in quartzose sandstones as a function of time, temperature, depth, stylolite frequency, and hydrocarbon saturation: American Association of Petroleum Geologists Bulletin, v. 82, no. 4, p. 637-648.

Bjorlykke, K., Aagaard, P., Dypvik, H., Hastings, D. S., and Harper, A. S., 1988, Diagenesis and reservoir properties of Jurassic sandstones from the Haltenbanken area, offshore mid Norway, *in* Spencer et al., ed., Habitat of Hydrocarbon on the Norwegian ContinentalShelf,, Norwegian Petroleum Society Graham and Trotman, p. 276-286.

Bjørnseth, H. M., and Gluyas, J., 1995, Petroleum exploration in the Ula Trend: Norwegian Petroleum Society Special Publications, v. 4, p. 85-96.

Bloch, S., Lander, R. H., and Bonnell, L., 2002, Anomalously high porosity and permeability in deeply buried sandstone reservoirs: Origin and predictability: American Association of Petroleum Geologists Bulletin, v. 86, no. 2, p. 301-328.

Bryant, S., Cade, C., and Mellor, D., 1993, Permeability prediction from geologic models: American Association of Petroleum Geologists Bulletin, v. 77, no. 8, p. 1338-1350.

Burley, S. D., 1984, Patterns of diagenesis in the Sherwood Sandstone Group (Triassic), United KIngdom: Clay Minerals, v. 19, no. 3, p. 403-440.

Cade, C. A., Evans, I. J., and Bryant, S. L., 1994, Analysis of permeability controls - a new approach: Clay Minerals, v. 29, no. 4, p. 491-501.

Chang, J. C., and Yortsos, Y. C., 1994, Lamination during silica diagenesis - effects of clay content and Ostwald ripening: American Journal of Science, v. 294, no. 2, p. 137-172.

Craig, H., 1957, Isotopic standards for carbon and oxygen correction factors for mass spectrometric analysis of carbon dioxide: Geochimeca et Cosmochemica Acta, v. 12.

Dixon, S. A., Summers, D. M., and Surdam, R. C., 1989, Diagenesis and preservation of porosity in Norphlet Formation (Upper Jurassic), southern Alabama: Americam Association of Petroleum Geologists Bulletin, v. 73, no. 6, p. 707-728.

Ehrenberg, S. N., 1990, Relationship between diagenesis and reservoir quality in sandstones of the Garn Formation, Haltenbanken, mid-Norwegian continental shelf: American Association of Petroleum Geologists Bulletin, v. 74, no. 10, p. 1538-1558.

Evans, J., Cade, C., and Bryant, S., 1997, A geological approach to permeability prediction in clastic reservoirs: In: Reservoir quality prediction in sandstones and carbonates (eds. Kupecz, J.A., Gluyas, J. and Bloch, S.) AAPG Memoir, v. 69, p. 91-102.

Folk, R. L., 1968, Petrology of sedimentary rocks, Austin, Texas: Hemphill.

French, M. W., Worden, R. H., Mariani, E., Horn, W. C., Kliewer, C. E., Lamberti, W. A., Mueller, R. R., and Fischer, C., 2010, Low temperature porosity preserving microquartz from Upper Cretaceous sandstones of the Subhercynian Basin (Germany): Geochimica et Cosmochimica Acta, v. 74, no. 12, p. A305-A305.

French, M. W., Worden, R. H., Mariani, E., Larese, R. E., Mueller, R. R., and Kliewer, C. E., 2012, Microcrystalline quartz generation and the preservation of porosity in sandstones: evidence from the Upper Cretaceous of the Sub-Hercynian Basin, Germany: Journal of Sedimentary Research, v. 82, no. 5-6, p. 422-434.

Friedman, I., and O'Neil, J. R., 1977, Compilation of stable isotope fractionation factors of geochemical interest, USGeological Survey Professional papers, Data of Geochemistry.

Gluyas, J. G., Robinson, A. G., Emery, D., Grant, S. M., and Oxtoby, N. H., 1993, The link between petroleum emplacement and sandstone cementation, *in* Parker, J., ed., Petroleum Geology of the North west Europe, Geological Society of London, v. 4, p. 1395-1402.

Haddad, S. C., Worden, R. H., Prior, D. J., and Smalley, P. C., 2006, Quartz cement in the Fontainebleau sandstone, Paris basin, France: Crystallography and implications for mechanisms of cement growth: Journal of Sedimentary Research, v. 76, no. 2, p. 244-256.

Hamar, G. P., Fjaeran, T., and Hesjedal, A., 1983 Jurassic stratigraphy and tectonics of the south-southeastern Norwegian offshore, *in* Kaasschieter, J. P. H., and Reijers, T. J. A., eds., Petroleum Geology of the Southeastern North Sea and the Adjacent Onshore Areas. , Volume 62, Geol. Mijnbouw, p. 103-114.

Harris, N. B., 2006, Low-porosity haloes at stylolites in the feldspathic Upper Jurassic Ula sandstone, Norwegian North Sea: An integrated petrographic and chemical mass-balance approach: Journal of Sedimentary Research, v. 76, no. 3-4, p. 444-459.

Hogg, A. J. C., Sellier, E., and Jourdan, A. J., 1992, Cathodoluminescence of quartz cements in Brent group sandstones, Alwyn South, UK North Sea, *in* Morton, A. C., and Hazeldine, S. R., eds., Geological Society, London, Special Publications, Volume 61, p. 421-440.

Home, P. C., 1987, Ula, *in* Spencer, A. M., Holter, E., Campbell, C. J., Hanslein, S. H., Nelsen, P. H. H., Nysteacher, E., and Ormaasen, E. G., eds., Geology of the Norwegian oil and gas fields: London, Graham and Trotman, p. 143-151.

Jahren, J., and Ramm, M., 2000, The Porosity preserving effects of microcrystalline quartz coatings in arenitic sandstones: Examples from the Norwegian Continental Shelf, *in* Worde, R. H., and Morad, S., eds., Quartz cementation in sandstones, Volume 29,

International Association of Sedimentologists Special edition. Blackwell Science, p. 271-280.

Karlsen, D. A., Nedkvitne, T., Larter, S. R., and Bjørlykke, K., 1993, Hydrocarbon composition of authigenic inclusions: application to elucidation of petroleum reservoir filling history: Geochimica et cosmochimica acta, v. 57, no. 15, p. 3641-3659.

Karlsen, D. A., and Skeie, J. E., 2006, Petroleum migration, faults and overpressure, part I: calibrating basin modelling using petroleum in traps—a review: Journal of Petroleum Geology, v. 29, no. 3, p. 227-256.

Knipe, R. J., Anderson, S., and Mitchell, A., 1991, Deformation processes and fault seal mechanisms: a combined microstructural analysis from the Ula field, Central Graben, North Sea: American Association of Petroleum Geologists Bulletin, v. 75, no. CONF-910403--.

Kraishan, G. M., Rezaee, M. R., and Worden, R. H., 2000, Significance of trace element composition of quartz cement as a key to reveal the origin of silica in sandstones: an example from the Cretaceous of the Barrow sub-basin, Western Australia: In: Quartz cementation in sandstones (eds. Worden, R.H. and Morad, S.) International Association of Sedimentologists Special Publications, v. 29, p. 317-332.

Land, L. S., 1983, The application of stable isotopes to studies of the origin of dolomite and to problems of diagenesis of clastic sediments, Society of Economic Paleontologists and Mineralogists, Short course, Stable isotopes in sedimentary geology: In Stable Isotopes in Sedimentary Geology, 4.1-4.22 p.:

Lima, R. D., and De Ros, L. F., 2002, The role of depositional setting and diagenesis on the reservoir quality of Devonian sandstones from the Solimões Basin, Brazilian Amazonia: Marine and Petroleum Geology, v. 19, no. 9, p. 1047-1071.

Macaulay, C. I., Fallick, A., McLaughlin, O. M., Haszeldine, R. S., and Pearson, M. J., 1998, The significance of d13C of carbonate cement in reservoir sandstones; a regional perspective from the Jurassic of the Northern North Sea: In: Carbonate cementation in sandstones (ed. Morad, S.) International Association of Sedimentologists Special Publications, v. 26, p. 395-408.

Marchand, A. M. E., Haszeldine, R. S., Smalley, P. C., Macaulay, C. I., and Fallick, A. E., 2001, Evidence for reduced quartz-cementation rates in oil-filled sandstones: Geology, v. 29, no. 10, p. 915-918.

McBride, E. F., 1989, Quartz cement in sandstones: a review: Earth Science Reviews, v. 26, no. C, p. 69-112.

Molenaar, N., Cyziene, J., and Sliaupa, S., 2007, Quartz cementation mechanisms and porosity variation in Baltic Cambrian sandstones: Sedimentary Geology, v. 195, no. 3, p. 135-159.

Morad, S., Al-Ramadan, K., Ketzer, J. M., and De Ros, L. F., 2010, The impact of diagenesis on the heterogeneity of sandstone reservoirs: A review of the role of depositional facies and sequence stratigraphy: American Association of Petroleum Geologists Bulletin, v. 94, no. 8, p. 1267-1309.

Nedkvitne, T., Karlsen, D. A., Bjorlykke, K., and Larter, S. R., 1993, Relationship between reservoir diagenetic evolution and petroleum emplacement in the Ula Field, North Sea: Marine and Petroleum Geology, v. 10, no. 3, p. 255-270.

O'Connor, S., Rasmussen, H., Swarbrick, R., and Wood, J., 2011, Integrating a hydrodynamically-titled OWC and a salt-withdrawal depositional model to explore the Ula Trend: Geofluids, v. 11, no. 4, p. 388-400.

O'Neil, J. R., and Epstein, S., 1966, Oxygen isotope fractionation in the system dolomite-calcite-carbon dioxide: Science, v. 152, no. 3719, p. 198-201.

O'Connor, S., Rasmussen, H., Swarbrick, R., and Wood, J., 2001, Integrating a hydrodynamically-titled OWC and a salt-withdrawal depositional model to explore the Ula Trend: Geofluids, v. 11.

Oelkers, E. H., Bjorkum, P. A., and Murphy, W. M., 1996, A petrographic and computational investigation of quartz cementation and porosity reduction in North Sea sandstones: American Journal of Science, v. 296, no. 4, p. 420-452.

Osborne, M. J., and Swarbrick, R. E., 1999, Diagenesis in North Sea HPHT elastic reservoirs - consequences for porosity and overpressure prediction: Marine and Petroleum Geology, v. 16, no. 4, p. 337-353.

Oxtoby, N. H., 1994, The Ula field, *in* Warren, E. A., and Smalley, P. C., eds., North Sea Formation waters: London, The Geological Society London. Memoir No. 15, p. 74.

Oxtoby, N. H., Mitchell, A. W., and Gluyas, J. G., 1995, The filling and emptying of the Ula Oilfield: fluid inclusion constraints, *in* J.M. Cubitt, and England, W. A., eds., The Geochemistry of Reservoirs Geological Society, London, Special Publications, Volume 86, p. 141-157.

Partington, M. A., Mitchener, B. C., Milton, N. J., and Fraser, A. J., 1993, Genetic sequence stratigraphy for the North Sea Late Jurassic and Early Cretaceous: distribution and prediction of Kimmeridgian–Late Ryazanian reservoirs in the North Sea and adjacent areas: Geological Society of London, v. 4, p. 347-370.

Petersen, H. I., Andersen, C., Holme, A. C., Carr, A. D., and Thomsen, E., 2012, Vitrinite reflectance gradients of deep wells with thick chalk sections and high pressure: implications for source rock maturation, Danish-Norwegian Central Graben, North Sea: International Journal of Coal Geology, v. Man, p. Muscript accepeted 19 June, 2012.

Ramm, M., 1992, Porosity depth trends in reservoir sandstones - theoretical models related to Jurassic sandstones offshore Norway: Marine and Petroleum Geology, v. 9, no. 5, p. 553-567.

Ramm, M., and Bjorlykke, K., 1994, Porosity depth trends in Norwegain reservoirs - assessing the quantitativ effects of varying pore-pressure, temperature history and mineralogy, Norwegian shelf data: Clay Minerals, v. 29, no. 4, p. 475-490.

Ramm, M., Forsberg, A. W., and Jahren, J., 1997, Porosity-depth trends in deeply buried Upper Jurassic Reservoirs in the Norwegian Central Graben: an example of porosity preservation beneath the normal economic basement by grain coating microquartz: In: Reservoir quality prediction in sandstones and carbonates (eds. Kupecz, J.A., Gluyas, J. and Bloch, S.) AAPG Memoir, v. 69, p. 177-200.

Rosenbaum, J., and Sheppard, S. M. F., 1986, An isotopic study of siderites, dolomites and ankerites at high temperatures: Geochimica et Cosmochimica Acta, v. 50, no. 6, p. 1147-1150.

Schmid, S., Worden, R. H., and Fisher, Q. J., 2004, Diagenesis and reservoir quality of the Sherwood Sandstone (Triassic), Corrib Field, Slyne Basin, west of Ireland: Marine and Petroleum Geology, v. 21, no. 3, p. 299-315.

Sheldon, H. A., Wheeler, J., Worden, R. H., and Cheadle, M. J., 2003, An analysis of the roles of stress, temperature, and pH in chemical compaction of sandstones: Journal of Sedimentary Research, v. 73, no. 1, p. 64-71.

Skjerven, J., Rijs, F., and Kalheim, J., 1983, Late Paleozoic to Early Cenozoic structural development of the south-southeastern Norwegian North Sea: Geologie en Mijnbouw, v. 62, p. 35-45.

Stewart, I. J., Structural controls on the Late Jurassic age shelf system, Ula trend, Norwegian North Sea1993, Volume 4, Geological Society of London, p. 469-483.

Stokkendal, J., Friis, H., Svendsen, J. B., Poulsen, M. L. K., and Hamberg, L., 2009, Predictive permeability variations in a Hermod sand reservoir, Stine Segments, Siri Field, Danish North Sea: Marine and Petroleum Geology, v. 26, no. 3, p. 397-415.

Underhill, J. R., 1998, Jurassic, *in* Glennie, K. W., ed., Petroleum Geology of the North Sea:Basic Concepts and Recent Advances, Blackwell Science, p. 656.

Vagle, G. B., Hurst, A., and Dypvik, H., 1994, Origin of quartz cements in some sandstones from the Jurassic of the Inner Moray Firth (UK): Sedimentology, v. 41, no. 2, p. 363-377.

Veizer, J., Ala, D., Azmy, K., Bruckschen, P., Buhl, D., Bruhn, F., Carden, G. A. F., Diener, A., Ebneth, S., Godderis, Y., Jasper, T., Korte, C., Pawellek, F., Podlaha, O. G., and Strauss, H., 1999, Sr-87/Sr-86, delta C-13 and delta O-18 evolution of Phanerozoic seawater: Chemical Geology, v. 161, no. 1-3, p. 59-88.

Walderhaug, O., 1994, Temperatures of quartz cementation in Jurassic sandstones from the Norwegian continental shelf - evidence from fluid inclusions: Journal of Sedimentary Research Section a-Sedimentary Petrology and Processes, v. 64, no. 2, p. 311-323.

Walderhaug, O., Lander, R. H., Bjorkum, P. A., Oelkers, E. H., Bjorlykke, K., and Nadeau, P. H., 2000, Modelling quartz cementation and porosity in reservoir sandstones: examples from the Norwegain continental shelf: In: Quartz cementation in sandstones (eds. Worden, R.H. and Morad, S.) International Association of Sedimentologists Special Publications, v. 29, p. 39-50.

Weibel, R., Friis, H., Kazerouni, A. M., Svendsen, J. B., Stokkendal, J., and Poulsen, M. L. K., 2010, Development of early diagenetic silica and quartz morphologies - Examples from the Siri Canyon, Danish North Sea: Sedimentary Geology, v. 228, no. 3-4, p. 151-170.

Wilhelms, A., and Larter, S. R., 1994, Origin of tar mats in petroleum reservoirs. Part II: formation mechanisms for tar mats: Marine and Petroleum Geology, v. 11, no. 4, p. 442-456.

Wilkinson, M., and Haszeldine, R. S., 2011, Oil charge preserves exceptional porosity in deeply buried, overpressured, sandstones: Central North Sea, UK: Journal of the Geological Society, v. 168, no. 6, p. 1285-1295.

Williams, L. A., and Crerar, D. A., 1985, Silica diagenesis; II, General mechanisms: Journal of Sedimentary Research, v. 55, no. 3, p. 312-321.

Williams, L. A., Parks, G. A., and Crerar, D. A., 1985, Silica diagenesis; I, Solubility controls: Journal of Sedimentary Research, v. 55, no. 3, p. 301-311.

Worden, R. H., and Burley, S. D., 2003, Sandstone diagenesis: the evolution from sand to stone, *in* Burley, S. D., and Worden, R. H., eds., Sandstone diagenesis, recent and

ancient. International Association of Sedimentologists Reprint Series, Volume 4, p. 3-44.

Worden, R. H., French, M. W., and Mariani, E., 2012, Amorphous silica nanofilms result in growth of misoriented microcrystalline quartz cement maintaining porosity in deeply buried sandstones: Geology, v. 40, no. 2, p. 179-182.

Worden, R. H., and Morad, S., 2003, Clay minerals in sandstones: Controls on formation, distribution and evolution: In: Clay mineral cements in sandstones (eds. Worden, R.H. and Morad, S.) International Association of Sedimentologists Special Publications, v. 34, p. 3-41.

Worden, R. H., Oxtoby, N. H., and Smalley, P. C., 1998, Can oil emplacement prevent quartz cementation in sandstones?: Petroleum Geoscience, v. 4, no. 2, p. 129-137.

Worden, R. H., Warren, E. A., Smalley, P. C., Primmer, T. J., and Oxtoby, N. H., 1995, Evidence for resetting of fluid inclusions from quartz cements in oil fields - discussion: Marine and Petroleum Geology, v. 12, no. 5, p. 566-570.

CHAPTER 6

6. Synthesis discussion and general conclusions

6.1 Context of the study: Recap

Assessing reservoir quality is one of the most important aspects of petroleum exploration. Sandstones continue to lose porosity and permeability through compaction and cementation after burial. Quartz is the most important porosity-destroying cement in medium and deeply buried sandstone reservoirs. This project deals with the diagenesis and the effect of early oil emplacement on diagenetic activities with emphasis on quartz cementation in oil field reservoirs of Ula and Tambar fields. Two opposing schools of thought have evolved over recent years: (1) that quartz cementation ceases or slows dramatically in oil (or gas) fields once petroleum has replaced water in the pores, thus leading to the preservation of porosity and permeability (Cox et al., 2010; Emery et al., 1993; Gluyas et al., 1993; Marchand et al., 2002; Saigal et al., 1992; Wilkinson and Haszeldine, 2011) because water is essential for the dissolution-transport-precipitation process that creates cement and (2) that quartz cementation is unaffected by the addition of water since quartz cementation is controlled by the rate of quartz precipitation and quartz grains remain water coated even in oil-filled sandstones due to residual water saturation (Aase and Walderhaug, 2005; Bjørkum et al., 1998; Ehrenberg, 1993; Giles et al., 1992; Molenaar et al., 2008; Ramm, 1992).

To try to deduce whether the first or second school of thought is correct, an integrated approach has been used involving detailed petrographic studies, fluid inclusion studies and stable isotope geochemistry. Sedimentological analysis was used to understand and select rocks of similar properties to be compared for reservoir qualities between zones of different fluid saturations. Sets of wireline logs were used to determine the exact fluid saturations of all petrographic (core) samples in all wells used in the study. Optical petrography, stable isotope geochemistry and XRD Fluid inclusion studies were used to determine qualitative and quantitative distribution of minerals, changes in water chemistry and the timing of quartz cementation relative to oil filing. Therefore, the outcome should help in understanding reservoir quality

distributions and controls in these fields which could enhance field appraisal and regional exploration activities.

6.2 General discussions and responses to key questions

6.2.1 What controls reservoir quality in the Ula and Tambar fields?

Reservoir qualities in Ula and Tambar have different controls. Reservoir quality in the Ula field is predominantly controlled by grain size, microquartz grain coats and early oil emplacement. The are three main facies types; very fine to fine intensely biotubated sandstones, fine to medium grained biotubated sandstones and coarse grained graded sandstones without biotubation. There reservoir quality is divided into two distinct classes (Fig. 6.1). The very fine to fine facies (which is texturally similar to the <125µm grain size class of the Tambar field) is characterised by grain-coating microquartz and moderate porosity and very low permeability (<<100mD) due to the abundance of clay minerals. The medium grained, biotubated facies and the medium to coarse grain have a range of reservoir qualities. The low water saturation units (<20% Sw) have high porosity and permeability (Fig. 4.6). The high water saturation units show low porosity and permeability in both facies. The coarse grained and graded facies show high amounts of quartz cement when they have high water saturation compared to the fine to medium grain with similar pore fluid.

In Tambar the main control on reservoir quality is microquartz whose distribution is controlled by grain size. The texture ranges from siltstone to fine grains sandstones (note that the coarser grain sizes found in Ula are absent from Tambar). The grain size are split into three classes; <125µm, 125-177µm and >177µm. The 125-177µm grain size class, here referred to as lower fine grain size, has the best reservoir quality of >20% porosity and >100mD permeability compared to the other two grain size classes (Fig. 5.25, 6.1). The <125µm grain has moderate porosity and poor permeability because of the great quantity of pore filling and pore throat blocking clays. The coarser grain size, >177µm, has the lowest porosity and permeability values. This grain size class has more quartz and feldspar cement than the finer grained size classes.

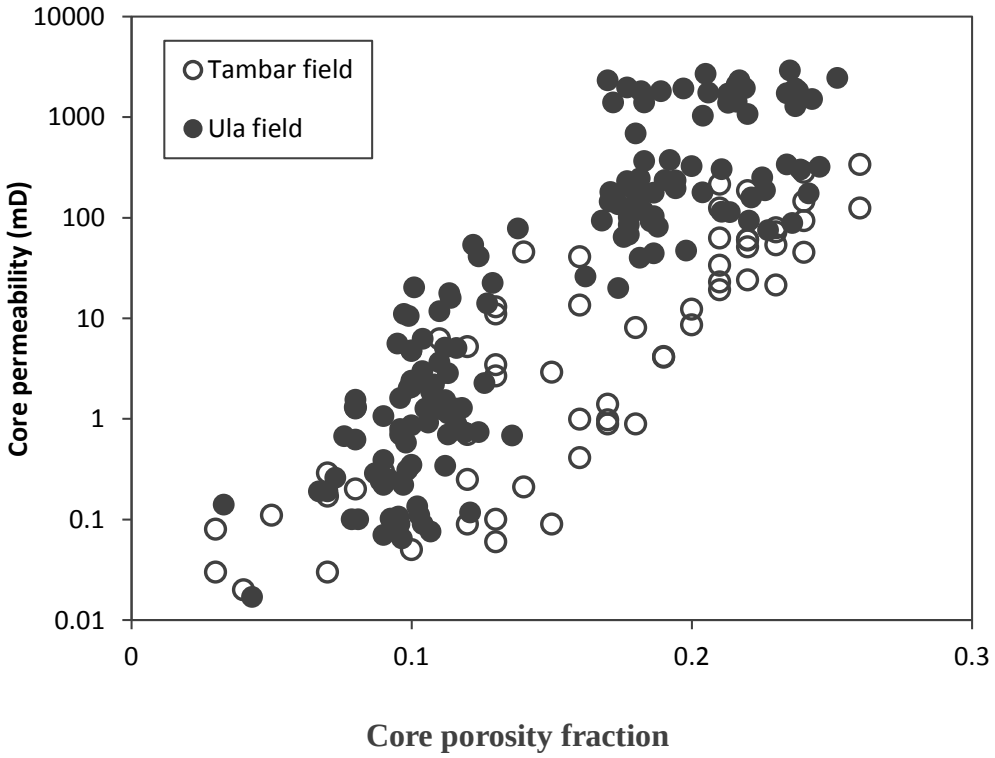

Figure 6. 1 Plot of porosity and permeability for Ula and Tambar fields. The high porosity and very high permeability data points for Ula field are samples with less than 20% water saturation.

6.2.2 What is the temperature and duration of quartz cementation?

Increases in temperature (and possibly lithostatic pressure) during diagenesis accelerate reaction kinetics by increasing the solubility of quartz and amorphous silica which provides greater amounts of soluble silica for quartz cementation (Dove and Rimstidt, 1994).

Aqueous fluid inclusion homogenization temperature have been used to determine quartz precipitation temperature and duration (Walderhaug, 1990). Quartz cement is typically assumed to begin growing at temperatures greater than approximately 80 ^{o}C (Lander and Walderhaug, 1999; McBride, 1989; Walderhaug, 2000; Worden and Morad, 2000). In the Ula field minimum homogenization temperature recorded in an aqueous fluid inclusion was 109 ^{o}C (Fig. 3.16, 6.2) with a mode between 140 and 159 ^{o}C. The maximum fluid inclusion temperature is 176 ^{o}C, close to present day in-situ temperature which suggested that quartz cementation may be taking place in the reservoir at the present time. Considering the wide range of homogenization temperatures (Fig 6.2) recorded by the fluid inclusions in quartz cements, (Fig 6.2a) and the burial history, indicates a long period of quartz cementation of about 25Ma.

In the Tambar field, the minimum homogenization temperature measured from aqueous fluid inclusion within quartz cement was 122 ^{o}C and the maximum temperature was 176 ^{o}C, close to the present day reservoir temperature (Fig. 5.19, 6.2). These values indicate that minimum quartz cement temperatures are high in these fields and the duration is very long time rather than episodic. Tambar quartz fluid inclusion homogenization temperatures are slightly higher than those from Ula, which may be due to higher reservoir depth of burial than of Ula field. Petroleum inclusions are fewer and have narrower range in Tambar field than Ula (Fig, 6.2). Probably the main phase of quartz cementation in Tambar took place before oil charge began. However, not known the minimum oil saturation required during quartz cementation in order to trap petroleum inclusions within the cement is not known (Worden and Morad, 2000; Worden et al., 1998).

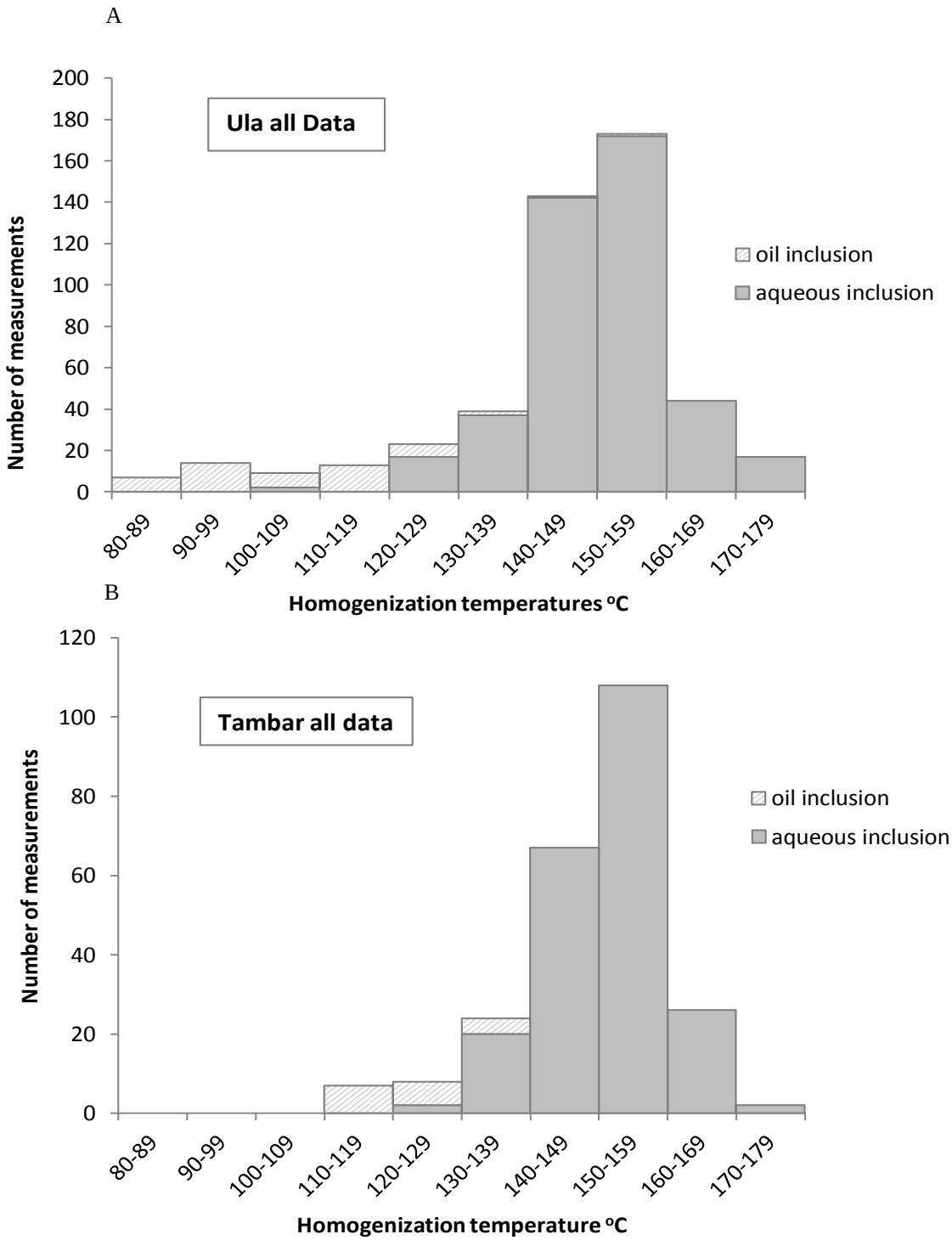

Figure 6. 2 Histograms for all fluid inclusion data (A) Ula field (B) Tambar field

6.2.3 Has oil emplacement retard/inhibit quartz cementation in oil leg relative to the water leg?

In order to answer this question, bulk comparisons of point count and petrophysical data from the oil legs and water legs were avoided since they include data from widely different grain sizes, sorting and sandstones affected by early diagenesis. The Ula reservoir rock is split to three different facies so that only similar rocks are compared. Water saturation for each point across the entire reservoir was determined (Fig. 4.5). The characteristics of the three different primary lithofacies above and below the oil-water contact (and in the transition zone) are summarized in Table 4.1. These three lithofacies (coarse grained graded sandstones, medium to fine bioturbated sandstones, very fine to fine bioturbated sandstones) have similar (uniform) grain size and sorting characteristics and have a narrow range of primary mineralogies (Fig. 4.7). They also have consistent quantities of detrital clay and grain-coating microcrystalline quartz. Samples cemented with poikilotopic calcite (i.e. with all pore space filled very soon after deposition) were not included in the analysis since they present entirely different characteristics.

In the Ula Formation reservoir, the oil leg has higher porosity and less quartz cement than the water leg for the coarse-grained graded sandstones and the fine to medium-grained bioturbated sandstone (Table 4.1). A water saturation and quartz cement plot (Fig. 4.14) shows high water saturation equates to elevated quantities of quartz cement for coarse-grained graded and the fine to medium grained facies that lack significant microquartz. Only the very fine to fine-grained biotubated facies did not show differences in quartz cement volume between high and low water saturations. The difference in quartz cement volume in Figure 4.14 cannot be explained by different amounts of microcrystalline quartz coating, grain-coating chlorite, other pore-filling cements (e.g. ferroan dolomite), grain size or any other primary lithofacies influence. The difference can be attributed to the composition of the pore fluid. Having oil in the sandstone during quartz cementation (as shown by oil inclusions in quartz cement; Fig.4.12) has led to a slower rate of quartz precipitation and less quartz cement. The reduced rate of quartz cementation could be the ultimate result of reduced rates of silica supply (presumably from internal, stylolite-related,

sources; Figs. 4. 9c and d), reduced rates of transport (either advection due to relative permeability effects or diffusion due to tortuosity effects) (Worden et al., 1998).

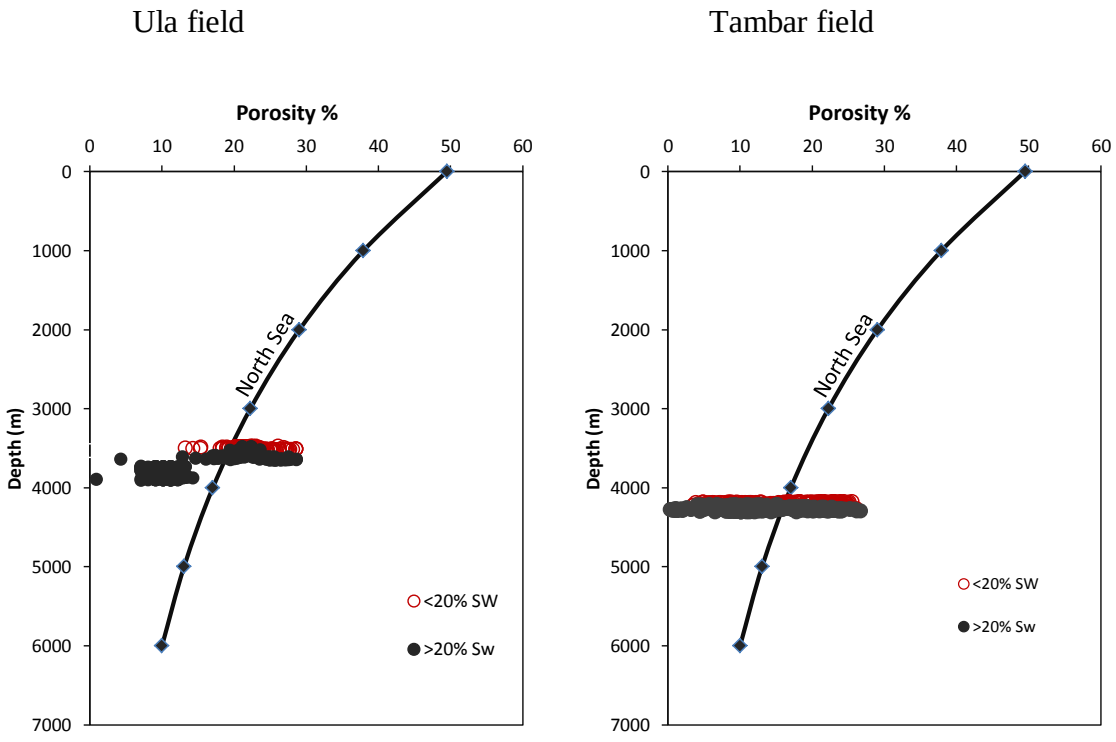

Figure 6. 3 Porosity-depth trend of the Ula and Tambar fields compared to average porosity depth trend of the North Sea by Sclater and Christie (1980).

In the Tambar field, reservoir only the upper fine grain (>177µm) class size show high quartz cement volume for high water saturation (Fig. 5.28). From the fluid inclusion evidence, oil emplacement is likely to have post-dated the main phase of quartz cementation in the Tambar field. If oil was introduced into the reservoir after quartz cementation, no difference in volume of quartz cement should be expected between high oil saturation and low oil saturation (Worden and Morad, 2000). The other factor in the Ula and Tambar sandstones is microcrystalline quartz that coat the grains at much lower temperature than the onset of quartz cementation. The microquartz stops quartz cement precipitation on the surface of the grain. Since there is a considerable amount of quartz cement (locally up to 15%) the most convincing factor that leads to similarity in volume of quartz cement in low water saturation and high water saturation in parts of the Tambar field is that cementation by quartz happened before the major oil charge. Oil emplacement has inhibited

quartz cementation in the Ula field but did not play a major role in the Tambar field (Fig. 6.3). Because the influence of compaction is not great, the Housenecht type plot for the Tambar field shows the greater influence of cementation than compaction in destroying the porosity.

6.2.4 What is the nature of microcrystalline quartz and its contribution in inhibiting quartz cementation?

In the Ula Formation sandstone reservoir of the Ula field, a rim of microcrystalline quartz coats detrital grains in the very fine to fine – grained biotubated facies as defined by many authors (French et al., 2010; Lima and De Ros, 2002; Vagle et al., 1994). There are two forms of microquartz; fine 2-5µm size and larger 4-10µm size (Fig. 3.12c and d). The finer form has traces of quartz overgrowth on it while the coarser form has no quartz cement growing on top (Fig. 3.12). In terms of distribution, microquartz is restricted to the very fine to fine grained biotubated facies. This facies with microquartz coatings has very low quartz cement relative to other facies (Fig. 4.15a) that lack microquartz.

In the Tambar field, microcrystalline quartz coatings are abundant and not strictly confined to specific facies or horizons. The microquartz sizes are the same as the coarse type of microquartz in Ula field. There is an inverse relationship between quartz cement volume and microcrystalline quartz coating grains (Fig. 3.24c-d, 5.29a-d) in both fields. Because the general texture of the Tambar field reservoir is siltstone to fine grain size, the coarse nature of the microcrystalline quartz (dominantly 4-10µm Fig. 5.11) have contributed to permeability-reduction in that field. There is clear evidence for the biogenic source of the microquartz as numerous circular pores representing dissolution of sponge spicules are observed especially in the Tambar field (Fig. 5.10a-b). In conclusion, microquartz has significantly inhibited the growth of quartz cement in the finest facies in Ula and Tambar.

6.2.5 Is there a link between stable oxygen isotope and oil emplacement in the reservoirs?

The present day formation water from the Ula Field has a $\delta^{18}O$ value of 3.26‰ V-SMOW. The $\delta^{18}O$ values for samples in the water leg range from (-5.48 to -12.4‰

PDB) average -10.5 and the oil leg values range from (-5.50 to -6.52‰ PDB) average -6.17‰ PDB. The temperature of dolomite growth, using the appropriate isotope fractionation equations (Fig. 5.22) (Land, 1983; O'Neil and Epstein, 1966), averaged 102 ^{0}C in the oil leg and water leg averaged 147^{o}C. In the Tamar field, similar to Ula field (same reservoir age, same detrital mineralogy, same stratigraphy, similar thermal and filling history), it was assumed to have similar present day formation water value as Ula (δ^{18}O value of 3.26‰ V-SMOW), using same fractionation equation used for Ula, crystallization temperature for dolomite in the water leg (average 152.7 ^{o}C) is higher than oil leg (average 86.08 ^{o}C) (Fig. 5.22, 6.4 Table 5.3). Dolomite in the water leg grew, or recrystallized, at close to the present day temperature while dolomite in the oil legs of the two fields appear to have grown at a significantly lower temperature (Table 4.2, 5.3), possibly before oil entered the reservoir (Fig. 6.4). This is a clear indication that oil emplacement into the reservoirs has significantly retarded dolomite precipitation. This may mean early oil emplacement has an impact on the general diagenesis of sandstones, and not just quartz cementation.

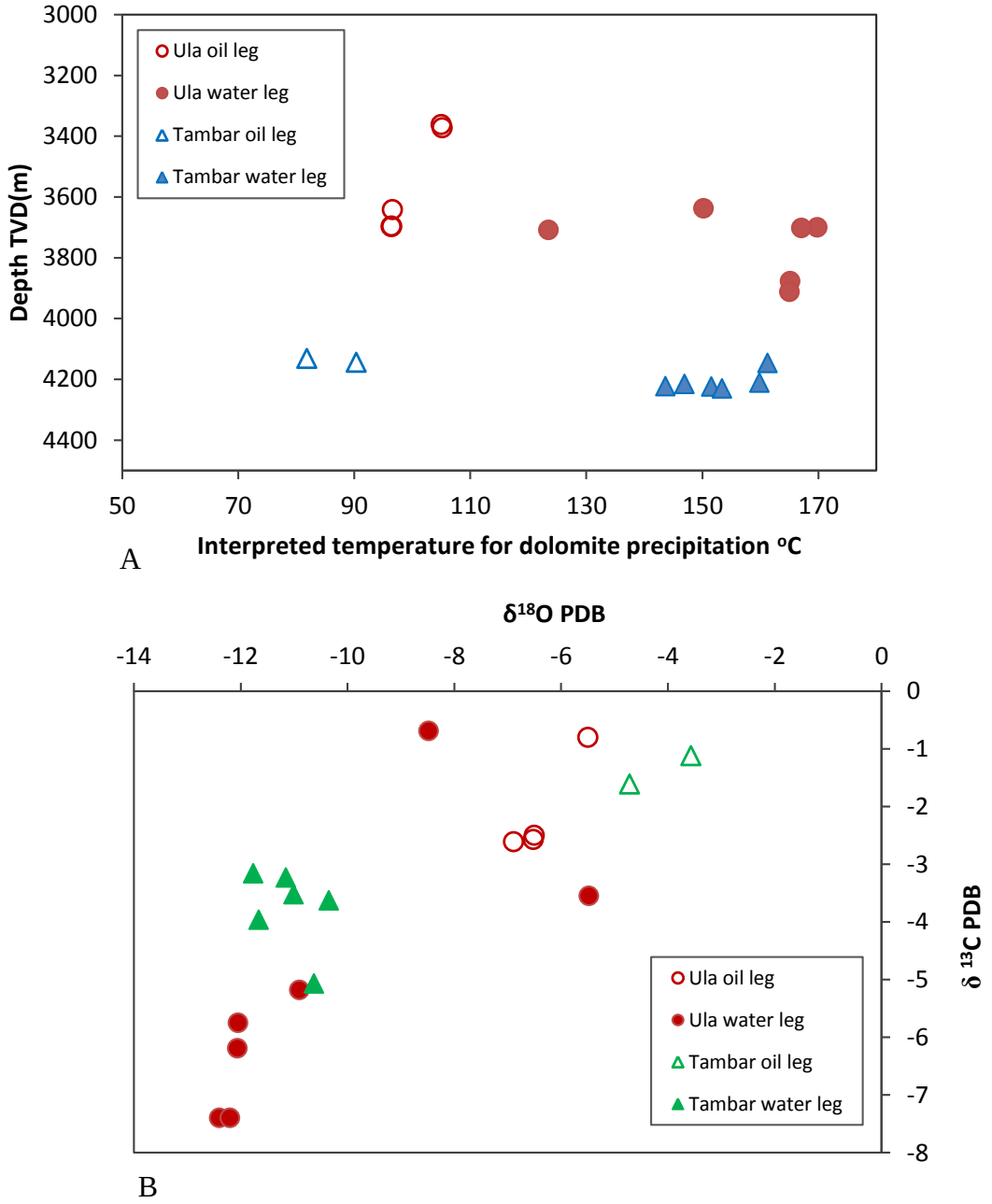

Figure 6. 4 Dolomite oxygen isotope plots for Ula and Tambar fields (A) Interpreted temperature of dolomite growth versus depth (B) Carbon isotope and oxygen isotope plots.

6.3 Implications for the petroleum industry

The conclusion made here that oil emplacement before onset of major quartz cementation in a reservoir will inhibit quartz cementation has economic significance. If the concept that early oil emplacement inhibits quartz cementation is disregarded, it will lead to prediction of no porosity - permeability variation in relation to filling history. This may result in inappropriate reserves calculation during appraisal stage, wrong prediction of aquifer performance during production, and lead to improper decisions on the number and positions of injection wells during the later life of the field.

6.4 Suggestions for future work

(1) This research work was carried out with a total of eight wells; five in the Ula and three in the Tambar field. Comparisons of all reservoir quality parameters for different water saturation zones of the reservoirs were carried out. It would be helpful if more wells from different fields could be used to carry out similar research for sandstones in different depositional settings.

(2) The duration of quartz cement precipitation was proposed for both Ula and Tambar fields based on long range homogenization temperature distribution of the aqueous fluid inclusions trapped in quartz cement. CL images of quartz cement did not show a clear zonation to suggest changes in water chemistry or discontinuities in cementations patterns. It would be useful if stable isotope analysis will be carried out on the quartz cement using SIMS (secondary ion mass spectroscopy, ion probe) to understand changes within the quartz cement from the detrital grain to the edge of the cement (Hervig et al., 1995; Marchand et al., 2000; Sullivan et al., 1997).

(3) One of the major porosity-preserving mechanisms in the Ula and Tambar fields is the grain coating microcrystalline quartz. This, and some previous works, has identified sponge spicules, radiolarian and diatoms as sources of saturated silica for microquartz precipitation. Other source of silica from meteoric fluids mixing with formation water has also been proposed (French et al., 2010; Haddad et al., 2006). A study of the sedimentology of sponge spicules and microquartz in modern

environments could serve as an analogue to help understand the source and distribution of microcrystalline quartz.

(4) To improve on our understanding of the effect of oil emplacement on quartz cementation and porosity preservation, the timing of oil emplacement could be fixed relative to time of oil charge. Barclay and Worden (2000) showed that early oil emplacement could halt quartz cementation in the oil leg. In contrast, oil emplacement after quartz cementation would have no effect on quartz cementation. Oil emplacement during quartz cementation could lead to progressive reduction in amount of quartz from crest to oil-water contact. Rapid versus slow oil charge into a reservoir will also result in different effects (Marchand et al., 2000). Most of the recent work on oil emplacement and quartz cementation used aqueous fluid inclusion to determine the time of quartz cementation and oil charge. Using petroleum inclusion PVT analysis to determine the actual time and duration of oil charge to constrain time and the rate of oil charge into reservoirs could help determine the precise timing of oil-filling relative to quartz cementation.

(5) Stable isotope analysis of the carbonate cements in both Ula and Tambar fields show lower precipitation temperatures for dolomite in the oil leg compared to precipitation temperatures in the water leg. More focus on carbonate and feldspar cements above and below oil water contact could be carried out in other field, and even other basins, to confirm if this pattern is consistent and universal.

(6) Petroleum fluid inclusions in quartz cement have been used as evidence of continuous quartz cementation in the presence of oil. However, the exact water saturation of the reservoir when petroleum inclusions were trapped has not been clearly determined. Petroleum geochemistry of the inclusions trapped in quartz cements could be carried out. The maturity of the petroleum in the inclusion could be compared to the reservoir petroleum as well as at different points within the cements to test whether inclusions were actually less mature (early generation) oil trapped at the onset of petroleum inclusions and there is gradual increase in maturation from early trapped inclusions to late trapped inclusions.

6.5 References

Aase, N. E., and Walderhaug, A., 2005, The effect of hydrocarbons on quartz cementation: diagenesis in the Upper Jurassic sandstones of the Miller Field, North Sea, revisited: Petroleum Geoscience, v. 11, no. 3, p. 215-223.

Bjørkum, P. A., Oelkers, E. H., Nadeau, P. H., Walderhaug, O., and Murphy, W. M., 1998, Porosity prediction in quartzose sandstones as a function of time, temperature, depth, stylolite frequency, and hydrocarbon saturation: American Association of Petroleum Geologists Bulletin, v. 82, no. 4, p. 637-648.

Cox, P. A., Wood, R. A., Dickson, J. A. D., Al Rougha, H. B., Shebl, H., and Corbett, P. W. M., 2010, Dynamics of cementation in response to oil charge: Evidence from a Cretaceous carbonate field, UAE: Sedimentary Geology, v. 228, no. 3-4, p. 246-254.

Dove, P. M., and Rimstidt, J. D., 1994, Silica-water interactions: Reviews in Mineralogy and Geochemistry, v. 29, no. 1, p. 259-308.

Ehrenberg, S. N., 1993, Preservation of anomalously high porosity in deeply buried sandstones by grain-coating chlorite: examples from the Norwegian continental shelf: American Association of Petroleum Geologists Bulletin, v. 77, p. 1260-1260.

Emery, D., Smalley, P. C., Oxtoby, N. H., Ragnarsdottir, K. V., Aagaard, P., Halliday, A., Coleman, M. L., and Petrovich, R., 1993, Synchronous oil migration and cementation in sandstone reservoirs demonstrated by quantitative description of diagenesis [and discussion]: Philosophical Transactions of the Royal Society of London. Series A: Physical and Engineering Sciences, v. 344, no. 1670, p. 115-125.

French, M. W., Worden, R. H., Mariani, E., Horn, W. C., Kliewer, C. E., Lamberti, W. A., Mueller, R. R., and Fischer, C., 2010, Low temperature porosity preserving microquartz from Upper Cretaceous sandstones of the Subhercynian Basin (Germany): Geochimica et Cosmochimica Acta, v. 74, no. 12, p. A305-A305.

Giles, M. R., Stevenson, S., Martin, S. V., Cannon, S. J. C., Hamilton, P. J., Marshall, J. D., and Samways, G. M., 1992, The reservoir properties and diagenesis of the Brent Group: a regional perspective, *in* Morton, A. C., Haszeldine, R. S., Giles, M. R., and Brown, S., eds., Geology of the Brent Group, Geological Society, London, Special Publications, v. 61, p. 329-350.

Gluyas, J. G., Robinson, A. G., Emery, D., Grant, S. M., and Oxtoby, N. H., 1993, The link between petroleum emplacement and sandstone cementation, *in* Parker, J., ed., Petroleum Geology of the North west Europe, Geological Society of London, v. 4, p. 1395-1402.

Haddad, S. C., Worden, R. H., Prior, D. J., and Smalley, P. C., 2006, Quartz cement in the Fontainebleau sandstone, Paris basin, France: Crystallography and implications for mechanisms of cement growth: Journal of Sedimentary Research, v. 76, no. 2, p. 244-256.

Hervig, R. L., Williams, L. B., Kirkland, I. K., and Longstaffe, F. J., 1995, Oxygen isotope microanalyses of diagenetic quartz: possible low temperature occlusion of pores: Geochimica Et Cosmochimica Acta, v. 59, no. 12, p. 2537-2543.

Land, L. S., 1983, The application of stable isotopes to studies of the origin of dolomite and to problems of diagenesis of clastic sediments, Society of Economic Paleontologists and Mineralogists, Short course, Stable isotopes in sedimentary geology: In Stable Isotopes in Sedimentary Geology, 4.1-4.22 p.:

Lander, R. H., and Walderhaug, O., 1999, Predicting porosity through simulating sandstone compaction and quartz cementation: American Association of Petroleum Geologists Bulletin, v. 83, no. 3, p. 433-449.

Lima, R. D., and De Ros, L. F., 2002, The role of depositional setting and diagenesis on the reservoir quality of Devonian sandstones from the Solimões Basin, Brazilian Amazonia: Marine and Petroleum Geology, v. 19, no. 9, p. 1047-1071.

Marchand, A. M. E., Haszeldine, R. S., Macaulay, C. I., Swennen, R., and Fallick, A. E., 2000, Quartz cementation inhibited by crestal oil charge: Miller deep water sandstone, UK North Sea: Clay Minerals, v. 35, no. 1, p. 201-210.

Marchand, A. M. E., Smalley, P. C., Haszeldine, R. S., and Fallick, A. E., 2002, Note on the importance of hydrocarbon fill for reservoir quality prediction in sandstones: American Association of Petroleum Geologists Bulletin, v. 86, no. 9, p. 1561-1571.

McBride, E. F., 1989, Quartz cement in sandstones: a review: Earth-Science Reviews, v. 26, no. 1, p. 69-112.

Molenaar, N., Cyziene, J., Sliaupa, S., and Craven, J., 2008, Lack of inhibiting effect of oil emplacement on quartz cementation: Evidence from Cambrian reservoir sandstones, Paleozoic Baltic Basin: Geological Society of America Bulletin, v. 120, no. 9-10, p. 1280-1295.

O'Neil, J. R., and Epstein, S., 1966, Oxygen isotope fractionation in the system dolomite-calcite-carbon dioxide: Science, v. 152, no. 3719, p. 198-201.

Ramm, M., 1992, Porosity depth trends in reservoir sandstones - theoretical models related to Jurassic sandstones offshore Norway: Marine and Petroleum Geology, v. 9, no. 5, p. 553-567.

Saigal, G. C., Bjorlykke, K., and Larter, S., 1992, The effects of oil emplacement on diagenetic processes - examples from the Fulmar Reservoir sandstones, central North Sea: American Association of Petroleum Geologists Bulletin, v. 76, no. 7, p. 1024-1033.

Sclater, J. G. and Christie, P. A. F. 1980 Continental stretching - an explanation of the post-mid- Cretaceous subsidence of the central North-Sea Basin. Journal of Geophysical Research, v. 85

Sullivan, M. D., Macaulay, C. I., Fallick, A. E., and Haszeldine, R. S., 1997, Imported quartz cement in aeolian sandstone grew from water of uniform composition but has complex zonation: Terra Nova, v. 9, no. 5-6, p. 237-241.

Vagle, G. B., Hurst, A., and Dypvik, H., 1994, Origin of quartz cements in some sandstones from the Jurassic of the Inner Moray Firth (UK): Sedimentology, v. 41, no. 2, p. 363-377.

Walderhaug, O., 1990, A fluid inclusion study of quartz cemented sandstones from offshore mid-Norway - possible evidence for continued quartz cementation during oil emplacement: Journal of Sedimentary Petrology, v. 60, no. 2, p. 203-210.

-, 2000, Modeling quartz cementation and porosity in Middle Jurassic Brent Group sandstones of the Kvitebjorn field, Northern North Sea: American Association of Petroleum Geologists Bulletin, v. 84, no. 9, p. 1325-1339.

Wilkinson, M., and Haszeldine, R. S., 2011, Oil charge preserves exceptional porosity in deeply buried, overpressured, sandstones: Central North Sea, UK: Journal of the Geological Society, v. 168, no. 6, p. 1285-1295.

Worden, R. H., and Morad, S., 2000, Quartz cementation in sandstones: a review of the key controversies *in* Worden, R. H., and Morad., S., eds., Quartz cementation in sandstones International Association of Sedimentologists Special Publication v. 29, p. 1-20.

Worden, R. H., Oxtoby, N. H., and Smalley, P. C., 1998, Can oil emplacement prevent quartz cementation in sandstones?: Petroleum Geoscience, v. 4, no. 2, p. 129-137.

7. Appendixes - See separate file and DVD enclosed with the hard copy

1. Modal and textural analysis data

2. Wireline data